2017

Green Thermosetting Factory: Novel Star-shaped Bio-based Systems and Their Thermosetting Resins; Synthesis and Characterization

Arash Jahandideh
South Dakota State University

GREEN THERMOSETTING FACTORY: NOVEL STAR-SHAPED BIO-BASED SYSTEMS AND THEIR THERMOSETTING RESINS; SYNTHESIS AND CHARACTERIZATION

BY

ARASH JAHANDIDEH

A dissertation submitted in partial fulfillment of the requirements for the

Doctor of Philosophy

Major in Agricultural, Biosystems and Mechanical Engineering

South Dakota State University

2017

GREEN THERMOSETTING FACTORY: NOVEL STAR-SHAPED BIO-BASED SYSTEMS AND THEIR THERMOSETTING RESINS; SYNTHESIS AND CHARACTERIZATION

This dissertation is approved as a creditable and independent investigation by a candidate for the Doctor of Philosophy in Agricultural, Biosystems and Mechanical Engineering and is acceptable for meeting the dissertation requirements for this degree. Acceptance of this does not imply that the conclusions reached by the candidate are necessarily the conclusions of the major department.

K. Muthukumarappan, Ph.D. Date
Dissertation Advisor

Van Kelley, Ph.D. Date
Head, Department of Agricultural and Biosystems Engineering

Dean, Graduate School Date

I dedicate this dissertation to my beloved family and my loving parents, Zahra and Ahmad. This would never have been possible without their supports.

ACKNOWLEDGEMENTS

I would like to thank my advisor, Dr. Muthukumarappan for his patience and continued support throughout my Ph.D. career. I am grateful for the numerous opportunities he gave me. I shall always remember his trust in me and the chances he has given me to succeed. I wish to thank the following people for their support in obtaining my Ph.D. degree: to my committee members who were more than generous with their expertise and precious time. To Dr. Bill Gibbons for his constant guidance and his trust in me in several projects. To Dr. Mikael Skrifvars and Dan Åkesson of University of Borås, Sweden, for sharing their expertise on star-shaped thermosets. To Nima Esmaeili from University of Bolton, UK, for his consultants and guidance on thermomechanical and characterization aspects of my project. To Dr. Gary Anderson for his smart insights on thermomechanical properties and statistical analysis of my work. To Dr. Halaweish for helping me with the NMR analysis. To Dr. Bishnu Karki for her insights and valuable time. To Dr. Tylor Johnson, for his advices, and help throughout lots of my projects. To my dear friends, Sepehr Nesaei and Samaneh Amiri. To Dr. Reza Ahmadi and Dr. Forough Jahandideh of university of Alberta for their kind help. I would particularly thank Dr. Asma Rashki of Tehran University of Medical Sciences, for critical evaluation of biomedical part of my dissertation. I also want to extend my deepest gratitude to Zari Alishiri and Dr. Ali Salehnia for their unconditional love, supports and help throughout these past three years. I extend my sincere appreciation to the entire faculty and staff in the department of Agricultural and Biosystems Engineering at South Dakota State University for their kind help and supports. Lastly and most importantly, I would like to express gratitude to my parents for making me feel unconditionally supported in every step I have taken.

TABLE OF CONTENTS

ABBREVIATIONS

LA: lactic acid

PLA: poly lactic acid

S-LA: star-shaped LA based resins

CP: condensation polymerization

ADC: azeotropic dehydration condensation

DP: direct polymerization

ROP: ring opening polymerization

EF: end-functionalization

NMR: Nuclear Magnetic Resonance

DMA: dynamic mechanical analysis

TGA: thermogravimetry analysis

MW: molecular weight

PLEG: poly lactic acid-ethylene glycol

PGA: poly glycolic acid

PEG: poly ethylene glycol

PENTA: pentaerythritol

IT: itaconic acid

MAAH: methacrylic anhydride

MAA: methacrylic acid

TEG: tetra (ethylene glycol)

THMP: 1,1,1-tri(hydroxy methyl)propane

DPE: dipentaerythritol

DSC: differential scanning calorimetry

DEA: dielectric analysis

TAN: Total Acid Number

FT-IR: Fourier transform infrared spectroscopy

USDA: U.S. Department of Agriculture

E: modulus of elasticity

UTS: ultimate tensile strength

HRR: heat release rate

FDA: Food and Drug Administration

DMA: Dynamic mechanical analysis

DSC: Differential scanning calorimetry

EF: End-functionalizing

EG: Ethylene glycol

ER: Erythritol

FTIR: Fourier-transform infrared spectroscopy

GL: Glycerol

IT: Itaconic acid

LA: Lactic acid

MAA: Methacrylic acid

MAAH: Methacrylic anhydride

PENTA: Pentaerythritol

PLA: Poly lactic acid

PLGA: Poly lactic-*co*-glycolic acid

ROP: Ring opening polymerization

S-LA: Star-shaped lactic acid based resins

TGA: Thermogravimetric analysis

THMP: 1,1,1-tri(hydroxy methyl)propane

LIST OF FIGURES

LIST OF TABLES

ABSTRACT

GREEN THERMOSETTING FACTORY: NOVEL STAR-SHAPED BIO-BASED SYSTEMS AND THEIR THERMOSETTING RESINS; SYNTHESIS, CHARACTERIZATION, OPPORTUNITIES AND DRAWBACKS

ARASH JAHANDIDEH

2017

Increasing attentions toward sustainable development, economic and environmental issues have led to many attempts at replacing the petroleum-based materials with renewables. Substitution of petroleum-based platforms with green alternative technologies is beneficiary in different ways. Using bio-renewables reduces the dependency of the national plastic industry to the petroleum resources and substantially promotes the environmental profile and sustainability of the product. It is expected that the emergence of the corn-based thermosetting industry generates substantial profits for the corn production sector. Developments in the emerging biobased thermosets are spectacular from a technological point of view. However, there are still several disadvantages associated with the current biobased thermosetting resins, e.g. low processability, environmental issues, expensive sources and poor thermomechanical properties. Use of natural fibers not only contributes to the production of a more environmentally friendly product, but also has advantages such as low-weight product and low manufacturing costs. The results of this study show a possibility of production of biocomposites made from natural fibers and star-shaped resin, synthesized

from corn-based materials (lactic acid and itaconic acid) and different multihydroxyl core molecules. These resins were synthesized via two-steps strategy: polycondensation of the monomers with the core molecules followed by end-functionalization of the branches by methacrylic anhydride or itaconic acid.

The results have shown that these resin are capable of competing with or even surpassing fossil fuel based resins in terms of cost and eco-friendliness aspect. Inexpensive biobased raw material, better environmental profile, low viscosity, and better processability of the matrix along with better thermomechanical properties of the produced biocomposites are of advantages expected for these systems.

Chapter 1 - Foreword

This dissertation is consisted of two different parts. Part A is entitled as "Synthesis, characterization and curing kinetics of novel star-shaped resins synthesized from lactic acid" in which the synthesis and characterization of various star-shaped resins with different core molecules will be discussed. The employed core molecules include: glycerin, pentaerythritol, ethylene glycol and xylitol. In the Part B which entitled as "the synthesis and characterization of novel star-shaped itaconic acid based thermosetting resins", star-shaped biobased thermoset resins will be synthesized employing itaconic acid molecules and glycerin core molecule. The objectives, incentives and the rationales for these studies will be presented below.

1.1 Part A: the Synthesis, characterization and curing kinetics of novel star-shaped resins synthesized from lactic acid.

The first objective of this phase is to synthesize and characterize the resins and optimize the curing process. Then, the effect of LA chain-length on the thermomechanical properties was investigated.

The second objective was to model the curing kinetics and the rheology. Finally, employing the curing and rheology models, the resin were employed for production of biocomposites reinforced by natural fibers. The results have shown that these resin are capable of competing with or even surpassing fossil fuel based resins in terms of cost and eco-friendliness aspect. Successful outcome of the project will result in synthesis and characterization of a novel star-shaped resin, suitable for biocomposite production with

possible wide range of applications. Inexpensive biobased raw material, better environmental profile, low viscosity, and better processability of the matrix along with better thermomechanical properties of the produced biocomposites are of advantages expected for these system.

1.1.1 Synopsis of the Part A study

Composites are engineered materials with wide range of applications which are currently produced from petroleum based resins and synthetic fibers. Due to a shortage of petroleum resources, and ecological-economic concerns associated to petroleum based resins, different biobased raw materials have been suggested for production of composites. Versatile and economical renewable sources of lactic acid (LA) make LA a suitable source for production of bioplastics.

Thermoplasts are a class of polymers with high molecular weight in which the chains are associated through intermolecular forces in which structure is weaken rapidly upon temperature increase. In contrast, thermosets form chemical bonds during the curing process and the structure cannot be reformed upon heating-cooling processes. Limitations in impregnation of the matrix to fibers, make the thermoplast processing to be slow and costly and also reduce the mechanical strength of the produced composites. In addition, PLA's hydrophobic nature makes it incompatible with natural fibers (Oksman, Skrifvars, and Selin 2003, Wambua, Ivens, and Verpoest 2003, Qin et al. 2011). The other privilege of the thermoset systems is that thermosets can be tailored for a certain functionality by altering the chemical structure or by changing crosslinking density which ultimately result in variety of resins (Raquez et al. 2010a). However, there are also several

disadvantages associated with current thermosetting resins, e.g. environmental issues, nonrenewable expensive sources and poor thermomechanical and impact properties.

Different studies have been performed on synthesis of star-shaped thermosetting resins from LA (Sachlos and Czernuszka 2003, Åkesson, Skrifvars, et al. 2010b, Bakare, Åkesson, et al. 2015, Bakare et al. 2014b). It is presumed that more hydroxyls of the core molecule provide a better extended network of the final thermosets. In addition, unsaturated hydroxyl groups of the core molecule may ultimately increase the hydrophilicity of the produced resin which makes the resin more compatible with hydrophilic inexpensive natural fibers. *The major goal of this phase is to produce biocomposites made from natural fibers and a novel star-shaped synthesized resins*.

The privilege of this state-of-the-art thermoset system over other systems is that this resin can be engineered for a certain functionality by changing the chemical structure or altering the crosslinking density. For example, substitution of the end-functionalization agent with groups containing phosphorous, can add flame retardancy features to the biocomposites, or by increasing the LA chain-length of the oligomer, the flexibility of the product is increased. The already established knowledge on biopolymer synthesis and biocomposite production, a network of experts working closely on different areas related to the subject, promising preliminary results and available resources required for conducting the experiments, have encouraged us to work on this project.

1.1.2 Rationale and Specific Objectives of Part A-Using Xylitol Core molecule

Substitution of current petroleum-based platforms with renewable-based technologies would be beneficiary in different ways. First, using the corn-based LA instead of conventional petroleum based monomers, will reduce the dependency of the national thermosetting plastic industry to the petroleum resources. Thus, in the long term,

it will *enhance the national energy security.* Second, compared to petroleum based products, using biobased materials will substantially *promote the environmental profile and sustainability* of the production chain. Third, using corn-based LA and inexpensive natural fibers as the raw materials, will subsequently *promote economic diversification in rural areas* of the United States.

It is expected that the emergence of the LA based thermosetting industry will generate substantial profits for individuals involved in the corn production sector. The multidisciplinary nature of this proposal promotes the collaborative partnerships between different participants, from agriculture-sector individuals to experts of different fields of agricultural engineering, chemical and polymer engineering and mechanical engineering. The incentives for suggesting xylitol as the core molecule in this star-shaped polymer are that 1) it is biobased and relatively inexpensive, 2) it lowers the viscosity of the final resin and enhances the resin's processability, 3) xylitol's hydroxyl groups provide a better extended network which results in better thermomechanical properties of the cured resin and 4) hypothetically, unsaturated branches of xylitol molecule, increase the hydrophilicity of the produced resin. Therefore, it leads to a resin which is more compatible with inexpensive natural fibers and it eventually increases the mechanical properties and lowers the final costs of the biocomposites produced from natural fibers and PLA thermosets.

Objectives: The specific objectives of this phase are as follows:

Objective 1: Resin Synthesis, Characterization and Optimization. In the first phase, the resins are synthesized and characterized and the curing process is optimized.

The thermomechanical properties of cured resins is also investigated and the effect of the LA chain-length on the thermomechanical properties of the resins will be investigated.

Objective 2: Cure kinetics and Rheology Characterization. Cure kinetics and Rheology of the synthesized resins is investigated by means of DSC and viscometer. These models then were applied for composite processing.

*Objective 3: Biocomposite production. B*iocomposites were prepared using natural fibers by compression molding method. The composite laminates were then prepared and cut with a laser cutting machine and the thermomechanical properties of composites were investigated.

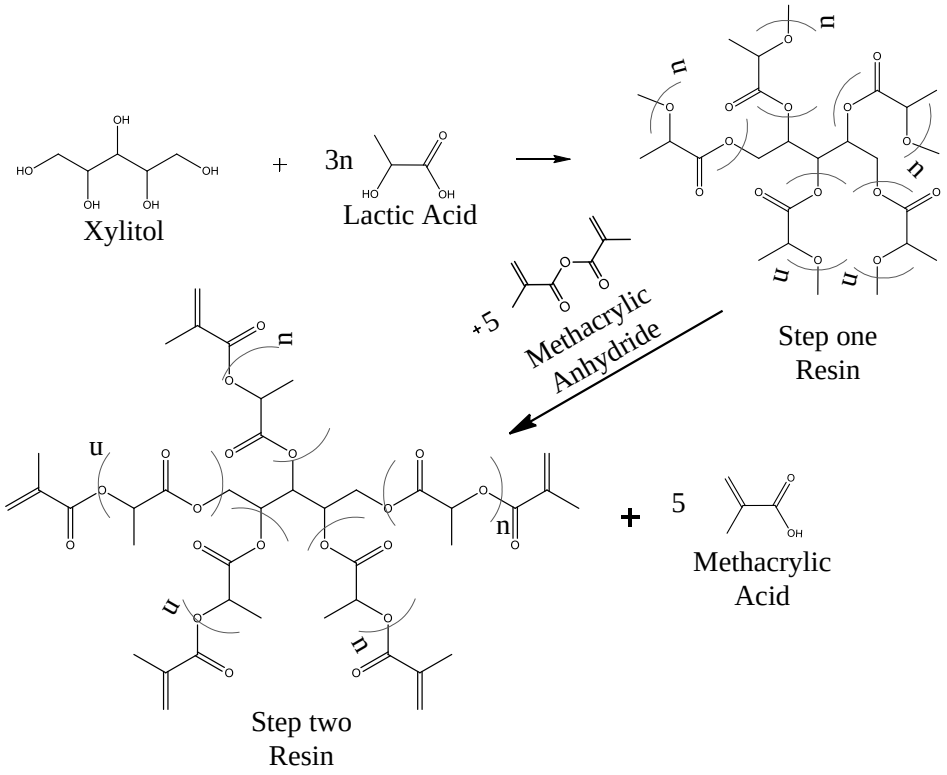

Figure 1. 1 Reaction scheme for the two-stage synthesis of methacrylate functionalized xylitol-LA resins

1.1.3 Summary of Methods Used in Part A

1.1.3.1 Objective 1.1- Resin Synthesis

The resins will be synthesized via a two steps method: poly-condensation and end-functionalization. The first-step reactions result in oligomers with a xylitol center and LA branches. In the poly-condensation reactions, LA and Xylitol will be mixed in presence of toluene and the catalyst, methanesulfonic acid. The condensation of LA will occur under toluene reflux from an azeotropic distillation apparatus. The ratio of the reacted to initial carboxylic groups in the reactants can be attributed to the degree of completion of the condensation reaction in the polymerization-condensation step.

The number of carboxylic groups will be measured based on an acid-base titration method (ASTM D974). The branches will be functionalized further to improve their reactivity by adding carbon double bonds. For this mean, in presence of hydroquinone, methacrylic anhydride will be added as the end-functionalizing agent. The chemical reactions and idealized structures are presented in Figure 1. The chemical structures of the resins will be confirmed by a ^{13}C NMR spectrometry at 400 MHz and the FTIR analysis which will be carried out on a spectrometer in the range of 4000–600 cm^{-1}.

1.1.3.2 Objective 1.2- Resin Optimization

The aim of the curing optimization is to obtain the complete, cured samples, which has no imperfections in the final casted product. For the curing purpose, benzoyl peroxide will be used as the radical-initiator. Different curing strategies will be investigated and the completion of the curing process will be confirmed by analyzing the exotherms of the DSC of the samples. Finally, mechanical strength of different neat samples will be checked and the best curing method will be introduced. The FTIR analysis of the cured samples will be carried out on a spectrometer in the range of 4000–

600 cm^{-1}. TGA of the cured resins will also be carried out to study the thermo-stability and DMA will be performed to check the viscoelastic properties of the biocomposites.

1.1.3.3 Objective 1.3- Effect of Chain-Lengths on Thermomechanical Properties.

In this part, the effect of LA chain-lengths on the thermomechanical properties of the resins will be investigated. The resins with three different LA chain-lengths of: 3, 5 and 7 will be synthesized in a similar way as explained in the resin synthesis part. Resins will be characterized by ^{13}C-NMR, FTIR, Viscoanalyzer, DSC, DMA, TGA and also by Flexural and Tensile tests. The resin with desired thermomechanical properties will be identified and used for production of biocomposites.

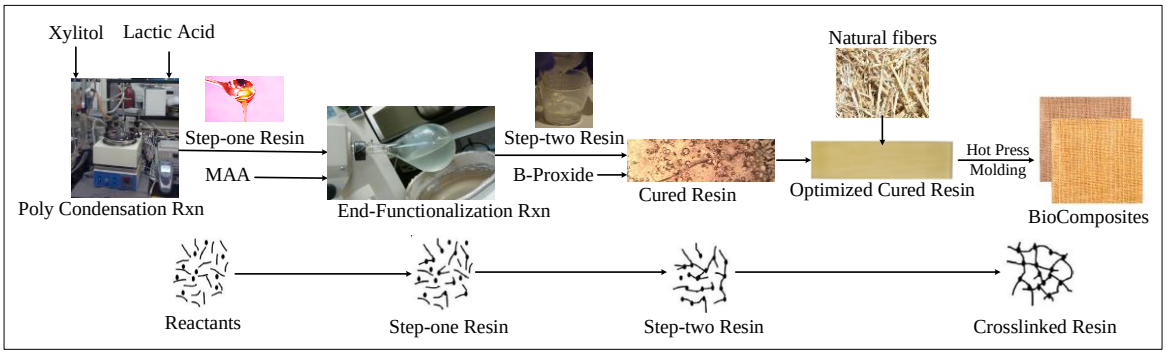

Figure 1. 2. Schematic of the methodology proposed in this proposal

1.1.3.4 Objective 2- Cure Kinetics and Rheology Characterization.

For cure kinetics, the DSC will be used to measure the heat flow of dynamic and isothermal curing processes. Non-isothermal curing experiments will also be performed to study the curing kinetics of the reactions. The curing process will be then modeled by the change of various kinetic parameters, reaction orders and evolutions of activated energy under the test reaction conditions. Rheology of the synthesized resins will also be investigated by a viscometer. The change in viscosity under isotheral conditions will be

measured and used for phenomenological modeling of the rheology. These models then will be applied for composite processing.

1.1.3.5 Objective 3: Biocomposite Production.

Biocomposites will be prepared using different natural fibers (e.g. Jute, flax and hemp) by a layout method. The optimized resin will be impregnated in to natural fiber reinforcements and then compression molded at elevated temperature to produce thermoset composites. The composite laminates will be cut with a laser cutting machine and the mechanical properties will be characterized by flexural and tensile testing. The thermal properties of composites will be also investigated by DMA and TGA. The water adsorption tests will be performed based on ASTM D 570 to determine the relative rate of water absorption of the biocomposite samples.

It is possible to manipulate the biocomposites' properties by changing the nature and the portion of the block units of copolymers of LA and xylitol. This manipulation could be in terms of changing the hydrophilicity as well as designing and altering the voids' sizes of the polymers network. It means that the next generation biocomposites can be engineered for a specific application. One future scope of this study might be to engineer the resins for a certain functionality, e.g. to add antimicrobial properties by embedding antioxidant agents or to add flame-retardancy property by adding phosphorus containing groups in the chains. Manipulation of both void's size and hydrophilicity will provide the unique opportunity for designing a polymeric matrix which is specifically designed for certain chemical component release or a desired drug delivery with a substantial control over release rate.

1.1.4 Deliverables expected for Part A

Successful outcome of the Part A of this project will result in synthesis and characterization of a novel, inexpensive, biobased, star-shaped resin, suitable for biocomposite production with possible wide range of applications. By studying the effect of LA chain-length the resin formulation will be optimized for a certain biocomposite production purposes. Curing kinetic and Rheology models will be developed and used for production of biocomposites in which the natural fibers are used as reinforcements. The outcome of this dissertation would be served as the cornerstone of future plans for more collaborative projects between different parties, working on the functionalized composites. The proposed platform will create a paradigm for future studies on engineered star-shaped thermosetting.

1.2 Part B: The Synthesis and Characterization of Novel Star-Shaped Itaconic acid based Thermosetting Resins

1.2.1 Synopsis of the Part B study:

In this part of this dissertation, the synthesis and characterization of corn-based thermosetting resins suggested based on itaconic acid and the star-shaped lactic acid based resins (S-LA). In part A of this dissertation, we have introduced the method for synthesizing the S-LA, and in this part, the substitution of the expensive methacrylic anhydride (MAA) with the corn-based itaconic acid has been proposed. MAA which is currently used for end functionalization of resins, is a toxic and reactive liquid which does not have a known renewable source. Itaconic acid (ITA) is a non-toxic, readily biodegradable chemical which is produced commercially by the fermentation of corn based carbohydrates using *Aspergillus terreus*.

These properties candidate ITA as a sustainable industrial building block. Inexpensive biobased raw material, better environmental profile, low viscosity and better processability of the matrix along with better thermomechanical properties and low weights of the produced biocomposites are of advantages expected for the ITA based S-LA composites. Successful outcome of this phase results in synthesis and characterization of an inexpensive, biobased, biodegradable resin, suitable for biocomposite production with possible wide range of applications.

a

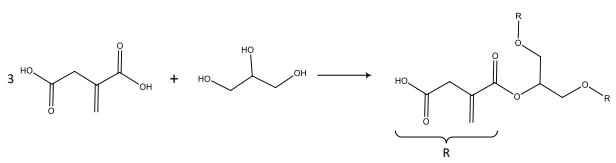

b

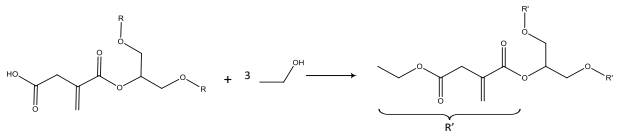

Figure 1. 3. Reaction scheme for a) the synthesis of star-Ita-Gly resins, and b) end-functionalization with ethanol to synthesis T*star*-Ita-Gly resins.

1.2.2 Commercial Potential of Itaconic based Resins

Commercial composites are typically manufactured from glass fibers and fossil fuel derived polymers. In this part of this dissertation, the synthesis of the corn-based thermosetting resins suggested based on itaconic acid and glycerol core molecules. ITA has been listed as one of the top 12 value-added chemicals by the U.S. Department of Energy which can be commercially produced from corn starch using fungi. Glycerol is an inexpensive abundant renewable compound which is the main byproduct of the biodiesel production. The produced star-shaped resins would be inexpensive, biobased, suitable for biocomposite production with possible wide range of applications.The previous results support that these resins are more compatible with inexpensive natural fibers which eventually increases the mechanical properties and lower the final costs of the biocomposites. These composites can be engineered for specific applications such as automotive, electrical, furnishing or food packaging.

We firmly believe that these thermoset resins are capable of competing with or even surpassing expensive commercial thermoset resins include polyesters, vinyl esters, epoxies, maleimides, polyimides, etc. (with a huge market demand) in terms of cost and eco-friendliness concerns. The composites' market is mainly dominated by the aerospace, wind energy and transportation appliances due to their excellent properties and low

weight. The suggested thermosetting resin is made up of up to 96 wt% corn-based raw materials with a high potential market demand for different industries. In addition, the global price of the MAA which is currently employed for end functionalization, is estimated to be around $10/kg while the global price of the ITA is expected to be around $1/kg. Therefore, substitution of the MAA with ITA in the thermosetting resins is believed to substantially improve the economy of the process.

1.2.3 Objectives of Part B

The specific objectives of this part of the dissertation are as follows:

Objective 1: Resin Synthesis, Characterization and Optimization. In the first phase, the resins will be synthesized and characterized and the curing process will be optimized.

Objective 2: Substitution of hydroxyl groups with more reactive groups. In the second phase, the resins will be synthesized by treating the resins with biobased and reactive alcohols. The resins will be then characterized and the curing process will be optimized.

1.2.4 Methods used in Part B of this study

1.2.4.1 Resin Synthesis:

We have already shown the synthesis of star-shaped oligomers in our previous studies via a two-step method. The first-step reactions result in oligomers with a glycerol center and LA branches. The degree of completion of the condensation reaction in the polymerization-condensation step will be measured based on an acid-base titration method. Previous results showed that although macromolecules have reactive groups, yet

the reacti1vity is not enough for efficient crosslinking. So far, MAA has been used for efficient end-functionalization of the thermoset resins which is toxic, expensive and doesn't have a biobased source. In this proposal, the ITA is proposed for end-functionalization. The chemical structures of the resin will be evaluated by H NMR, ^{13}C NMR and FTIR analysis.

1.2.4.2 Curing Optimization:

The aim of the curing optimization is to obtain the completely cured samples, which has no imperfections in the final casted product. Different curing strategies will be investigated and the completion of the curing process will be confirmed by analyzing the exotherms of the DSC of the samples. Finally, mechanical strength of different neat samples will be checked and the best curing method will be introduced. TGA of the cured resins will also be carried out to study the thermo-stability and DMA will be performed to check the viscoelastic properties of the crosslinked resins.

Chapter 2- Star-shaped lactic acid based systems and their thermosetting resins; synthesis, characterization, potential opportunities and drawbacks

Arash Jahandideh*, Kasiviswanathan Muthukumarappan

Agricultural and Biosystems Engineering Department, South Dakota State University, PO Box 2120, Brookings, SD 57007, USA

This chapter has been published in European polymer Journal.

*Corresponding author: *arash.jahandideh@sdstate.edu*

List of abbreviations:

LA: lactic acid

PLA: poly lactic acid

S-LA: star-shaped LA based resins

CP: condensation polymerization

ADC: azeotropic dehydration condensation

DP: direct polymerization

ROP: ring opening polymerization

EF: end-functionalization

NMR: Nuclear Magnetic Resonance

DMA: dynamic mechanical analysis

TGA: thermogravimetry analysis

MW: molecular weight

PLEG: poly lactic acid-ethylene glycol

PGA: poly glycolic acid

PEG: poly ethylene glycol

PENTA: pentaerythritol

IT: itaconic acid

MAAH: methacrylic anhydride

MAA: methacrylic acid

TEG: tetra (ethylene glycol)

THMP: 1,1,1-tri(hydroxy methyl)propane

DPE: dipentaerythritol

DSC: differential scanning calorimetry

DEA: dielectric analysis

TAN: Total Acid Number

FT-IR: Fourier transform infrared spectroscopy

USDA: U.S. Department of Agriculture

E: modulus of elasticity

UTS: ultimate tensile strength

HRR: heat release rate

FDA: Food and Drug Administration

Abstract

Shortcomings of the conventional PLA synthesis methods have encouraged researchers to investigate on alternative methods for PLA synthesis. Utilization of chain extenders is an effective way to achieve high MW polymers. The concept of using star-shaped resins as the reinforced matrices for biocomposites or in biomedical applications is gaining more and more attention day by day. Star-shaped lactic acid based resins are a

class of branched resins with a multifunctional core molecule and lactic acid branches. In order to increase the reactivity of branches, the star-shaped resin oligomers can get end-functionalized which yields in a crosslinkable product. Changing the architecture of a polymer from a linear to a multiarm or hyperbranched one, would change its chemical, diffusional and physical-mechanical properties.

This review paper presents the current state and recent advances in the synthesis, characterization, properties and applications of the star-shaped resins made from lactic acid or lactide and multi-hydroxyl core molecules with a focus on the role of the morphology of the polymer on the properties of resins. Rheological, physiochemical and thermomechanical properties of to date synthesized star-shaped resins are compared and discussed. Special emphasis would be made on potential opportunities, probable applications and also gaps and drawbacks concerning these systems. This review aims to provide useful information to help future development of efficient, highly engineered bioresins which can be especially designed for a certain application.

Keywords

Star-shaped; Lactic acid; Thermosetting resins; Applications; Limitations

Highlights

- Recent advances in the synthesis and properties of the star-shaped resins are discussed.
- Physiochemical and thermomechanical properties of S-LA resins are compared and discussed.
- Opportunities, probable applications and also drawbacks of the star-shaped resins are discussed.

2.1. Introduction

Different studies have been published on the synthesis of resins from lactic acid (LA) or lactide and branching point molecules. In order to increase the MW of PLA and induce branching points in the structure, different techniques have been employed, including free-radical branching in the presence of epoxides (Takamura et al. 2008), beam irradiation (Wang et al. 2011), copolymerization with cyclic monomers having hydroxyl groups in the cycle (Wolf and Frey 2009) or use of polyfunctional chain extenders. Generally, the star-shaped thermosetting resins are synthesized via a two-step strategy: poly-condensation of LA with the core molecule followed by end-functionalization of the branches. So far, star-shaped LA based resins (S-LA) were synthesized employing core molecules, including ethylene glycol, xylitol, glycerol and pentaerythritol for different applications.

The rationales for employing a core molecule in the structure of star-shaped polymers are that it potentially changes the properties of the polymer, increases the MW of the oligomers, lowers the viscosity and enhances processability of the resin; this technique is also provides a better extended network resulting in better thermomechanical properties of the cured resin. In addition, the core molecule will provide reactive sites which can be further used for the addition of a special functionality, e.g. a flame retardant agent, a drug carrier, an anti-microbial agent, etc. It is also possible to manipulate the biocomposites' properties by changing the nature and the portion of the block units of copolymers of LA and the core molecule. This manipulation could be in terms of changing the hydrophilicity or designing and altering the voids' sizes of the crosslinked polymer's network. For example, by employing longer oligomers, it is possible to

increase the size of the voids in the network and by using hydrophilic monomers, the hydrophilicity of the product can be tailored. Manipulation of both void's size and hydrophilicity will provide the unique opportunity for designing a polymeric matrix for certain component release or a desired drug delivery with a substantial control over release rate.

Different methods have been introduced for synthesizing and characterizing the S-LA. The differences between the S-LA properties, resulted from employing of different core molecules, different lengths of the LA monomers (or co-polymers) in branches, utilization of different end-functionalization (EF) agents, employing different curing techniques as well as using different curing initiators. Choosing a combination of these factors results in a unique product with specific characteristics which could be suitable for a certain purpose. The concept of using star-shaped resins as the reinforced matrices for biocomposites or in biomedical applications is gaining more and more attention day by day.

The increasing number of publications during the recent years, concerning the synthesis and characterization of star-shaped resins for different applications, including biocomposites (Bakare et al. 2014b, Bakare, Åkesson, et al. 2015, Bakare et al. 2016, Åkesson et al. 2011b), coating (Åkesson, Skrifvars, et al. 2010b), biomedical (Zeng et al. 2013, Kim, Kim, and Kim 2004), drug delivery (Park et al. 2003, Lin and Zhang 2010, Lin, Zhang, and Wang 2012), tissue engineering (Sakai et al. 2013), smart packaging, functionalized polymers (Finne and Albertsson 2002, Biela et al. 2005) and so on, reflects the growing importance of these new resins. To date, there is no comprehensive study exists on the different synthesis methods and characteristics of the synthesized S-LA.

This review paper presents the recent advances in the synthesis, characterization, properties and applications of S-LA and their thermosetting systems using a multi-hydroxyl clustering core molecule. The synthesis, chemical and thermomechanical properties of S-LAs are assessed. Special emphasis would be made on potential opportunities, probable applications and also drawbacks concerning the use of the multi-hydroxyl core molecules in the structure of the S- LA. Finally, the limitations and technological gaps of these systems are highlighted. This paper will not address other branched LA based polymers, including dendritic (Mezzenga, Boogh, and Månson 2001), hyperbranched (Hult, Johansson, and Malmström 1999), grafted or comb-like polymers (Plate and Shibayev 1971); and also, synthetic fiber reinforcements for bio composites are out of the scope of this paper. In addition, studies on fiber treatment for composite productions are excluded from this review article.

This review paper consisted of four different sections. In the first part, the synthesis of the S-Las and linear PLA systems are explored. Different synthesis methods of PLA are discussed and currently applied multi-hydroxyl monomers as the core molecule for S-LAs are introduced. The role of EF and attributed methods of end-functionalizing of the branches as well as different methods for curing of the resins are emphasized.

In the second part, the characterization of the S-LAs are discussed, including chemical characterization, general properties and thermomechanical properties. In chemical characterization, titration, nuclear magnetic resonance (NMR) and Fourier transform infrared spectroscopy (FT-IR) of S-LAs are briefly discussed. Special emphasis are made on rheological properties of the star-shaped crosslinkable resins. The

general properties section presents the current knowledge on water absorption properties and the biobased contents of the S-LAs. Finally, the thermomechanical properties of the cured resins are discussed based on the reported results of dynamic mechanical analysis (DMA), flexural and tensile analysis. The third part will discuss different applications of these systems, including biocomposites, drug delivery and tissue engineering. In the fourth part, the limitations and future of these systems are discussed.

2.2. Introduction to PLA synthesis methods

Lactic acid (2-hydroxy propionic acid) exists as the two stereo isomers of L-LA and D-LA, and can be produced via bacterial fermentation of carbohydrates or chemical synthesis. The LA produced by the chemical rout is an optically inactive racemic mixture (50/50 L-D) while fermentation-derived LA exists almost exclusively as L-LA (Lunt 1998). Due to major limitations of chemical synthesis, the fermentation pathway is often preferred (Datta and Henry 2006, Jamshidian et al. 2010). Poly lactic acid (PLA), an aliphatic polyester made up of LA monomers, is a biodegradable and compostable thermoplastic, which has extensive applications in biomedical fields, including bone fixation, drug delivery and tissue engineering (Lasprilla et al. 2012). The applications of PLA are not limited to biomedical field and it has potential for use in a wide range of applications, including food applications, packaging, structural composites, furnishings, etc. (Jamshidian et al. 2010, Madhavan Nampoothiri, Nair, and John 2010).

Synthesis of PLA from LA can follow two different routes of polymerization, condensation polymerization (CP) of LA and polymerization through lactide formation (presented in Fig. 1) (Jamshidian et al. 2010). The condensation polymerization route includes direct condensation-polymerization of LA (see Fig. 1, Pathway A) and

azeotropic dehydration condensation (ADC) of LA (see Fig. 1, Pathway C). In direct condensation polymerization, esterification of monomers happens with the aid of solvents and the consequent water is removed progressively at high temperatures and partial vacuum. The molecular weight of the condensation derived polymer is low, which results in poor mechanical properties (Jamshidian et al. 2010, Hartmann 1998). In the ADC method, the azeotropic solution and catalysts are employed to produce a high molecular weight PLA. The azeotropic solution helps to reduce the distillation pressure and enables the separation of the PLA from the solvent. In general, PC methods require a good control over the reaction for achieving a PLA with desired MW, and water, as a byproduct of the condensation, must be efficiently removed from the solution for achieving a high MW PLA (Drumright, Gruber, and Henton 2000).

In the lactide formation pathway or ring opening polymerization (ROP) (see Fig. 1, Pathway C), first LA is dimerized to lactide. Adding a proper catalyst at elevated temperatures under vacuum, the PLA is synthesized with relatively high MW. Reaction time, temperature, purity of lactide and type of the employed catalysts are of key parameters in ROP method (Xiao, Wang, et al. 2012). The ROP of LA is a complicated and expensive method for production of high MW PLA and condensation methods result in low MW PLA (Esmaeili and Javanshir 2013).

2.2.1. Synthesis of the PLA by chain extension

In direct polymerization DP (also called solution poly-condensation or melt poly-condensation), LA is condensate polymerized to yield a low MW brittle glassy polymer. Presence of water, the high viscosity of the polymer melt, the presence of impurities, low concentration of reactive groups and occurrence of the unwanted “back biting” reactions

which result in lactide formation are of reasons for achieving a low MW polymer (Ajioka et al. 1995, Hartmann 1998). Therefore, the resulted polymer is not suitable for any application without further utilization of the chain extenders which are employed to increase the MW of the polymer (Hartmann 1998). Azeotropic condensation-polymerization is also sensitive to the presence of impurities of the supplied LA. The impurities endcap the polymer and limit the chain growth and have a large effect on the MW of the final polymer. In addition, in azeotropic condensation-polymerization, various diacids, diols or hydroxyl acids interfere with polymerization step and affect the purity of the produced polymer. Residual catalysts in the products is another drawback of this method (Hartmann 1998).

From the other hand, the yield and efficiency of ROP method heavily depend on the type of the employed catalyst and the employed polymerization mechanism. Cationic (Kricheldorf and Dunsing 1986), anionic (Kurcok, Matuslonicz, and Jedlinski 1995) and coordination-insertion (Hartmann 1998) are the three mechanisms of catalytic reactions in the ROP, which are sensitive, complex and expensive (Ray and Bousmina 2005). Tin compound catalysts, e.g. tin (II) bis-2-ethylhexanoic acid ($C_{16}H_{30}O_4Sn$, referred to as tin octoate, stannous octoate, octoate or $Sn(Oct)_2$) are the most common catalysts used in the ROP method (Garlotta 2001b). It is shown that the rate of chain growth varies greatly, depending on the presence of lactide impurities and also by formation of crystalline phase during polymerization. It is believed that the presence of impurities does not significantly affect the rate of polymerization, but it dramatically reduces the final MW of the polymer. However, carboxylic impurities have an inhibitory effect on the rate of polymerization as well, which could be due to deactivation of the catalyst by forming a

complex. Substantial sensitivity of the ROP method to impurities, indicates that a rigorous purification of lactide is required beforehand in those processes which impose substantial costs to the process (Hartmann 1998, Gu et al. 2008).

Shortcomings of the DC methods and complexity of ROP, encouraged researchers to investigate on alternative methods for PLA synthesis. Utilization of chain extenders is an effective way to achieve high MW polymers. Generally, chain extenders are multifunctional low MW chemicals which are attached to the low MW oligomer and link it into a polymer with higher MW. The most common chain extenders for polyesters which contain –OH and –COOH groups include diisocycanates, diepoxides, bisoxazolines, dianhydrides and bisketeneacetals (Gu et al. 2008, Hartmann 1998).

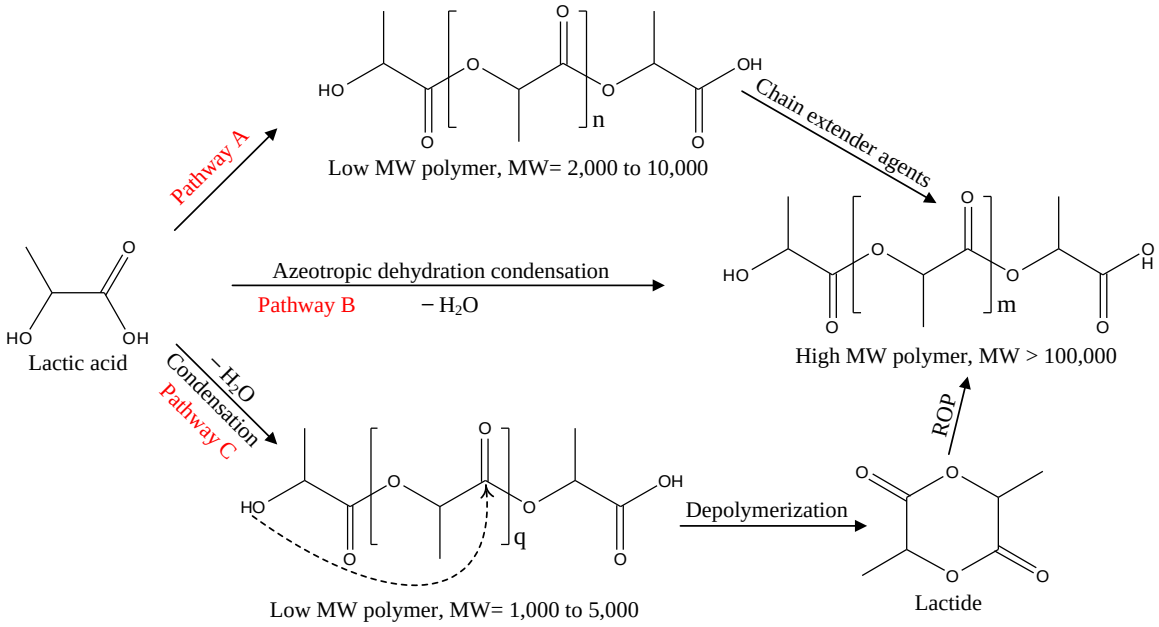

Figure 2. 1. Synthesis methods for high molecular weight PLA. Condensation/coupling (Pathway A), Azeotropic dehydration condensation (Pathway B) and Ring Opening Polymerization (ROP) of lactide (Pathway C) (Hartmann 1998).

2.2.2. Synthesis of star-shaped resins

Currently, polymers are designed for a certain application. In order to add especial physical properties, it is sometimes desirable to change the architecture of the polymer from linear to a star-shaped polymer (Finne and Albertsson 2002). Changing the architecture of a polymer to achieve a multiarm or hyperbranched one would change its morphological and physical-mechanical properties (Alward et al. 1986). Different methods for achieving star-shaped polymers have been introduced, including employ of multifunctional linking agents or multifunctional initiators (Kanaoka, Sawamoto, and Higashimura 1991, Finne and Albertsson 2002, Fukui, Sawamoto, and Higashimura 1994, Dong et al. 2001, Marsalko, Majoros, and Kennedy 1993, Lutz and Rempp 1988). However, a few studies have been devoted to syntheses of star-shaped polyesters. The early star-shaped polyesters have been synthesized by the reaction of multifunctional hydroxyl compounds and $Sn(Oct)_2$ using an ROP approach (Kim et al. 1993, Choi, Bae, and Kim 1998).

Currently, different polyol molecules with various hydroxyl groups have been employed as the core molecule in S-LA. In the next part of this review article, the recent methods for synthesis of different star-shaped resins using these polyols are explored. In addition, although the two-armed PLA systems, with 2 hydroxyl group compound chain extenders, doesn’t have a star shaped architecture and are linear, due to similarities between these systems and other S-LA systems in terms of synthesis, physiochemical properties, and applications, the two armed linear PLA systems are also discussed in the next part.

Two-arm linear LA based polymers: Modification of linear PLA is a technique often employed for controlling the degradation rate or increasing the flexibility of the polymers for biomedical application (Baiardo et al. 2003). PLEG often produced from poly ethylene glycol and poly lactic acid or lactide (Fig. 2.1) by direct conjugation method (Cheng et al. 2007) for modification of the PLA polymers. Poly lactic acid-ethylene glycol, PLEG, has also been synthesized from lactide and ethylene glycol using $Sn(Oct)_2$ as catalyst at 200 °C (Sawhney, Pathak, and Hubbell 1993, Tsuji et al. 2008). Biela et al. employed diethylene glycol and synthesized hydroxyl group terminated R-$(PLA\text{-}OH)_2$ according to the procedure explained by Arvanitoyannis et al. (Arvanitoyannis et al. 1995) employing $Sn(Oct)_2$ as co-initiator. Sealed glass ampules using a standard high vacuum technique were employed for polymerization at 120 °C (Biela et al. 2003) (Fig. 2.4). Tetra(ethylene glycol), TEG, has also been used as the chain extender and telechelic polylactides having two CH-OH end groups were obtained. The ratio of LA to TEG was set to 20:1 mole and dry chlorobenzene was added under an atmosphere of dry nitrogen. The reactants were heated to 120 °C and after 5 min, $Bi(OAc)_3$ was added – with a ratio of 0.02 mole to mole of TEG (Kricheldorf, Hachmann-Thiessen, and Schwarz 2004).

The two-armed lactic/glycolic acid polymers (PLGA) have been used to fabricate devices for drug delivery and tissue engineering applications for several decades (Makadia and Siegel 2011, Kumari, Yadav, and Yadav 2010) owing to their outstanding biocompatibility and nontoxic and absorbable degradation end-products (Wise 1995). Physical properties of PLGA are dependent on multiple factors, including the MW of the

polymer, the ratio of lactide to glycolide (or lactic to glycolic acid) in the structure, time of exposure to water and the surface shape (Houchin and Topp 2009).

Generally, PLGA copolymers are synthesized by ring-opening copolymerization of lactide and glycolide and common catalysts used include $Sn(Oct)_2$, tin(II) alkoxides, or aluminum isopropoxide (Jeong et al. 2000, Astete and Sabliov 2006). Wang et al. reported the synthesis and characterization of a series of PLGA with various molar ratios of lactic to glycolic acid with various molecular weights, using the ROP method (Fig. 2.2). The PLGA polymers were amorphous, glassy with a T_g, ranged from 21 °C to 52 °C, depending on the MW and the composition (Wang et al. 2000, Wu and Wang 2001).

Butanediol is also used as the chain extender in the synthesis of the S-LA (Fig. 2.3). The oligomers were polymerized via ROP method from lactide at 160 °C for 3 h. In the presence of 0.02 mole % $Sn(Oct)_2$ as an initiator, the appropriate amount of the extender to LA molecules were added in which the ratio of the LA monomer to butanediol was varied between 100:12.5 to 100:5 (Helminen, Korhonen, and Seppälä 2002). Wang et al. reported the synthesis and characterization of linear PLA polymers with two arms, using the 1,6-hexanediol and lactide through ROP method at 125 °C (Fig. 2.5). In the reported synthesis method, $Sn(Oct)_2$ was used as the catalyst (Wang and Dong 2006). The summary of the synthesis methods is presented in the table 1.

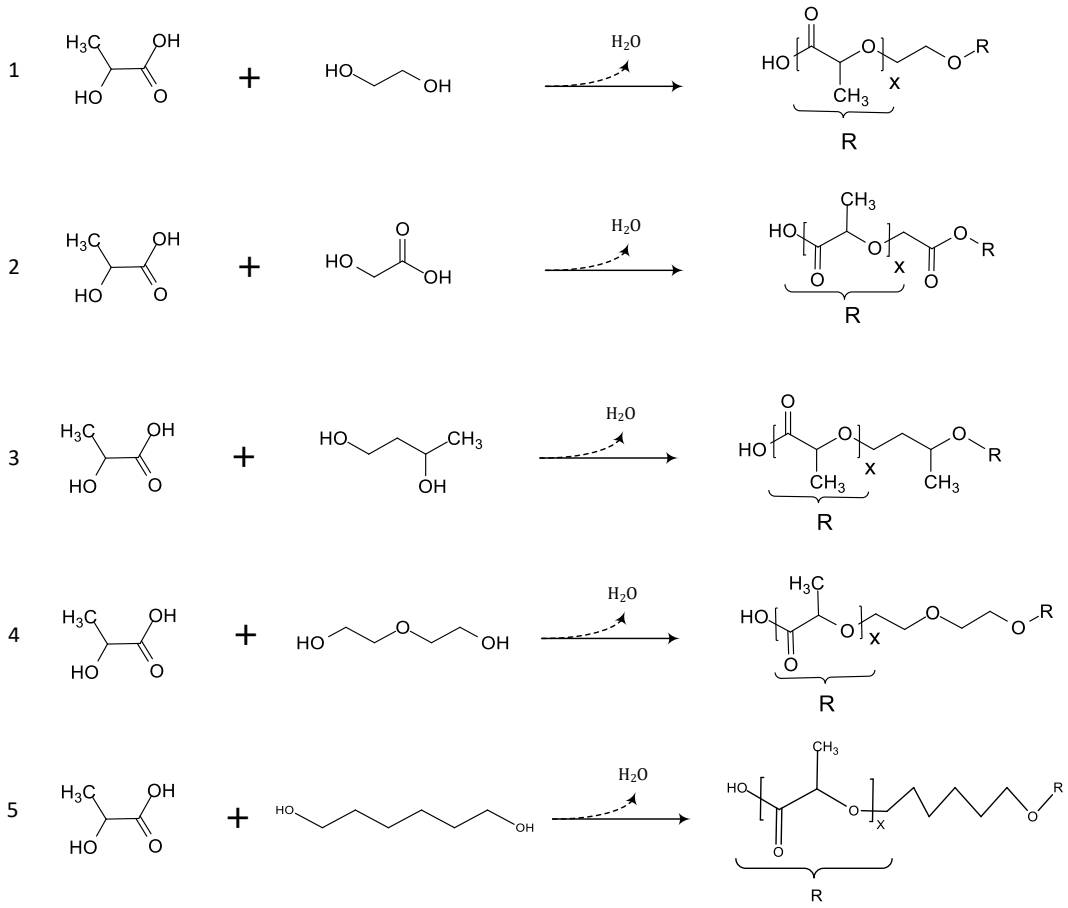

Figure 2. 2. Synthesis of PLLAs with different chain extenders with two hydroxyl groups. Chain extenders used: 1) ethylene glycol, 2) glycolic acid, 3) 1,4-butanediol, 4) diethylene glycol and 5) 1,6-hexanediol.

Core molecules with three hydroxyl groups: Early S-LA polymers with three hydroxyl groups' core molecules were synthesized by reaction of lactide and glycerol by Arvanitoyannis et al (see Fig 3.1). The star shaped polymers were synthesized through a ROP method using pressurized ampoules in presence of $Sn(Oct)_2$ or tetraphenyltin as catalysts at 130 °C in a duration of 4 days. Amorphous polymers obtained when the ratio of lactide to glycerol was below 20:1 (mol:mol) and semicrystalline thermoplast obtained

when this ratio is higher than 20:1. In addition, MW of the polymers decreased proportionally to the glycerol content in the polymer (Arvanitoyannis et al. 1995). Bakare et al. synthesized a thermoset S-LA with glycerol core molecules. The thermoset resins was synthesized in two stages: direct condensation reaction of LA with glycerol and EF of the oligomers with MAAH. Resins with different LA chain lengths of 3, 7 and 10 were synthesized. Condensation reactions performed in the presence of toluene reflux from an azeotropic distillation apparatus as an auxiliary solvent for water removal containing 0.1 *wt*% of the catalyst, methanesulfonic acid. The temperature was set to 145 °C for two hours, increased to 165 °C for another two hours and to 195 °C for one more hour.

For EF, in the presence of 0.1 *wt*% of hydroquinone as the stabilizer, 3.3 mole MAAH per mole of glycerol was added under a nitrogen atmosphere. The resin was purified from the remained water/toluene and the produced MAA by a rotary evaporator at 13 mbar at 60 °C for 2 hours (Bakare et al. 2014b). 1,1,1-tri(hydroxymethyl)propane (THMP) (see Fig 3.2) has also been used as the core molecule where a three-armed S-LA with three CH-OH end groups was formed. The ratio of lactide to THMP was 20:1 mole to mole and dry chlorobenzene was added under an atmosphere of dry nitrogen. The reactants were heated to 150 °C for homogenization before cooling to 120 °C and after 5 min, $Bi(OAc)_3$ was added with a ratio of 0.02 mole to mole of THMP (Biela et al. 2003, Kricheldorf, Hachmann-Thiessen, and Schwarz 2004). In another similar study, the same core molecule, THMP, was used with $Sn(Oct)_2$ as initiator in which lactide was polymerized with the polyol, at 120 °C (Biela et al. 2005).

In a more recent study, tri(hydroxymethyl)benzene (see Fig 3.3), used as the core molecule using a $Sn(Oct)_2$ catalyst, for producing S-LA oligomers with 10 lactide

monomer units arms. Polymerization reaction was performed at 125 °C for 8 h under nitrogen atmosphere. The precipitation in cold methanol was employed for separation of the polymers from the reactants (Perry and Shaver 2011). The summary of the synthesis methods is presented in the table 1.

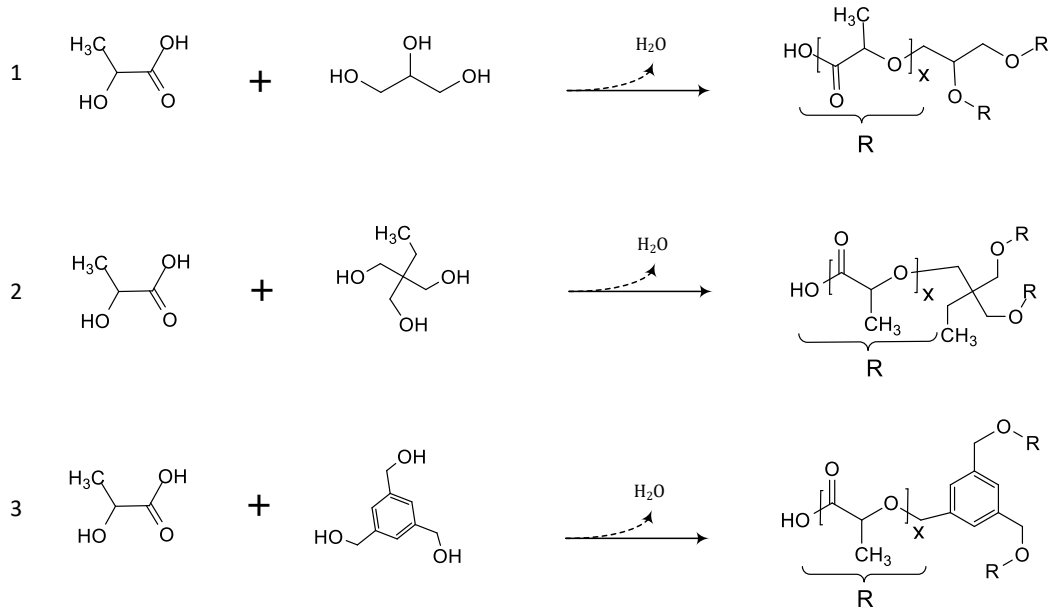

Figure 2. 3. Synthesis of S-LA with different core molecules with three hydroxyl groups. Core molecules used: 1) glycerol, 2) 1,1,1-tri(hydroxymethyl)propane, 3) 1,3,5-benzenetrimethanol.

Core molecules with four hydroxyl groups: Kim et al. showed the possibility of the preparation of higher MW S-LA with pentaerythritol (PENTA) (see Fig 4.1) as the core molecule. The used catalyst was $Sn(Oct)_2$ and the resulted resin showed a lower intrinsic viscosity compared to those of the linear ones, which confirms the lower viscosity of the star-shaped architecture (Kim et al. 1993, Kim et al. 1992). Åkesson et al. synthesized a crosslinkable thermoset resin from LA and PENTA core molecules. The

resin was synthesized via direct condensation reaction of LA with PENTA and itaconic acid (IT) followed by EF of the oligomers with MAAH. At 120 °C, the catalyst, 0.05 *wt*% of $Sn(Oct)_2$, was added, and the reaction temperature was set to 180 °C. The total polymerization time was 15 h and the resulted product was a yellowish, transparent, rigid, brittle resin. It is assumed that IT was only reacted with one branch of PENTA. For EF at 100-110 °C, first, 0.1 *wt*% of hydroquinone was added as the stabilizer and then, 15 *wt*% of MAAH was added dropwise.

The reaction continued at 120 °C for 3 h under nitrogen purge (Åkesson, Skrifvars, et al. 2010b). In another study, Biela et al. synthesized four hydroxyl groups terminated R-$(PLA\text{-}OH)_4$ employing di(trimethylolpropane) (see Fig 4.2) as the core molecule according to the procedure explained by Arvanitoyannis et al. (Arvanitoyannis et al. 1995) employing $Sn(Oct)_2$ as catalyst in which sealed glass ampules used for ROP polymerization at 120 °C (Biela et al. 2003). The summary of the synthesis methods is presented in the table 1.

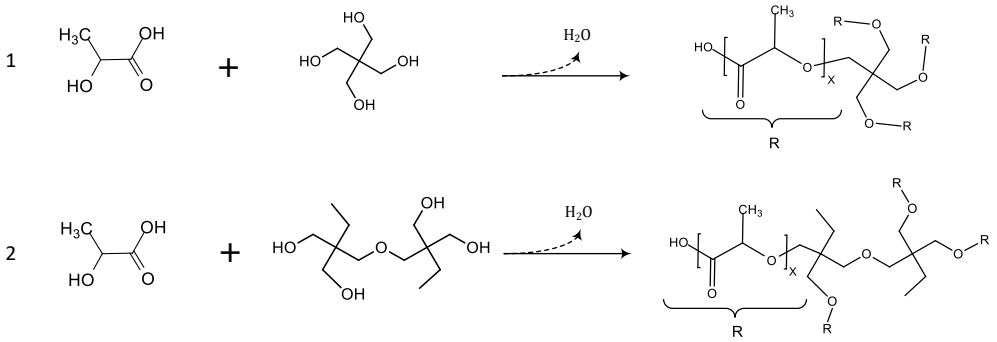

Figure 2. 4. Synthesis of S-LA with different core molecules with three hydroxyl groups. Core molecules used: 1) pentaerythritol (PENTA) and 2) di(trimethylolpropane).

Core molecules with five hydroxyl groups: In a recent study, the utilization of xylitol (see Fig 5.1) molecule was examined and evaluated as the core molecule in a thermoset S-LA resin. The resin was synthesized via direct condensation reaction of LA with xylitol, in the presence of toluene reflux from an azeotropic distillation apparatus. 50 g toluene per mole of LA was initially added as an auxiliary solvent for water removal containing 0.1 *wt*% of the catalyst, methanesulfonic acid. The reaction temperature was set to 145 °C for two hours and then increased to 165 °C for 7 hours. The branches were then end-functionalized at 90 °C with methacrylic anhydride (5.5 mole MA per mole of LA) in the presence of 1 *wt*% hydroquinone. Finally, under partial vacuum, the residual toluene and the released methacrylic acid were removed - ~10 mbar, 1 h at 60 °C and two hours at 90 °C (Jahandideh and Muthukumarappan 2016a).

S-LA thermoplasts have also been synthesized from lactide and xylitol core molecules. Teng et at. reported synthesizing of S-LA polymers with xylitol core molecules by ROP of lactide in glass ampoules (see Fig 5.2). In this method, lactide and xylitol were first transferred in 10 mL ampoules and deoxygenated frozen ampoules were then filled with argon, thawed and immersed in a 130 °C oil bath. After 24 hours of

polymerization, the products were dissolved in dichloromethane and isolated by vacuum filtration resulting in a white solid powder (Teng et al. 2015). The summary of the synthesis methods is presented in the table 1.

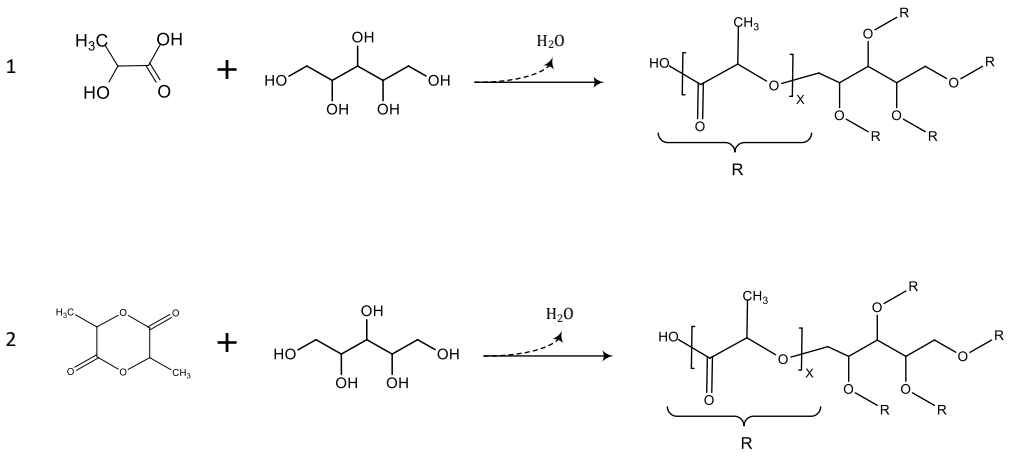

Figure 2. 5. Synthesis of S-LA with xylitol core molecules with five hydroxyl groups. Using 1) LA and 2) lactide.

Core molecules with more hydroxyl groups: Biela et al. reported the synthesis of S-LA with six hydroxyl groups. The dipentaerythritol (DPE) (see Fig 6.1) core molecules were used to produce 6 arms S-LA with $Sn(Oct)_2$ coinitiator with ROP in glass ampoules at 120 °C. Perry and Shaver also synthesized and characterized a S-LA, using cyclic hexa(hydroxymethyl)benzene core molecule (see Fig 6.2) and a $Sn(Oct)_2$ catalyst with 10 lactide monomer units in arms. Polymerization reaction was performed at 125 °C for 8 h under nitrogen atmosphere (Perry and Shaver 2011). The ROP method with glass ampoules was also employed for synthesizing a 13 arms S-LA polymer with poly(3-ethyl-3-hydroxymethyloxetane) (see Fig 6.3) core molecule (Biela et al. 2002). In this method, $Sn(Oct)_2$ catalyst was used and polymerization was occurred at 120 °C. The summary of the synthesis methods is presented in the table 1.

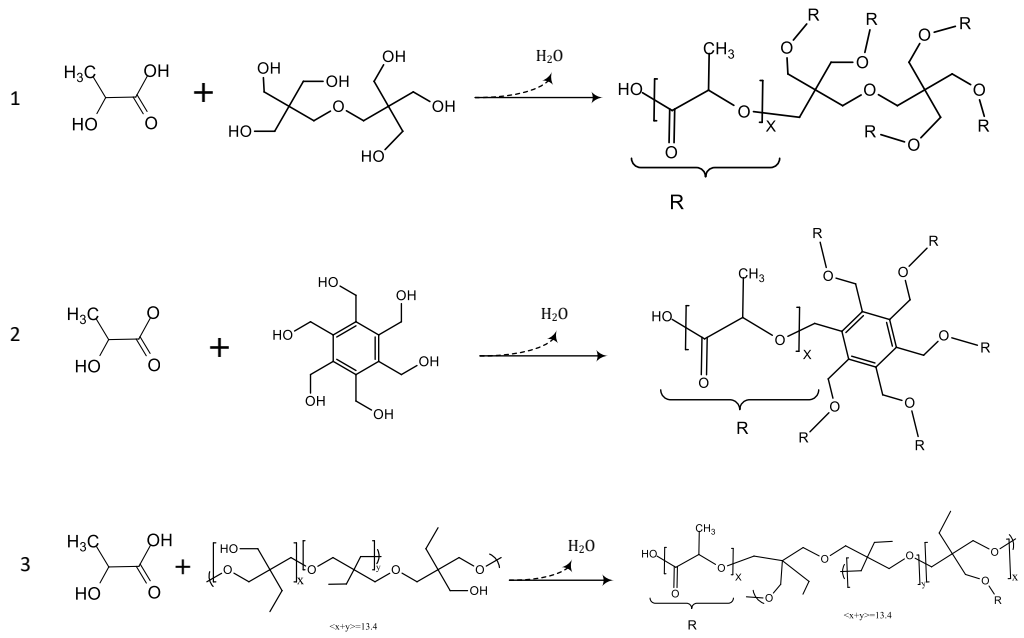

Figure 2. 6. Synthesis of S-LA with different core molecules with hydroxyl groups >3. Core molecules used: 1) dipentaerythritol, 2) hexa(hydroxymethyl)benzene and 3) poly(3-ethyl-3-hydroxymethyloxetane).

Table 1. 1. Synthesis of multiarm PLA systems

Chain monomer	Arms	Chain extender/ core molecule	Synthesis method	Catalyst	Reaction Temperature	Ref
Lactic	2	Glycolic acid	ROP	Stannous 2-ethyl-hexanoate	150	(Wang et al. 2000)
Lactic	2	Glycolic acid	DMC	Tin chloride dehydrate /p-toluenesulfonic acid	180	(Lan and Jia 2006)
Lactide	2	Glycolide	ROP-A	$Fe(acac)_3$ – $Fe(OEt)_3$	100-150	(Dobrzynski et al. 2002)
Lactide	2	Ethylene glycol	ROP	$Sn(Oct)_2$	200	(Sawhney, Pathak, and Hubbell 1993)
Lactide	2	Tetra ethylene glycol	ROP-A	$Bi(OAc)_3$	120	(Kricheldorf, Hachmann-Thiessen, and Schwarz 2004)
Lactide	2	Diethylene glycol	ROP-A	$Sn(Oct)_2$	120	(Biela et al. 2003)
Lactide	2	Butanediol	ROP	$Sn(Oct)_2$	160	(Helminen, Korhonen, and Seppälä 2002)
Lactide	2	1,6-hexanediol	ROP	$Sn(Oct)_2$	125	(Wang and Dong 2006)
LA	3	glycerol	PCP	Methanesulfonic acid	145-190	(Bakare et al. 2014b)
Lactide	3	glycerol	ROP-A	$Sn(Oct)_2$-tetraphenyltin	130	(Arvanitoyannis et al. 1995)
Lactide	3	tri(hydroxymethyl)benzene	ROP	$Sn(Oct)_2$	125	(Perry and Shaver 2011)
Lactide	3	THMP	ROP	$Bi(OAc)_3$	150	(Kricheldorf, Hachmann-Thiessen, and Schwarz 2004)
Lactide	3	THMP	ROP-A	$Sn(Oct)_2$	120	(Biela et al. 2005)
Lactide	4	PENTA	ROP-A	$Sn(Oct)_2$	130	(Kim et al. 1992)
LA	4	PENTA	DCP	$Sn(Oct)_2$	180	(Åkesson, Skrifvars, et al. 2010b)
Lactide	4	di(trimethylol propane)	ROP-A	$Sn(Oct)_2$	120	(Biela et al. 2003)
LA	5	xylitol	PCP	Methanesulfonic acid	165	(Jahandideh and Muthukumarappan 2016a)
Lactide	5	xylitol	ROP-A	$Sn(Oct)_2$	130	(Teng et al. 2015)
Lactide	6	dipentaerythritol (DPE)	ROP-A	$Sn(Oct)_2$	120	(Biela et al. 2003)
Lactide	6	hexa(hydroxymethyl)benzene	ROP	$Sn(Oct)_2$	125	(Perry and Shaver 2011)
Lactide	13	poly(3-ethyl-3-hydroxymethyloxetane)	ROP-A	$Sn(Oct)_2$	120	(Biela et al. 2003)

2.2.3. End functionalization of oligomers

The star-shaped oligomers, resulted from the condensation reaction of LA with a multifunctional hydroxyl core molecule, have reactive groups (either the terminal LA's hydroxyl

groups or the core molecules' unreacted hydroxyls) but yet, the groups are not reactive enough for a satisfactory cross-linking or further esterification (Jahandideh and Muthukumarappan 2016a, Åkesson, Skrifvars, et al. 2010b). Esterification of lactic acid oligomers can be promoted by post reaction with brassylic acid, fumaric acid, and acid anhydrides such as maleic and succinic (components with two carboxylic end groups). This modification, results in conversion of the hydroxyl end-groups to carboxyl ones (Hartmann 1998, Ibay and Tenney 1993). The option of free radical crosslinking can also be added to the oligomers, using unsaturated compounds for the end-functionalization (Ibay and Tenney 1993).

In order to produce a thermoset, capable of efficient crosslinking, branches must be further functionalized- or end capped- with an EF agent. The role of EF is to improve the reactivity of branches, generally by adding carbon-carbon double bonds. The stoichiometric amount of the EF agent is calculated from the theoretical molecular weight of the synthesized oligomer and the functionality of the co-initiator (Helminen, Korhonen, and Seppälä 2002). Common EF agents, used in the S-LA thermoset systems presented in the literature are MAAH (Jahandideh and Muthukumarappan 2016a, Bakare et al. 2014b, Bakare, Ramamoorthy, et al. 2015, Liu, Madbouly, and Kessler 2015, Chang et al. 2012b) (see Fig. 7.A.1), MAA (Åkesson et al. 2011b) (see Fig. 7.A.2), IT (Åkesson et al. 2011b) (see Fig. 7.A.3) and 2-Butene-1,4-diol (Wang et al. 2008) (see Fig. 7.A. 4). The content and the reactivity of the olefinic bonds of the EF molecule are two essential factors in the final crosslinking density. Therefore, the two olefinic bonds of the MAAH, bestow a higher reactivity to the molecule and make it more desired for EF purpose, compared to other EF agents. The schematic of different end-functionalization reactions are presented in the Fig. 7.B. Usually, a stabilizer agent, e.g. hydroquinone, is used to protect the olefinic carbon-bonds during the EF reactions and avoid subsequent cross-linking reactions and gelation. Generally, EF reactions are sensitive to high temperatures, which induce gelation inside the reactor; therefor, a good control over the temperature is required.

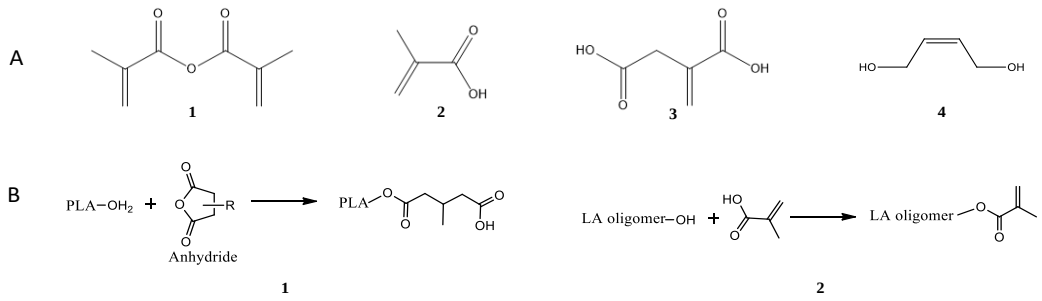

Figure 2. 7. A. End functionalization agents: A.1.: methacrylic anhydride (MAAH), A.2: methacrylic acid (MAA), A.3: itaconic acid (IT) and A.4: 2-Butene-1,4-diol. B: End functionalizing reactions. B.1.: PLA esterification promotion functionalization, B.2.: End functionalized LA oligomers capable of free radical crosslinking.

2.2.4. Thermal curing of the resins

Curing involves the irreversible transformation of low molecular weight oligomers of a resin into a solid network (Vergnaud and Bouzon 2012). The liquid resin is usually composed of several ingredients (e.g. fillers, blowing agents, coupling agents, surfactants, colorants, etc. (Ratna 2009)) with three or more reactive groups per molecule that can react by an external action, such as heating or UV irradiation which results in a tridimensional cross-linked structure (Auvergne et al. 2013). Generally, thermal curing of resins consists of two different stages: the heating period and the curing reaction phase. During the heating phase, the heat is transferred by conduction through the resin which is heated up to a temperature at which the cure reactions start. In the curing reaction phase, the heat *evolved* from the overall cure reaction zone at a constant temperature which can be described by an Arrhenius equation (Vergnaud and Bouzon 2012).

Often, in the S-LAs, a free-radical polymerization method is employed for curing in which the reaction starts by the assistance of a radical initiator. Common studied initiators for free radical polymerization include benzoyl peroxide (Jamshidian et al.

2010, Esmaeili et al. 2015, Bakare et al. 2014b), 2,5-bis(tert-butylperoxy)-2,5-dimethylhexane (Sakai et al. 2013), 2-butanone peroxide (Helminen, Korhonen, and Seppälä 2002), cobalt naphthenate (Finne and Albertsson 2002), *tert*-butyl peroxybenzoate (Åkesson, Skrifvars, et al. 2010b), N,N-dimethylaniline (Bakare, Åkesson, et al. 2015) and *tert*-butyl peroxybenzoate (Chang et al. 2012b, Åkesson et al. 2011b). Different factors are involved in free radical curing reactions, including the nature of the initiator, initiator-to-resin ratio, applied heat regimes, retention times and cooling strategies. Often, 1-2 *wt*% of the initiator is utilized for the thermal curing. Using excess amount of the curing agent or applying high temperatures for curing may result in higher exotherms, faster gelation and more shrinkage due to excessive thermal zoning (Jahandideh and Muthukumarappan 2016a, Pereira and d'Almeida 2016). Fig. 8 presents the reaction Scheme for the synthesis steps and the curing reaction.

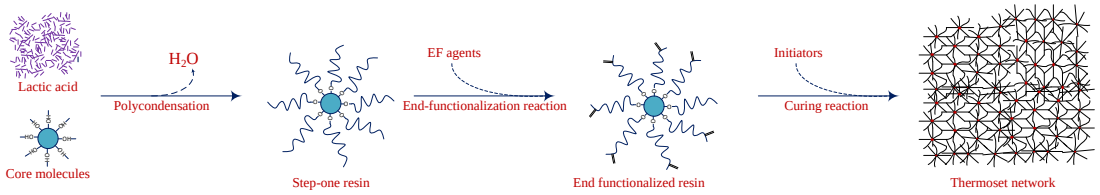

Figure 2. 8. Reaction Scheme for the two-step synthesis of the S-LA and the thermosetting network

Differential scanning calorimetry (DSC), Raman spectroscopy, and dielectric analysis (DEA) are of common techniques used for analyzing the curing behavior of the unsaturated polyesters and thermosets (Zhao et al. 2002, Hardis et al. 2013, Martín, Cadenato, and Salla 1997, Xu, Shi, and Shen 2004). The analytical models of cure kinetics have wide applications in numerical simulations of composite manufacturing processes (Du et al. 2004, Kamal and Sourour 1973, Kamal 1974, Liang and

Chandrashekhara 2006, Cole 1991). Phenomenological –also called empirical- modeling approach is commonly employed for the analytical expression of the cure kinetics based on an Arrhenius type equation in which the approximated relationship of the curing parameters of the mathematical model are compared with the experimental data (Liang and Chandrashekhara 2006).

Several phenomenological models are presented in the literature for modeling the curing kinetics of the thermosetting resins (Du et al. 2004, Kamal and Sourour 1973, Kamal 1974, Liang and Chandrashekhara 2006, Cole 1991); however, a few studies performed for the modeling of the curing kinetics of the S-LAs (Liang and Chandrashekhara 2006, Chang et al. 2012b). Chang et al. studied the curing kinetics of a set of methacrylated four-armed S-LA systems with PENTA core molecule. The effect of architecture and the LA chain length (with 5 to 15 LA units) on the curing behavior were investigated using DSC analysing for non-isothermal and isothermal curing. Chang et al. successfully applied an *autocatalytic* phenomenological model (presented in the equation 1) for the modeling and the parameters of the model were obtained.

$$\frac{d\alpha}{dt} = K\alpha^m(1-\alpha)^n \qquad \text{Equation 1}$$

where α is the degree of cure and presents the extent of the curing reaction, K is the reaction rate constant which is presented based on an Arrhenius equation, and m and n are the reaction orders obtained from the experimental data (Chang et al. 2012b). The autocatalytic model represents the autocatalytic effect of the curing reactions. This model considers a single rate constant for the reaction and the maximum reaction rate is supposed to take place in the intermediate conversion stage. Their experimental results have shown that the curing time is dependent to the thermal initiation condition and can

vary from several minutes to more than an hour. The authors have also reported that changing the LA arm length of the S-LA (with 4 arms) affects the curing process and results in different curing parameters, reaction orders and evolutions of activation energy (Chang et al. 2012b).

2.3. Characterization of the S-LA systems

2.3.1. Chemical characterization

Titration: The condensation retention time is a crucial factor in poly-condensation reactions. From one hand, insufficient retention time in the reactor results in unreacted reactants and from the other hand, excessive reaction times result in promoting transesterification reactions, which gradually degrades the structure of the oligomers (Jahandideh and Muthukumarappan 2016a). The progress of the condensation reaction can be evaluated by determination of the *Total Acid Number* (TAN) for residual acidic constituents (carboxyl groups) during the poly-condensation step. According to the ASTM D974-12, the TAN is defined as the quantity of KOH (in mg), required for the titration of 1 g of the sample which is dissolved in a specified solvent system (Knothe 2006). The samples are diluted in predefined solvent systems, capable of dissolving the S-LA, and then, titrated with a base in the presence of an indicator, e.g. phenolphthalein 1% (Murillo, Vallejo, and López 2011).

The currently used solvent systems for the TAN determination are 1:1 v/v xylene/isopropyl alcohol solutions (Jahandideh and Muthukumarappan 2016a, Bakare et al. 2014b, Murillo, Vallejo, and López 2011), acetone (Shao and Agblevor 2015) and a mixture of toluene and isopropyl alcohol (based on the ASTM D664 and D974-12). The ratio of the *reacted* to *initial* available carboxylic groups, indicates the degree of

completion of the condensation reaction (Knothe 2006). The titration data for S-LA systems is very rare in the literature. Moreover, the reported conversion rates of the polycondensation reactions for different S-LA systems cannot be directly compared. In other words, the conversion rates of S-LA systems depends on several factors, including the type and the load of the used catalysts, the employed solvents, reaction temperatures and other factors. Bakare et al. showed that the condensation reaction of lactic acid oligomers and the glycerol core molecules almost starts immediately at 160 °C with methanesulfonic acid as the catalyst (Bakare et al. 2014b); however, using the same polymerization method, the same reaction temperature and the same solvents, Jahandideh et al. reported that reaction of xylitol core molecules with LA oligomers delayed for 100 min.

In addition, 95% of conversion achieved after 360 min for glycerol, while 94% of conversion for xylitol S-LA systems achieved after 720 min. using the same polymerization method, the differences between the conversion rates can be attributed to the differences between the number of hydroxyl groups in the glycerol and xylitol core molecules. Therefore, increasing in the number of the hydroxyl groups of the core molecule in the S-LA architecture results in lower conversion rates, during the polycondensation phase (Bakare et al. 2014b, Jahandideh and Muthukumarappan 2016a).

NMR: The Nuclear magnetic resonance (NMR) is a technique frequently used for identifying the chemical structure of the synthesized resins as well as LA chain length in the branches. The ^{13}C NMR data for different S-LA is presented in the literature (Jahandideh and Muthukumarappan 2016a, Bakare et al. 2014b, Åkesson, Skrifvars, et al. 2010b, Park et al. 2003, Lin and Zhang 2010, Choi, Bae, and Kim 1998, Helminen,

Korhonen, and Seppälä 2002, Murillo, Vallejo, and López 2011, Xiong et al. 2014, Abiko, Yano, and Iguchi 2012). Of particular interest is the carbonyl region (160-180 ppm) (Jahandideh and Muthukumarappan 2016a, Bakare, Åkesson, et al. 2015). For neat S-LA, different types of carbonyl bonds are expected, including a) main-chain carbonyls, b) LA carbonyl groups adjacent to the (–O-CH_2) branches of the core molecule, and c) carbonyls of the LA end-group for unreacted LA. For the end-functionalized resins, signals in the carbonyl area would be broad, because signals for carbonyls of LA next to the core molecule (or next to the end-capping agent) differ from that of LA in chains. In addition, the end-group agent may add other carbonyl bands. The other class of chemical shifts used for characterization, belongs to a carbon atom adjacent to an oxygen atom which is revealed in the range of 60–75 ppm (Xiao, Mai, et al. 2012).

These CH groups could be a) in the structure of the core molecule, b) next to the reacted LA carbonyl groups and an oxygen atom, or c) adjacent to the hydroxyl end-group. The other expected groups are methyl groups. The LA methyl groups are detected in the 16–22 ppm range (Jahandideh and Muthukumarappan 2016a). Hydroxyl functionalized end-group of methyl groups are present in the S-LA, but not present in the EF resins. The probable CH_3 groups of the end-capped agent in the resin structure and the olefinic carbon sites of the end-groups are other characteristic signals of the EF resins. Moreover, the NMR technique can also be used for measuring the chain length of the branches (Bakare, Åkesson, et al. 2015), the percentage of the LA in forms of reacted with the core molecule as well as the percentage of the LA reacted into free oligomers (Jahandideh and Muthukumarappan 2016a, Bakare et al. 2014b).

FT-IR: The FT-IR analysis of the S-LA is often performed for verifying the structure of polycondensation resins, the end functionalized resins and also the cured samples. Infrared spectroscopy data of the S-LAs' functional groups is presented in the literature (Bakare et al. 2014b, Bakare, Åkesson, et al. 2015, Xiong et al. 2014, Nouri, Dubois, and Lafleur 2015b, Cui et al. 2003, Lin, Zhang, and Wang 2012, Chang et al. 2012b, Xiao, Mai, et al. 2012, Åkesson, Skrifvars, et al. 2010b, Hisham et al. 2011) and summarized in the Table 2. Different groups might appear in the IR spectra of the S-LA, end functionalized resins and the cured samples. Generally (─OH) Stretch spectra is just present in polycondensation resins as hydroxyl groups will react with an EF agent during the end-capping reactions. The spectra for (─CH─ stretch and bend), (─C=O carbonyl stretch) and (─C─O─C─ Stretch), generally presented in both neat and crosslinkable S-LA systems. The spectra for (─C=C─ stretch) and (=CH_2 bending) are just expected in EF resins in which carbon-carbon double bonds are present.

Table 1. 2. Infrared spectroscopy data of the S-LAs' functional groups.

Assignment	Peak position, cm^{-1}
─OH Stretch (free)	3380 (Cui et al. 2003), 3428 (Bakare, Åkesson, et al. 2015), 3491 (Xiong et al. 2014), 3500 (Bakare et al. 2014b, Bakare, Åkesson, et al. 2015), 3506 (Lin, Zhang, and Wang 2012), 3508 (Chang et al. 2012b), 3520 (Nouri, Dubois, and Lafleur 2015b, Cui et al. 2003)
─CH─ stretch	2870 (Lin, Zhang, and Wang 2012), 2879 (Nouri, Dubois, and Lafleur 2015b), 2900 (Bakare et al. 2014b), 2994- 2943 (Xiong et al. 2014), 2947 (Lin, Zhang, and Wang 2012), 2990 (Xiao, Mai, et al. 2012)
─CH─ bend	1382-1454 (Xiong et al. 2014), 2947 (Lin, Zhang, and Wang 2012)
─C=O carbonyl stretch	1705 (Cui et al. 2003), 1722 (MAAH) (Chang et al. 2012b), 1734 (Lin, Zhang, and Wang 2012), 1749 (Chang et al. 2012b), 1755 (Xiong et al. 2014), 1757 (Bakare, Åkesson, et al. 2015), 1758–1763 (Nouri, Dubois, and Lafleur 2015b), 1759 (Bakare, Åkesson, et al. 2015)
─C=C─ stretch	1635 (Bakare et al. 2014b), 1638 (Chang et al. 2012b), 1640 (Åkesson, Skrifvars, et al. 2010b, Bakare et al. 2014b, Bakare, Åkesson, et al. 2015)

$=CH_2$ bending	815 (Hisham et al. 2011), 816 (Bakare et al. 2014b, Bakare, Åkesson, et al. 2015, Chang et al. 2012b, Hisham et al. 2011)
$-CH_3$	1453, 2999 (Lin, Zhang, and Wang 2012)
–C=O bend	757 (Nouri, Dubois, and Lafleur 2015b)
–C–O–C– Stretch	1095–1130 (Nouri, Dubois, and Lafleur 2015b), 1170 (Lin, Zhang, and Wang 2012), 1271-1188-1093 (Xiong et al. 2014)
–CH ring of lactide	932–934 (Nouri, Dubois, and Lafleur 2015b)

2.3.2. Thermomechanical properties

The thermomechanical tests currently employed in characterizing thermomechanical properties of the S-LA and their thermosets include DMA tests, tension tests, bending or flexural tests and impact tests. The type of the employed testing methods on the specimen depends on the service expected for the produced thermoset. The more testing applied on a specimen, the more information acquired for the intended S-LA. It is believed that the mechanical properties of S-LA is very dependent on the molecular weight and the structure of the network. Generally, employ of a star branching point in the S-LA systems, results in lower melting temperatures (T_m), lower glass transition temperatures (T_g) and lower crystallization temperatures (T_c) for polycondensation resins compared to linear PLA (Kim, Kim, and Kim 2004).

However, analyzing a series of S-LA systems with flexible polyols (PENTA and dipPENTA) and rigid polyols (tri(hydroxymethyl) benzene and hexa(hydroxymethyl)benzene) as core molecules, Perry and Shaver concluded that the length of LA chain primarily determines the physical properties, including glass, melt, crystallization, and decomposition temperatures (Perry and Shaver 2011, Zhao et al. 2002). The lower T_c indicates that the staring points make the material harder to

crystallize, while lower T_m indicates that it makes stacking of the polymers more difficult (Corneillie and Smet 2015, Choi, Bae, and Kim 1998). Abiko et al. reported that changing the terminal groups of S-LA systems from hydroxyl to carboxyl groups slightly affects the thermal properties, while it greatly increases the solubility and degradability of these S-LA polymers (Abiko, Yano, and Iguchi 2012).

Presence of cracks in the casted resins is a common problem in determining the mechanical properties of the casted S-LA thermosets (Jahandideh and Muthukumarappan 2016a). Therefore, it is very hard to determine the mechanical properties such as flexural and tensile properties of neat casted resins. However, the viscoelastic properties of the neat S-LA thermosets have been reported in the literature. The viscoelastic properties of crosslinked S-LA can be acquired with dynamic mechanical analysis. In DMA, a sinusoidal stress is applied to the specimen and the resulting displacement (strain) is measured. Properties such as storage modulus, loss of modulus, lag phase and T_g are measured with this technique (Menard 2008). The storage modulus, which measures the stored energy, represents the elastic characteristic of a polymer.

The storage modulus G' is related to the molecular packing density in the glassy state (Vergnaud and Bouzon 2012, Chang et al. 2012b) and higher G' means the better mechanical properties. Jahandideh et al. reported that applying a stepwise curing method for curing of the methacrylated S-LA with xylitol core molecules results in higher G' compared to continues heating curing method or immediate heating method. Stage curing of crosslinkable S-LA allows gradual solidification and more relaxed state with less built in stresses and result in lower G' (Jahandideh and Muthukumarappan 2016a, Vergnaud and Bouzon 2012). The G' is decreasing upon elevated temperatures when the polymer

chain is in the rubbery plateau region (Bakare, Ramamoorthy, et al. 2015) due to the free movements of the polymer chains.

The same trend was reported for curable S-LA resins with different core molecules including glycerol (major changes between ~45 °C to 80 °C), PENTA (major changes between 65 °C to 105 °C) and xylitol (major changes between 48 °C to 83 °C). The loss modulus, G", measures the energy dissipated as the heat and represents the viscous part. Generally, smaller G" suggests better mechanical properties and the strong tendency for reversibility in the samples (Bakare, Ramamoorthy, et al. 2015) and in the reported crosslinked S-LA thermosets, a rather small and broad loss modulus curve can be seen (Jahandideh and Muthukumarappan 2016a). At the glass transition temperature, T_g, the G' decreases dramatically while G" reaches its maximum. The T_g value of polymers and thermoset systems can be reported based on DSC analysis, loss modulus analysis or peak of tan δ. In order to compare the T_g of different systems, it is inevitable to use the same technique.

The T_g of the crosslinked S-LA systems, often presented based on the peak of tan δ in DMA curves. The peak of tan δ for the linear PLA is reported as ~50 °C (Oksman, Skrifvars, and Selin 2003); however, rather higher T_g values are reported for S-LA thermoset systems. The T_g values reported for crosslinked S-LA systems with glycerol core molecule (LA chain length of 5), PENTA core molecule (LA chain length of 4) and xylitol core molecule (LA chain length of 3) were reported as 83 °C, 97°C and 98 °C, respectively (Bakare et al. 2014b, Jahandideh and Muthukumarappan 2016a, Åkesson, Skrifvars, et al. 2010b). The T_g of the crosslinked S-LA systems is a function of chain length and the number of arms in the cured S-LA. A direct comparison between these

reported systems is not valid, as both the chain length and number of arms differ between these systems; however, all the reported T_g values for the crosslinked S-LA are higher than the T_g of the thermoplast PLA. In addition, even higher T_g values, and consequently better mechanical properties are expected if the reinforcement fibers applied to the crosslinkable S-LA (Adekunle, Åkesson, and Skrifvars 2010, Bakare, Ramamoorthy, et al. 2015).

Helminen et al. reported that the crosslinking density of methacrylated S-LA thermosets is increasing with an increase in the number of arms of the core molecule (butanediol, PENTA and polyglycerine used as the core molecules with 2, 3 and 4 arms, respectively) and also, the compressive yield strength will built up (Helminen, Korhonen, and Seppälä 2002). The same trend was also confirmed for methacrylated S-LA systems with glycerol and xylitol core molecules with 3 and 5 arms, respectively (Jahandideh and Muthukumarappan 2016a, Bakare et al. 2014b). Jahandideh et al. have shown that in S-LA thermosets with xylitol core molecule, different factors affect the final distribution and propagation of cracks, including the mix ratio of the curing agent to S-LA resin, severity of the mixing, applied mixing method and the mixing temperature. They have shown that cracks can occur, propagate and terminate due to the presence of bubbles in the casted product; however, the crack's problem fully resolved by changing the mixing method, applying partial vacuum and implementing a stage curing technique for the xylitol S-LA system (Jahandideh and Muthukumarappan 2016a).

The flexural modulus and strength of S-LA with xylitol core molecule with different LA chain lengths of 3, 5 and 7 have also been reported by Jahandideh et al. The authors reported higher flexural strengths for S-LA casted samples with longer LA length

chains. However, Chang et al. have reported inferior mechanical properties for S-LA with PENTA core molecule with higher LA chain lengths (Chang et al. 2012b). The DMA results also provides evidences showing that in S-LA with xylitol core molecule, the short LA chain of three imposes steric hindrance which finally reduced the flexural properties. By increasing the chain length, this hindrance is decreased and flexural properties improved. However, the trend showed that when the chain length is long enough and doesn't impose the steric hindrance, the length of the arms adversely affect the mechanical properties. The same trend was also reported for the tensile strength and the maximum elongation (Jahandideh and Muthukumarappan 2016a).

It is believed that the tensile properties of the star-shaped structure are different with linear oligomers. The strength can be lower for networks with flexible extension units, or higher for structures with rigid staring points. It is reported that S-LA systems with high crosslinking density demonstrate similar mechanical properties to those of other biodegradable composites; however, longer LA chains will decrease tensile properties (Helminen, Korhonen, and Seppälä 2002). Helminen et al. reported lower tensile strength for butanediol-LA systems (despite higher crosslinking density), which was ascribed to the flexible butanediol units used in the linear oligomers (Helminen, Korhonen, and Seppälä 2002). However, it is believed that the tensile strength is a function of crosslinking density and generally, a higher crosslinking density results in higher tensile strength (Storey et al. 1993). In summary, star branching point in the S-LA systems results in lower T_m, lower T_g and lower T_c compared to linear PLA, while the length of the LA chain in S-LA systems primarily determines the glass, melt, crystallization, and decomposition temperatures. In S-LA thermoset systems, the

crosslinking density of methacrylated S-LA thermosets is increasing with an increase in the number of arms of the core molecule and by increasing the arm length, the flexural and tensile modulus are decreased; thus longer chains reduce the crosslinking density and result in inferior mechanical properties.

Water absorption: The water absorption rates of polymers and composites are of interest, especially when the material is supposed to exposure to relatively humid conditions. The moisture content affects polymers' properties such as electrical insulation resistance, dielectric losses, mechanical strength, appearance, and dimensions. It is believed that the diffusion of water into polymer matrix is dependent to several factors, including a) the square root of immersion time, b) the type of immersion, c) dimensions and shape of the specimen and d) the inherent properties of the polymer (Jahandideh and Muthukumarappan 2016a, Qiu and Bae 2006). In composites, the type and characteristics of the reinforced fiber also affect the water uptake. For example, using the same matrix, the flax/basalt composites showed a lower water uptake than the flax composites (Bakare et al. 2016, Nawab et al. 2013). The fiber volume fraction of the composite is also believed to be proportional to the water uptake rate of the composite (Yousefi, Lafleur, and Gauvin 1997, Murillo, Vallejo, and López 2011).

The *water absorption tests* are generally carried out based on the ASTM D 570-98 in 3 modes: *Long-Term Immersion, Two-Hour Boiling Water Immersion* and *Immersion at 50°C.* In Long-Term Immersion, the sample is immersed in a distilled water bath at 23ºC and the total water absorption versus time is recorded, in the two-hour-boiling-test, the water absorption is measured after 2 hours of immersion in the boiling distilled water bath and in the Immersion at 50°C mode, water absorption is measured at

50°C at different time intervals. Tests are continued until the samples get substantially saturated (achieved water absorption rates to be ≤ 1% or 5 mg between intervals). The initial slope of the water-absorption versus time curve is proportional to the diffusion constant of water in the matrix (Qiu and Bae 2006).

Biobased content: The biobased content or *"Percent biobased"* is a measure of the proportion of the biobased carbon fraction to the total carbon in the product. The ASTM D6866 has set a standard method based on radiocarbon analysis for the calculation of the biobased content included in a resin, which is frequently used for measuring the biobased content of resins (Jahandideh and Muthukumarappan 2016a, Bakare, Ramamoorthy, et al. 2015, Tiwari et al. 2012). This standard method is also used by the U.S. Department of Agriculture (USDA) BioPreferred program[1] to calculate the biobased content included in a material. Based on this standard, the biobased standard can be calculated using the following formula:

$$\text{Biobased content} = \frac{biobased\ carbon\ content}{total\ carbon\ content} \times 100$$

The total carbon content includes both renewable based and petroleum based carbons.

2.3.3. Rheological properties of the star-shaped crosslinkable resins

Viscosity of the resins: Inadequate and poor impregnation of a viscous matrix to fibers is a major problem in composite manufacturing. It makes the production process to be slow and also reduce the mechanical strength of the product [12, 13]. The viscosity is of importance for manufacturing processes, maximizing the production efficiency, improving processability as well as for improving the impregnation efficiency of the

[1] https://www.biopreferred.gov/BioPreferred/

matrix to the reinforcement fiber for composite production (Komkov, Tarasov, and Kuznetsov 2015). It is believed that the linear PLA shows a long Newtonian plateau typical in polymers having a linear chain structure (at low to moderate oscillation frequencies <100 rad/sec). For the S-LA systems however, a non-Newtonian behavior has been reported. Also, the S-LA systems show an intensified shear thinning response (similar to comb-like PLA) compared to the linear PLA (Nouri, Dubois, and Lafleur 2015a, Kim, Kim, and Kim 2004). In composite manufacturing industry, low viscosity of thermoset resin is a crucial factor for several processing methods, including vacuum infusion, spray and hand lay-up, filament winding, and pultrusion (Åkesson, Skrifvars, et al. 2010b).

A proportional relationship between the MW and the viscosity of the PLA systems has been reported (Nouri, Dubois, and Lafleur 2015a, Cooper-White and Mackay 1999, Othman et al. 2011). Comparably lower viscosities of thermosets, suggest better processability and better impregnation in these systems and make thermosets desirable as a matrix for reinforced composite applications. Generally, the lower the viscosity, the better rheological properties and more desired matrix to be used for reinforced composite applications (Liang and Chandrashekhara 2006). For a satisfactory composite manufacturing, Li et al., suggests that the resin flow viscosity needs to be below 5 Poise (0.5 Pa s) (Li, Wong, and Leach 2010). It is believed that employing a core molecule in the structure of oligomers can reduce the viscosity of the resins. This reduction can be ascribed to the coiling character of polymers (Corneillie and Smet 2015); therefore, as the star-shaped polymers have smaller hydrodynamic volume compared to that of linear

polymers with the same molecular weight, the viscosity will be lower (Chang et al. 2012b, Finne and Albertsson 2002, Choi, Bae, and Kim 1998).

However, the contradictory observations have also been reported by Nouri et al. in which higher viscosity and elastic modulus was observed for branched PLA structures (Nouri, Dubois, and Lafleur 2015a). The viscosity of the S-LA is generally measured based on stress viscometry technique at different temperature intervals. Increasing the length of the LA branches will increase the MW and the viscosity. Bakare et al. reported the same trend for S-LA thermosets with glycerol core molecules with different LA chain lengths in which resins with shorter arms proportionally had lower viscosities. The same trend was reported for the S-LA thermosets resins with xylitol core molecules, and similarly up on increasing the temperature, the viscosity of resins substantially dropped down. Low viscosity, even at elevated temperatures (up to curing temperature), is substantially important as low viscosity facilitates the impregnation of the resin into the fiber reinforcement at higher temperatures. There is not a considerable number of studies exist on the effect of star-shaped structures and the Table 3 summarizes the viscosities reported for to date synthesized S-LAs.

Table 1. 3. The effect of the core molecule and the LA chain length on the viscosity of the crosslinkable S-LA.

Core molecule	LA Chain length	End-functionalization	Number of branches	Viscosity at 25 °C Pa. s	Viscosity min Pa. s	Ref
Unsaturated polyester	-	none	-	0.3	0.1 at 70 °C	(Bakare et al. 2016)

xylitol	3	MAAH	5	2.97	0.06 at 85 ℃	(Jahandideh and Muthukumarappan 2016a)
pentaerythritol	5	IT-MAAH	4	7000	4 at 80 ℃	(Åkesson, Skrifvars, et al. 2010b)
glycerol	3	MAAH	3	1.09	0.04 at 100 ℃	(Bakare et al. 2014b)
glycerol	7	MAAH	3	80	0.33 at 100 ℃	(Bakare et al. 2014b)
glycerol	10	MAAH	3	900,000	1.05 at 100 ℃	(Bakare et al. 2014b)
pentaerythritol	5	MAAH-Allyl alcohol	4	0.02	0.01 at 70 ℃	(Bakare et al. 2016)

Curing kinetics: Curing involves the irreversible transformation of low molecular weight oligomers into a solid network. Thermal curing of thermosets consists of the heating period stage and the curing reaction stage. During the heating period, the resin is heated up to a temperature at which the curing reaction starts, while in the curing reaction stage, the heat evolved from the overall curing mass at a constant temperature (Vergnaud and Bouzon 2012). Often, in the S-LA thermosets, curing reaction starts by the assistance of a radical initiator. The tuning of curing parameters, including temperatures, pressures, time, etc. (Liang and Chandrashekhara 2006) is of importance, especially in thermosets, as it affects the properties of the final product and applying improper conditions for curing, may result in higher exotherms, faster gelation and more shrinkage due to excessive thermal zoning (Jahandideh and Muthukumarappan 2016a, Pereira and d'Almeida 2016). Understanding of the cure process is substantially important, especially for more complex systems such as industrial formulations, as a variety of additives are interfering in the curing procedure, resulting in a more complex cure kinetics. These factors indicate that an excellent control over curing process is required for production of

thermosets with desired properties (Yousefi, Lafleur, and Gauvin 1997, Nawab et al. 2013). The cure process can be evaluated based on two methods: a) monitoring the changes in concentration of the reactive groups and b) by monitoring the changes in the physiomechanical properties of the sample (Yousefi, Lafleur, and Gauvin 1997). Cure kinetics correlate heat release rate (HRR) with the temperature (or time) and the resultant degree of cure (Liang and Chandrashekhara 2006). The analytical models of cure kinetics have wide applications in numerical simulations of composite manufacturing processes. Phenomenological –also called empirical- modeling approach is commonly employed for the analytical expression of the cure kinetics based on an Arrhenius type equation in which the approximated relationship of the curing parameters of the mathematical model are compared with the experimental data (Liang and Chandrashekhara 2006). Several phenomenological models are presented in the literature for modeling the curing kinetics of the thermosetting resins; however, a few studies are performed for the modeling the curing kinetics of the S-LAs (Liang and Chandrashekhara 2006, Chang et al. 2012b). The degree of cure, α, presents the extent of the curing reaction and is proportional to the amount of heat released by bond formation. The degree of cure is defined as:

$$\alpha = \frac{H}{H_u}$$

where H is accumulative reaction heat up to time t, and H_u is the total heat released during curing reaction. H_u is evaluated by

$$H_u = \int_0^{t_{fd}} \left(\frac{dQ}{dt}\right)_d dt$$

where t_{fd} is the total reaction time and $(dQ/dt)_d$ is the instantaneous heat flow during the dynamic scanning. The curing rate which is proportional to the rate of heat generation, is defined as:

$$\frac{d\alpha}{dt} = \frac{1}{H_u}\left(\frac{dH}{dt}\right)$$

Table 3 provides a summary of suggested phenomenological models in the literature.

Table 1. 4. phenomenological models suggested for curing kinetics of the thermosetting systems.

Model	Equation	Parameters	Dependent parameters	Ref
nth- order rate	$\frac{d\alpha}{dt} = K(1-\alpha)^n$	*K*: reaction rate constant $K = K_0 \exp\left(-\frac{\Delta E_A}{RT}\right)$	K_0: Arrhenius frequency factor ΔE_A: activation energy R: universal gas constant T: absolute temperature	(Du et al. 2004)
Autocatalytic	$\frac{d\alpha}{dt} = K\alpha^m(1-\alpha)^n$	K: reaction rate constant. $K = K_0 \exp\left(-\frac{\Delta E_A}{RT}\right)$ m, n: reaction orders defined by experimental data.	K_0: Arrhenius frequency factor ΔE_A: activation energy R: universal gas constant T: absolute temperature	(Kamal and Sourour 1973)
Kamal	$\frac{d\alpha}{dt} = (K_1 + K_2\alpha^m)(1-\alpha)^n$	Ki: reaction constants. $K_i = K_{i0} \exp\left(-\frac{\Delta E_i}{RT}\right), (i = 1,2)$ m, n: reaction orders defined by experimental data.	K_{i0}: Arrhenius frequency factors. ΔE_i: activation energy R: universal gas constant T: absolute temperature	(Kamal 1974)

Modified Kamal	$\frac{d\alpha}{dt} = (K_1 + K_2\alpha^m)(\alpha_{max} - \alpha)^n$	Ki: reaction constants. $K_i = K_{i0}\exp\left(-\frac{\Delta E_i}{RT}\right), (i = 1,2)$ m, n: reaction orders defined by experimental data. α_{max}: maximum degree of cure at a given temperature	K_{i0}: Arrhenius frequency factors. ΔE_i: activation energy R: universal gas constant T: absolute temperature	(Liang and Chandrashekhara 2006)
Cole	$\frac{d\alpha}{dt} = \frac{K\alpha^m(1-\alpha)^n}{1+e^{C(\alpha-(\alpha_{c0}+\alpha_{CT}T))}}$	*K*: reaction rate constant. $K = K_0\exp\left(-\frac{\Delta E_A}{RT}\right)$ *m, n*: reaction orders defined by experimental data. C: diffusion constant. α_{c0}: critical degree of cure at T=0 K. α_{CT}: increase in critical resin degree of cure with temperature.	K_0: Arrhenius frequency factor ΔE_A: activation energy R: universal gas constant T: absolute temperature	(Cole 1991)

The *nth- order* rate equation is the simplest phenomenological model proposed for predicting the rate of the curing reaction in thermosets. The *nth-order* reaction predicts the maximum curing rate at the beginning of the curing phenomenon and does not account for the autocatalytic effect (Du et al. 2004). The *autocatalytic* models represent the autocatalytic effect of the curing reactions. This model considers a single rate constant for the reaction and the maximum reaction rate is supposed to take place in the intermediate conversion stage. A more accurate model has been proposed by Kamal and Sourour considering two rate constants for the curing kinetics (known as *Kamal's model*) (Kamal 1974, Kamal and Sourour 1973).

However, more parameters in the model have made the model to be more complicated. The limitation of all the mentioned models is that they are just valid when the kinetic of bond formation, is considered to be the only rate controlling step in the

curing reactions. The vitrification effect (transforming to a non-crystalline amorphous solid) has been considered in a modified version of Kamal's model in which the fractional conversion has been considered to not exceed the degree of cure associated with vitrification. In the *Cole's model*, another controlling mechanism for the curing is considered in expressing the curing kinetic equation. This diffusion constant term in the equation, explicitly accounts for shifting from the kinetics to the diffusion control (Cole 1991, Liang and Chandrashekhara 2006).

2.3.4 Thermomechanical properties

In this part, the effect of external forces on the behavior of cured S-LA thermosets and their composites are discussed and the thermomechanical tests currently employed in determining various properties, including elastic modulus, yield stress, ultimate strength, toughness, flexural modulus, storage modulus, flexural modulus and glass transition temperature are highlighted. The mechanical tests currently employed in characterizing thermomechanical properties of S-LA thermosets, including DTMA tests, tension tests, compression tests, bending or flexural tests, hardness tests, fatigue tests, creep tests, thermogravimetry analysis, dynamic scanning calorimetry and impact tests. The type of the employed testing methods on the specimen depends on the service expected for the produced thermoset. However, the more testing applied on a specimen, the more information acquired for the intended S-LA. The mechanical properties of S-LA is very dependent on the molecular weight and the structure of the network. Generally, employ of a star branching point in the S-LA systems, results in lower melting temperatures (T_m), lower glass transition temperatures (T_g) and lower crystallization temperatures (T_c) for polycondensation resins. The lower T_c indicates that the staring points make the material

harder to crystallize, while lower T_m indicates that it makes stacking of the polymers more difficult (Corneillie and Smet 2015). The following section provides a short description of the current mechanical testing methods and the type of information obtained from these methods.

Tension or tensile tests are the most fundamental tests employed for characterizing mechanical properties of S-LA based matrices. In tensile tests, a specimen is subjected to a controlled tension until failure happens and stress to strain curve is obtained. The modulus of elasticity (Young's modulus), E, is a measure of the stiffness of the sample in the linear region of the curve in which the specimen can return to its exact initial conditions, if the load is removed; the yield strength is the stress applied to the material at which plastic deformation starts to occur; and ultimate tensile strength (UTS) is the maximum load the specimen sustains during the test. Increasing the temperature generally increases the ductility (the extent of plastic deformation before fracture) and the toughness of a material while decreases the yield stress, tensile strength and the modulus of elasticity (Callister and Rethwisch 2007, Kalpakjian, Schmid, and Sekar 2014).

It is believed that the tensile properties of the star-shaped structure are different with linear oligomers. The strength can be lower for networks with flexible extension units, or higher for structures with rigid staring points. It is reported that S-LA systems with high crosslinking density demonstrate similar mechanical properties to those of other biodegradable composites, however, longer LA chains will decrease tensile properties (Helminen, Korhonen, and Seppälä 2002). Helminen et al. reported lower tensile strength for butanediol-LA systems (despite higher crosslinking density), which was ascribed to the flexible butanediol units used in the linear oligomers (Helminen,

Korhonen, and Seppälä 2002). However, it is believed that the tensile strength is a function of crosslinking density and generally, a higher crosslinking density results in higher tensile strength (Storey et al. 1993).

In *compression tests*, the specimen is subjected to a compressive load usually by a solid cylindrical object between two well-lubricated flat platens. For the brittle materials, a disk test is applied instead, in which the disk is subjected compression and uniform tensile stresses develop perpendicular to the centerline of the disc (Hodgkinson 2000, Kalpakjian, Schmid, and Sekar 2014). *The bending, flexural or transverse beam test* measures behavior of brittle materials (usually with a rectangular cross section) by applying vertical load in which tensile stress produced on the convex side of the specimen and compression stress in the concave side. The load is applied on either one point (3 point bending) or two points (four-point bending) and the specimen deflection is measured by the crosshead position.

The bending test provides values for the modulus of elasticity in bending (E_f), flexural stress (σ_f), flexural strain (ϵ_f) and the flexural stress-strain response of the material. Usually, the 3-point bending test is applied to polymers and the values like flexural strength and flexural modulus are reported. Flexural strength is defined as the maximum stress in the outermost fiber, the modulus of rupture is defined as the stress at fracture in bending and the flexural modulus is the slope of the stress-deflection curve (Mujika 2006, Wool and Sun 2011).

Hardness, which is defined as the resistance to permanent indentation, is an indicator of the strength of a material and its resistance to scratching or wear. The

resistance to indentation depends on the shape of the indenter and the applied load; therefore, several hardness test methods have been developed to measure the hardness of a material, including Brinell test (using a steel or tungsten-carbide ball indenter (Biwa and Storåkers 1995)), Rockwell test (using a diamond cone or steel ball indenter (Herrmann 2011)), Vickers test (using a diamond pyramid indenter), Knoop test (using a diamond pyramid indenter) and Scleroscope and Leeb test (using a diamond-tipped indenter) (Herrmann 2011, Kalpakjian, Schmid, and Sekar 2014).

Impact tests measure the ability of a specimen to resist high-rate loading and it is used for determining the energy absorbed in fracturing a test specimen at high velocity which is important for estimating the service life of a test piece. Typically, this test is performed by placing a notched specimen in an impact tester (supported at both ends in Charpy test, or at one end in Izod test) and breaking it with a swinging pendulum. In brittle materials, less energy is required for starting a crack, and a little more to propagate it to the shattering climax (Kalpakjian, Schmid, and Sekar 2014).

Dynamic mechanical, thermal analysis (DMTA) is another technique frequently employed to characterize the viscoelastic properties of polymers, in which a sinusoidal stress is applied to the specimen and the resulting displacement (strain) is measured. Properties such as storage modulus, loss of modulus, lag phase (between stress and strain) and glass transition temperature can be measured with this technique (Menard 2008). The storage modulus, which measures the stored energy, represents the elastic characteristic of a polymer. The storage modulus G' is related to the molecular packing density in the glassy state (Vergnaud and Bouzon 2012, Chang et al. 2012b) and higher G' means the better mechanical properties. The G' is decreasing upon elevated

temperatures when the polymer chain is in the rubbery plateau region (Bakare, Ramamoorthy, et al. 2015) due to the free movements of the polymer chains. The loss modulus, G", measures the energy dissipated as the heat and represents the viscous part. Generally, smaller G" suggests better mechanical properties and the strong tendency for reversibility in the samples (Bakare, Ramamoorthy, et al. 2015). At the glass transition temperature, T_g, the G' decreases dramatically while G" reaches its maximum. Temperature sweep tests, frequency sweep tests and dynamic stress-strain tests are the most common test modes employed for characterizing the viscoelastic properties of polymers in DTMA studies.

Thermogravimetric analysis (TGA), is a technique currently employed for measuring changes in physical and chemical properties versus temperature (constant heating rate mode) or time (constant temperature or mass loss mode). As the temperature increases, various components of the sample decomposed. Commonly, in TGA, the percentage of weight loss or the rate of weight loss would be presented versus temperature, which are referred to as the thermogravimetric curve and the differential thermogravimetric curve, respectively (Gabbott 2008). For thermosets, TGA can provide information about the thermal stability, loss of volatiles, decomposition rate and oxidation-reduction reactions and it is employed to study of degradation mechanisms and reaction kinetics (Chatterjee 2009). The degradation in thermoset systems starts with decomposition of the crosslinked network and follows by the random scission of the linear chains (Adekunle, Åkesson, and Skrifvars 2010).

2.4. Applications

2.4.1. Biocomposites

Inexpensive biobased raw material, better environmental profile, low viscosity and better processability of the matrix along with better thermomechanical properties of the produced biocomposites are of advantages expected for the crosslinkable S-LA based composites. The employ of multihydroxyl core molecules in the structure of S-LA polymers for biocomposite production has many advantages. A class of employed polyols (e.g. glycerol and xylitol) has biobased sources and are relatively inexpensive; therefore, employ of these molecules in the structure of S-LA reduces the final costs for the produced composites. In addition, employ of these core molecules lowers the viscosity of the final crosslinkable resins and enhances the resin's processability, which are crucial factors in biocomposite manufacturing.

Also, the core molecules' hydroxyl groups provide a better extended network which results in better thermomechanical properties of the cured resins and the biocomposite. Finally, it is believed that the unsaturated branches of the core molecule, increase the hydrophilicity of the produced resin. The higher hydrophilicity, makes the resin more compatible with inexpensive natural fibers and it eventually increases the mechanical properties and lowers the final costs of the biocomposites produced from natural fibers and S-LA thermosets.

To date, composites of crosslinkable S-LA matrix and different reinforcements, including viscose fiber (Esmaeili et al. 2015), flax fibers (Åkesson et al. 2011b, Bakare et al. 2016), surface modified cellulose fibers (Ramamoorthy et al. 2015) and flax/basalt (Bakare et al. 2016) have been produced. Esmaeili et al. reported rather good mechanical properties for biocomposites made from methacrylated glycerol based S-LA, reinforced by up to 70 *wt*% regenerated cellulose fiber using different fiber alignments. Using the

same matrix, better mechanical properties obtained for unidirectional alignment of the reinforcements (tensile modulus: 11-14 GPa, flexural modulus: 10-11.5 GPa, impact strength: 130-150 kJ/m^2) and lower mechanical properties reported for bidirectional and nonwoven fiber alignments (Esmaeili et al. 2015). Bakare et al. synthesized a crosslinkable S-LA thermoset with low viscosity from LA, allyl alcohol and PENTA and used it as the matrix for production of biocomposites reinforced with flax and basalt fibers (up to 40 and 60 *wt*% fiber loads, respectively). Rather good mechanical properties were reported for flax/ballast composites (tensile modulus: 9-14 GPa, flexural modulus: 10-12 GPa, impact strength: 46-54 kJ/m^2) and lower mechanical properties reported for pure flax composites (Bakare et al. 2016).

Ramamoorthy et al. produced composites from silane and alkali treated regenerated cellulose fibers (Ramamoorthy, Skrifvars, and Rissanen 2015) and methacrylated glycerol S-LA thermosets. Good mechanical properties reported for these biocomposites (tensile modulus: 9.5 GPa, flexural modulus: 6.2 GPa, impact strength: 28 kJ/m^2 (Ramamoorthy et al. 2015). It has been shown that unsaturated branches of the core molecule increase the hydrophilicity of the produced resin and make it more compatible with inexpensive natural fibers which eventually increases the mechanical properties and lower the final costs of the biocomposites. However, sometimes a hyper branched core molecule in the structure of the S-LA thermoset can adversely affect the thermomechanical properties, and also it is plausible that unsaturated groups available in the core molecule of the polymer affect the water absorption capacity of the matrix which results in altering the electrical and physiochemical properties of the product.

2.4.2. Biomedical

Drug delivery: Wide diversity in the topology and the chemistry, ease of formulation for various devices, excellent bio-compatibility, biodegradability and desired mechanical strength have introduced a class of FDA approved aliphatic polyesters such as PLA, PGA, and PLGA to be used in controlled release of drugs, especially for cancer therapy (Tiwari et al. 2012, Bummer 2004, Qiu and Bae 2006, Xiong et al. 2014, Makadia and Siegel 2011). It is believed that the architecture of the polymer, called topology, often influences the physicochemical properties and effects the microsphere preparation and drug delivery properties (Qiu and Bae 2006, Wolf and Frey 2009). The polymer architectures plays a crucial role in the drug delivery control and in the fabrication of drug delivery systems; however, it is relatively unfamiliar to pharmacists.

Different polymer topologies have been studied for drug delivery, which can be categorized in to linear, branched, cross-linked, block (Cheng et al. 2007, Ghahremankhani, Dorkoosh, and Dinarvand 2008, Jeong, Bae, and Kim 2000), star-shaped and dendrimer topology (Qiu and Bae 2006). Compared to linear polymers with the same MW, the star-shaped polymers provide smaller hydrodynamic radius and so, a lower solution viscosity. The star-shaped polymers can be synthesized via *arm-first* or *core-first* methods. In the arm-first methods, the linear arms are prepared via a controlled polymerization pathway; then, the chains are reacted with multifunctional terminating agents. The core-first method which is the dominant employed technique, provides a better control over the process and starts with a multifunctional initiator and the propagation of the arms through a controlled polymerization pathway. Research on S-LA polymers as drug vectors seem rather limited so far and the study experience on different PLA architectures and new drug carriers is still quite limited. Thus, so far there are not

enough experimental data exists to explain the exact role of polymer architectures on the fate of the conjugated drugs (Qiu and Bae 2006). However, different core molecules have been suggested so far for the drug delivery purposes, including, PEG (Choi, Bae, and Kim 1998), THMP (Biela et al. 2003, Biela et al. 2005), PENTA (Kim et al. 1992), di(trimethylolpropane) (Biela et al. 2003), cholic acid (Xiao, Mai, et al. 2012) and luminescent ruthenium tris(bipyridine) (Wang et al. 2011).

Different drug carries have been suggested when star shaped polymers are used for drug delivery purpose, including unimolecular micelles and injectable hydrogels (sol-gel transitions). The drug encapsulation is an important property when star-shaped architecture polymers are used along with unimolecular micelle drug carrier. When injectable hydrogel drug carriers employed, lower critical solution temperature and gel strength is resulted in star-shaped polymers. The controlling factors for the release rate in star shaped polymers include the dimension of the hydrophobic core, the arm number and the arm length. In the linear two-arm PLA-PEG structure, manipulation of the molecular weights of EG to LA in the structure is an important factor in designing a system with high control over the hydrophilic/hydrophobic balance and core protection (Qiu and Bae 2006).

Zeng et al. developed a cholic acid functionalized star-shaped PLGA-b-TPGS for sustained and controlled delivery of docetaxel for treatment of cervical cancer (Zeng et al. 2013). Choi et al. reported the synthesis of star shaped PEO-PLA polymers by a divergent synthetic method which could be used as the delivery carrier for polypeptide. The authors also reported that the melting point, crystallinity, and phase separation are decreasing with an increase in the degree of branching (Choi, Bae, and Kim 1998). Jeong

et al. have also shown the capability of employing star-shaped PEO–PLA block copolymers to be used as parenteral injectable drug delivery (Jeong et al. 1999).

Tissue engineering: Tissue engineering aims to apply engineering methods to create artificial substitutes for defective tissues and organs (Shin, Jo, and Mikos 2003, Tabata 2000). The matrix can be served as a substrate for attachment, grow and migration of cells or can be utilized as a drug carrier to activate cellular function in the region (Saltzman and Olbricht 2002, Shin, Jo, and Mikos 2003). Biodegradable polymers, by providing exogenous matrices suitable for facilitating tissue regeneration, play an important role in most tissue engineering strategies (Whang, Goldstick, and Healy 2000). Successful utilization of biomaterials for tissue engineering is dependent on several factors. The biomaterial must resorb after its service and should provide conditions for sufficient growth rate and effective cell adhesion, while it is -or its degradation materials are- nontoxic, when implanted *in vivo.*

The material which is designed for tissue engineering should also meet certain physical properties, including but not limited to having a) high porosity (≤90% for providing enough surface area in a 3D structure), b) minimum diffusional constraints (sufficient to meet the metabolic requirements), c) sufficient space for extracellular matrix regeneration and d) adjustable degradation rate (to match the rate of tissue regeneration *in vivo*) (Sheridan et al. 2000, Langer 1994). The microarchitecture of the device is also of importance as it influences the interconnection between the pores for cell proliferation. In addition, as scaffolds are subjected to remain in intimate contact with the cells for prolonged periods, the influence of the polymeric materials on viability, growth,

and function of the attached or adjacent cells is of crucial importance (Saltzman and Kyriakides 2014, Wu, Wang, and Li 2015).

Different biodegradable polymers, including linear PLA, polylactide, polyglycolide and PLG have been employed for cell transplantation or for various tissue regeneration, including bone, cartilage, liver, and skin (Langer 1994, Whang, Goldstick, and Healy 2000). The mechanical strength and the rate of degradation of the PLG is typically adjusted based on the ratio of lactic to glycolide and polymer's degree of polymerization. Although the polymer blends must be well optimized by refining their properties to be used for tissue engineering, yet, polymer properties are not the only crucial factors in tissue engineering. The interaction of the cells with the surface of the polymer is another crucial factor and polymers that allow surface modification like PLG are particularly promising for tissue engineering purposes (Lucke et al. 2000).

Go et al. synthesized a heparin-conjugated S-LA by coupling heparin to the S-LA with PENTA core molecules. Authors reported a lower protein adsorption and platelet adhesion as well as higher cell activity on the surface of the S-LA-Hep along with a higher cell spreading area on the surface. These features candidate the S-LA-Hep to be used as blood-tissue compatible materials for implantable medical devices (Go et al. 2008). Cai et al. reported the synthesis of star-shaped polylactide attached to poly(amidoamine) polymers with potentials to be used for hydrophilic drug delivery of growth factor and antibodies in tissue engineering (Cai et al. 2003). Cheng et al. also synthesized a functionalized S-LA polymer with a cholic acid core molecule which had better wettability and higher surface energy compared to the linear PLA. These features result in higher cell adhesion and better cell proliferation (Fu et al. 2007).

2.5. Perspectives, opportunities and limitations

2.5.1. Perspectives and opportunities

Substitution of current petroleum-based platforms with renewable-based technologies would be beneficiary in different ways. First, using the corn-based LA instead of conventional petroleum based monomers, will reduce the dependency of the national thermosetting plastic industry to the petroleum resources. Thus, in the long term, it will enhance the national energy security. Second, compared to petroleum based products, using biobased materials will substantially promote the environmental profile and sustainability of the production chain. In addition, the biodegradability of the products will alleviate carbon footprint and the environmental burdens associated with the final product. Third, using corn-based LA and inexpensive natural fibers as the raw materials, will subsequently promote economic diversification in rural areas. It has been shown that the S-LAs are capable of competing with or even surpassing fossil fuel based resins in terms of cost and eco-friendliness concerns (Jahandideh and Muthukumarappan 2016a, Bakare et al. 2014b, Bakare et al. 2016, Åkesson et al. 2011b, Lin and Zhang 2010).

Modifications for biomedical use: Using a core molecule with adjustable functional groups at the center of the S-LA provides the unique opportunity of designing and controlling over properties of the resin. It is presumed that more hydroxyl groups of the core molecule, provide a better extended network to the final product. The unsaturated hydroxyl groups of the core molecule ultimately increase the hydrophilicity of the produced resin which make the resin more compatible with hydrophilic systems. The privilege of these thermoset systems over other systems is that these resins can be

engineered for a certain functionality by changing the chemical structure or altering the crosslinking density. Moreover, by changing the nature and the portion of the block units of copolymers chain, it is possible to further manipulate the polymers properties.

This manipulation could be in terms of changing the hydrophilicity properties as well as designing and manipulation of the void sizes of the polymer network. By employing longer arms which will act as plasticizers, it is possible to increase the size of the voids in the network and by using hydrophilic monomers in copolymers the hydrophilicity of the polymer network can be tailored. Manipulation of both void sizes and the hydrophilicity of voids will provide the unique opportunity for designing a polymeric matrix which is specifically designed for certain chemical component release or a desired drug delivery –based on drugs chemical structure, molecular weight, polarity, etc. with a substantial control over the release rate. In these systems, the polymer's network can be tailored based on different parameters, including substitution of LA hydrophobic groups with a more hydrophilic group such as glycolic acid, by changing the ratio of the chain extender to the oligomer units or by changing the cross-linking density of the cured thermoset system. Using short oligomer chains in the network of the polymer leads to a compact network structure results in more resistance on diffusion. In addition, by reducing the ratio of methyl groups to the carbonyl groups in the structure (which results by applying higher ratios of glycolic acid units to lactic ones in the PGLA polymer), more hydrophilic structure is achieved.

Smart packaging applications: The S-LA thermosets provide an adjustable polymeric network, which potentially can be tailored for active packaging of productions. Active packaging (also called intelligent or smart packaging), means having active

functions beyond the inert, passive containment and protection of the product and refers to packaging systems currently employed for foods, pharmaceuticals, and several other types of products (McCabe-Sellers and Beattie 2004, Byun, Kim, and Whiteside 2010). Nowadays, PLA is employed as an active packaging material for antibacterial packaging with the ability of controlled release of antimicrobial or antioxidant compounds. Antioxidant packaging is a well-known, promising technique for increasing food quality and extending food production shelf life (Byun, Kim, and Whiteside 2010). The addition of antioxidants to the polymeric packages has two facets. First, available antioxidants in the polymer formulations protect the ester bonds of the polymer structure from degradation (Dainelli et al. 2008, Yam, Takhistov, and Miltz 2005, Jamshidian et al. 2010).

Second, it helps protecting the food contents by migration of antioxidants from packaging material to the food medium. It is believed that antioxidant compounds can defuse and migrate from the packaging material to the food product and help maintaining the quality of the food. Previously, antioxidants have been successfully incorporated into different polymeric matrices, including low density polyethylene (LDPE), polyvinyl chloride (PVC) and polypropylene (PP), for various foods (Wessling, Nielsen, and Giacin 2001, Wessling et al. 1999, Jamshidian, Tehrany, and Desobry 2012). The release of antioxidants is a result of the biodegradation of the polymer matrix as well as the diffusion phenomenon. In the diffusion of antioxidants, the migrant diffuses through the polymer matrix toward the interface and then partitioned between the polymer matrix and the food medium until the equilibrium. Therefore, antioxidant release can be presented as

a result of diffusion, dissolution and finally, the equilibrium process (Soto-Cantú et al. 2008, Jamshidian, Tehrany, and Desobry 2012).

Flame retardancy: Many additives have been developed and employed to reduce the risk of fire hazards and to pass safety specifications in polymers. A flame retardant additive reduces the flammability of the product and the smoke generation capability (Morgan and Gilman 2013, Bourbigot and Fontaine 2010). In the S-LA systems, the flame-retardancy feature can be potentially obtained by adding the phosphorus containing groups (or other flame retardant groups) to the structure of the network. In these systems, the core molecule provides different reactive sites (hydroxyls) which may be employed for addition of a special functionality. The other sites which may be used to add a functional group, are the chains. In addition, using an EF agent with groups containing a flame retardant component, can potentially add flame retardancy feature to the S-LA thermosets.

2.5.2. Gaps and limitations

In this section, shortcomings and gaps of S-LA systems are discussed. S-LA and their composites have been synthesized and employed for several applications for decades. Employing a core molecule makes the structure of these systems more complex compared to linear thermoplast PLA. Moreover, the combination of different polymerization steps, EF reactions and curing reactions have imposed more complexity to these systems. In addition, numerous applications are considered for these systems, including biomedical applications, adhesives, coatings and biocomposites, and each certain application requires certain characteristics. In order to manipulation of the S-LA for a specific desired property, these systems must be thoroughly characterized.

Shortcomings and gaps in the different steps must be well studied. The aim of the following section is to discuss drawbacks associated with different steps of preparation and characterization of these systems. These gaps are classified into two categories: the synthesis and manufacturing concerns and the characterizing issues.

Generally, using a chain extender imposes more complexity to the system which inevitably leads to a comparably poor control over the polymerization. The choice of the core molecule would be one of the most important factors. It can directly effect on the crosslinking density, mechanical properties, thermostability, degradation rate and the hydrophobicity of the system. The ratio of the core molecule to the LA monomers is another important factor which affects the crosslinking density and the final properties of the produced network. Too much core molecule makes the resin brittle and reduces the diffusion rates. The thermostability of the core molecule is of importance, as the synthesis often occurs at high temperatures and molecules with susceptible bonds can be degraded during the synthesis.

Steric hindrance, increased by employing the core molecules with multi-hydroxyl branches and may result in an incomplete reaction of branches with the hydroxyl groups which leaves unsaturated sites in the core molecule. Even if the complete reaction of hydroxyl groups ensured, still the length of chains might vary between oligomers which results in unpredictable mechanical and diffusional properties for the batch to batch resins. This is problematic, especially when the resin is expected to be used for the drug delivery and biomedical applications. In addition, the polycondensation synthesis pathway, which is commonly employed for the synthesis of the S-LAs, is an energy extensive step, due to the long reaction times at high temperatures. It also requires large

quantities of organic solvents for effective water removal which must be recycled through the azeotropic condensation.

This purification and water removal step imposes a substantial environmental load. Thus, there is a need for optimization of the required energy for the synthesis. The energy inputs can be alleviated by optimization of the process and choosing more effective solvents, more efficient catalyst systems or choosing an alternative synthesis method. The EF reaction is the other important synthesis step. Despite the condensation step, the EF reactions occur at moderate temperatures and shorter reaction durations. However, this step requires a crucial control over the temperature as at elevated temperatures, the undesired partial crosslinking happens and the risk of gelation is increased. In this step, in order to avoid unwanted crosslinking, an inhibitor agent often used for protecting the olefinic carbon bonds. The origin of the EF agents, the presence of releasing products during the reaction, e.g. MAA, the progress of EF reactions and the degradation products are of other concerns, especially when the cured resin is intended to service *in-vivo* in biomedical applications.

The optimization of the EF reactions would be a tackle as applying insufficient reaction times and temperatures result in poor crosslinking density and subsequently inferior mechanical properties of the product, and applying excess reaction times and elevated temperatures increase the risk of gelation. Therefore, successful substitution of the nonrenewable EF agents with nontoxic renewable ones is of interest. The rheological properties of these systems are the other hotspot. The rheological properties of the S-LA systems have not been studied intensively in the literature. Although employing a core molecule in the structure of oligomers is believed to reduce the viscosity of the resins

(Chang et al. 2012b, Finne and Albertsson 2002), yet, resulted viscosities are still far from the desired viscosity for manufacturing processes. It is believed that a proportional relationship exists between the MW and the viscosity of these systems (Nouri, Dubois, and Lafleur 2015a, Cooper-White and Mackay 1999, Othman et al. 2011).

Employing core molecules with fewer hydroxyl groups, reduction in the LA chain length of branches and an efficient functionalization of the remaining hydroxyl groups can further reduce the viscosity of resins. The curing procedure is also of importance and must be well optimized as it can affect the properties of the final product. Applying improper curing techniques result in undesired mechanical strength on the matrix (Gledhill et al. 1978). Different factors are involved in the free radical curing reactions which are often employed for curing of the S-LA systems, including the nature of the initiator, *initiator: resin* ratio, applied heat regimes, retention times and cooling strategies. Using excess curing agent or applying high temperatures for the curing may result in higher exotherms, faster gelation and more shrinkage due to excessive thermal zoning (Jahandideh and Muthukumarappan 2016a, Pereira and d'Almeida 2016).

There are also shortcomings exist in the characterization methods of these systems. Currently, the titration method is employed for monitoring the progress of the polycondensation step which is based on TAN measurements titration of available acidic groups. The samples are diluted in the predefined solvent systems, capable of dissolving the S-LA, and then titrated with KOH. However, these solvent systems have been optimized for petroleum based materials and might not be capable of efficient dissolving of the high MW oligomers of the S-LA which results in unrealistic high conversion degrees. In addition, comparably more complex structure of these systems makes the

interpretation of the FT-IR and NMR analysis to be hard. Therefore, too many peaks often can be found in the spectrums, especially in the carbonyl area of the EF resins, which can obscure the results and make them very hard to interpret. In addition, these techniques provide no solid information about the degree of completion of the polycondensation and EF reactions.

2.6. Conclusions

The need for designing polymers for a certain application and the shortcomings associated with the conventional synthesis methods, encouraged researchers to explore for the alternative PLA synthesis routes. Utilization of chain extenders and core molecules are of promising ways to achieve a high MW polymer capable of being engineered for a certain functionality. It is well known that changing the architecture of the linear PLA would change its properties. The concept of using star-shaped resins for biocomposites or in biomedical applications is gaining more and more attention day by day. The polymer architecture is a crucial factor for the drug delivery control; however, it is relatively unfamiliar to pharmacists. Employing a multifunctional core molecule at the center of the S-LA systems, provides the unique opportunity of designing and controlling over release properties of the resin. Adjustable structure of these aliphatic polyesters, provides the chance for altering the chemistry, ease of formulation, excellent bio-compatibility and biodegradability and makes them a suitable candidate for the controlled release of drugs, especially in cancer therapy. In addition, altering the linear structure of the PLA, often results in lower viscosity, better extended network and better thermomechanical properties.

Comparably lower viscosities of the S-LA thermosets, results in better processability and better impregnation of the matrix to the reinforcing fibers which is beneficiary for the composite applications. It is believed that often unreacted hydroxyl groups of the core molecule increase the hydrophilicity of the matrix and make it more compatible with hydrophilic natural fibers which results in the better mechanical properties of the biocomposites. However, in some cases, worse mechanical properties may result depending on the type of the employed core molecule. It is also plausible that unsaturated groups increase the water absorption capacity which results in altering the electrical and physiochemical properties of the matrix.

Developments in the emerging S-LA systems are spectacular from a technological point of view. However, these systems still suffer from different limitations and technological gaps and have a long way to go. These limitations can be categorized into the synthesis deficiencies and the characterization gaps. Firstly, employ of a core molecule makes the structure of these systems relatively more complex and reduce the control over the polymerization step. Association of multi-step reactions, including different polymerization steps, EF reactions and curing reactions also impose more complexity to these systems. The steric hindrance, increased by employ of the core molecule, may result in an incomplete reaction which leaves unsaturated hydroxyl groups in the network. Even if the complete reaction ensured, still the risk of inconsistent product remains as the length of chains cannot be efficiently controlled. The former results in the unpredictable mechanical and diffusion properties of the batch to batch product. The properties of the S-LA is dependent on several factors, including the

molecular weight, the architecture of the network, rigidity of the core molecule, length of branches, crosslinking density and the degree of conversion.

These interrelated factors, make the optimization and characterization to be complicated and hard. In addition, the type of the employed testing methods depends on the expected service for the product. The tuning of the curing parameters is also a challenge, especially for more complex systems such as industrial formulations. Applying improper curing method results in inferior mechanical properties, higher exotherms, faster gelation and more shrinkage in the cured resins. In addition, the polycondensation synthesis is known as an energy extensive step. Large quantities of organic solvents required also impose substantial environmental load.

This is a very exciting period in the development of biocompatible polymers, in particular, biobased S-LA resins. Although these state of the art, adjustable S-LA systems look very interesting and promising for various applications, yet their usage is limited. Therefore, future use of these systems requires systematic optimization and invention of better characterization methods.

Acknowledgement

The authors would like to acknowledge the funds provided by Agricultural Experiment Station, South Dakota State University and North Central Sun Grant through US Department of Agriculture, Washington, DC in support of this research work. The authors also appreciate the critical evaluation of biomedical part of this manuscript by Dr. Asma Rashki of School of Medicine, Tehran University of Medical Sciences.

Chapter 3 - Synthesis, Characterization and Curing Optimization of a Biobased Thermosetting Resin from Xylitol and Lactic Acid

Arash Jahandideh[1,*], Kasiviswanathan Muthukumarappan[1]

[1] Agricultural and Biosystems Engineering Department, South Dakota State University, PO Box 2120, Brookings, SD 57007, USA

This chapter has been published in European Polymer Journal.

* Corresponding author current address: Agricultural, Biosystems & Mechanical Engineering Department, 1400 North Campus Drive Box 2120, Brookings, SD 57007, USA. Tel.: +1 (605) 6885670

Corresponding author: arash.jahandideh@sdstate.edu

Abstract

A biobased thermoset resin was synthesized by direct condensation reaction of lactic acid with xylitol followed by the end-functionalization of the hydroxyl groups of branches by methacrylic anhydride. Chemical structures of resins were evaluated and confirmed by ^{13}C NMR and Fourier-transform infrared spectroscopy (FT-IR). Different techniques were employed for the optimization of the curing process. Techniques including Microscopy, Differential Scanning Calorimetry (DSC) and Dynamic Mechanical Thermal Analysis (DMTA) were employed for characterization of the cured resins. Thermogravimetric analyses (TGA) were also carried out to check the thermal stability of the cured resins. The viscosity of the neat resin was measured at different temperatures and different stress levels. Water adsorption tests were also carried out to

check the water absorption properties of cured resins. The glass temperature (Tg) of the resin was 98°C, and the viscosity of the resin was 2.97 Pa s at room temperature which drops to 0.07 Pa s upon increasing the temperature to 85°C. The biobased content of the resin was calculated as 77%. Cheap raw materials, high biobased content, biodegradability, good thermomechanical and rheological properties, good processability and good thermal stability are of advantages of the synthesized resin which makes the resin comparable with commercial unsaturated polyester resins.

Keywords: synthesis; thermosets; crosslinking; renewable resources; lactic acid; thermal mechanical properties

---

3.1. Introduction

Due to a shortage of petroleum resources, ecological and economic concerns associated to petroleum based resins, different biobased raw materials have been suggested for production of biobased resins including vegetable oils (Mashouf Roudsari, Mohanty, and Misra 2014, Liu, Madbouly, and Kessler 2015, Xiong et al. 2013), polyols and polyphenols (Auvergne et al. 2013, Bakare et al. 2014b) and lactic and itaconic acid (Ma et al. 2013). Poly lactic acid (PLA) is a biodegradable aliphatic polyester which is derived from lactic acid (Lunt 1998). Versatile and economical renewable sources of lactic acid (LA), and biodegradability of the products makes LA a suitable source for production of bioplastics (Martinez et al. 2013, Jimenez, Peltzer, and Ruseckaite 2014). Thermoplasts are a class of polymers with high molecular weight where the chains are associated through intermolecular forces and their structure is weaken rapidly upon temperature increase. In contrast, thermosets form chemical bonds during the curing

process and the structure cannot be reformed upon further heating-cooling processes (Raquez et al. 2010b, Jimenez, Peltzer, and Ruseckaite 2014). Thermosets can be tailored for a desired property by changing cross-linking density or structure which makes them capable of being engineered for a certain functionality.

Limitations in impregnation of viscous matrix to fibers is a major problem in composites. Poor impregnation makes the production process to be slow and also reduces the mechanical strength of the composites (Komkov, Tarasov, and Kuznetsov 2015, Han et al. 2015). Low viscosity of thermosets results in better processability and better impregnation of fibers making thermosets desirable as a matrix for reinforced composite applications (Liang and Chandrashekhara 2006). In addition, PLA's hydrophobic nature makes it incompatible with natural fibers (Oksman, Skrifvars, and Selin 2003, Wambua, Ivens, and Verpoest 2003, Qin et al. 2011). Hydrophilic fibers cannot be efficiently employed for reinforcing the PLA matrix as the adhesion of the fiber to the hydrophobic resin is poor which contributes to poor mechanical properties of the produced composites (Garlotta 2001a). Several studies carried out to enhance the compatibility of the natural fibers in the matrix include treating the fibers with hydrophobic functional groups such as maleic anhydride (Sutivisedsak et al. 2012, Kabir et al. 2012), ultrasonic and plasma treatment (Liu et al. 2008, Bozaci et al. 2013) and co-polymerization of PLA with a more hydrophilic monomer like glycolic acid monomers (Makadia and Siegel 2011).

Different studies have been performed on synthesis of LA based thermosetting resins suitable for different applications including structural composites, biomedical applications, drug-delivery applications, tissue engineering, coating applications or smart packaging. (Bakare, Ramamoorthy, et al. 2015, Åkesson, Skrifvars, et al. 2010b, Bakare,

Åkesson, et al. 2015, Sakai et al. 2013, Chang et al. 2012b, Åkesson et al. 2011b, Makadia and Siegel 2011). Recently, thermoset resins prepared by direct condensation of LA with glycerol (Bakare et al. 2014b), allyl alcohol terminated LA oligomers (Bakare, Åkesson, et al. 2015), and pentaerythritol (Åkesson, Skrifvars, et al. 2010b) have been introduced for biocomposite productions. Star-shaped molecules resulted after direct condensation of the core molecule with LA were further functionalized with an end-capping agent (Åkesson et al. 2011b). It is presumed that more hydroxyl groups of the core molecule provide a better extended network of the final thermosets (Moon et al. 2001). In addition, unsaturated hydroxyl groups of the core molecule may ultimately increase the hydrophilicity of the produced resin and make the resin more compatible with natural fibers which ultimately increases the mechanical properties of biocomposites produced from natural fibers and PLA thermoset.

In this study, the possibility of producing resins from LA and xylitol have been investigated. Thermoset resin was synthesized in a two-step synthesis procedure: a direct condensation-polymerization followed by an end-functionalization reaction. The structure of the resin was confirmed using ^{13}C-NMR and FTIR. The curing process was optimized and the thermomechanical properties of cured resins was investigated using dynamic mechanical thermal analysis (DMTA), differential scanning calorimetry (DSC) and thermogravimetric analysis (TGA). The advantages of using xylitol as the core molecule are that 1) it is biobased and relatively inexpensive, 2) it lowers the viscosity of the final resin enhancing its processability, 3) xylitol has more hydroxyl groups providing a better extended network which results in better thermomechanical properties of the cured resin

and 4) unsaturated branches of xylitol molecule, increase the hydrophilicity of the produced resin leading to a resin which is more compatible with natural fibers.

3.2. Materials and Methods

3.2.1 Materials

L (+)-lactic acid (≥90%; Acros Organics) and xylitol (≥99%; Sigma-Aldrich) were used as the main reactants. Toluene (≥99.8%; Sigma-Aldrich) as the solvent, Methanesulfonic acid (≥99.0%; Sigma-Aldrich) as the catalysts, Hydroquinone (≥99.5%; Sigma-Aldrich) as the inhibitor, Methacrylic anhydride (≥ 94%; Sigma-Aldrich) as the end-functionalization agent were also used in synthesis. Benzoyl peroxide (≥98%; Sigma-Aldrich) was used as the free radical initiator for crosslinking phase. Xylenes (≥98.5%; Sigma-Aldrich) and Isopropyl alcohol (99.5%; Sigma-Aldrich) were employed for the titration. Potassium hydroxide (≥85%; Sigma-Aldrich) solution in absolute ethanol was used as the titrant with phenolphthalein (1% in ethanol, Fluka) as the indicator.

3.2.2 Synthesis

The resin was synthesized by direct condensation reaction of LA with xylitol and further end-functionalizing of the hydroxyl groups of branches by methacrylic anhydride. Xylitol molecules played the role of a clustering agent in the final polymer structure. Eventually, a star-shaped oligomer of xylitol and LA was prepared in the step-one reaction. In the step-two reactions, branches were end-functionalized with methacrylic anhydride. The chemical reactions and idealized structures are presented in figure 1.

3.2.2.1 Step-one reactions: poly-condensation of LA with xylitol

The first synthesis step was carried out employing a direct condensation polymerization technique in the presence of toluene as an auxiliary solvent for water removal. LA (1.5 moles) was added to 0.1 mole of xylitol diluted in 75 g of toluene containing 0.1% *wt* of the catalyst methanesulfonic acid (see figure 1). The components were transferred to a three-neck, round-bottom flask, equipped with a magnetic stirrer in which one neck was connected to a nitrogen flow and toluene reflux from and the azeotropic distillation apparatus. The other two necks were used for toluene reflux from an azeotropic distillation unit and connecting a thermometer. In the third neck, an azeotropic distillation unit was connected to a condenser for toluene recovery. The flow of the nitrogen in the system was ensured by employing a mini gas bubbler in the outlet of the condenser. The temperature inside the flask was set to 145°C for two hours and then increased to 165°C for seven hours.

3.2.2.2 Step-two reactions: End functionalization of the Oligomers

The oligomers resulted from condensation reactions would have reactive groups but yet, the groups are not reactive enough for a satisfactory cross-linking. The branches were further functionalized with methacrylic anhydride to improve their reactivity by adding carbon double bonds. The resulted resin was cooled to 90°C and 1% *wt* hydroquinone was added to the reaction mixture for stabilization as well as inhibiting unwanted cross-linking reactions and gelation. Under a constant stirring rate and nitrogen purge flow, 0.55 mole of methacrylic anhydride was added dropwise and the temperature was maintained at 90°C for four hours. The medium was then transferred to a drop-shaped glass flask connected to a rotary evaporator under partial vacuum conditions (~10 mbar, 1 hour at 60°C and two hours at 90°C) to remove the residual toluene and released

methacrylic acid. The chemical reactions and idealized structures are presented in figure 1.

3.2.3 Curing optimization

The thermal curing was performed by a free-radical polymerization method which forms a rigid three dimensional network. Different curing methods were investigated to obtaining an optimal curing procedure including different initiators: resin ratios, applying different heat regimes, applying different temperatures and retention times, applying different pressures and also applying different cooling strategies. The aim of the curing optimization was to obtain completely cured samples with no cracks or bubbles with the desired mechanical properties. To avoid premature cracks, the dispersion of the curing agent in the form of a fine powder and in the form of dissolved in toluene were examined.

For identifying the sufficient ratio of the initiator to the neat resin, curing was performed with different ratios of 0.5, 1, 1.5, 2 and 3 wt%. For fully cured samples, a microscopy technique was applied for checking the samples to stablish the presence and cause of cracks and bubbles in the cast resins. Using the proper initiator to resin ratio, the temperatures in the range of 90 to 140°C for 20 minutes periods were applied for thermal curing. Three different post curing methods, called a, b and c, were investigated and effects of the methods on mechanical properties of the final samples were investigated. In method a, curing was started by heating samples from room temperature to 150°C at a heat rate of 5°C/min.

Samples were kept at 150°C for 20 minutes and after curing, they were cooled at room temperature. In method b, curing was started at 50°C for 10 minutes followed by

another 10 minutes at 90°C. Finally, samples were post cured at 150°C for 20 minutes and cooled and stored at room temperature. In method c, curing was started at 150°C in a preheated oven and continued for 20 minutes. After curing, samples were cooled and stored at room temperature. Completion of the curing processes were investigated by analyzing the DSC residual exotherms. Finally, mechanical strength of different cured samples cured via different techniques were evaluated through mechanical testing and the best curing method was identified.

3.2.4 Characterization

The progress of the condensation reaction was monitored by titrating the residual carboxyl groups during the step-one resin synthesis. The conversion progress was determined by titrating aliquot samples (1 g) taken hourly during the condensation reaction. The samples were first diluted with 20 mL of 1:1 *v/v* xylene/isopropyl alcohol solutions and then titrated with 0.5 M KOH in absolute ethanol with phenolphthalein 1% as the indicator.

The chemical structure of step-one and step-two resins were determined with a Carbon Nuclear Magnetic Resonance (^{13}C NMR) spectrometry (Bruker BioSpin GmbH, Germany) at 400 MHz. Sample concentration in 5 mm tubes was 10% by weight in $CDCl_3$ and the measurement temperature was 45ºC. The internal standard was tetramethylsilane, TMS, and the shifts were expressed in ppm.

IR spectra of step-one, step-two and cured samples were recorded at room temperature on Nicolete 6700 spectrometer, supplied by Thermo Fisher Scientific,

Massachusetts, USA in the range of 4000–600 cm^{-1}. Each spectrum was recorded after the sample was scanned 60 times.

Calorimetric analyses were carried out by a DSC on a TA Instrument Q 100 (V9.9 Build 303- supplied by Water LLC, New Castle DE) thermal analyzer. Samples of approximately 10 mg were sealed in aluminum hermetic pans and tested under a nitrogen atmosphere. The calorimeter was calibrated using an indium standard (heat flow calibration) and an indium– lead–zinc standard (temperature calibration). Uncured resin was analyzed from -20°C to 220°C at a heating rate of 10°C/min in order to investigate the crosslinking reaction. Isothermal curing of resins was also performed at 90°C, 100°C, 120°C, 130°C, 140°C and 150°C for 20 minutes and residual exotherms were analyzed from 25°C to 200°C at a heating rate of 10°C/min.

Thermogravimetric analyses of the cured resins were carried out with a Q50 from a TA Instrument supplied by Waters LLC. Samples with an approximate mass of 10 mg were heated from 30°C to 600°C, at a heat rate of 10°C/min under a N_2 purge gas stream of 20 mL/min. Weight percent data versus time was plotted.

Dynamic Mechanical Thermal Analysis was performed on cured samples from different methods on a DMTA (Q800 from TA Instruments, supplied by Waters LLC). The tests were performed on samples with dimension of approximately 60×15×3 mm from -20°C to 150°C in a dual cantilever bending mode with a heat rate of 5°C/min; the frequency was 1 Hz, the amplitude was 15 μm and the tests were performed under a nitrogen atmosphere.

The viscosity of the uncured resin was determined using a viscoanalyzer rheometer (TA instrument, Sweden). All measurements were done with a truncated cone

plate configuration (Ø15 mm, 5.4°C). Viscosities of uncured resins were measured in a temperatures range of 25 to 85°C in increments of 10°C. Shear stress ranged from 0.2 to 400 Pa.

3.2.5 Water adsorption tests

The water adsorption tests were carried out based on ASTM D 570–98 standard to determine the relative rate of absorption of water by the cured samples when immersed. The dimension of test specimens were 60 × 60 × 1 mm. The tests were perform in 3 modes: Long-Term Immersion, Two-Hour Boiling Water Immersion and Immersion at 50°C. In Long-Term Immersion, the specimens were placed in a container of distilled water maintained at a temperature of 23 ± 1°C and the total water absorbed by samples versus time were measured. In the two-hour-boiling-test, adsorption of samples was measured after 120 min of immersion, in the boiling distilled water and in Immersion at 50°C mode, water adsorption was measured at a temperature of 50°C for different time intervals.

3.3. Results and discussion

3.3.1 Titration

The proper condensation-reaction time is essential, as insufficient reaction time results in unreacted reactants and excessive reaction time results in transesterification reactions which degrades the structure (Bakare et al. 2014b). The ratio of the reacted to initial carboxylic groups in the polymerization-condensation step is related to the degree of completion of the condensation reaction in the polymerization-condensation step. In this step, -COOH groups are reacting with the -OH groups of xylitol core molecules (see

figure 1). As the reaction proceeds, the -COOH groups react and the length of LA arm increases. The number of carboxylic groups was measured with an acid-base titration method (Murillo, Vallejo, and López 2011, Xiao, Mai, et al. 2012).

The solvent system was chosen based on ASTM D974. The conversions during the first 720 minutes of the reaction were calculated based on the mL of consumed KOH by the 1 g samples. From figure 2, it can be seen that the reaction started almost after 100 minutes. The conversion reaction proceeds rapidly during the next 320 minutes. The reaction continues until 720 minutes and after that the conversion rate did not change due to transesterification reactions. Based on the titration results, a 12 hours condensation reaction period was considered for the first-step reaction which results in a 94% conversion of the carboxylic groups. Bakare et al. employed a similar acid-base titration method for measuring the degree of reaction of LA with glycerol and reported 95% reaction competition after 360 minutes (Bakare et al. 2014b). The less reaction times required for LA- glycerol reaction compared to that of LA-xylitol reaction can be explained by the differences between the number of hydroxyl groups in glycerol and xylitol.

3.3.2 ^{13}C-NMR spectroscopic analysis

The NMR analysis was performed to confirm the chemical structure of the step-one and step-two resins and also for measuring the obtained LA chain length. The ^{13}C-NMR spectra of the step-one and end-capped resins are shown in figure 4. The expected and observed chemical shifts and assignments are shown in table 1. Shifts for different carbon environments have been assigned based on data from the literature (Åkesson, Skrifvars, et al. 2010b, Bakare, Åkesson, et al. 2015, Bakare et al. 2014b, Adekunle,

Åkesson, and Skrifvars 2010, Xiao, Mai, et al. 2012) Carbon environments for the ideal structures of step-one and step-two resins are presented in figure 3a. and 3b., respectively. As it can be seen in figure 3a. for the step-one resin, 9 different carbon environments were expected: $A_{1,2}$ for methyl groups, B_{1-4} for CHs adjacent to different groups (shown in table 1), $C_{1,2}$ for carbonyl groups and the CH_2 (B_4, B_5) in the central xylitol structure.

The number of expected chemical shifts would be even greater in the end-capped resins case as the chemical structure is more complex. Apart from chemical shifts of methyls (A), CHs (B) and carbonyls (C), another chemical shift for C=C bond is also expected.

In the carbonyl area (160 – 180 ppm) (Bakare, Åkesson, et al. 2015), two peaks for the carbonyl groups of LA were expected: C_1 for the main-chain carbonyl C=O and C_2 for LA carbonyl group adjacent to the –O–CH_2– branch of the xylitol core molecule which both of them were clearly raised at 169.59 (C_1) and 169.89 (C_2) (Bakare, Åkesson, et al. 2015). Also, another weak peak was observed in the step-one resin at 174.80 ppm which can be assigned to C=O of the LA end-group, for the remaining unreacted LA (Bakare et al. 2014b, Lunt 1998).

For the end-capped resin however, in the carbonyl area, the signal is broad, as LA carbonyls next to the xylitol core molecule, and next to the methacrylic end, will give different signals compared to a LA carbonyl next to another LA component (Fig 4b.). In addition, another carbonyl group belongs to a methacrylic end-group is also expected which can be seen at 166.57 ppm. Another weak peak was also observed at 171.19 ppm which can be assigned to carbonyl of methacrylic acid, released during the end-capping

reactions. The weak peak which is seen at 163.18 ppm is corresponded to carbonyl groups of methacrylic anhydride (Raquez et al. 2010b).

The chemical shifts for carbon atom adjacent to an oxygen atom would be in the range of 60–75 ppm (Xiao, Mai, et al. 2012). CH groups of xylitol core molecules showed signals in range of 68 ppm to 71 ppm- the CH next to the reacted LA carbonyl group and an oxygen atom gives a broad signal from 68 ppm to 71 ppm (Xiao, Mai, et al. 2012) and it is assigned as $B_{2,3}$ and $B_{\sim 6}$. B_4 and B_5 peaks represent the CH groups in the xylitol core molecule with chemical shifts of 68.7 ppm and 70.2 ppm, respectively. The CH adjacent to the hydroxyl end-group, B_1, gives a signal at 66.61 ppm. The CH_2 group in the xylitol core group can be seen as a weak peak at 68.71 ppm (Murillo, Vallejo, and López 2011). No signal was detected around 64.4 ppm for the CH_2 group of unreacted xylitol molecules suggesting that the reaction of xylitol molecules and LA molecules was complete.

The LA methyl groups were detected in the 16–22 ppm range (Wambua, Ivens, and Verpoest 2003). The hydroxyl functionalized end-group of methyl groups, A_1, are present in the step-one resin and were detected at 20.28 ppm. The CH_3 groups in the LA chains, A_2, were also detected in the range of 16.59-16.67 ppm (Xiao, Mai, et al. 2012). The same signals were identified in the end-capped resin for the A_2 position. Absence of the A_1 signal in the step-two resins, indicates that the end-functionalization reactions were complete. The methyl groups of methacrylate in the end-capped resins A_3, were detected at a range of 17.83 – 18.07 ppm (Kabir et al. 2012).

The olefinic carbon sites, D_1 and E_1, presented in the methacrylated end-groups give signals in range of 126–127 ppm and 135-136 ppm. In addition, presence of free

methacrylic acid, which is formed during the end-capping reaction was confirmed by observing the signal at 129.2 ppm which belongs to the olefinic carbon (Liu et al. 2008).

The NMR analysis confirmed that oligomers from the first synthesis step mainly have

alcohol end-groups. The reaction of xylitol and LA was also confirmed, because there was no evidence of carboxylic acid groups in the NMR spectrum of the step-one resin. The length of the xylitol-LA chains was estimated based on the carbonyl peak areas based on the method described by Bakare et al [25]. The percentage of the LA in forms of reacted with the xylitol and in form of LA reacted in to free oligomers were also calculated based on the same method. From the peak areas of the LA end-groups at 169.59 ppm and the main-chain lactic acid components at 170.8 ppm, the average chain length of the branches was estimated as around three lactic acid units. The branch lengths was measured as 3.3 LA and the percentage of LA reacted to oligomers or lactide was 14%. The percentage of lactic acid reacted with xylitol was measured to be 82.3% and the percentage of chain ends reacted with methacrylic anhydride was 86.7%. The reaction of methacrylic anhydride with the alcohol groups of chains was confirmed by detecting the corresponding signals.

3.3.3 FTIR spectroscopy analysis

The FTIR analysis was applied for further analysis of the synthesized resins. Figure 5, shows the FTIR spectra of step-one, step-two and cured samples. The spectra of the first synthesis step shows a signal at 3500 cm^{-1} which can be attributed to an alcohol end-group (Xiao, Mai, et al. 2012, Bakare et al. 2014b, Bakare, Åkesson, et al. 2015). As expected, this group is not presented in methacrylic anhydride functionalized resins

where hydroxyl end groups were reacted with methacrylic anhydride. The peak for the CH group bond around 2990 cm^{-1} (Xiao, Mai, et al. 2012) can be found in all three spectra; while cured resins show two peaks in the carbonyl range 1740 – 1750 cm^{-1} which indicates two different C=O groups in the structure (Xiao, Mai, et al. 2012, Bakare et al. 2014b).

The presence of signals which correspond to carbon-carbon double bonds at 1635 cm^{-1} (stretching C=C) (Bakare et al. 2014b) and 815 cm^{-1} (bending CH_2) (Hisham et al. 2011) confirm that the end functionalization by the methacrylic anhydride did occur. These bonds are not present in step-one resin spectra. In addition, disappearance of signals related to C=C bond in the cured resin spectra and an increase in the bond –CH stretching from 2850 to 3000 cm^{-1} indicates that the crosslinking reaction did occur (Bakare et al. 2014b, Bakare, Åkesson, et al. 2015).

3.3.4 Biobased content

The biobased content of the resin was calculated based on ASTM D6866 standard using the following formula:

$$\text{Biobased content} = \frac{biobased\ carbon\ content}{total\ carbon\ content} \times 100$$

$$= \frac{X_m + LA_m - W_m}{X_m + LA_m - W_m + MAA_m - MA_m} \times 100$$

Where, X_m is the weight of Xylitol core molecule, LA_m is the weight of LA, W_m is the weight of released water during condensation polymerization. MAA_m is the weight of methacrylic anhydride and MA_m is the weight of the released methacrylic acid during the end-capping reactions (Bakare, Åkesson, et al. 2015).

$$C_5H_{12}O_5 + 15C_3H_6O_3 \longrightarrow C_{50}H_{72}O_{35} + 15H_2O$$
$$C_{50}H_{72}O_{35} + 5C_8H_{10}O_3 \longrightarrow C_{70}H_{92}O_{40} + 5C_4H_6O_2$$

Bio based content is found to be 76.7%.

3.3.5 Curing optimization

Presence of cracks in casted resins dramatically reduces the mechanical strength of the matrix (Gledhill et al. 1978). The proper mix ratio, severity of mixing, applied mixing method and mix temperatures would affect final distribution and propagation of cracks (Phillips, Scott, and Jones 1978, Carfagna, Amendola, and Giamberini 2013, Heinrich et al. 2013). Improper mix ratio of the curing agent and resins results in higher exotherms, faster gelation and subsequently more shrinkage due to excessive thermal zoning (or hot spots) during the curing process (Pereira and d'Almeida 2016, Le Corre et al. 2012). Investigating different mix ratios, demonstrates that 1% *wt* curing agent was proper for the synthesized resin. However, poor dispersion of solid state benzoyl peroxide results in benzoyl peroxide rich areas causing different rates of curing within the mixed product and subsequently, initiation of cracks. In other words, gradients in concentration of the hardener causes microcracks to be initiated during gelation phase which develop as the material cures or during thermal cycling (Campbell Jr 2003).

Figure 6a. shows the initiation of cracks in the cured samples. As it can be seen, the cracks can occur due to presence of bubbles. However, propagation of the cracks can also be terminated when they reach the microbubbles (figure 6b.) as well as another crack propagating in the other direction (figure 6a.). The twofold effect of the bubbles can be better seen in figure 6c. were the microcrack is been initiated from one micro bubble and is also terminated at the other end by colliding with another microbubble. It can be seen in the figure 6d. that presence of benzoyl peroxide solid particles results in the initiation

of cracks. When curing agent was added in form of powder, micro particles are inevitable. This problem was overcome by dissolving the curing agent in a solvent and mixing the solvent with the matrix at elevated temperatures (up to 50°C) for better mixing.

The presence of bubbles in the casted samples was another problem which reduces the mechanical strength of the product and causes microcracks. Uncured resins were kept at ambient temperature under partial vacuum (20 millibars) for an hour which resulted in evaporation of the added solvent as well as eliminating the bubbles in the matrix. By changing the mixing method, applying partial vacuum and implementing a stage curing technique, the cracking and bubble problems were fully resolved.

3.3.6 Differential Scanning Calorimetry

DSC technique is currently applied to investigate curing of resins by detecting crosslinking reaction exotherms as well as residual exotherms of cured samples at different temperatures (Liang and Chandrashekhara 2006, Mohan, Ramesh Kumar, and Velmurugan 2005, Bakare, Ramamoorthy, et al. 2015). Figure 7 presents the exothermic heat reaction of the curing reaction.

From the thermogram, it was observed that the resin cured between 100°C and 140°C, (revealing an exothermic peak). The reaction heat was measured as 275.5 J/g, and the peak temperature was 117.25°C. The onset temperature is defined as the intersection of the tangent of the peak with the extrapolated baseline, and measured as 108.10°C. Bakare et al. reported a curing temperature range of 80°C to 130°C with exothermic heat evolved at 227.4 J/g for a glycerol-LA thermoset resin with a length chain of 3 LAs (Bakare et al. 2014b). In a more recent study, a curing temperature range of 90°C to

150°C and a heat of reaction of 194 J/g for an allyl alcohol-LA resin was reported (Bakare, Åkesson, et al. 2015).

The peak exotherms in figure 7a. present the residual exotherms of DSC analysis from 25°C to 200°C at a heating rate of 10°C/min for resin samples cured at 90°C, 100°C, 110°C, 120°C, 130°C, 140°C and 150°C for 20 minutes. Presence of substantial residual heat in the DSC curves is an evidence showing that samples cured at temperatures below 110°C did not cured completely. However, there is a substantial reduction in exotherms of samples cured at temperatures above 110°C which is explained as the onset temperature of the resin was measured as 108.1°C. The residual exotherms were also shifted to higher temperatures for samples cured at 120°C, 130°C and 140°C. The absence of residual exotherms for samples cured at 150°C for 20 minutes, indicates that the curing reaction is fully completed. Therefore, in this study, the post curing conditions for curing was selected as 20 minutes at 150°C.

3.3.7 Thermogravimetric analysis

Oxidative temperature is a measure of thermal stability. Higher oxidation temperature is associated with better overall quality of the tested products (Mashouf Roudsari, Mohanty, and Misra 2014). The degradation in thermoset systems, occurs after decomposition of the crosslinked polymer network as well as the random scission of the linear chains (Adekunle, Åkesson, and Skrifvars 2010). In this study, the TGA was performed to check the thermal stability of resins by recording the percentage weight loss of the cured samples versus time. The sample was heated from 30°C to 600°C, at the uniform heat rate of 10°C/min in a N_2 gas purge stream of 20 mL/min. The thermogravimetric curves of cured resin at 150°C for 20 minutes is presented in figure 8.

The degradation occurred in the temperature region of 170°C to 462°C. The maximum rate of decomposition which indicates the maximum rate of oxidation was observed at 380°C. The char weight percent was 3.6% *wt* and the appearance of weak multiple peaks is an evidence for the presence of volatile substances in the resin.

3.3.8 Dynamic Mechanical Thermal Analysis

DMTA was performed to characterize the crosslinked resins, cured via different methods. There is evidence that stage curing increased mechanical properties of cured samples as it allows gradual solidification which results in a more relaxed state with less built in stresses (Vergnaud and Bouzon 2012). Figure 9a. shows the storage modulus G' in the temperature range of -20°C to 150°C for samples cured by the different methods. The measured storage modulus with standard deviations at 25°C are given in table 2. The storage modulus is related to the molecular packing density in the glassy state (Vergnaud and Bouzon 2012, Chang et al. 2012b). Storage modulus curves in figure 9a. show that the resin cured with method b has a higher storage modulus than all other analyzed resins.

Therefore, better mechanical properties are expected for the resins cured with this method. Due to the free movement of the polymer chain in the rubbery plateau region (Bakare, Ramamoorthy, et al. 2015), the storage modulus of samples decreases in this temperature interval. The temperature range for major changes in storage modulus for method b cured resins is observed between 48°C and 83°C. This interval for resins cured with method a was 36°C to 75°C showing that stage curing was effective for increasing mechanical properties.

Figure 9b. shows the loss modulus G" curves for the samples cured with different methods and in table 2 the loss modulus of different samples at 25°C is given. The loss

modulus is broader and shorter in samples cured with method b, suggesting better mechanical properties. The rather low value of the loss modulus was due to the rubbery plateau state of the cured resin and indicates the strong tendency for reversibility in the samples (Bakare, Ramamoorthy, et al. 2015).

Figure 9c. shows the tan δ curves for the samples cured by the different methods and in table 2, peaks of tan δ for the different cured resins are presented. The tan δ peaks were recorded at 93°C, 98°C and 95°C for resins cured via method a, b and c, respectively. The higher tan δ peak values for resins cured with method b indicates better mechanical properties. The tan δ peak for thermoplast PLA was reported at 50°C (Oksman, Skrifvars, and Selin 2003). However, in LA based thermoset systems, tan δ values would be comparably higher. Åkesson et al. reported a tan δ of 83°C for a synthesized resin from pentaerythritol and LA. The observed tan δ for a Glycerol-LA thermoset resins was observed at 97°C (Bakare et al. 2014b). In addition, the tan δ value is believed to shift to higher temperatures after applying reinforcement fibers. The better adhesion of the fiber to the matrix generally results in the higher tan δ value and better mechanical properties (Adekunle, Åkesson, and Skrifvars 2010, Bakare, Ramamoorthy, et al. 2015).

3.3.9 Viscosity measurements

The viscosity for thermoset resins is of importance because the resin must flow around and impregnate the reinforcement (Komkov, Tarasov, and Kuznetsov 2015). The viscosity of the resin was monitored using stress viscometry at temperatures 25°C, 35°C, 45°C, 55°C, 65°C, 75°C and 85°C and is presented in figure 10. The resin has a viscosity of 2.97 Pa s which drops to 0.06 Pa s upon increasing the temperature to 85°C. Åkesson

et al. previously reported a viscosity of 7000 Pa s at room temperature and 4 Pa s at 80°C for a four armed, star-shaped oligomer, synthesized by reacting pentaerythritol with LA (Åkesson, Skrifvars, et al. 2010b). The high viscosity at room temperature makes the resin unsuitable for impregnation of to the fiber reinforcement by the resin, even at elevated temperatures (Komkov, Tarasov, and Kuznetsov 2015). In a more recent study, Bakare et al. synthesized a glycerol-LA resin with a better processability at room temperature with a viscosity of 1.09 Pa s and 0.04 Pa s at temperatures above 100°C (Bakare et al. 2014b).

3.3.10 Water adsorption tests

The moisture content of a polymer affects its properties such as electrical insulation resistance, dielectric losses, mechanical strength, appearance, and even its dimensions. Diffusion of water into polymer matrix is a function of the square root of immersion time, type of water exposure, dimensions and shape of the specimen, and inherent properties of the plastic (ASTM D570-98(2010)e1 2010). In this study, the water adsorption tests were performed to determine the effects of exposure to water on water absorption rate of cured samples based on ASTM D 570–98. In the performed tests, samples with water adsorption rates of less than 1 % or 5 mg between intervals, were considered as substantially saturated, and the duration time that it took the samples to reach the saturation state was considered the water saturation time. The water saturation time is dependent on specimen thickness and the difference between the substantially saturated weight and the dry weight was reported as the water absorbed.

Figure 11a. presents the percent of absorbed water versus immersing time at 50°C. For long-term immersion, the increase in weight was reported as a function of the

square root of immersion time- presented in figure 11b. The initial slope of the graph is proportional to the diffusion constant of water in the matrix which is 0.252 and 0.699 at 23°C and 50°C, respectively. The water saturation for long-term immersion at 23°C was 504 h. The water saturation for immersion at 50°C was 110 h. Percentage water adsorbed after saturation of 50°C immersion and Long term immersion at 23°C were 14.02 ±0.35 and 8.08 ± 0.61%, respectively. Saturated water adsorption based on Two-Hour Boiling Water Immersion was 7.27 ± 0.42 %.

3.4 Conclusion

In this study, a biobased thermoset resin was synthesized by poly-condensation of LA and xylitol followed by end-functionalization of branches with methacrylic anhydride. Chemical structure of resins were confirmed employing ^{13}C NMR and FTIR techniques. The resins were thermally cured employing a free-radical polymerization strategy. Different curing strategies and techniques were investigated for optimization and characterization of the curing process. Thermogravimetric analyses of the cured resin was also carried out to check the thermal stability of the cured resins. The viscosity of neat resins was measured at temperatures in the range of 25°C to 85°C. It is observed that at room temperature the resin has a viscosity of 2.969 Pa s which drops to 0.056 Pa s upon increasing the temperature to 85°C. Finally, water adsorption tests were carried out to check the water absorption properties of cured resins. Water absorbed percentage after saturation for 50°C immersion and Long term immersion at 23°C were 14.02 ±0.35 and 8.08 ± 0.61%, respectively. Saturated water adsorption after Two-Hour Boiling Water Immersion was 7.27 ± 0.42 %. The synthesized thermoset resin showed a Tg, substantially higher than that of thermoplast PLA, at 98°C. The biobased content of the

resin was calculated as 76.7%. High biobased content of the structure, good thermomechanical and rheological properties and good thermal stability are of advantages of the synthesized resin.

Acknowledgement

The authors would like to acknowledge the funds provided by Agricultural Experiment Station, South Dakota State University and North Central Sun Grant via Department of Energy, Colorado in support of this research work.

Figures and Tables

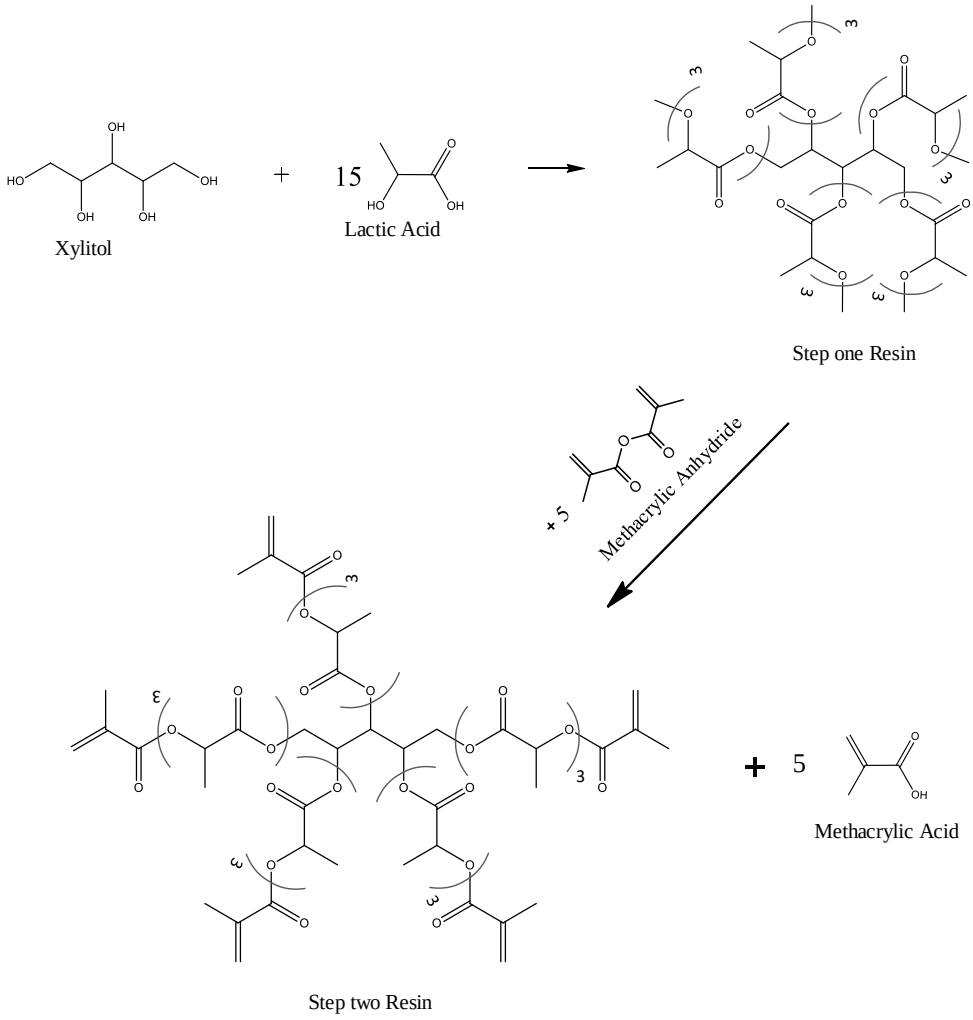

Figure 3. 1. Reaction scheme for the two-stage synthesis of methacrylate functionalized xylitol-LA resins with LA chain of 3

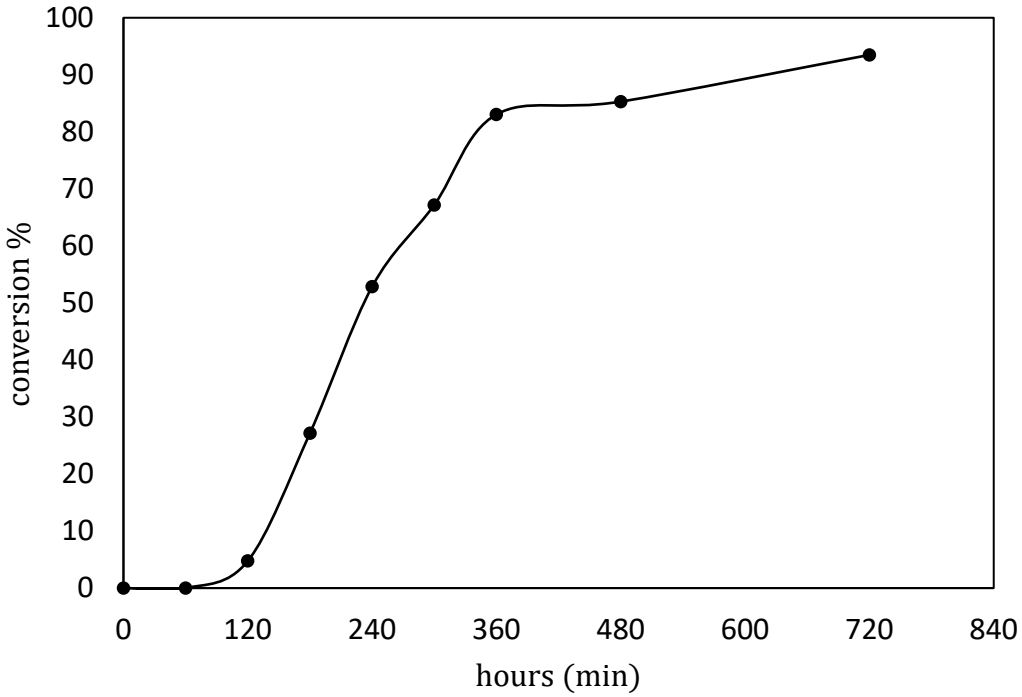

Figure 3. 2. Conversion of carboxyl groups in poly condensation reaction

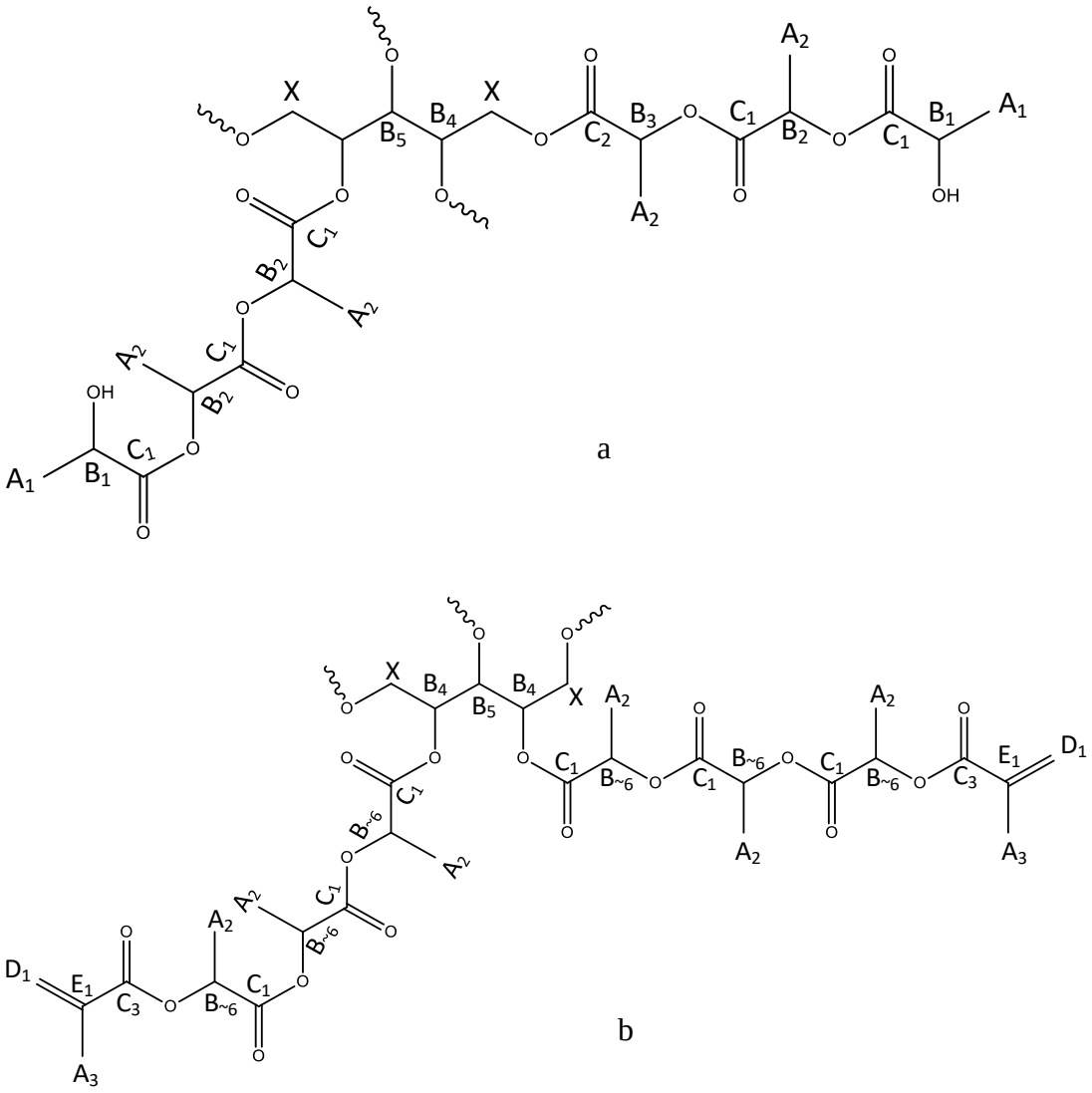

Figure 3. 3. Carbon environments for the ideal structures of a) step-one and b) step-two resins

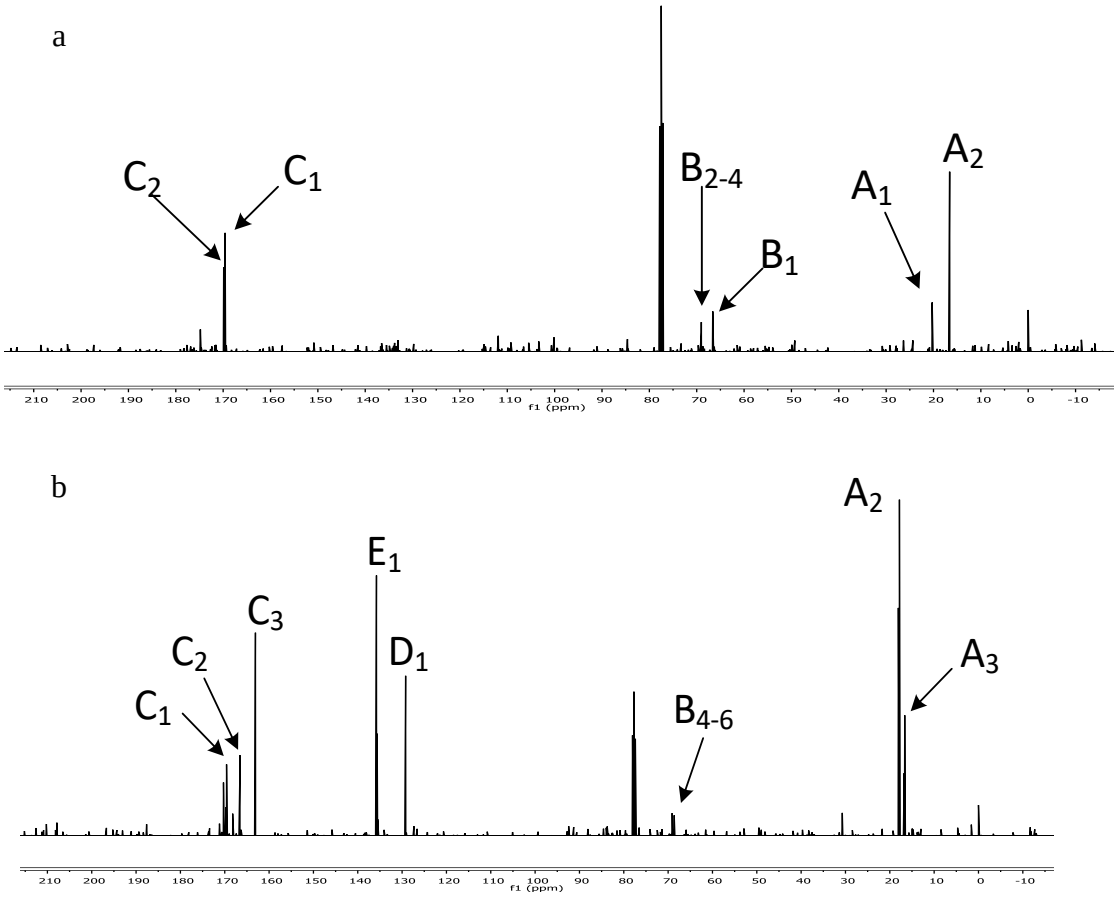

Figure 3. 4. 13C-NMR spectra of the step-one (a) and the end-capped resins (b)

c

b

a

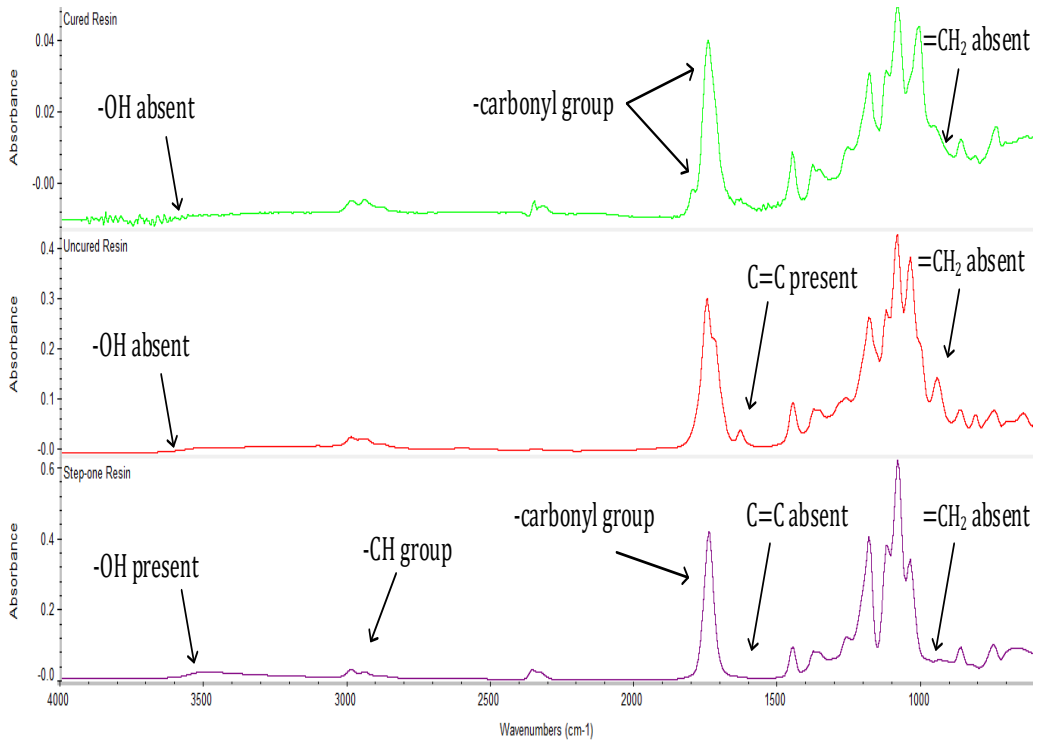

Figure 3. 5. The FTIR spectra of step-one (a), step-two (b) and cured samples (c).

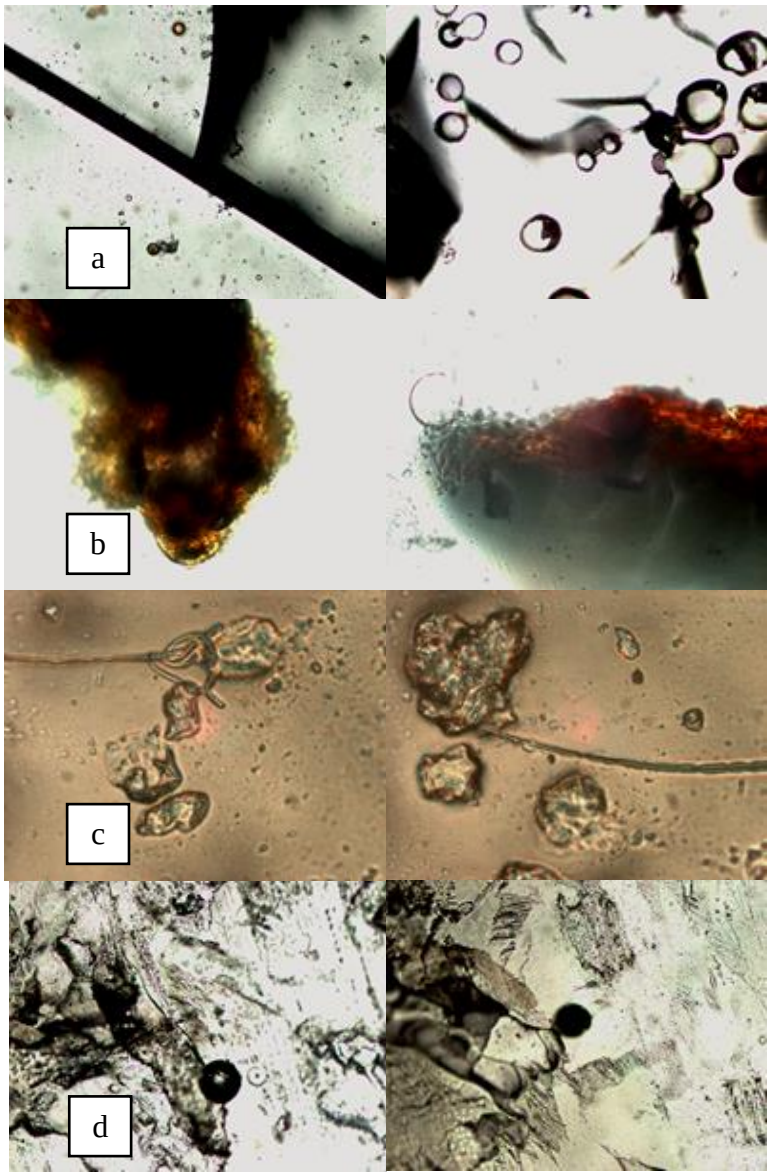

Figure 3. 6. Effect of curing method on distribution and propagation of bubbles and cracks-100X

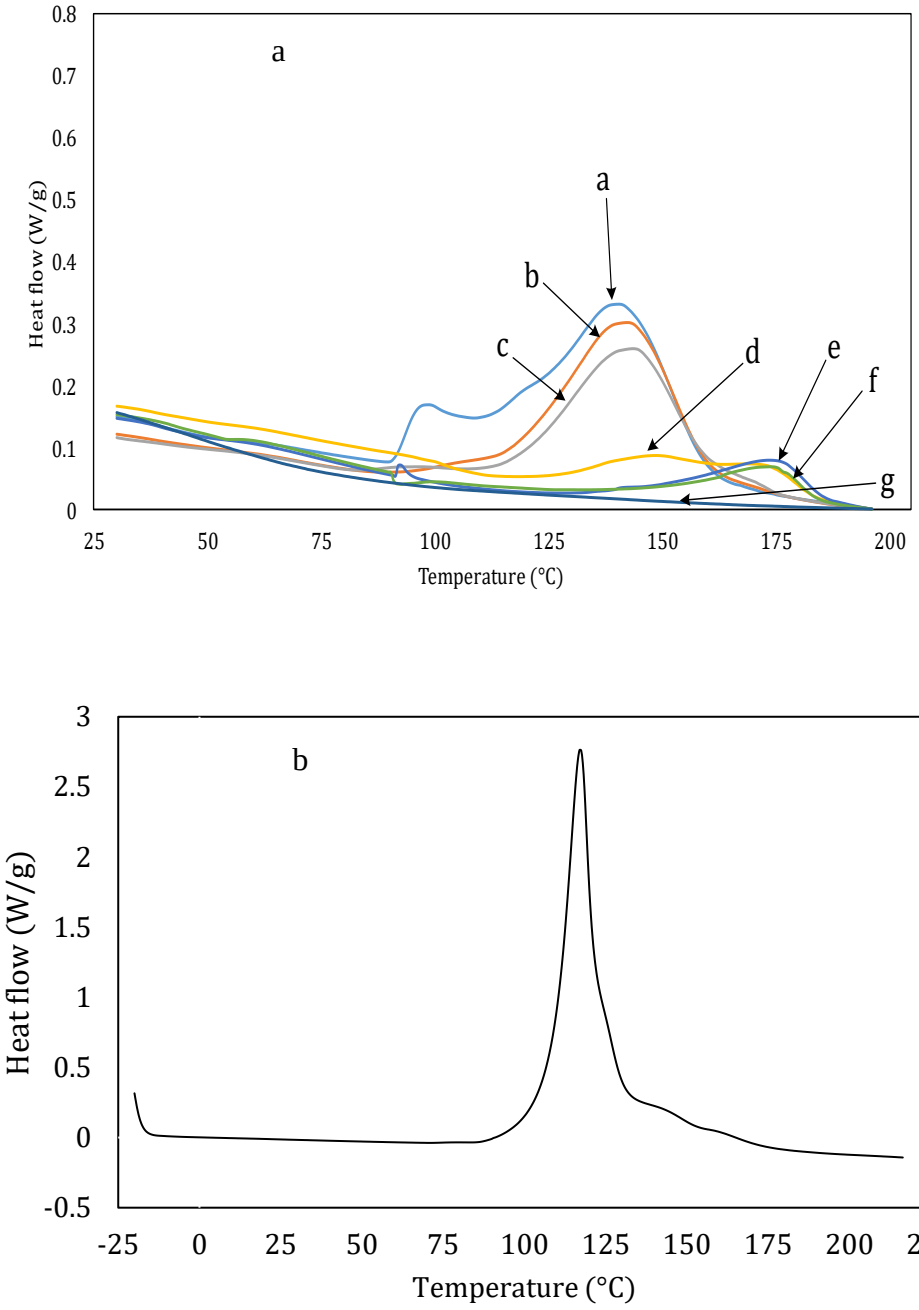

Figure 3. 7. a) DSC curves for residual exotherms for samples cured for 20 minutes at 90°C (a), 100°C (b), 110°C (c), 120°C (d), 130°C (e), 140°C (f) and 150°C (g) b) DSC curve for unreacted xylitol-LA at a heat rate of 10°C/min in the heat range of -20 to 220°C/min

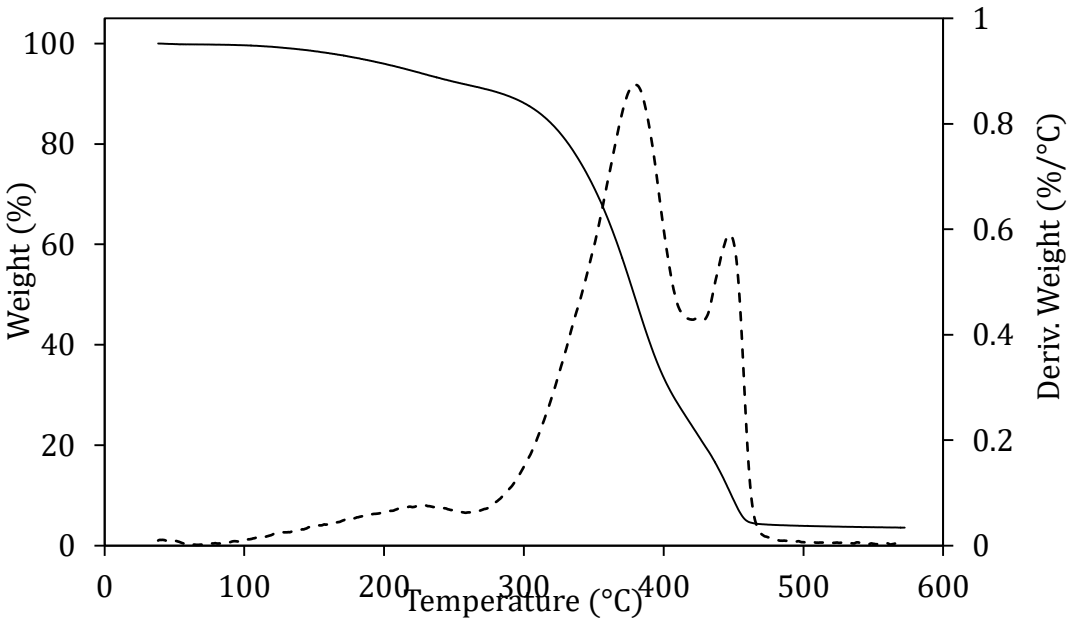

Figure 3. 8. TGA curves for cured resin, solid-line presents Weight (%) and dashed-typed pattern shows Derivative Weight (%/°C)

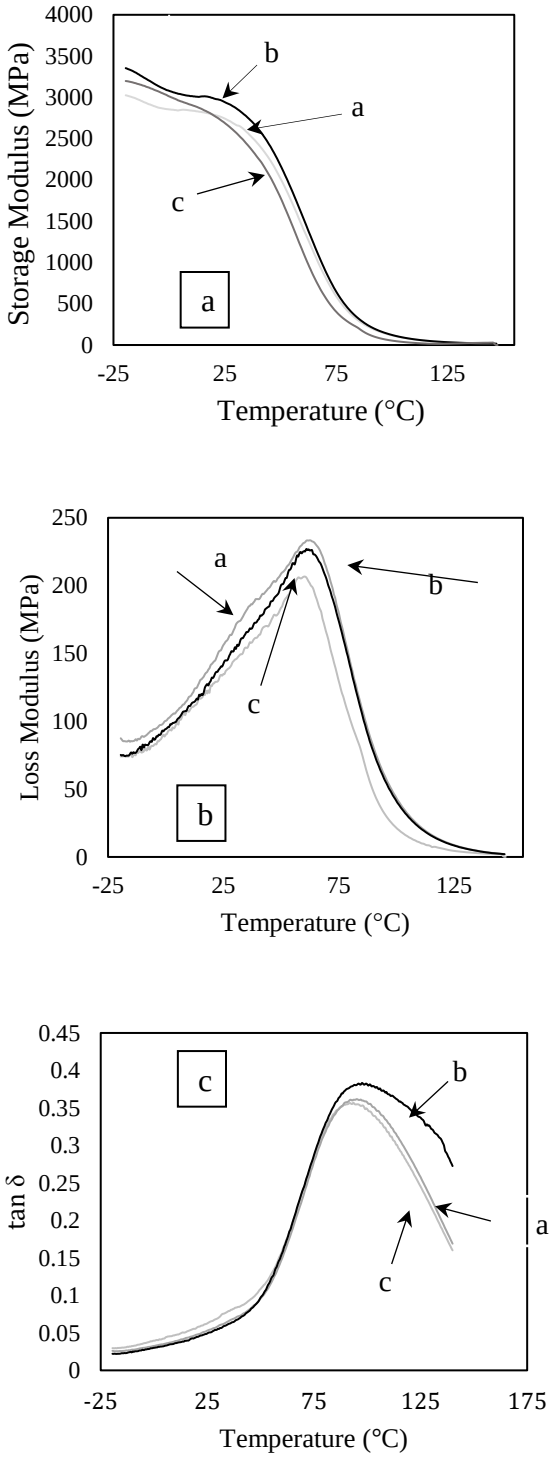

Figure 3. 9. DMA curves ((a) Storage modulus, (b) Loss modulus and (c) tan δ) for samples cured via different methods, a, b and c).

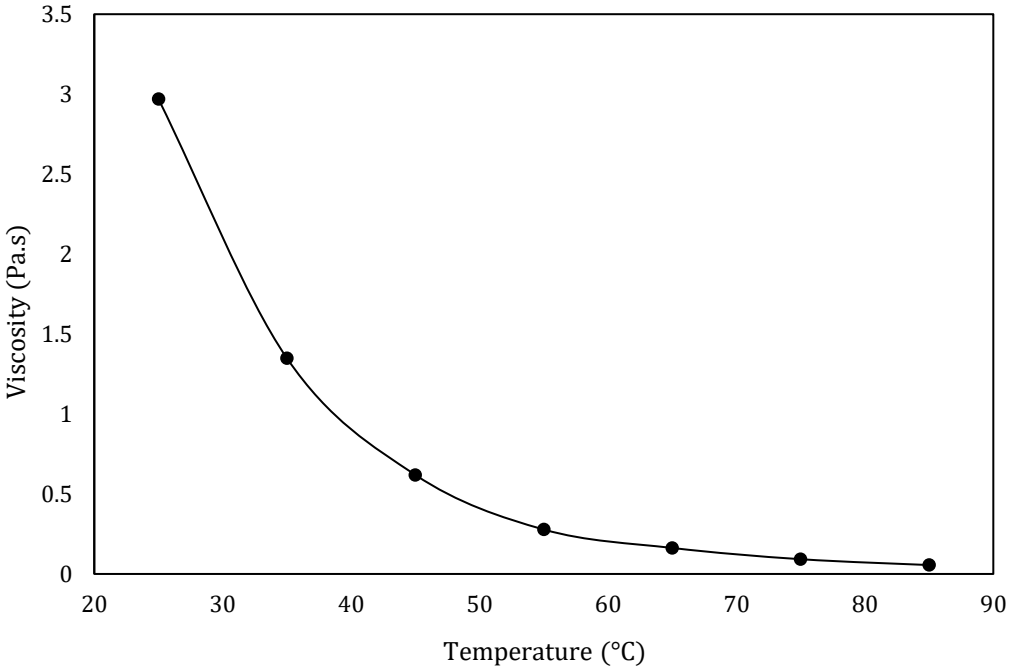

Figure 3. 10. Viscosity of resin as a function of temperature

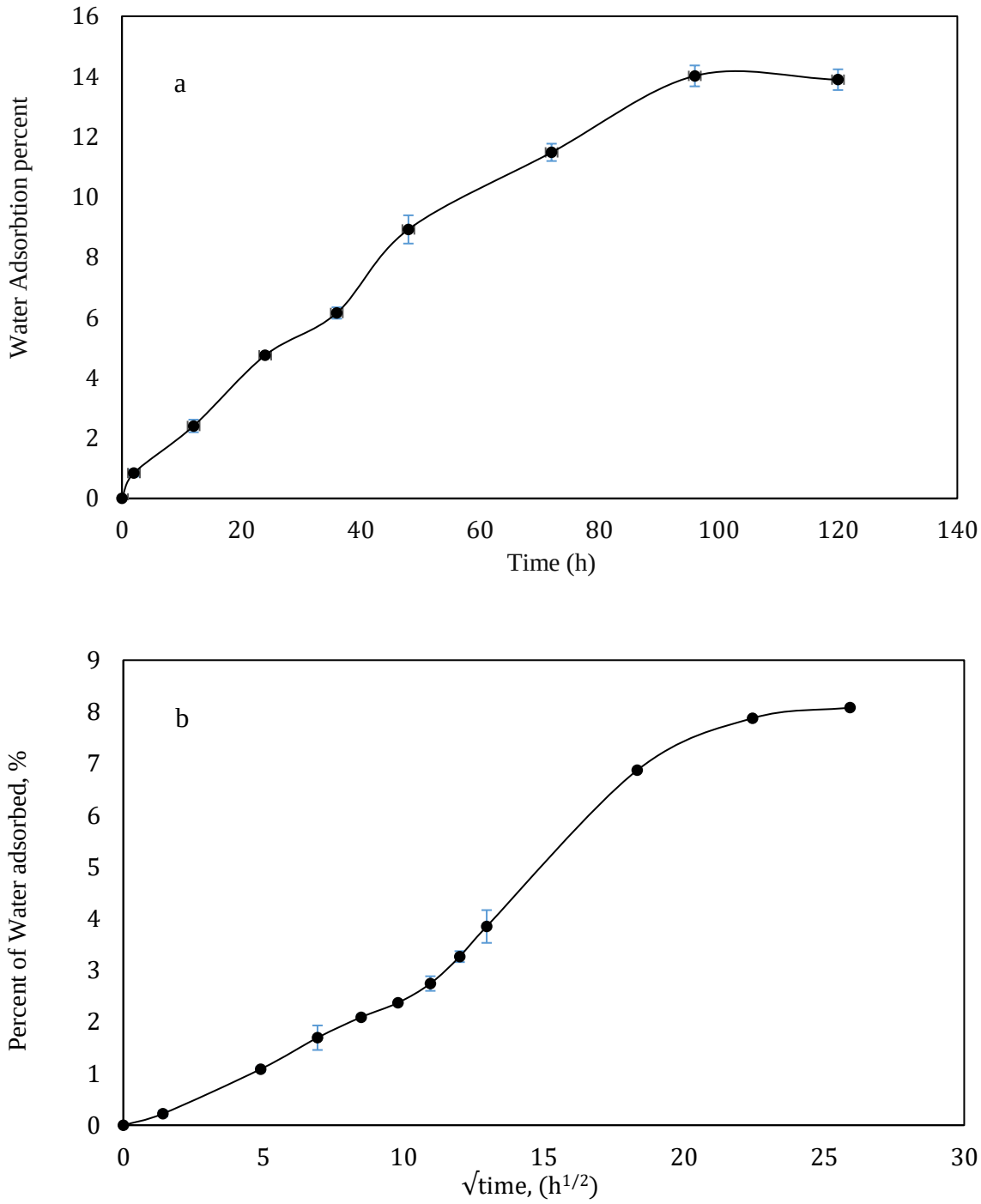

Figure 3. 11. a) percent of absorbed water versus immersing time at 50°C, b) long-term immersion procedure water adsorption; reported as a function of the square root of immersion time

Table 3. 1, Assignment of peaks from ^{13}C-NMR

Peak	Exp Chem shift (ppm)	Obs Chem Shift (ppm)	Assignment
A_1	21.5	20.3	CH_3 -Hydroxyl terminated
A_2	16.5	16.6-16.7	CH_3 of lactic acid–C(=O)–O–
A_3	17.9	17.8 – 18.1	CH_3 of methacrylate
B_1	65.6	66.6	CH–C(=O)–OH–CH_3
B_2	70.6	70-71	CH–C(=O)–O–CH_3
B_3	70.3	70-71	CH–C(=O–O)–O–CH_3
B_4	68.7	68.7	CH–CH_2–O–CH
B_5	70.2	70.2	CH–CH–CH–O
$B_{\sim 6}$	70.4-70.7	71-71	CH– End-capped main chain
C_1	170.8	169.9	C=O–Main chain–
C_2	169.0	169.6	C=O–O(CH_2)–CH
C_3	167.2	166.57	C=O–O–C
D_1	125.2	126–127	CH_2= C–
E_1	136.0	135-136	C=CH_2–C–CH_3

Table 3. 2, Thermal-Mechanical Characterization Results of the Resin

DSC				
	Heat of exotherm for uncured resin (J/g)		275.5	
	Curing temperature interval		100 -140°C	
	Heat of exotherm for cured resin (J/g) at 150°C		0	
	Peak temperature		117.25°C	
	Onset temperature		108°C	
DMA				
		method a	method b	method c
	tan δ peak (T_g °C)	93°C	98°C	95°C
	Storage modulus (MPa) at 25°C	2739 ± 102	2938 ± 101	2875 ± 101
	Loss modulus (MPa) at 25°C	171 ± 14.6	155.8 ± 14.5	141.7 ± 15.2
TGA				
	Degradation temperature range		170 – 462°C	
	Degradation temperature at 10 wt % loss (°C)		269°C	
	Maximum degradation (°C)		380°C	
	Second derivative peak (°C)		435°C	

Chapter 4 - Effect of lactic acid chain lengths on thermomechanical properties of *star*-LA-xylitol resins and jute reinforced biocomposites

Arash Jahandideh[2,*], Nima Esmaeili[2], Kasiviswanathan Muthukumarappan[1]

[1]Department of Agricultural and Biosystems Engineering, South Dakota State University, PO Box 2120, Brookings, SD-57007, USA

[2]Institute for Materials Research and Innovation, University of Bolton, Deane Road, Bolton, BL3 5AB, UK

This chapter has been published in Polymer International Journal

Abstract

Star-shaped bio-based resins were synthesized by direct condensation of lactic acid (LA) with xylitol followed by end-functionalizing of branches by methacrylic anhydride with three different LA chain lengths (3, 5 and 7). Thermomechanical and structural properties of resins were characterized by ^{13}C NMR, FT-IR, Rheometer, DSC, DMA, TGA and flexural and tensile tests. An evaluation of the effect of chain length on synthesized resins showed that the resin with five LAs exhibited the most favorable thermomechanical properties. Also, the resin's glass transition temperature (103 °C) was substantially higher than that of the thermoplast PLA (~55 °C). The resin had low viscosity at its processing temperature (80 °C). The compatibility of the resin with natural fibers was investigated for biocomposite manufacturing. Finally, composites were

* Corresponding author current address: Agricultural, Biosystems and Mechanical Engineering Department, 1400 North Campus Drive Box 2120, Brookings, SD 57007, USA. Tel.: +1 (605) 6885670
arash.jahandideh@sdstate.edu

produced from the n5-resin (80 *wt*% fiber content) using jute fiber. The thermomechanical and morphological properties of the biocomposites were compared with jute-PLA composites and a hybrid composite made of the impregnated jute fibers with n5 resin and PLA. SEM and DMA showed that the n5-jute composites had better mechanical properties than the other composites produced. Inexpensive monomers, good thermomechanical properties and good processability of the n5 resin make the resin comparable with commercial unsaturated polyester resins.

Keywords: Synthesis; Thermosets; Star-shaped; Lactic acid; Biocomposites; Thermomechanical properties

---

4.1 INTRODUCTION

Due to the global burden on petroleum-derived materials and ecological and economic concerns associated with petroleum based resins, different bio-based raw materials have been evaluated for the production of composites. Lactic Acid (LA) is a renewable resource abundantly available via the fermentation of carbohydrates.(Martinez et al. 2013, Jimenez, Peltzer, and Ruseckaite 2014, Lunt 1998) A limitation of the impregnation of fibers with the thermoplast Polylactic Acid (PLA) viscous matrix is that it slows down the manufacturing process and also reduces the mechanical strength of the composites.(Komkov, Tarasov, and Kuznetsov 2015, Han et al. 2015) Thermosets have the inherent advantage of the lower viscosity, which results in better processability and improved impregnation of fibers. These characteristics make thermosets desirable for reinforced composite applications.(Liang and Chandrashekhara 2006) The star-shaped LA (*star*-LA) based thermosetting resins and their potential for composite manufacturing have been investigated previously by researchers.(Bakare, Åkesson, et al. 2015,

Adekunle, Åkesson, and Skrifvars 2010, Sakai et al. 2013, Chang et al. 2012b, Åkesson et al. 2011b) To make the LA based resins cross-linkable, the hydroxyl terminal groups of the LA chains are substituted with unsaturated groups, which can be used in the crosslinking reactions to create a rigid three-dimensional network structure. Another strategy for increasing the crosslinking density of thermosets is to employ a core molecule in the structure of the LA oligomers which consequently improves the mechanical properties of the crosslinked thermoset.(Sachlos and Czernuszka 2003, Bakare, Åkesson, et al. 2015, Åkesson, Skrifvars, et al. 2010b)

In our research group's previous work, star-shaped resin from LA and xylitol was synthesized and characterized.(Jahandideh and Muthukumarappan 2016a) Resins were synthesized via a two-step synthesis strategy: direct condensation polymerization and an end-functionalization reaction. The aim of this study was to synthesize and characterize *star*-LA-xylitol resins with chain lengths of 3, 5 and 7 LA monomers. The chemical structure of these resins were determined by Nuclear Magnetic Resonance (^{13}C NMR) spectroscopy and Fourier Transform Infrared Spectroscopy (FT-IR) techniques. The thermomechanical properties of the cured resins were also investigated via Rheometer, Dynamic Mechanical Analyzer (DMA), Differential Scanning Calorimetry (DSC), Thermogravimetric Analyzer (TGA) and flexural and tensile testing. The compatibility of the produced resins with natural fibers was also investigated employing jute fibers. The mechanical properties of the biocomposites compared with that of the jute-PLA and hybrid composites made up of n5 resin-impregnated jute fibers and PLA, respectively. These composites were further characterized by Scanning Electron Microscopy (SEM) and DMA.

4.2. EXPERIMENTAL

4.2.1. Materials

All chemicals used in this study were purchased from Sigma-Aldrich (MO, USA) at the highest purity available and used as recieved. L (+)-lactic acid and xylitol were used as the primary reactants, toluene was used for water removal, and methanesulfonic acid was used as catalysts during polycondensation reactions. Benzene-1,4-diol was used as the inhibitor and methacrylic anhydride was used for end-functionalization. Dibenzoyl peroxide was used as the free radical initiator for crosslinking. Xylenes, propan-2-ol, potassium hydroxide and phenolphthalein (1% in ethanol) were used for the titration. Commercial jute fibers provided by James Thompson & Co Inc., 100% (NY, USA) was used as reinforcement in the biocomposites. Acetone was used for fiber preparation. NatureWorks Ingeo™ 4043 (MN, USA) PLA pellets were used for preparation of PLA sheets.

4.2.2. Resin synthesis and curing

The *star*-LA-xylitol resins with LA chain lengths of 3, 5 and 7 were synthesized via a direct condensation reaction of LA with xylitol and end-functionalizing of branches with methacrylic anhydride, which has been described in a previous study by our research group.(Jahandideh and Muthukumarappan 2016a) The reaction schemes are presented in Fig. 1A and 1B. The thermal curing was performed using an optimized free-radical polymerization method.(Jahandideh and Muthukumarappan 2016a) Resins were mixed with 1 *wt%* dibenzoyl peroxide dissolved in toluene, at 50 °C, in order to avoid premature curing(Chang et al. 2012b) and then thermally cured using a heating regime. Curing was initiated at 50 °C for 10 minutes followed by 10 minutes at 90 °C, and then post-cured at 150 °C for 20 minutes. The same curing

procedure was then applied for the production of biocomposites via a compression molding method.

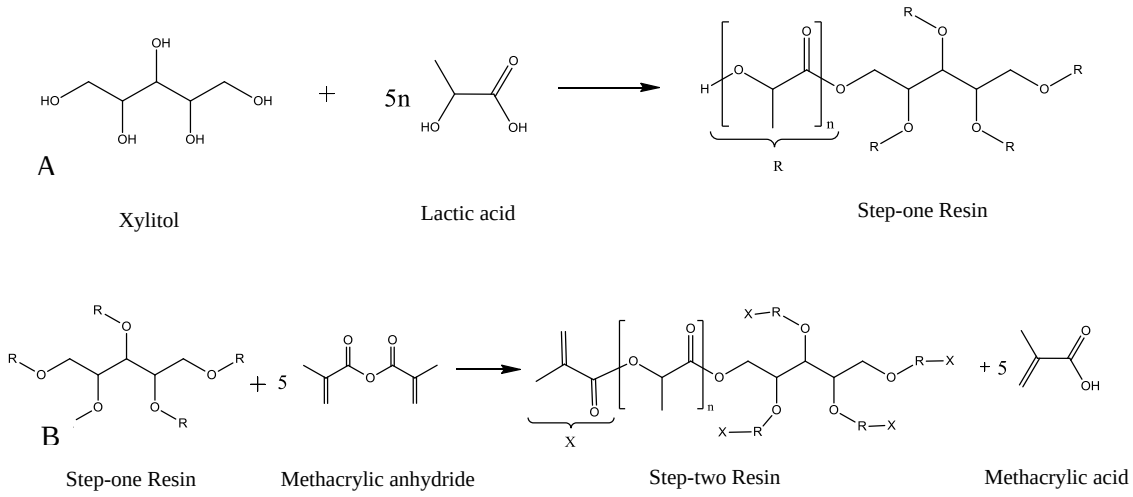

Figure 4. 1. Reaction scheme for A: the step-one resins, and B: the step-two (functionalized) resins- n=3, 5 and 7.

4.2.3. Resin characterization

An acid-base titration method was employed to evaluate the progress of the polycondensation reactions. In this method, aliquot samples (1 g), taken hourly for 12 h, were diluted with 20 mL of 1:1 (mol mol^{-1}) xylene/ propan-2-ol solutions, and then titrated with 0.5 M KOH in absolute ethanol in the presence of 1 *wt%* phenolphthalein.

The chemical structure of resins was determined via ^{13}C NMR spectrometry (Bruker BioSpin GmbH, Germany) at 400 MHz. The sample's concentration in 5 mm tubes was 10 *wt%* in $CDCl_3$. The internal standard was tetramethylsilane (TMS) and the shifts were expressed in ppm.

The FT-IR analysis were carried out using Nicolete 6700 spectrometer (ThermoFisher Scientific, MA, USA) in the range of 600-4000 cm^{-1} using 60 scans and 4 cm^{-1} resolution.

Calorimetric analyses were carried out by a DSC on a TA Instrument Q 100 (V9.9 Build 303, Water LLC, DE, USA) thermal analyzer. Approximately, 10 mg samples of uncured resins were sealed in hermetic aluminum pans and analyzed under nitrogen atmosphere from 0 °C to 220 °C at a heating rate of 10 °C min^{-1}.

TGA of the cured resins were carried out on a Q50 (TA Instruments, Waters LLC, DE, USA). Approximately, 10 mg samples were heated from 30 °C - 600 °C, with a heat rate of 10 °C min^{-1} under a N_2 purge of 20 mL min^{-1}.

Dynamic mechanical analysis was performed on a DMA (Q800, TA Instruments, Waters LLC, DE, USA). The dimensions of the samples were approximately 60 mm × 15 mm × 3 mm and the tests were performed in a temperature range of -20 °C - 150 °C in a dual cantilever bending mode with the heat rate of 5 °C min^{-1} and frequency of 1 Hz at an amplitude of 15 µm. These tests were performed under nitrogen atmosphere.

The viscosity of the neat resins was determined using a viscoanalyzer (ATS Rheosystems, Rheologica Instrument Inc., NJ, USA) using a truncated cone plate configuration (Ø15 mm, 5.4 °C) in temperature range from 20 °C - 120 °C. The shear stress ranged between 0.2-400 Pa, 70-1280 Pa and 200-1280 Pa for n3, n5 and n7 resins, respectfully.

The cured samples were further characterized by a three-point bending flexural test and tensile test according to ASTM D790-03 and ASTM D638-10, respectively using

a MTS Insight 5 (MTS Systems Corporation, USA). For flexural tests, the machine was equipped with a 5 kN load cell. The cross head speed was 1.5 mm min^{-1} and the span was 35 mm. For the tensile tests, the machine was equipped with a 10 kN load cell and a mechanical extensometer. A minimum of five test specimens were tested.

4.3. Composites preparation

The reinforcement mats were cut into 20 cm × 20 cm pieces, washed thoroughly with acetone, and dried in a vacuum oven at 15 mbar and 105 ºC for 2 h. For the n5-jute composites, impregnation was carried out via the hand lay-up method. The neat resin was mixed with 1 *wt%* dibenzoyl peroxide in toluene and then applied on the surface of the fiber mats. The fabric laminates included six sheets of resin impregnated jute mats. The hybrid (n5-PLA)-jute composites were fabricated by an initial impregnation of the mats with the n5 resin. The n5 resin (10 *wt%*) was spread on the dried sheets at ambient temperature, and the fibers were pressurized at 2 MPa to obtain satisfactory impregnation. The stacks were kept under partial vacuum at ~15 mbar. The PLA pellets were compress molded to produce PLA sheets of 18 cm × 18 cm with approximately 0.3 mm thickness. The sheets were then placed between the impregnated jute mats and the stack was placed in a Teflon frame. Laminate stacks consisted of 6 layers of impregnated mats and 5 PLA sheets containing 80 *wt%* fiber, 10 *wt%* n5 resin and 10 *wt%* PLA. PLA-jute composites were prepared utilizing the prepared PLA sheets with a fiber load of 80 *wt%*. The samples were compression molded with a hydraulic press (automatic hydraulic 30-ton press, Carver-Wabash, USA) at 2-4 MPa to produce composites. The exact fiber weight load was measured by weighing the dry fiber sheets and the final composites. The schematic of composites preparation methods is presented in Fig. 2.

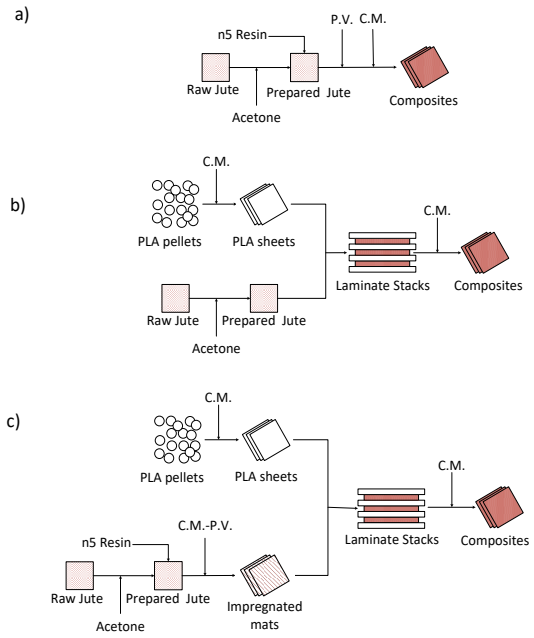

Figure 4. 2. Schematic of composites preparation methods. a) n5-jute composites, b) PLA-jute composites and c) hybrid (n5-PLA)-jute composites. P.V. represents the applied partial vacuum and C.M. represents compression molding.

4.4 Composites characterization

Dynamic mechanical analysis was performed using a DMA (Q800 from TA Instruments, Waters LLC, DE, USA). The dimensions of samples were: 35 mm × 8 mm and thickness of ~3 mm. The tests were performed in a temperature range of -20 °C - 150 °C in a dual cantilever bending mode with a heat rate of 5 °C min^{-1} and a frequency of 1 Hz at an amplitude of 15 µm. Fractured surfaces of the composites were studied with a SEM (Hitachi S-3400N, Tokyo, Japan) with an accelerate voltage of 25 kV. The sample surfaces were sputter coated with gold (CrC-150 sputtering-10nm Au layer) to avoid charging.

4.5. RESULTS AND DISCUSSION

The star-shaped resins were synthesized by polycondensation of LA with xylitol followed by end-functionalizing of branches by methacrylic anhydride. Insufficient retention time in the polycondensation reactions results in unreacted reactants and excessive reaction time promotes transesterification reactions, which degrades the structure of the macromolecules.[25] The conversion rate carboxylic groups was defined based on the ratio of the *reacted* to *initial* available carboxylic groups.(Knothe 2006) For all resins, the concentration of carboxylic groups were unchanged for the first 100 min and reduced rapidly during the next 320 min. After 720 min, the reaction was completed with a final conversion of ~94%.

Using the same technique, Bakare *et al.* reported that the polycondensation reaction of LA and glycerol core molecules started almost immediately and reached a conversion rate of 95% after 360 min.(Bakare et al. 2014b) In these studies, the LA chain lengths had a minimal effect on the conversion rates. The differences between the conversions of the polycondensation reactions in xylitol and glycerol star-shaped resins, can be attributed to the differences in the number of hydroxyl groups in the glycerol and xylitol core molecules. Therefore, increasing in number of hydroxyl groups in the core molecule of the *star*-LA architecture resulted in slower conversions (compare 720 min to 360 min for xylitol and glycerol), during the polycondensation phase.

NMR was conducted to investigate the chemical structures and the LA chain lengths in the different resins used in this study. The assignments of the peaks was based on the literature and previously reported data.(Adekunle, Åkesson, and Skrifvars 2010, Bakare, Åkesson, et al. 2015, Bakare et al. 2014b, Xiao, Mai, et al. 2012, Murillo,

Vallejo, and López 2011, Wambua, Ivens, and Verpoest 2003, Kabir et al. 2012, Liu et al. 2008, Raquez et al. 2010b, Jahandideh and Muthukumarappan 2016a) The shifts at 60–75 ppm were attributed to the carbon atoms adjacent to oxygen atoms. The CH groups of xylitol core molecules showed signals in the range of 68 ppm -71 ppm. The CHs adjacent to the hydroxyl end-groups, showed a peak at ~ 66.6 ppm and the CH_2 group of the xylitol core molecules showed a peak at ~ 68.7 ppm. There was no evidence of the presence of the CH_2 group of unreacted xylitol molecules, which suggests the reaction was complete.

The signals detected in the 16-22 ppm range were attributed to methyl groups. Of these signals, those in the 16.5-16.7 ppm range were attributed to the methyl groups in the LA chains and signals in the 20-21 ppm range were attributed to the methyl groups at the end of the chains, next to the hydroxyl group. The completion of the end-functionalization reaction was confirmed by two results: the absence of signal shifts at 20-21 ppm in the step-two resins spectra, and the presence of signal shifts in the 17.8 – 18.1 ppm range. The absence of the first peak in the spectra indicates that the unreacted hydroxyl end-groups were not present in the step-two resins. Therefore, hydroxyl end-groups have been fully reacted with the end-functionalizing agent.

Also, the presence of signal shifts in the 17.8 – 18.1 ppm range represent the methyl groups of methacrylate in the end-functionalized chains, which indicates the end-functionalization reactions occurred. The presence of the olefinic carbon shifts of methacrylated end-groups (the shift for CH_2 at 126–127 ppm and the shift at 135-136 ppm for C=C) provides further evidence of the successful end-functionalization reaction. In addition, the shift of the olefinic group (~129.2 ppm) of methacrylic acid, which is

released during the end-functionalization reactions, provides further evidence the end-functionalization occurred.

The ^{13}C NMR spectra of the carbonyl area (160-180 ppm) of the step-one and end-functionalized resins are shown in Fig. 3 for n3, n5 and n7 resins. In the carbonyl area, two signals for the carbonyl groups of LA were observed: the signal for the main-chain carbonyl (~169.6 ppm) and a signal for the LA carbonyl group adjacent to the –O–CH_2– branch of the xylitol core molecule (~169.9 ppm). The LA end-group carbonyls are located at 174.5 - 175.5 ppm, which include both LA-xylitol branches and the LA oligomers. In addition, the presence of peaks at 172-173 ppm in the spectra of n5 and n7 resins can be attributed to the carbonyl adjacent to the hydroxyl groups. The presence of the peaks in the 170-171 ppm range of the step-two resins is attributed to the carbonyl group of methacrylic acid, which further suggests the reaction did occur as expected and methacrylic acid was formed.

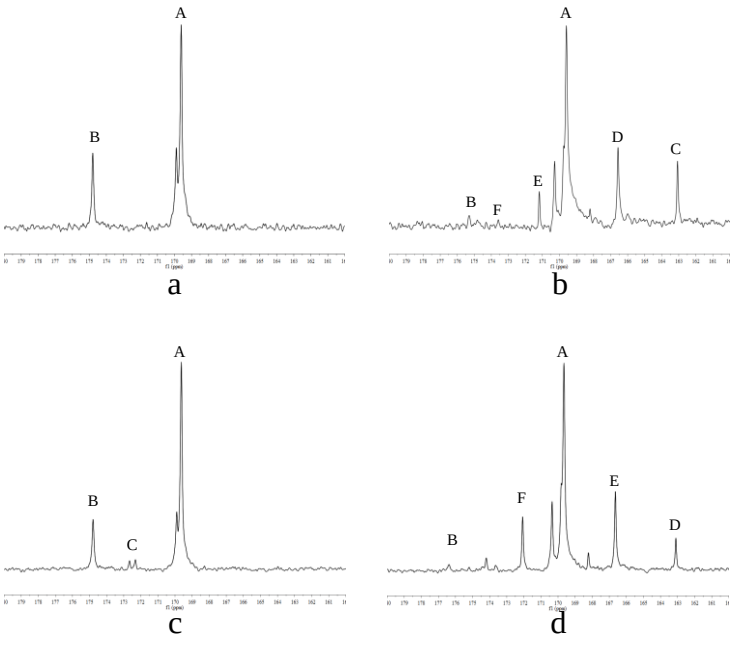

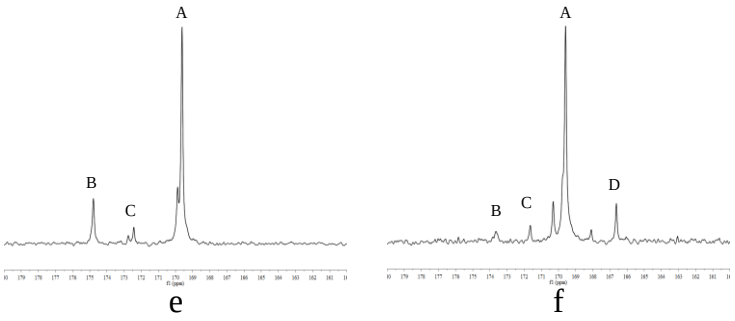

Figure 4. 3. Carbonyl area ^{13}C NMR spectra for a) step-one n3 resin, b) end-functionalized n3 resin, c) step-one n5 resin, d) end-functionalized n5 resin, e) step-one n7 resin and, f) end-functionalized n7 resin.

The length of the LA chains were estimated based on the carbonyl peak areas from the method described by Bakare *et al.* (Bakare et al. 2014b) The percentage of LA in form of reacted with the xylitol, and in form of LA reacted in free oligomers were also calculated based on the same method. Table 1 presents the branch lengths, percentage of LA reacted, percentage of LA as lactide and oligomers, and also the percentage of the chain-ends reacted for all resins.

Table 4. 1. Summary of the ^{13}C NMR Results

Feature	n3 resin	n5 resin	n7 resin
% LA reacted with xylitol	82.3	85.9	86.7
% LA reacted into LA oligomers	14.0	10.0	0.11
% LA as lactide	3.7	4.1	3.2
Chain length of X-LA polymer	3.8	5.1	6.6
% ends reacted with MA	86.7	93.3	87.5

FT-IR spectroscopy data of the functional groups of the *star*-LA based thermosettings have been previously reported in the literature(Bakare et al. 2014b, Bakare, Åkesson, et al. 2015, Xiong et al. 2014, Nouri, Dubois, and Lafleur 2015b, Cui et

al. 2003, Lin, Zhang, and Wang 2012, Chang et al. 2012b, Xiao, Mai, et al. 2012, Åkesson, Skrifvars, et al. 2010b, Hisham et al. 2011) and were used for assigning the signals in this study. Figure 4, illustrates the FT-IR spectra of the step-one, step-two and cured samples for resins with different chain lengths. The (─OH) stretch spectra (a signal at 3500 ppm cm^{-1}) was only present in the polycondensation resins as the hydroxyl groups reacted during the end-functionalization reactions.(Xiao, Mai, et al. 2012, Bakare et al. 2014b, Bakare, Åkesson, et al. 2015) The peak at 2990 cm^{-1} was attributed to (─CH─ stretch and bend), and was present in all FT-IR spectra.(Xiao, Mai, et al. 2012)

In addition, the end-functionalization was confirmed by observing the signals at 1635 cm^{-1} for the stretching carbon-carbon double bond,(Bakare et al. 2014b) and the signal at 815 cm^{-1} which can be attributed to the bending CH_2 group.(Hisham et al. 2011) The occurrence of the cross-linking reaction was confirmed by the signals for –CH from 2850 to 3000 cm^{-1}, as well as the disappearance of signals related to C=C bond in the cured resin.(Bakare et al. 2014b, Bakare, Åkesson, et al. 2015)

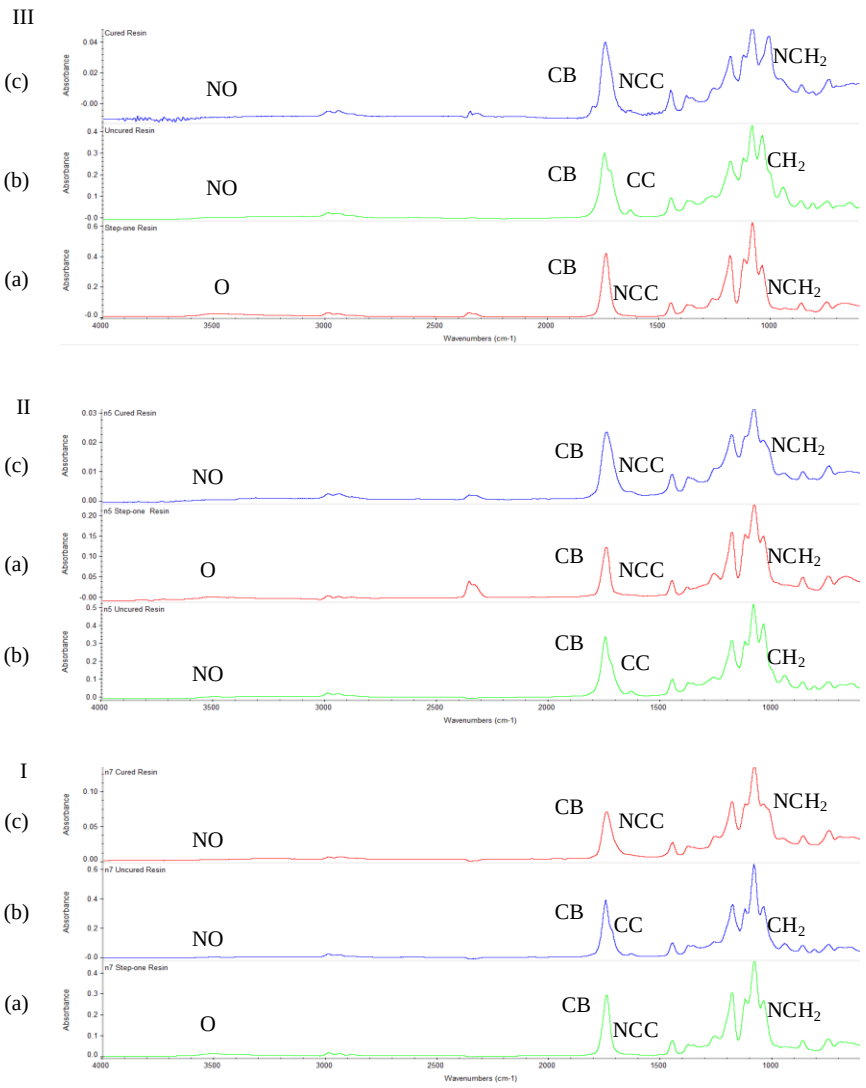

Figure 4. 4. The FT-IR spectra of the step-one (a), step-two (b) and cured samples (c) for I: n7, II: n5 and III: n3 resins. O: presence of OH group, NO: absence of OH group, CB: carbonyl group, CC: presence of carbon double bond, NCC: absence of carbon double bond, CH_2: presence of CH_2 group, NCH_2: absence of CH_2.

The bio-based content of resins were calculated based on the ASTM D6866 standard.(Jahandideh and Muthukumarappan 2016a, Bakare, Åkesson, et al. 2015) The bio-based contents of n3, n5 and n7 resins were 76.7%, 83.9% and 87.7%, respectively.

This indicates that the bio-based content of resins increased as the LA chain lengths increased. Bakare *et al.* evaluated the effect of chain lengths on the bio-based contents of the *star*-LA-glycerol based thermosettings, and reported a similar trend (78% for n=3, 89% for n=7 and 92% for n=10). The density of the resins was measured based on the ASTM D1475 standard as 1.23 g mL^{-1}, 1.24 g mL^{-1} and 1.25 g mL^{-1} for n3, n5 and n7 resins, respectively. This is comparable to the density of the other thermosets, including the epoxy resins, phenolic resins and the unsaturated polyester. It is apparent that by increasing the chain length, the bio-based content and density of resins increased.

Figure 5 illustrates the exothermic heat reaction (thermograms) of the curing reactions for the n3, n5 and n7 resins and these results are summarized in Table 2. The results showed that the evolved heat reactions decreased when the chain lengths increased. Bakare *et al.* reported a similar trend for *star*-LA-glycerol resins with chain lengths of 3, 7 and 10, with heat reactions of 227.4 J g^{-1}, 162.2 J g^{-1} and 94.3 J g^{-1}, respectively.(Bakare et al. 2014b) A similar trend was also reported by Chang *et al.* for *star*-LA-pentaerythritol resins with chain lengths of 5, 10 and 15, with 106 J g^{-1}, 75 J g^{-1} and 56 J g^{-1}, respectively.(Chang et al. 2012b)

The exothermic peak of the commercial unsaturated polyester occurred between 50 °C and 150 °C, with reaction heat of ~198 J g^{-1}.(Bakare, Åkesson, et al. 2015) The exothermic peak of methacrylated LA-allyl alcohol resins occurred between 90 °C and 150 °C, with reaction heat of 194 J g^{-1}. Employing pentaerythritol (PENTA) core molecules in the structure of the same resin resulted in substantially lower reaction heat (~26 J g^{-1}), in the same interval.(Bakare, Åkesson, et al. 2015) Figure 5 illustrates the

substantial reduction in the reaction heats which are shifted to lower temperatures by increasing the chain length of the *star*-LA-xylitol resins.

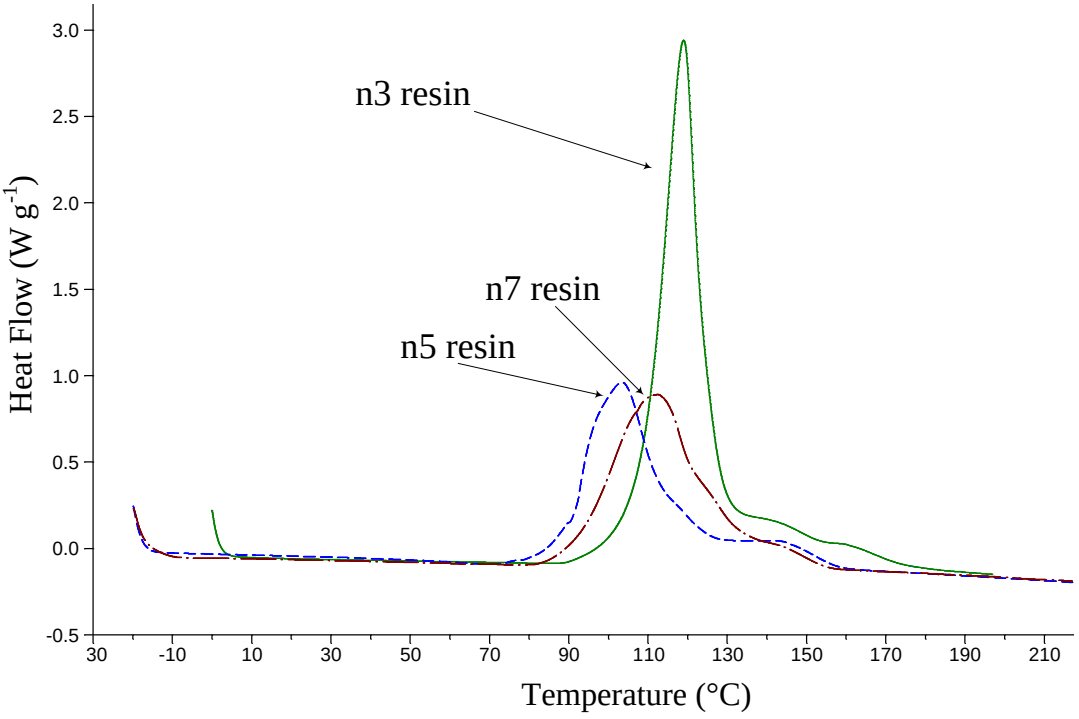

Figure 4. 5. DSC curve for unreacted *star*-LA-xylitol resins

DMA was performed to characterize the viscoelastic properties of the crosslinked resins. Figure 6a shows the elastic modulus (*G'*) values for resins. The *G'* values for different resins at 25 °C are shown in the Table 2. The *G'* of resins decreased substantially in the temperature intervals related to the rubbery plateau region, due to the free movement of the polymer chains.(Bakare et al. 2014b) The same trend was also observed for crosslinkable *star*-LA resins with different core molecules including glycerol (~45 °C to 80 °C) and PENTA (65 °C to 105 °C).(Bakare et al. 2014b, Bakare,

Åkesson, et al. 2015) The temperature range for major changes in the *G'* for n3 resins occurred between 44 °C and 82 °C. This temperature interval shifted from 56 °C to 87 °C for n5 resins. These results show that the *G'* values increased 14% by increasing the resin chain length from 3 to 5.

This indicates that the n5 resins had an increased packing density in the glassy state,(Vergnaud and Bouzon 2012, Chang et al. 2012b) which occurred due to improved crosslinking during the curing process. This observation does not concur with the results of Chang *et al.*, which reported inferior mechanical properties for *star*-LA-PENTA with longer chain lengths.(Chang et al. 2012b) The contrasting results can be explained due to the increased steric hindrance which is imposed by the shorter LA chain lengths in 5-armed core molecules. Increasing the chain lengths resulted in a 5% reduction in the elastic modulus values. By increasing the chain length from 3 to 5, the hindrance decreased and the elastic modulus improved. Bakare *et al.* reported the same trend for *star*-LA-glycerol based resins in which the *G'* values were decreased by an increase in the chain lengths.(Bakare et al. 2014b)

Table 4. 2. Thermomechanical characterization results of resins

Resins		n3 resin	n5 resin	n7 resin
DSC				
	Heat of exotherm for uncured resin (J g^{-1})	279.1	191.9	187.5
	Curing temperature interval (°C)	100 -150	87-160	85-160
	Peak temperature (°C)	117.3	115.3	105.7
	Onset temperature (°C)	108	90	90
DMA				
	tan δ peak (°C)	96	103	81

	Elastic modulus (MPa) at 25 °C	2884	3525	3335
	Viscous modulus (MPa) at 25 °C	142	95	160
TGA				
	Degradation temperature range (2%-99%) (°C)	170 – 449	201-438	167-457
	Degradation temperature at 10 *wt%* loss (°C)	268	289	266
	Maximum degradation (°C)	368	373	378
	Second derivative peak (°C)	438	443	419

Based on the results of this study, we conclude that the optimal chain length was 5. The shorter LA chains resulted in higher crosslinking density, and in this resin, the shorter LA chain lengths impel steric hindrance, which consequently hinders the crosslinking reactions. The *G'* values for n5 and n7 resins were higher than *G'* value reported for the commercial polyester resin (2956 MPa at 25 ºC).(Bakare et al. 2014b)

Figure 6b shows the viscous modulus *G"* for resins with different chain lengths. The *G"* of the n3 resins is broader and shorter in height than that of n5 and n7 resins. This can be attributed to the n3 resin's higher crosslinking density compared to n5 and n7 resins. However, rather low values of the *G"* above the glass transition temperatures indicates the strong tendency for reversibility.(Bakare, Åkesson, et al. 2015) The peak value of *G"* increased ~40% by increasing the chain length from 3 to 5. Figure 6c shows the *tan δ* curves of crosslinked resins. The glass transitions temperatures (T_g) were 96 ºC, 103 ºC and 81 ºC for n3, n5 and n7 resins, respectively. The higher *tan δ* peak value for the n5 resin suggests comparably better mechanical properties.

The T_g of the thermoplastic PLA (based on the *tan δ* peak) was reported as ~50 °C.(Oksman, Skrifvars, and Selin 2003) However, higher T_g values were reported for the LA based thermosets. For example, the T_g of 83 °C was reported for a crosslinked *star-*

LA-PENTA thermoset (LA chain length of 4) and a T_g of 97 °C was reported for *star*-LA-glycerol thermosets (LA chain length of 5).(Bakare et al. 2014b, Adekunle, Åkesson, and Skrifvars 2010) Generally, by increasing the crosslinking density, *tan* δ becomes broader and smaller.(Bruining et al. 2000) The T_g value is dependent on the chain length and the number of arms in the crosslinked resins. Therefore, a direct comparison between the T_g values of the *star*-LA based resins is not possible. However, the reported T_g values for the *star*-LA based thermosets are relatively higher than the T_g value of the thermoplast PLA.

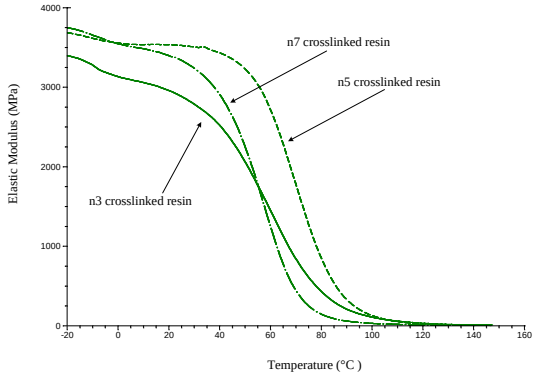

a)

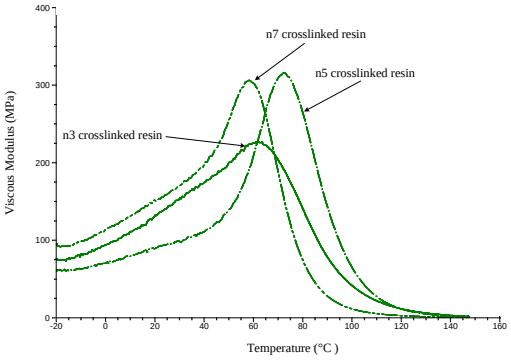

b)

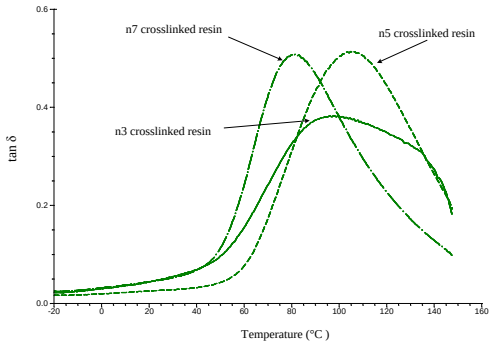

c)

Figure 4. 6. DMA curves ((a) elastic modulus, (b) viscous modulus and (c) tan δ) for cured samples of different resins.

Thermal stability of the crosslinked resins was evaluated by TGA and presented in Fig. 7 and summarized in Table 2. The thermal degradation of thermosets occurs via decomposition of the crosslinked network, followed by random scission of the linear chains.(Adekunle, Åkesson, and Skrifvars 2010) Bakare *et al.* and Chang *et al.* previously reported that shorter arms result in higher crosslinking and subsequently, better thermal stability.(Chang et al. 2012b, Bakare et al. 2014b) This trend was also observed for n5 and n7 resins. However, the n3 resins showed inferior thermal stability because of the imposed steric hindrance in the structure. Thermal degradation led to a

two stage weight loss from the decomposition of the network followed by degradation of the methacrylic anhydride homopolymer.(Finne and Albertsson 2002)

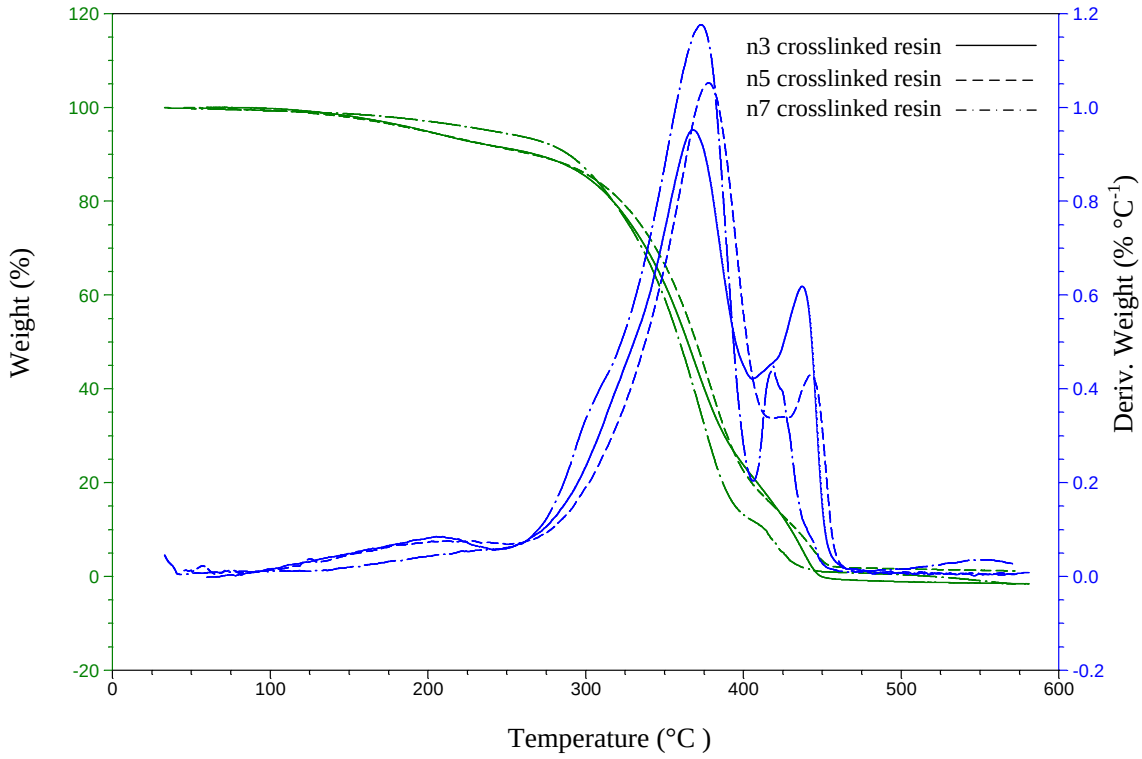

Figure 4. 7. TGA curves for cured resins with LA chain length of 3, 5 and 7.

The viscosity of resins was measured using stress viscometry at temperatures ranging from 20 ºC to 120 ºC (Fig. 8). The viscosity of n3, n5 and n7 resins at 25 ºC were 2.97 Pa s, 86.67 Pa s and 293.91 Pa s, respectively. When the temperature was increased to 85 ºC, the viscosity of n3, n5 and n7 resins decreased to 0.06 Pa s, 0.12 Pa s and 0.42 Pa s, respectively. The viscosity at this temperature is of great significance as this temperature can be considered the conservative processing temperature for the mixture of resins and the hardener. Figure 8 also shows that n3 and n5 resins have moderate

viscosities at higher temperatures, which facilitates the impregnation into the fiber reinforcement.

Åkesson *et al.* reported a viscosity of 7000 Pa s at 25 °C and 4 Pa s at 80 °C for *star*-LA-PENTA thermoset resins.(Adekunle, Åkesson, and Skrifvars 2010) The high viscosity makes the resin unsuitable for impregnation of the fiber. Bakare *et al.* synthesized a *star*-LA-glycerol thermoset resin which showed a better processability with a viscosity of 1.09 Pa s at room temperature and 0.04 Pa s at temperatures above 100 °C.(Bakare et al. 2014b) To achieve satisfactory composite manufacturing, the resin viscosity must be below 0.5 Pa s.(Li, Wong, and Leach 2010) It is believed that changing the architecture of the oligomers from linear to star-shaped reduces the viscosity of the resins due to the coiling character and the smaller hydrodynamic volume of polymers.(Corneillie and Smet 2015) (Chang et al. 2012b, Finne and Albertsson 2002, Choi, Bae, and Kim 1998)

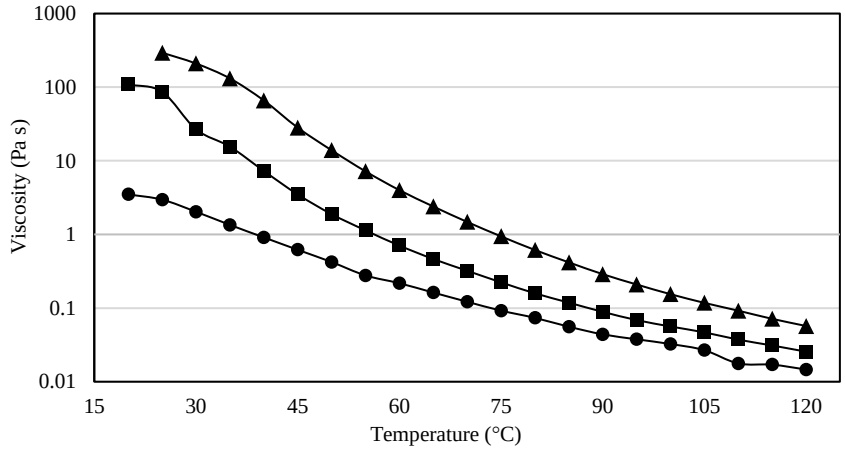

Figure 4. 8. Viscosity of resins as a function of temperature. (●) represents n3 resin, (■) represents n5 resin and (▲) shows n7resin.

Table 3 provides the flexural and tensile properties of the crosslinked resins. These results suggest that the flexural strength was increased as the LA length chain increased. These results do not concur with results reported by Chang *et al.*, in which the

mechanical properties deteriorated when the chain length of the oligomer increased.(Chang et al. 2012b) The different results among these two studies occurred due to the differences in the imposed steric hindrance associated with *star*-LA-xylitol oligomers with lactide-PENTA oligomers. The imposed steric hindrance led to a lower crosslinking density. The flexural strength increased 16% when the LA chain increased from 3 to 5.

However, increasing the chain length slightly affected the ultimate stress of the synthesized resins. Yield stress values for n3, n5 and n7 resins were 59.90, 74.98 and 88.91 MPa, respectively. It was observed that by increasing the chain length, the yield stress values of resins increased. The tensile strength at break and the maximum elongation were increased when the chain length increased. We conclude that by increasing the chain length of LA, the flexural and tensile modulus are decreased, which indicates the stiffness of the resin is decreased. However, the maximum elongation, flexural strength and tensile strength at break have been increased.

Table 4. 3. Flexural and tensile properties for resins with different LA chain lengths.

	n3 resin	n5 resin	n7 resin
Flexural properties			
Flexural Strength (MPa)	88.23 ± 3.25	102.05 ± 1.95	108.36 ± 3.16
Yield Stress (MPa)	59.90 ± 5.99	74.98 ± 20.06	88.91 ± 4.97
Modulus of Flexure (GPa)	4.07 ± 0.46	4.08 ± 0.15	3.31 ± 0.31
Max Strain %	2.78 ± 0.14	2.53 ± 0.10	4.60 ± 0.55
Tensile Properties			
Tensile strength at break (MPa)	34.70 ± 1.7	47.13 ± 2.4	59.87 ± 8.4
Max elongation %	1.43 ± 0.09	4.70 ± 0.48	5.51 ± 2.18

Modulus of Tensile, *E* (GPa)	2.87 ± 0.46	2.62 ± 0.12	2.49 ± 0.04

4.6. Characterization of the composites

SEM micrographs of the cross-sections of n5-jute, (n5-PLA)-jute and PLA-jute composites with 80 *wt%* fiber load are shown in Fig. 9. The micrographs of the fractured surface of the PLA-jute composites are presented in Fig. 9a. Figure 9a1 shows the individual fibers surrounded by the PLA (arrow F) and the fiber pull-out, which occurred at the surface of the fractured composites. This indicates weak bonding between the fibers and the matrix. The G and H arrows in Fig. 9a2 and 9a3 show that the fibers are partially impregnated and there are gaps between fibers and the matrix, which indicates poor adhesion between the fibers and the matrix. The micrographs of the (n5-PLA)-jute composite are presented in Fig. 9b, which shows that a comparably high portion of the fibers are still poorly impregnated.

This indicates that fiber content has been too much. However, there is no evidence of fiber pull-out, which resulted because of comparably improved adhesion. The better adhesion of the fibers and the matrix can also be seen in Fig. 9b2 and 9b3. Evidence of this can be observed because the cracks are very narrow or not present (arrows J and K). The improved adhesion of the fibers is a result of the initial impregnation of the fibers with the n5 resin. The cracks occurred at the interface of the PLA and the resin in the matrix. Figure 9b provides evidence that compared to the PLA-jute composite, the adhesion between the fibers and the matrix is improved, however still is not optimal. Figure 9c shows the electron micrographs of the surface of the n5 resin-jute composites. Figure 9c1 shows the individual fibers surrounded by the resin (arrow

L). In this figure, it is apparent that the fiber pull-out has not occurred at the surface of the fractured composites, which indicates better adhesion of the fibers and the matrix (arrows M and N). It can also be observed that cracks are very narrow or not present, which provides evidence of a better adhesion between the fibers and the n5 resin.

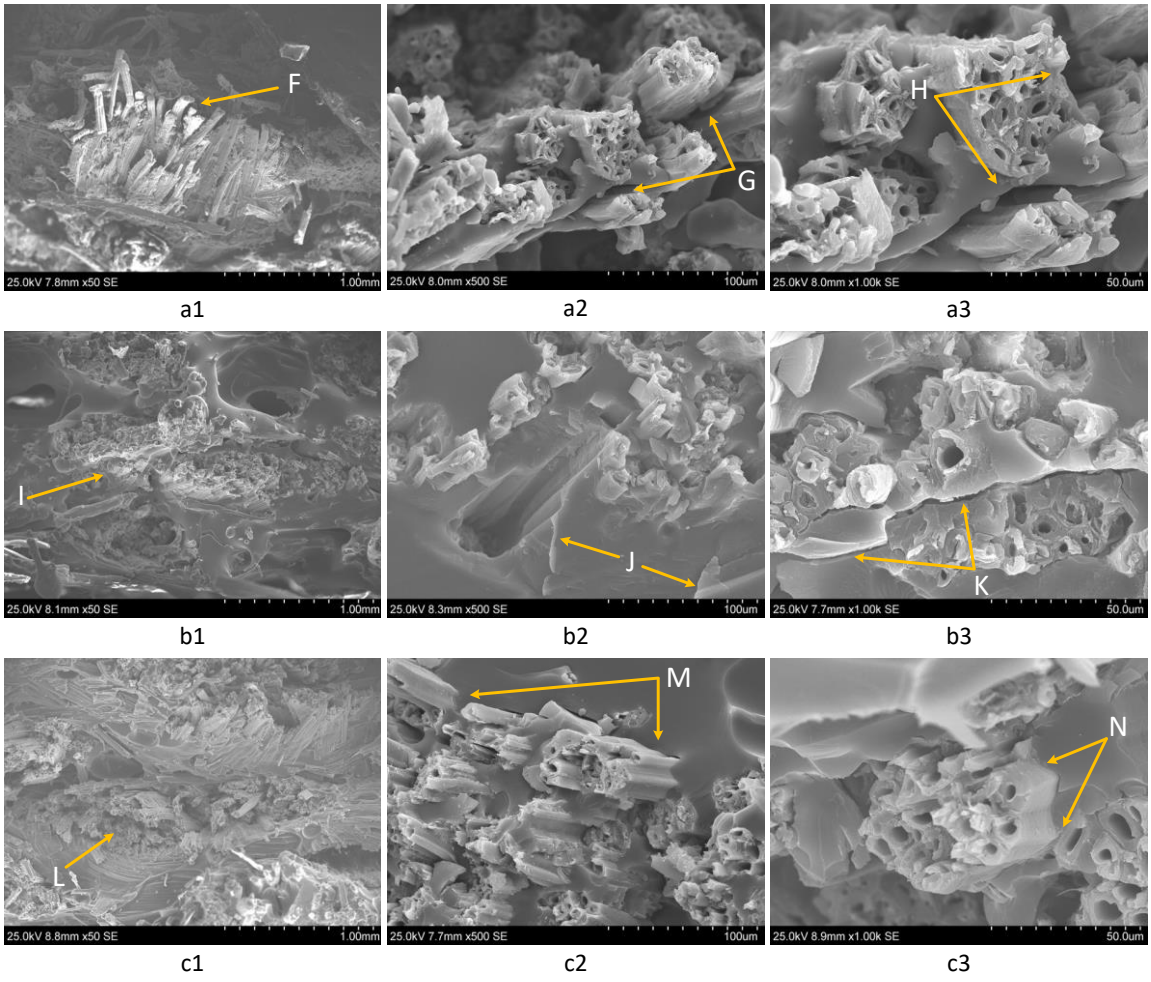

Figure 4. 9. SEM micrographs of the cross-sections of a) PLA-jute, b) (n5-PLA)-jute and c) n5-jute composites with different magnifications. All composites were prepared with 80 *wt%* jute fiber load.

DMA was performed to characterize the viscoelastic properties of the composites (Fig. 10). The elastic modulus for different composites were measured at 20 °C and were

approximately 4290 ± 47 MPa, 5245 ± 32 MPa and 6101 ± 107 MPa for the PLA-jute, (n5-PLA)-jute and n5-jute composites, respectively (see Fig. 10a). The glass transitions temperatures were 105 ºC, 77 ºC and 55 ºC for n5-jute, n5-PLA-jute and PLA-jute composites, respectively (see Fig. 10b). The higher *tan δ* peak value for the n5-jute composite suggests comparably better mechanical properties for this composite. Generally, higher T_g values are expected when the matrix is reinforced with fibers. However, this depends on the adhesion of the fiber to the matrix.(Adekunle, Åkesson, and Skrifvars 2010, Bakare, Åkesson, et al. 2015)

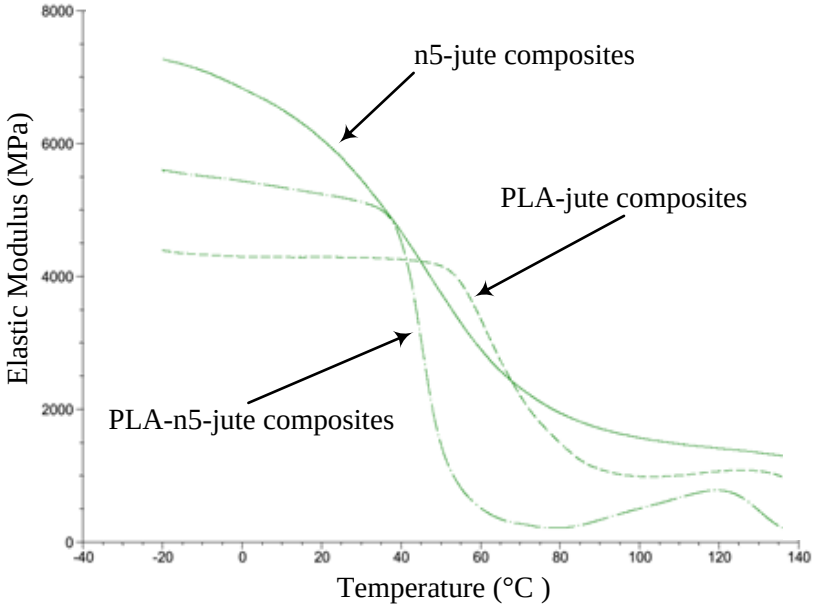

a

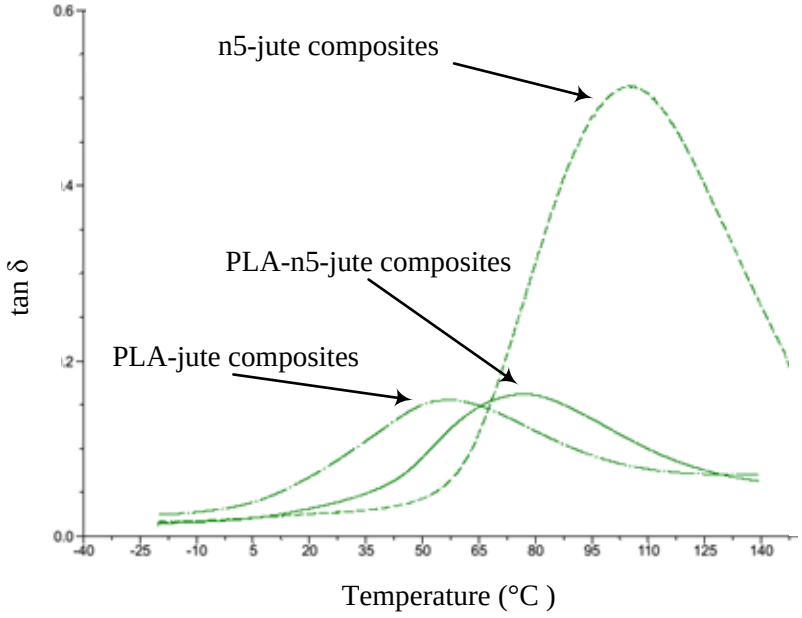

b

Figure 4. 10. DMA curves of composites. a) elastic modulus vs temperature, b) *tan δ* versus temperature for different composites

4.7. CONCLUSION

In this study, biothermosets with different LA chain lengths were synthesized and characterized. The results of this study showed that by increasing the chain length, the bio-based content and the viscosity of resins increased. The resin with an LA chain length of 5 showed a substantially higher T_g compared to other resins and to PLA. The higher *tan* δ peak value for the resin with LA chain length of 5 suggests comparably better mechanical properties for this resin. Relatively high bio-based content with good thermomechanical, rheological properties and thermal stability are all advantages of the n5 resin. The compatibility of this resin with natural fibers was also investigated. The composites were prepared utilizing jute fibers as reinforcements with 80 *wt*% fiber content.

The thermomechanical and morphological properties of the biocomposites were then compared to jute-PLA composites and a hybrid composite made from the impregnated jute fibers with n5 resin and PLA. These results showed that the n5-jute composites had improved mechanical properties compared to conventional PLA-jute composites and the hybrid resin-impregnated PLA composites. A future direction of this study is to investigate, the mechanical properties of composites from this resin reinforced with different natural fibers.

ACKNOWLEDGEMENT

The authors would like to acknowledge the funds provided by Agricultural Experiment Station, South Dakota State University and North Central Sun Grant through funds from US Department of Agriculture, Washington, DC in support of this research work. The

authors acknowledge the critical evaluation of this manuscript by Dr. Tylor J. Johnson of the University of Tennessee.

Chapter 5 - Synthesis and Characterization of Methacrylated Star-Shaped Poly(Lactidc Acid) Employing Core molecules with Different Hydroxyl Groups

Arash Jahandideh[c§], Nima Esmaeili[a,b§*], Kasiviswanathan Muthukumarappan[c], Dan Åkesson[a], Mikael Skrifvars[a]

[a]*Swedish Centre for Recourse Recovery, University of Borås, 501 90 Borås, Sweden*

[b]*Institute for Materials Research and Innovation, University of Bolton, Deane Road, Bolton, BL3 5AB, UK*

[c]*Agricultural and Biosystems Engineering Department, South Dakota State University, PO Box 2120, Brookings, SD 57007, USA*

This chapter has been published in Applied Polymer Science Journal.

§ Both authors contributed equally to this work

*Corresponding author: nima.esmaeili@gmail.com

Abstract

A set of novel bio-based star-shaped thermoset resins was synthesized via ring-opening polymerization of lactide and employing different multi-hydroxyl core molecules, including ethylene glycol, glycerol and erythritol. The branches were end-functionalized with methacrylic anhydride. The effect of the core molecule on the melt viscosity, the curing behaviour of the thermosets and also, the thermomechanical properties of the cured resins were investigated. Resins were characterized by Fourier-transform infrared spectroscopy (FTIR), ^{13}C NMR and ^{1}H NMR to confirm the chemical structure. Rheological analysis and differential scanning calorimetry (DSC) analysis were

performed to obtain the melt viscosity and the curing behaviour of the studied star-shaped resins. Thermomechanical properties of the cured resins were also measured by dynamic mechanical analysis (DMA). The erythritol-based resin had superior thermomechanical properties compared to the other resins and also, lower melt viscosity compared to the glycerol-based resin. These are of desired characteristics for a resin, intended to be used as a matrix for the structural composites. Thermomechanical properties of the cured resins were also compared to a commercial unsaturated polyester resin and the experimental results indicated that erythritol-based resin with 82% bio-based content has superior thermomechanical properties, compared to the commercial polyester resin. Results of this study indicated that although core molecule with higher number of hydroxyl groups results in resins with better thermomechanical properties, number of hydroxyl groups is not the only governing factor for average molecular weight and melt viscosity of the un-cured S-LA resins.

Keywords: Star-shaped; Thermosets; Biomaterials; Resins; Mechanical properties

Abbreviations

DMA: Dynamic mechanical analysis

DSC: Differential scanning calorimetry

EF: End-functionalizing

EG: Ethylene glycol

ER: Erythritol

FTIR: Fourier-transform infrared spectroscopy

GL: Glycerol

IT: Itaconic acid

LA: Lactic acid

MAA: Methacrylic acid

MAAH: Methacrylic anhydride

PENTA: Pentaerythritol

PLA: Poly lactic acid

PLGA: Poly lactic-*co*-glycolic acid

ROP: Ring opening polymerization

S-LA: Star-shaped lactic acid based resins

TGA: Thermogravimetric analysis

THMP: 1,1,1-tri(hydroxy methyl)propane

5.1. Introduction

Currently, composites are produced from petroleum-based materials and synthetic fibres. Utilization of bio-based materials and natural fibres for composite production, contributes to the production of a more environmentally friendly product(Mahalle et al. 2014, Huda et al. 2005). Lactic acid (LA), with versatile economical sources, is an interesting renewable candidate for substitution of conventional petroleum-based materials which is used for production of poly lactic acid (PLA) (Lunt 1998, Lim, Auras, and Rubino 2008, Garlotta 2001b). PLA is a biodegradable thermoplastic with wide range of applications, and can potentially be used for composite applications. However, the PLA, being a thermoplastic resin, suffer from limitation in impregnation of the matrix to natural fibres, which leads to a slow and costly process, and final composites with poor mechanical strength (Olabisi and Adewale 2016, Rowell 2007). Thermosets bestow a lower viscosity and the capability of tailoring for a certain functionality by altering the

chemical structure or by changing the crosslinking density. These features have made thermosets the main resin to be utilized in reinforced composite applications (Liang and Chandrashekhara 2006, Pascault et al. 2002).

Two different methods exist for polymerization of LA to PLA, including direct condensation of LA and polymerization through ring opening polymerization (ROP) of lactide. In condensation polymerization method, LA monomers are directly condensed to PLA and water is released during polymerization. Poly-condensation yields a low MW polymer due to the reversible esterification mechanism, which results in poor mechanical properties. To achieve a high molecular weight it is therefore necessary to effectively remove the water formed in the condensation reaction, and also to use LA of high purity, to ensure the stoichiometric balance (Drumright, Gruber, and Henton 2000). Presence of the residual catalysts in the products is another drawback of this method (Hartmann 1998). In the lactide formation method or ROP, lactides are polymerized with the assistance of a catalyst to yield a high MW PLA. As the lactide is used, no water is formed in the reaction, which avoids the reversible transesterification reaction. The important parameters in the ROP include but are not limited to the purity of the lactide, catalysts type, reaction time and the employed temperature (Xiao, Wang, et al. 2012). Although the ROP yields a high MW PLA, the process is costly and complicated, and the MW of the produced PLA heavily depends on the type of the employed catalyst (Esmaeili and Javanshir 2013). This method is found to be very sensitive to the presence of the lactide impurities and therefore, a rigorous lactide purification step is required which imposes substantial costs to the process (Hartmann 1998, Gu et al. 2008).

Limitations of these methods encouraged researchers to investigate on alternative synthesis routes to yield a higher MW PLA. It is known that the utilization of chain extenders can increase the MW of the synthesized PLA. The role of the chain extender is to attach low MW oligomers to each other and to form a higher MW polymer (Gu et al. 2008, Hartmann 1998). Another route has been to synthesise branched PLA, mainly for the use as thermosets. Different techniques have been employed for inducing branching points in the structure of PLA, including free-radical branching in the presence of peroxides (Esmaeili et al. 2014, Jahandideh and Muthukumarappan 2017). The crosslinkable branched-structure lowers the melt viscosity of the un-cured resin, which enhances processability of the un-cured resin and in the same time increases MW of the cured resin which in turn improves mechanical properties of the cured resin. In addition, in the branch-structure, the better extended network bestows better thermomechanical properties to the cured resin.

Different methods have been reported for production of branched polymers; however, a few studies have been dedicated to star-shaped architecture (Tunca 2013, Jahandideh and Muthukumarappan 2017, Jahandideh, Esmaeili, and Muthukumarappan 2017, Jahandideh and Muthukumarappan 2016a, Bakare et al. 2016, Esmaeili et al. 2015). The star-shaped lactic acid based resins (S-LA) are synthesized by condensation of LA with the core molecule, followed by end-functionalization of the branches with an end-functionalizing (EF) agent (Åkesson, Skrifvars, et al. 2010b). The aims of the EF agent are to add unsaturated carbon-carbon bonds to the structure and to increases the reactivity of the branches. Different EF agents have been employed in the star-shaped structures, including methacrylic acid (MAA) (Åkesson et al. 2011b), methacrylic

anhydride (MAAH) (Helminen, Korhonen, and Seppälä 2002, Liu, Madbouly, and Kessler 2015, Sakai et al. 2013, Åkesson, Skrifvars, et al. 2010b, Bakare et al. 2014b, Bakare, Åkesson, et al. 2015, Chang et al. 2012b, Bakare et al. 2016, Åkesson et al. 2011b) or itaconic acid (IT) (Åkesson et al. 2011b). Often, for curing purpose, a free-radical polymerization method is employed in which the curing starts by assistance of radical initiators. Factors such as the employed polymerization method, the nature of the core molecule, the length of the LA arm and the type of the EF agent result in different properties in the produced S-LA systems.

Changing the architecture of the polymer will change the morphological and physiomechanical properties for the polymer. Historically, the star-shaped polyesters have been produced by the reaction of multifunctional compounds catalysed by tin(II)-2-ethylhexanoate using an ROP method (Kim et al. 1993, Choi, Bae, and Kim 1998). So far, different polyols have been utilized as the core molecule for the synthesis of the S-LA. Poly lactic-*co*-glycolic acid (PLGA) is a copolymer of PLA and glycolic acid (with two hydroxyl groups), with wide applications in drug delivery and tissue engineering (Makadia and Siegel 2011). The MW of the PLGA, the ratio of the lactide to glycolide, time of exposure to water and the surface shape are of factors affecting the physical properties of the specimen (Houchin and Topp 2009). A tree-armed S-LA has been synthesized from 1,1,1-tri(hydroxymethyl)propane (THMP) as the core molecule and LA using tin(II)-2-ethylhexanoate, as the initiator (Biela et al. 2003, Kricheldorf, Hachmann-Thiessen, and Schwarz 2004). The four-armed, high MW S-LA has also been synthesized using pentaerythritol (PENTA) as the core molecule using the same initiator. The intrinsic viscosity of the four-armed S-LA was found to be lower than that of linear PLA

with the same MW, which confirms the lower viscosity of the star-shaped architecture (Kim et al. 1993, Kim et al. 1992). Åkesson et al. also reported the synthesis of a four-armed resin based on LA and itaconic acid resin with PENTA core molecules in which the arms were end-functionalized by MAAH (Åkesson, Skrifvars, et al. 2010b).

In our research group's previous work, a number of three-armed S-LA resins using glycerol as the branching point and oligomer arms of 3, 7 and 10 repeating LA units in each branch, had been synthesized and characterized using direct condensation method for the synthesis of oligomers from glycerol and LA (Bakare et al. 2014b) in order to investigate effect of chain length on viscosity of resin and thermomechanical properties of the cured resins. S-LA resins utilizing core molecules with different number of hydroxyl groups have been synthesized and characterized in separate studies but considering that different LA chain length, polymerization methods and EF agents utilized for preparation of these resins, effect of core molecule of properties of these resins cannot be directly investigated. The purpose of this study is to synthesize and characterize methacrylated branched PLA by the ROP and also to investigate the effect of number of hydroxyl groups of the core molecule on the properties of the methacrylated branched PLA, using ethylene glycol (EG), glycerol (GL) and erythritol (ER) with 2, 3 and 4 hydroxyl groups, respectively.

5.2. Materials and methods

5.2.1. Materials

L-actide (Puralact L polymer grade ≥99%, PURAC Biochem, Netherlands), glycerol (99.5%; Scharlau, USA), erythritol (≥99%, Sigma Aldrich, USA), ethylene glycol

(Puriss. p.a., ≥99.5%, Sigma Aldrich, USA) and methacrylic anhydride (94%; Alfa Aesar, UK) were used as received as the primary reactants. Toluene (99.99%; Fisher Scientific, USA) was used as solvent and tin(II)-2-ethylhexanoate (95%, Sigma Aldrich, USA) was used as received as catalyst for the ROP. Hydroquinone (99%, Sigma Ardrich, USA) was used as premature free radical initiation inhibitor during the EF reactions. Benzoyl peroxide (moistened with 25% water, Merck Schuchardt, Germany) was used as the free radical initiator for crosslinking of the synthesized resins. All reactions were performed in an atmosphere of nitrogen. Polylite 440-M850 (Reichhold AS, USA) which is a medium reactive orthophthalic polyester resin containing 43 ± 2 wt% styrene was used as a reference when evaluating the synthesized resin properties. Methyl ethyl ketone peroxide (33%, BHP Produkter AB, Sweden) was used as the initiator for curing of the resins.

5.2.2. Synthesis

The synthesis was performed in two stages. In the first stage (the ring-opening reaction stage), oligomers with two, three and four branches were synthesized by ROP reaction of EG, GL and ER with lactide. Tin(II)-2-ethylhexanoate was used as the catalyst for the ROP and the molar equivalent of 4 lactic acid monomers for each branch was assigned. Average length of each branch was adjusted by setting stoichiometry of the core molecule and the LA components. Four, six and eight moles of lactide was added to 1 mole of EG, GL and ER, respectively. In the second step, oligomers were end-functionalized by reacting with MAAH. Ideal structures of the oligomers and the final resins are shown in Fig. 1.

5.2.2.1. Ring-opening reaction (ROP) of the lactide (first stage of the synthesis)

In the presence of 0.1 wt% tin(II)-2-ethylhexanoate, glycerol (0.1 mole) and lactide (0.6 mole) were mixed with 50 g of toluene, in a three-neck round-bottom flask, continually stirred with a magnetic stirrer. The round-bottom flask was placed in an oil bath, under a nitrogen atmosphere, and was equipped with a condenser for toluene recovery. The temperature was initially set to 150 ºC for 2 h, then increased to 170 ºC for 1 h and finally increased to 190 ºC for 1 h. The same procedure was used to prepare oligomers with EG and ER polyols, in which 0.4 and 0.8 mole of lactide were added to 0.1 mole of EG and ER, respectively.

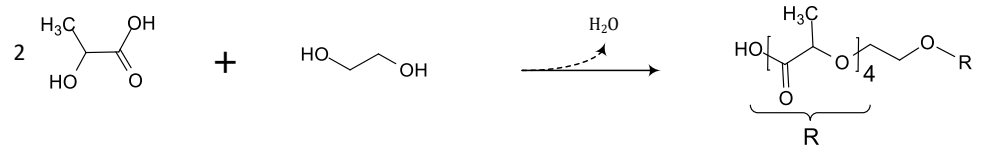

A1

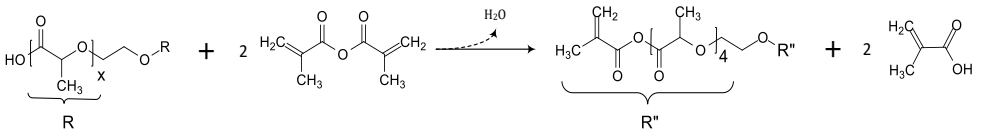

A2

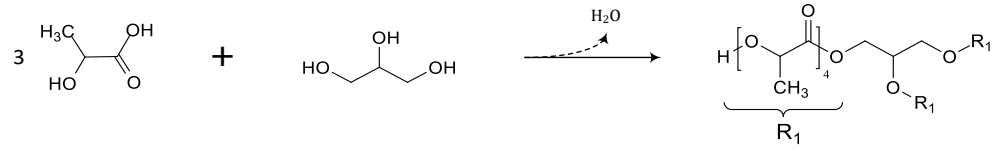

B1

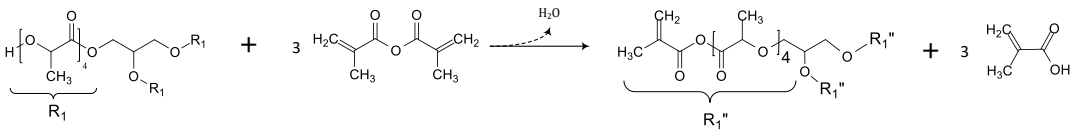

B2

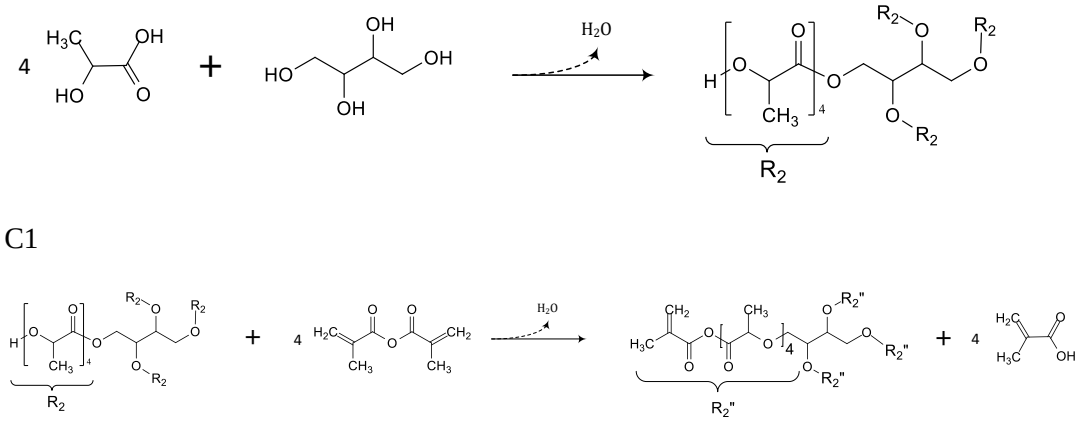

C1

C2

Figure 5. 1. Reaction schemes for A1: the synthesis of star-shaped ethylene glycol based resin, A2: end-functionalization of star-shaped ethylene glycol based resin with methacrylic anhydride, B1: the synthesis of star-shaped glycerol based resin, B2: end-functionalization of star-shaped glycerol based resin with methacrylic anhydride, C1: the synthesis of star-shaped erythritol based resin, and C2: end-functionalization of star-shaped erythritol based resin with methacrylic anhydride.

5.2.2.2. End-functionalization of the oligomers (second stage of the synthesis)

After the ROP step, the obtained hydroxyl-terminated oligomers were cooled to 105 ºC. Hydroquinone (0.1 wt%) was added for inhibiting the unwanted radical reactions and to prevent premature crosslinking and gel formation. In the first hour of the reaction, 0.22, 0.33 and 0.44 mole of MAAH were added dropwise to the EG, GL and ER resins, respectively. After 3 hours of reaction at 105 ºC, resins were cooled to 60-70 ºC, and the residual toluene was evaporated using a rotary evaporator at 3-10 mbar vacuum.

5.2.3. Curing of the resins

In this study, a free-radical polymerization method was employed for curing. The reactions were started by the assistance of a radical initiator (benzoyl peroxide 2 wt%) and continued by placing the mixture to a 160 °C pre-heated oven for 15 minutes. The presence of the residual exotherms were investigated by DSC. Cured resins were further analysed by DMA, TGA and FTIR.

5.2.4 Characterization

The chemical structure of the polymerized and the end-functionalized samples of different resins were evaluated with a proton and carbon nuclear magnetic resonance (^{1}H NMR and ^{13}C NMR) spectrometry (Bruker BioSpin GmbH, Germany) at 400 MHz and 45 °C. Sample's concentration in 5 mm tubes was ~10 wt% in $CDCl_3$.

The first stage resins, final resins and the cured ones were further characterized using Fourier transform infrared (FTIR) spectroscopy, on a Nicolet 6700 spectrometer, from Thermo Fisher Scientific, Massachusetts, USA in the range of 4000–600 cm^{-1}. Each spectrum was recorded after the sample was scanned 60 times.

The rheological properties of the uncured resins were analysed using Modular Compact Rheometer, Physica MCR 500. A cone-plate configuration was used for all measurements with truncated cone-plate configuration (1mm, 25 °C) and was ran in rotational mode. Viscosities were measured in the temperature range from 25 to 105 °C, with 10 °C intervals. The shear stress ranged from 0.5 to 500 Pa. The curing viscosity of samples were also investigated by heating the sample to 200 °C, using the similar setup and employing a 5 °C/min heating rate.

Curing of the resins were also investigated using differential scanning calorimetry technique on a TA Instrument Q 1000, supplied by Waters LLC, New Castle, USA. Samples of the neat resin were mixed with 1 wt% initiator and were placed in the sealed aluminium pans and heated from -20 to 200 °C at a heating rate of 10 °C /min in a nitrogen atmosphere. The cured resins at 150 °C for 15 minutes were also investigated by DSC to detect any possible residual exotherms.

Thermomechanical properties of the cured resins were analysed by dynamic mechanical analysis (DMA Q800 from TA Instrument, supplied by Waters LLC, New Castle, USA). Analysis was performed in the dual cantilever bending mode, with sample dimension of ~ 35 mm × 2 mm × 8 mm. The temperature ranged from -20 to 150 °C with a heating rate of 3 °C/min under a nitrogen atmosphere at frequency of 1 Hz and amplitude of 15 µm.

Thermal stability of the cured resins was investigated by the thermogravimetric analysis (TGA, Q500 from TA Instrument supplied by Waters LLC, New Castle, USA). Sample of ~20 mg were heated from 30 to 600 °C at a heating rate of 10 °C/min in a nitrogen purge stream.

5.3. Results and discussion

5.3.1. Nuclear Magnetic Resonance

The NMR is a technique frequently employed for verifying the chemical structure as well as the LA chain length in the branches of S-LA resins. Shifts for different carbon environments have been assigned based on the data presented in the literature and authors previous reports (Jahandideh and Muthukumarappan 2016a, Bakare, Åkesson, et al.

2015, Bakare et al. 2014b, Åkesson, Skrifvars, et al. 2010b, Park et al. 2003, Lin and Zhang 2010, Choi, Bae, and Kim 1998, Helminen, Korhonen, and Seppälä 2002, Murillo, Vallejo, and López 2011, Xiong et al. 2014, Abiko, Yano, and Iguchi 2012). Figure 2 presents the ^{13}C NMR results with the assigned peaks presented in the Table 1. Figures 2A and 2B present the spectra of the star-shaped EG oligomer, and the end-functionalized EG based resin. Figures 2C and 2D present the spectra of the star-shaped GL based oligomer and the end-functionalized GL based resins, and Fig. 2E and Fig. 2F present the spectra of the star-shaped ER based oligomer and the end-functionalized ER-based resins. Carbon and proton atoms in different environments within the molecule for the ideal structures of the synthesized polymerized and end-functionalized resins are presented in Fig. 3A-F. In the carbonyl area (160-180 ppm), different signals were observed, including a) main-chain carbonyls, b) LA carbonyl groups adjacent to the ($–O–CH_2$) branches of the core molecule, and c) carbonyls of the LA end-group for the unreacted LA. These peaks were observed at ~169.5, ~169.8 and ~174-5 ppm, respectively (see Fig. 2A, Fig. 2C and Fig. 2E). The signals at ~168 ppm in the polymerized resins is ascribed to the carbonyl group next to the core molecule (see Fig. 2A, Fig. 2C and Fig. 2E). In the spectra of the end-functionalized resins, signals for the carbonyls of the LA, next to the core molecule (or next to the end-capping agent) differ from that of the LA in chains. A peak at 162.9 ppm in the end-functionalized resins of different samples can be attributed to the carbonyl group of the MAAH in the structure (see Fig. 2B, Fig. 2D and Fig. 2F). The peak at ~170 ppm in the end-functionalized samples can be assigned to the carbonyl of MAA, released during the end-functionalized reactions.

The chemical shifts for the carbon atoms adjacent to the oxygen atoms revealed in the range of 60–75 ppm (Xiao, Mai, et al. 2012). The methine groups could be in the structure of the core molecule, next to the reacted LA carbonyl group or adjacent to the hydroxyl end-group. The CH groups of the core molecules (EG, GL and ER) and the CH next to the reacted LA carbonyl group and an oxygen atom showed broad signals in range of 68 ppm to 70 ppm (Fig. 2). The CH adjacent to the hydroxyl end-group, gives a signal at ~66 ppm (not marked in the figure). No signal was detected around 63-64 ppm for the CH_2 groups of the probable unreacted EG, GL and ER molecules, suggesting that the reaction of the core molecules and LA molecules were complete.

The LA methyl groups are detected in the 16–22 ppm range (Jahandideh and Muthukumarappan 2016a). Hydroxyl functionalized end-group of methyl groups are just present in the polymerized resins. The presence of a signal at ~21.3 ppm in the spectra of the polymerized resins (which can be attributed to the methyl group of the terminal LA) and the absence of this peak in the spectra of the end-functionalized resins, indicates that the EF reactions were complete for all samples.

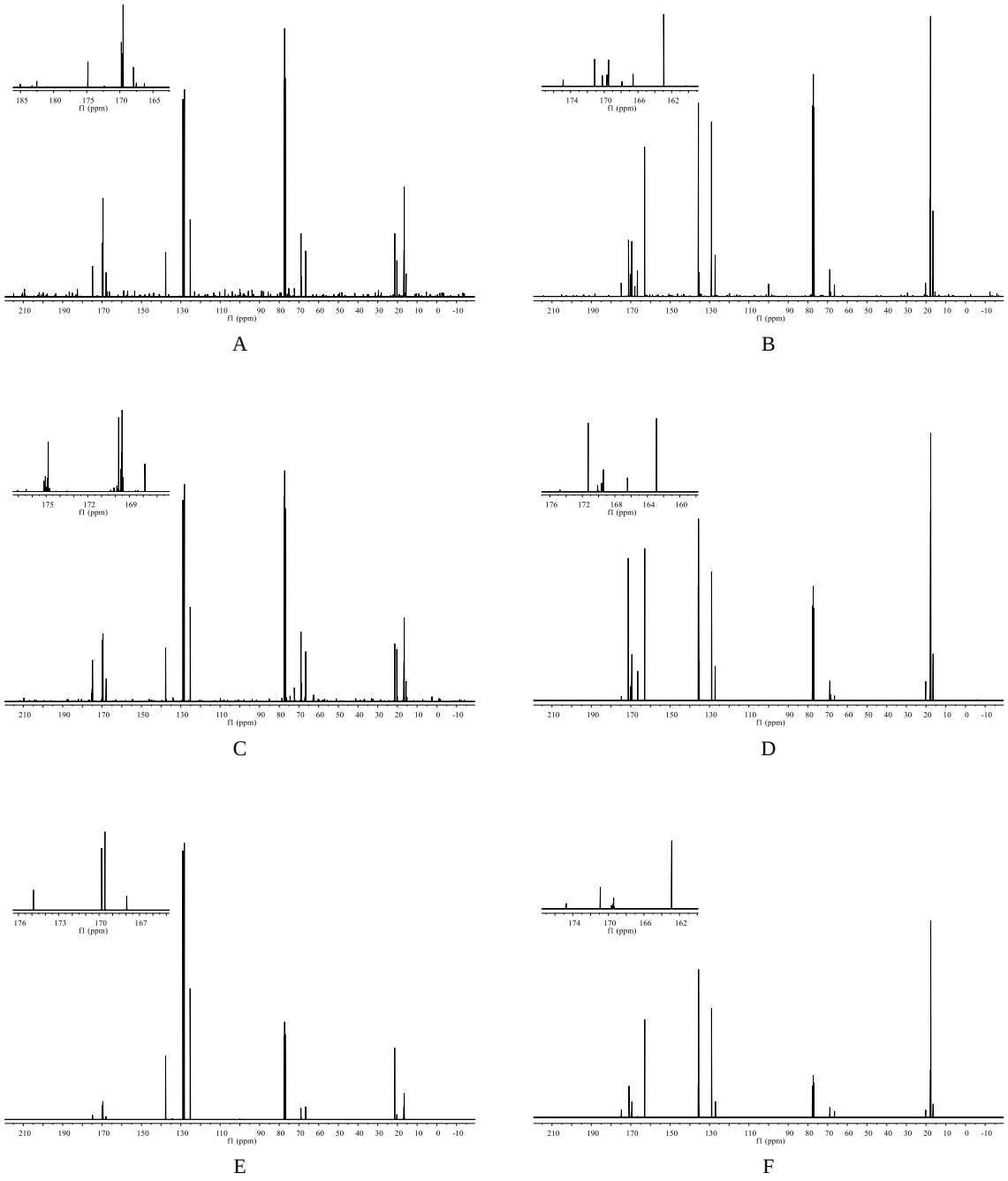

Figure 5. 2. The ^{13}C NMR spectra of the resins. A: star-shaped EG based oligomer, B: the end-functionalized EG based resin, C: star-shaped GL based oligomer, D: the end-

functionalized GL based resin, E: star-shaped ER based oligomer, and F: the end-functionalized ER based resin.

Signals for the CH_3 groups of the methacrylates in the end-functionalized resins were detected at a range of 17.6-17.8 ppm.

The C=C bonds of the methacrylated end-groups which are present in the end-functionalized samples (see Fig. 2B, Fig. 2D and Fig. 2F), result in signals at ~127 and ~135 ppm. In addition, the presence of the spectrum for the C=C bonds of MAA in the step-two resins (~129.0 ppm), confirms the successful end-functionalization which resulted in release of the methacrylic acid.

Table 5. 1. Assignment of peaks from ^{1}H and ^{13}C NMR

Assignment	Chemical shifts (ppm)
^{13}C NMR	
─C=O main-chain	~169.5
─C=O terminal unreacted LA	~174-5
─C=O adjacent to the (–O–CH_2) of core molecule	~169.8
─C=O next to the core molecule	~168
─C=O methacrylic anhydride end	~162.9
─C=O of methacrylic acid released	~170
─CH─ core molecule	~68-70
─CH─ adjacent to ─OH	~66
─CH_3 of lactic acid (─(C=O))(-OH)	~16–22
─CH_3 terminal LA	~21.3
CH_2 = methacrylated end-groups (C─)	~127

$C=CH_2$ in end-functionalized samples	~135
CH_2 = of methacrylic acid	~129.0
^1H NMR	
CH_3─ terminal LA	~1.44
CH_3─ in the chain	~ 1.54
OH─ chains terminal	~ 3.5
–CH_2– core molecule	~4.3
–CH in the chain	~5.1
CH_3 at the end-functionalized	~1.9
C=C	~6

The ^{1}H NMR technique was also employed for better characterization of the produced resins. Figure 3 and Table 1 present the ^{1}H NMR results with the assigned carbon environments for the ideal structures of the star-shaped oligomers and the end-functionalized resins. Figures 3A and 3B are the proton spectra of the star-shaped GL based oligomers and the end-functionalized GL based resin. Figures 3C and 3D are the proton spectra of the star-shaped EG based oligomer and the end-functionalized resins; and Fig. 3E and Fig. 3F are the proton spectra of the star-shaped ER based oligomer and the end-functionalized ER based resin. The peak at ~1.44 ppm can be attributed to the methyl bond of the terminal LA in the chains of the polymerized resins with one neighbouring hydrogen (see Fig. 3A, Fig. 3C and Fig. 3E). The next peak is revealed at ~ 1.54 ppm in all poly-condensate samples; it can be attributed to the methyl groups in the chain (same figure). The single weak peak at ~3.5ppm can be attributed to the terminal hydroxyl group providing evidence of successful hydroxyl functionalizing of the branches. The peaks at ~4.3 and ~5.1 ppm can be attributed to –CH_2– of the core

molecule and the methine group in the structure of the chains, respectively. The triplet weak peak at ~7.2 ppm (marked as f in the Fig. 3) resulted from the chloroform-d solvent (also seen at ~77.3 ppm in all ^{13}C NMR spectra). The single peak at ~1.9 ppm can be attributed to the terminal methyl group of the end-functionalized samples (see Fig. 3B, Fig. 3D and Fig. 3F). The new chemical shift, revealed in the end-functionalized resins at ~6 ppm can be attributed to the C=C site. Moreover, the branch lengths of the star-shaped resins were also estimated based on the method described in authors' previous works (Jahandideh, Esmaeili, and Muthukumarappan 2017, Bakare et al. 2016) as ethylene glycol chain length: 3.88, glycerol resin chain length: 3.98 and erythritol resin chain length: 3.30. Based on the acquired chain lengths, the molecular weights of the EG based oligomer, GL based oligomer and the ER based oligomers are estimated as 752, 1158 and 1296 g/mole, respectively.

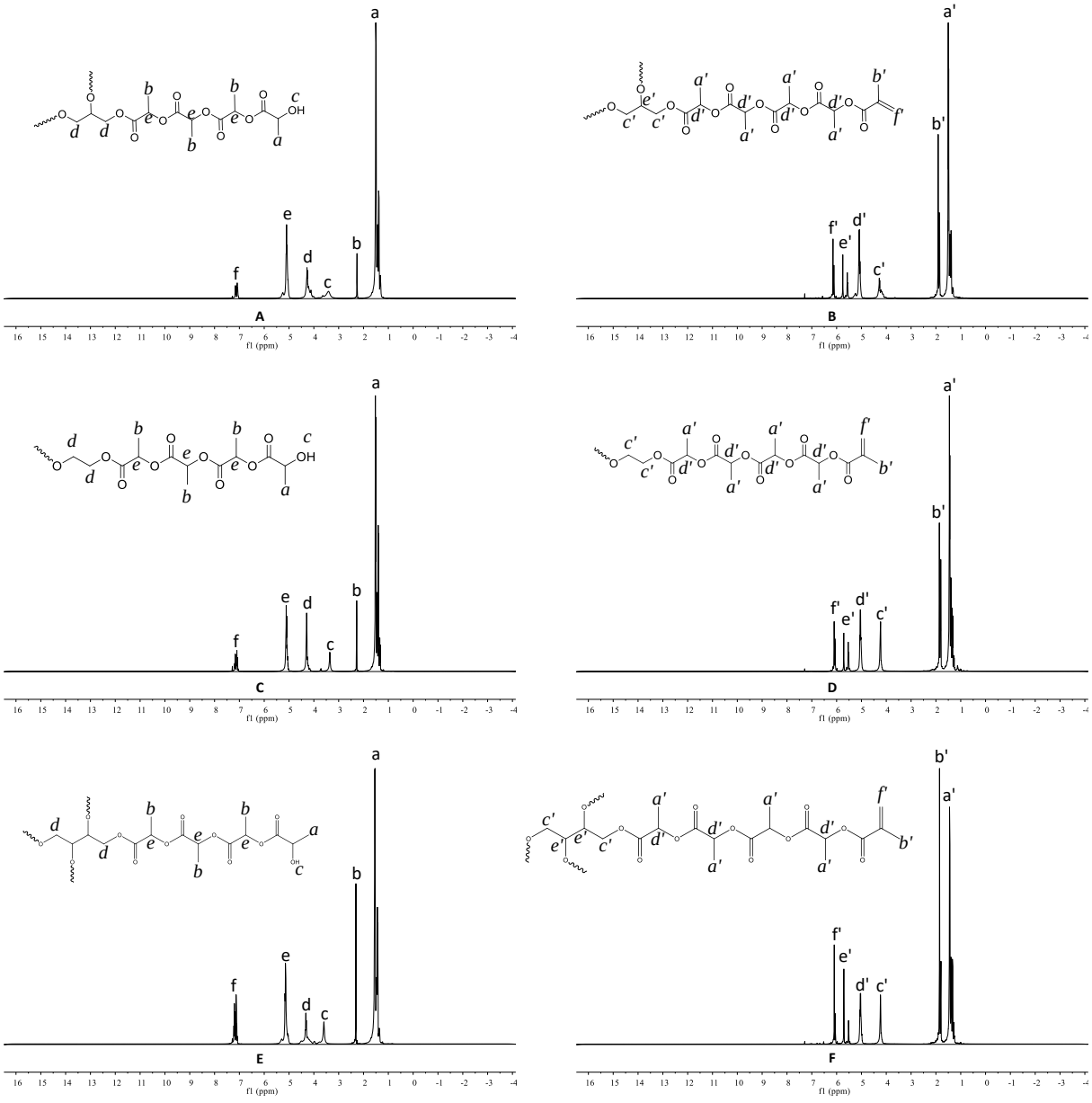

Figure 5. 3. The ^{1}H NMR spectra of the resins. A: star-shaped GL based oligomer, B: the end-functionalized GL based resin, C: star-shaped EG based oligomer, D: the end-functionalized EG based resin, E: star-shaped ER based oligomer, and F: the end-functionalized ER based resin.

5.3.2. Fourier-transform infrared spectroscopy

Chang et al. have compared the FTIR spectrum of the linear PLA with a star shaped LA based oligomer and the end-functionalized resin. The appearance of the broad absorption at 3508 cm^{-1} areas in the spectrum of the synthesized oligomer was an evidence for the presence of hydroxyl end groups. The disappearance of the hydroxyl peaks after EF reaction of the resin, indicates that the end-functionalization has been successful and hydroxyl groups have been reacted with MAAH (Chang et al. 2012b).

Figures 4a-c present the FTIR results for the ER, GL and EG based resins, respectively for the first-step resin, final uncured resin and the cured resin. The absorptions at 3508 cm^{-1} indicate the presence of the free hydroxyl groups in the all first-step resins. These broad peaks are almost disappeared in the spectrum of the methacrylated resins (second-step resin), which indicates successful functionalization. After the end-functionalization reaction, four new absorptions at 1722 cm^{-1} (attributed to C=O stretching vibrations for methacrylate (Chang et al. 2012b)), 1696 cm^{-1} (attributed to the C=C stretching for H_2C=CHOCOR), 1636 cm^{-1} (for C=C stretching (Bakare et al. 2014b)) and 814 cm^{-1} (attributed to =CH_2 twisting vibration (Hisham et al. 2011)) appeared. All these absorption peaks were disappeared in the spectra of the cured resins. It indicates that the curing was relatively complete, and even olefinic bonds of the excess MAA were reacted and became a part of the network.

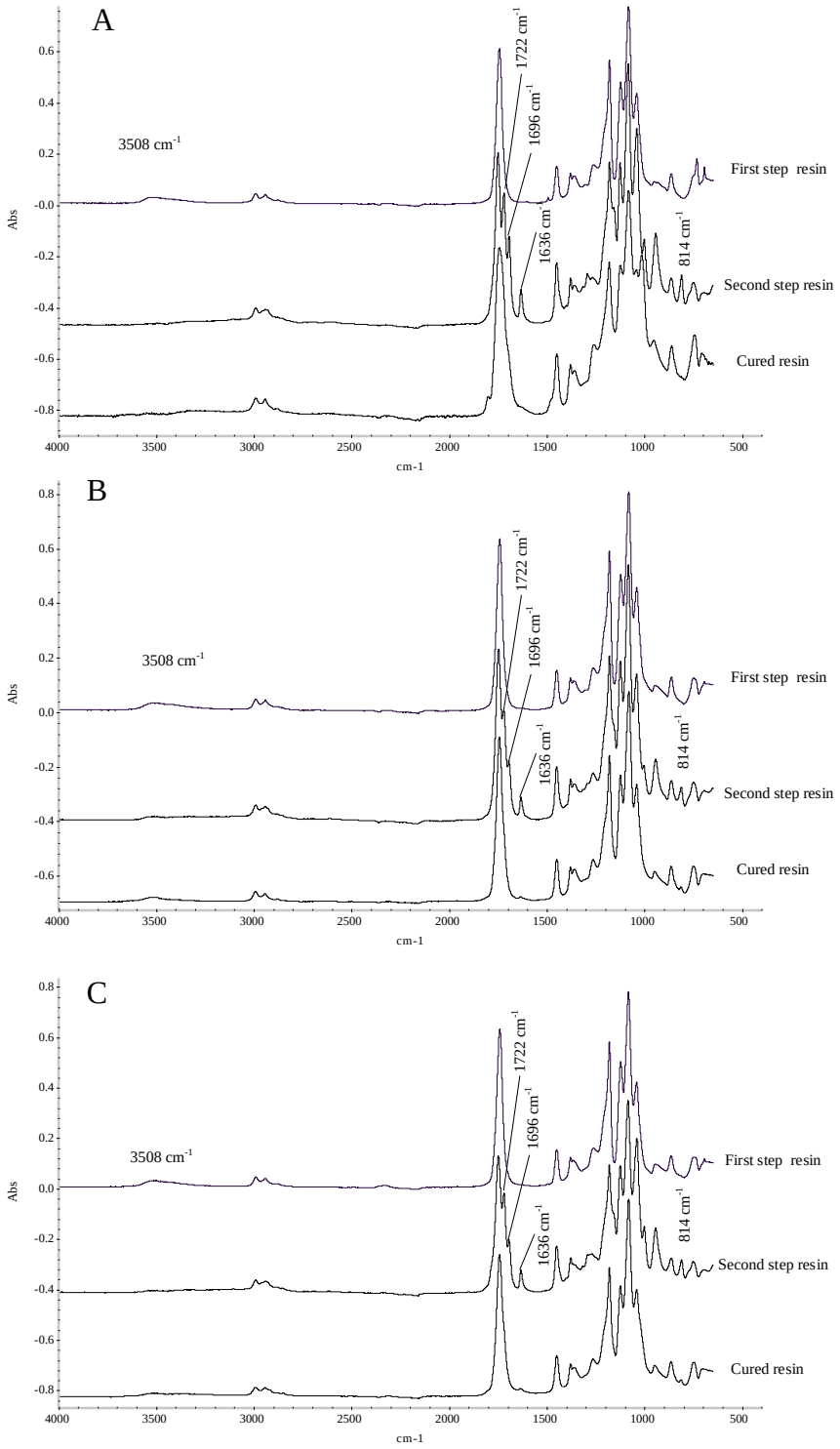

Figure 5. 4. The FTIR results for the first-step resin, final uncured resin and the cured resin for a) ER, b) GL, and c) the EG based resins.

5.3.3. Constant stress rheometry

Rheological properties of resins are of importance and greatly affect the processing conditions. The poor impregnation of the matrix to the reinforcement fibres is a severe problem in composite manufacturing which makes the process to be slow and also, reduces the mechanical strength of the product (Komkov, Tarasov, and Kuznetsov 2015). Low viscosity is desired for thermoset systems and is a crucial factor for several processing methods, including vacuum infusion, spray and hand lay-up, filament winding, and pultrusion (Åkesson, Skrifvars, et al. 2010b). The viscosity of resins were measured using stress viscometery at temperatures of 25, 35, 45, 55, 65, 75, 85, 95 and 105 °C. Figure 5 presents the viscometery results of the three resins. Results show that at room temperature, the GL resin has the highest viscosity followed by ER resin and the EG resin showed the lowest viscosity.

The huge difference in viscosity between GL and ER can be due to that the synthesis of the ER is not complete and does not follow the ideal structure, where all hydroxyl groups of the core molecule have reacted with the LA and with the assigned number of LA units. The ER has two primary and two secondary hydroxyl groups, while GL has two primary and one secondary hydroxyl groups. It seems that ER is more difficult to react completely concerning the last secondary OH. The average chain length of the oligomers which were estimated using NMR data based on the method described in the literature (Jahandideh, Esmaeili, and Muthukumarappan 2017, Bakare et al. 2014b), showed that unlike the EG and GL based resins, the average chain length of the ER based resin being 3.30, was lower than the ideal chain length expected for the resin (due to the higher chemical hindrance in the ER based resins). It is an evidence of incomplete

reaction of hydroxyl groups of the ER and the lactide molecules. Therefore, the unreacted lactide molecules and/or subsequent unreacted MAAH, may be remained in the medium. The presence of these free small components in the resin might be one of the reasons for the comparably lower viscosity observed in the ER based resin. The other probable reason for the lower viscosity of the ER based resin compared to the GL based, might be explained based on the lower coiling character (Chang et al. 2012b, Finne and Albertsson 2002, Choi, Bae, and Kim 1998) of the ER based resin compared to that of GL based resin. The ER based resin (with 4 arms) might present a smaller hydrodynamic volume (Corneillie and Smet 2015) compared to GL based resin (with 3 arms).

Upon increasing the temperature, the viscosity of all resins substantially dropped down. At temperatures above 75 °C, which are below the curing temperatures of resins, the viscosity of all resins dropped below 0.2 Pa.s, which facilitates impregnation of fibres for composite fabrication. Bakare et al. synthesized resins with similar structure to the GL resin, with 3, 7 and 10 repeating lactic acid units in each branch. At room temperature, authors reported viscosities of 1.09, 5 000 and 600 000 Pa.s for resins with 3, 7 and 10 LA units in the chain, respectively (Bakare et al. 2014b). In this study, the GL resin which had 4 repeating lactic acid units on each branch, had a viscosity of 43.8 Pa.s. Considering the dramatic effect of the chain length on the melt viscosity of star-shaped resins, an increase from 1.05 to 43.8 Pa.s by increasing chain length from 3 to 4 is logical. Åkesson et al. reported a viscosity of 7 000 Pa.s for a methacrylated crosslinkable PLA resin with pentaerythritol (PENTA) as the core molecule, with approximately 5 lactic acid units on each branch.

PENTA has four primary hydroxyl groups so all of them are of similar reactivity, so it is likely that hydroxyl groups of the PENTA are fully reacted, and therefore a higher MW and viscosity is achieved.

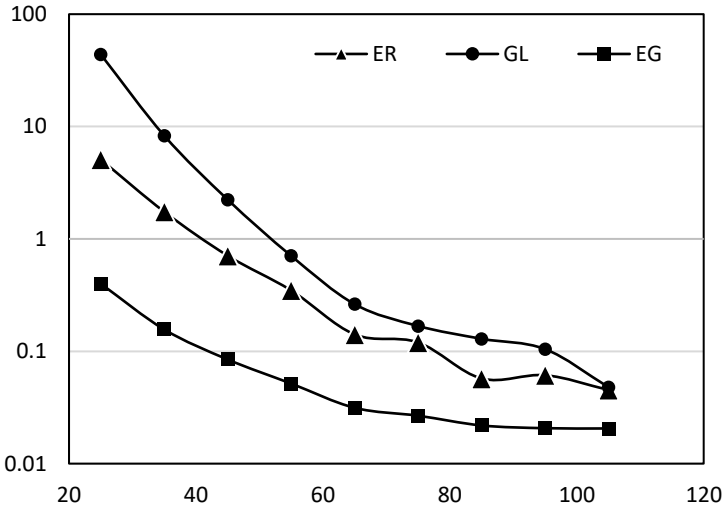

Figure 5. 5. Viscometery results of the erythritol based (▲), the glycerol based (●), and the ethylene glycol based (■) end-functionalized resins.

Figure 6 presents the complex viscosity of curing of resins, at a heating rate of 5 °C/min, from room temperature to 200 °C. Results show that at temperatures below 90 °C, in which curing has not been initiated yet, the GL and the EG resins show highest and lowest viscosities, respectively. Upon increasing the temperature, the viscosity of the ER, GL, and EG based resins started to rise rapidly at around 95, 105 and 85 °C, respectively. The rapid change in the viscosity of these resins can be ascribed to the initiation of the curing phenomenon. Considering the wide temperature interval before this rapid increase, in which viscosity is low enough (0.1-0.3 Pa.s) for effective impregnation of the fibres for composite fabrication, this does not affect the processability of these resins. The ER and EG resins showed the highest and lowest complex viscosities after curing at higher

temperatures. The complex viscosity of the resin after curing is an indicator of stiffness of the solidified resin at the elevated temperature thus ER and EG resins are most and least stiff resins among these resins at elevated temperature.

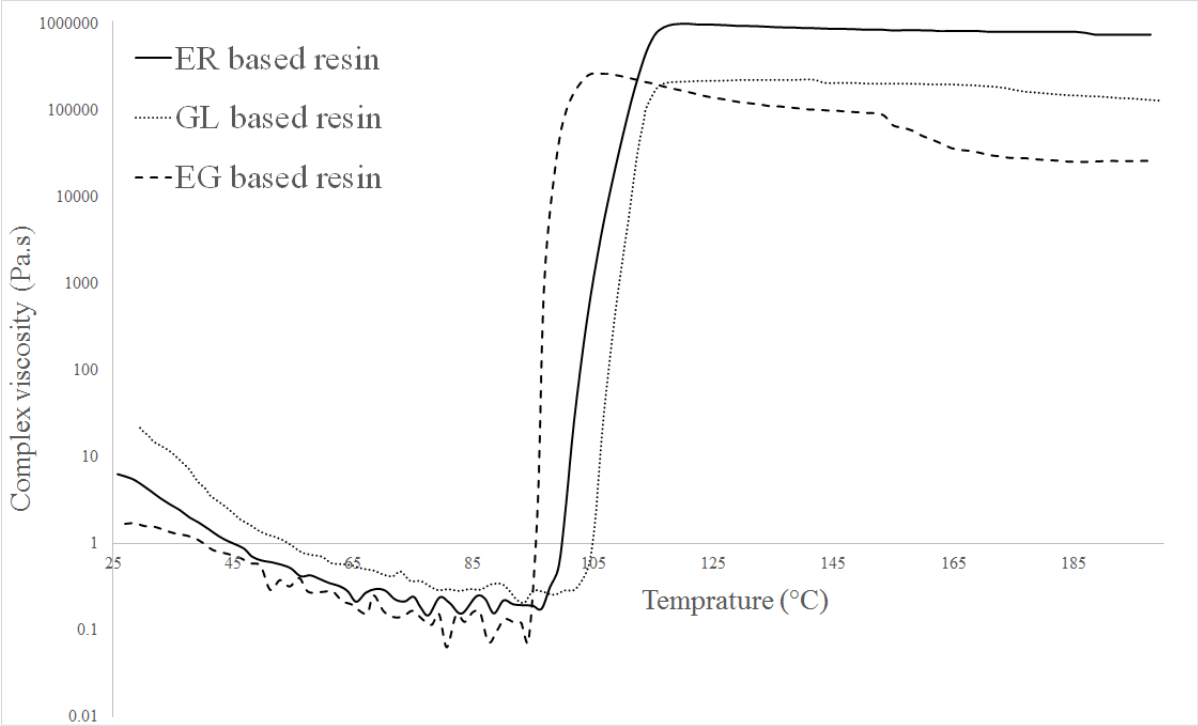

Figure 5. 6. The complex viscosity of curing of resins, at a heating rate of 5 °C/min, from room temperature to 200 °C; a) Ethylene glycol based resin, b) glycerol based resin, and c) erythritol based resin.

5.3.4. Differential scanning calorimetry

DSC is a technique frequently employed to investigate the curing and the crosslinking reaction efficiency (Liang and Chandrashekhara 2006, Mohan, Ramesh Kumar, and Velmurugan 2005, Bakare, Åkesson, et al. 2015). Figure 7 A) demonstrate DSC data for curing behaviour of the resins. Onset of curing of the resins are 73.4, 89.6 and 84.1 °C for the EG, GL and ER based resins respectively which shows EG resin has

the highest degree of reactivity compared to GL and ER based resins. Results also showed EG based resin had a slightly higher exothermic heat evolved at 227.4 J/g than the GL and ER based resins had exothermic heat evolved at 130.3 and 143.9 J/g, respectively, and the heat flow for the EG based resin reaches to its maximum at 73.9 °C which is considerably lower that of GL and ER based resins which are 114.9 and 118.5 °C respectively, as listed in table 2. These results can be justified by that by initiation of the curing for ER and GL based resins, a 3D network structure is formed which limits proximity of un reacted C=C bonds which in turn limits reactivity of the resins but considering the linear structure of the EG based resin, the absence of a 3D network structure, hence facile access of un reacted C=C bonds makes it more reactive compared to ER and GL based resins.

The cured samples of all resins were investigated by DSC in order to detect possible residual exotherms. Figure 7 B) shows the DSC curves for samples cured at 160 °C for 15 minutes. Absence of the residual exotherms in the DSC thermogram indicates that curing condition was optimum for all resins. In a proceeding study, the curing behaviour and the curing kinetics of these star-shaped resins will be investigated.

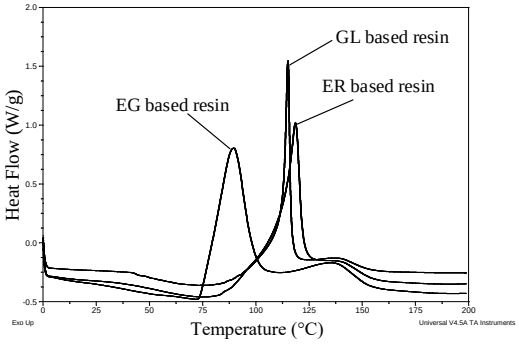

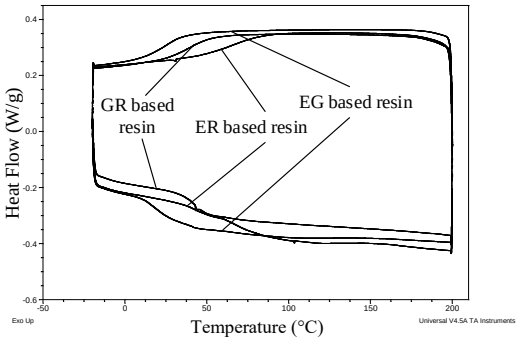

A B

Figure 5. 7. The residual DSC curves for different samples cured at 160 °C for 15 minutes.

Table 5. 2. DSC characterization of cured and uncured resins.

Resin type	Heat of exotherm for uncured resin (J/g)	Heat of exotherm for cured resin (J/g)	Onset of curing (°C)	Temperature of maximum heat flow
ER	143.9	0	73.4	89.3
GL	130.5	0	89.6	114.9
EG	178.8	0	84.1	118.5

5.3.5. Dynamic mechanical analysis

The type of the employed testing methods depends on the expected application for the product. The main desired application for these resins is to be used as a matrix for structural composites, thus their mechanical and thermomechanical properties are of great importance. Polylite 440-M850 as a commercial crude oil based thermosetting unsaturated polyester resin (CPE) was also selected to be compared with the star-shaped resins studied here. DMA is a common technique for characterizing the viscoelastic properties of polymers, in which a sinusoidal stress is applied to the test specimen and the resulting strain is measured. Properties such as storage modulus and lag phase (between stress and strain) and glass transition temperature can be measured with this technique (Menard 2008). DMA analysis was performed on all cured resins. Figures 8a and 8b present storage modulus and tan δ for all resins, respectively; and Table 3 summarizes the results. The peak of tan δ indicates glass transition of the polymer. Results show that the EG and GL based resins have lower T_g, compared to the CPE, while the ER based resin

has considerably higher T_g which makes it superior to the oil based resin for high-temperature applications.

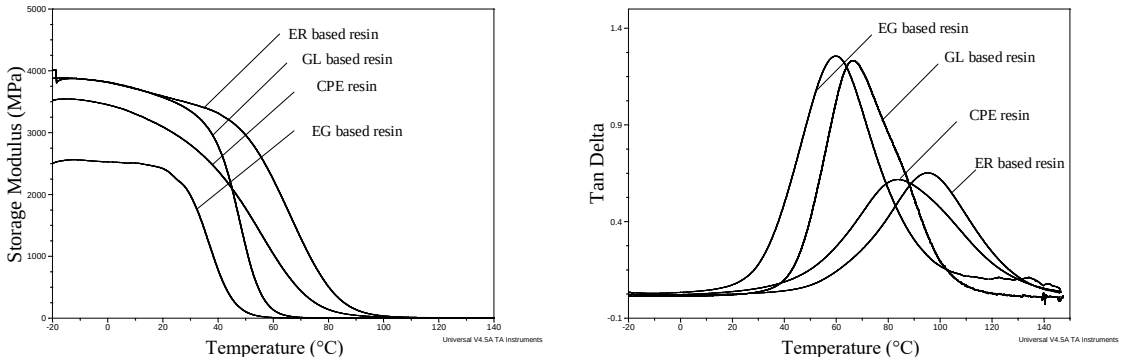

A B

Figure 5. 8. The DMA curves for cured samples of different resins. a) storage modulus, (b) tan δ

The storage modulus G' measures the stored energy and represents the elastic characteristic of a polymer. The storage modulus G' is an indicator of the molecular packing density of the specimen in the glassy state (Vergnaud and Bouzon 2012, Chang et al. 2012b) and the higher G', the better mechanical properties. The G' is decreased at elevated temperatures, as the polymer chain would be in the rubbery plateau region (Bakare et al. 2016), and free movements of the polymer chains results in a lower G'. The storage modulus at each temperature is an indicator of the stiffness of the polymer and can be compared to the flexural elastic modulus of the polymer. Results show that up to room temperature, the ER and GL based resins show considerably higher storage modulus compared to the CPE. The ER based resin shows a higher storage modulus for all the tested temperatures, which indicates that it is comparably superior to other resins

investigated in this study. It is also observed that the GL based resin`s storage modulus declines faster than that of the CPE upon increasing temperatures, and at temperatures above 50 °C it drops below that of the CPE. The EG based resin possess the lowest storage modulus between the studied resins at all temperatures.

Storage modulus of the neat thermoplastic PLA has been reported in range of 2.5 and 3 GPa at room temperature (Iwatake, Nogi, and Yano 2008, Jonoobi et al. 2010, Suryanegara, Nakagaito, and Yano 2009, Baghaei, Skrifvars, Rissanen, et al. 2014, Baghaei, Skrifvars, Salehi, et al. 2014, Baghaei, Skrifvars, and Berglin 2015, 2013) and its glass transition temperature (based on tan δ) has been reported in range of 65-70 ºC (Jonoobi et al. 2010, Baghaei, Skrifvars, Rissanen, et al. 2014, Baghaei, Skrifvars, Salehi, et al. 2014, Baghaei, Skrifvars, and Berglin 2015, 2013). Åkesson et al. reported the storage modulus of 1.6 GPa at room temperature and the glass transition temperature of 83 °C for the PENTA resin (Åkesson, Skrifvars, et al. 2010b). Bakare et al. reported room temperature storage modulus of 4.3, 3.8 and 1.7 GPa for the GL resins with 3, 7 and 10 lactic acid units on each chain, respectively. The glass transitions of 97, 80 and 54 ºC were also reported for the same set of resins with 3, 7 and 10 lactic acid units on each chain, respectively (Bakare et al. 2014b). Table 3 summarizes the storage modulus of resins synthesized in this study at room temperature and the glass transition temperatures. Comparing the storage modulus of these studied resins with that of other reported resins elsewhere, shows that an increase in the number of hydroxyl groups of the core molecule in the branched structure of PLA, does not necessarily result in an increase in the stiffness and the glass transition temperature.

By considering the similarities between the structures of the GL based resins synthesised in this study and the glycerol based resins reported by Bakare et al. (Bakare et al. 2014b), and considering the reverse effect of the chain length on the storage modulus and the glass transition temperature (reported by Bakare et al.), it was expected to observe a storage modulus in range of 4.3 to 3.8 GPa and a glass transition temperature between 97 and 80 ºC for the GL based resin in this study; however, both values were slightly less than what was expected. One probable reason could be that the actual chain length of the resins synthesized by ROP is higher than that of the resins synthesized by direct condensation polymerization method, which consequently results in a less crosslinking density. The other plausible reason could be that either the solvent extraction was less efficient in this study (results in remaining toluene in the system) or the released methacrylic acid had not been extracted completely in the other study (presence of MAA in the resins).

Table 5. 3. The storage modulus and the glass transition temperatures of different resins at 25 ºC

Resin type	Storage modulus at 25ºC (GPa)	SD	tan δ (°C)	SD
ER	3.567	0.032	94.00	0.54
GL	3.478	0.039	66.11	0.69
EG	2.517	0.015	60.22	2.25
CPE	2.935	0.048	84.37	1.27

5.3.6 Thermogravimetric analysis

Thermal stability of all the cured resins were investigated using the TGA technique by heating the samples from room temperature to 600 °C at 10°C/min heating rate, under a nitrogen atmosphere. As the temperature increases, various components of the sample decomposed, results in a continual weight loss. Commonly, in TGA, the percentage of weight loss or the rate of weight loss is presented versus temperature (Gabbott 2008). Figure 9 shows the TGA curves of the cured resins, and presents the percentage of weight loss as a function of temperature and corresponding derivative weight losses. Results show the onset of weight loss (5% weight loss) is 240, 260 and 265 °C for the EG, GL, and ER based resins, respectively. The ER-based resin leaves roughly 3 wt% char at 600 °C, while the EG and the GL-based resins leave ~1 wt% char at the same temperature. It is believed that the degradation in thermoset systems starts with decomposition of the crosslinked network, follows by the random scission of the linear chains (Adekunle, Åkesson, and Skrifvars 2010) result in two main decomposition stages. All three resins showed these two main decomposition stages at roughly same temperatures in a nitrogen atmosphere.

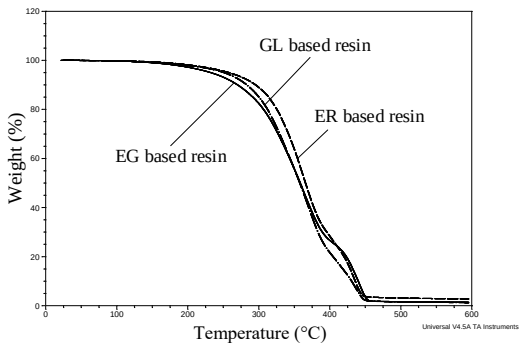

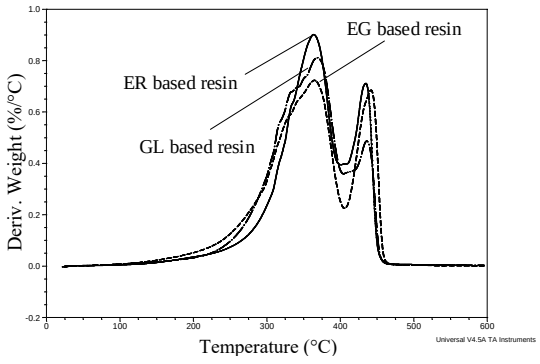

A B

Figure 5. 9. TGA curves for the ER, GL and the EG based resins.

5.4. Conclusions

Bio-based thermoset resins with three different core molecules were synthesized and characterized by the reaction of EG, GL and ER as the core molecule and lactide in two synthesis stages. In the first stage, L-lactide was reacted with the core molecule by ROP to obtain hydroxyl-group terminated oligomers with four repeating LA monomers in each chain; in the second stage, the obtained oligomers were end-functionalized by reacting with MAAH to obtain unsaturated LA polyester resins. This synthesis method is straightforward and less energy intensive compared to the direct-condensation polymerization method, which is a positive point for scale up for industrial production of these resins. The EG and GL based resins had a bio-based content of 82%, and this value for the EG-based resin was 74%. A commercial unsaturated crude oil based polyester resin was also compared with the bio-based resins. The results of this study indicated that the ER based resin has superior thermomechanical properties compared to other studied resins; and also, it has a lower viscosity than the GL-based resin. These results indicate although employing core molecules with higher number of hydroxyl group results in S-LA resins with better thermomechanical properties hypothetically due to more branched 3D network of crosslinked resins, the number of hydroxyl groups of the core molecule is not the only governing factor for the melt viscosity of the un-cured resin and factors such as geometry of the core molecule and type of the hydroxyl group (primary/secondary hydroxyl groups) play an important role in the molecular weight thus viscosity of S-LA resins. The complex viscosity of the EG, GL and the ER-based resins drops to 0.1, 0.2,

and 0.3 Pa.s at temperatures below the initiation of their curing, which is an advantage for impregnation of the resin into fibres for the preparation of bio-based composites. A future direction of this study is to investigate the curing kinetics of these star-shaped resins.

Acknowledgements

The authors would like to acknowledge the funds provided by Agricultural Experiment Station, South Dakota State University, US Department of Agriculture, Washington, DC and North Central Sun Grant through funding from USDA in support of this research work.

Chapter 6 - Glass fibre reinforced composites prepared from a lactic acid based thermosetting resin and their hygroscopic ageing properties

Nima Esmaeili[b,c§], Arash Jahandideh[a§], Kasiviswanathan Muthukumarappan[a], Dan Åkesson[b], Mikael Skrifvars[b]

[a]*Agricultural and Biosystems Engineering Department, South Dakota State University, PO Box 2120, Brookings, SD 57007, USA*

[b]*Swedish Centre for Recourse Recovery, University of Borås, 501 90 Borås, Sweden*

[c]*Institute for Materials Research and Innovation, University of Bolton, Deane Road, Bolton, BL3 5AB, UK*

[§] Both authors contributed equally to this work

Abstract

Three different type of thermoset glass fiber composites were produced using bio-based thermoset resin synthesized from lactic acid and glycerol, its blend with styrene and a commercial oil-based polyester resin. Fibers were impregnated by conventional hand layup technique with 70% fiber load and cured using compression moulding in room temperature and post-cured at elevated temperature. Composites were characterized by dynamical mechanical thermal analysis (DMTA) and flexural and tensile tests. Ageing behaviour of the composites was also studied in a climate chamber.

Results showed that bio-based composites had roughly similar mechanical properties in room temperature but thermomechanical properties in higher temperatures were considerably superior compared to commercial polyester composites. Ageing test results showed that bio-based resin composites deteriorate by ageing while commercial polyester composites remain intact but co-polymerizing with styrene improves the ageing behaviour of the bio-based resin and make it suitable for many applications.

6.1 Introduction

In the last decades industry`s interest have shifted from monolithic materials to composites. Composites are engineered materials composed of two or more distinct materials which demonstrate a combination of physical and chemical properties of each constituent material. Polymer matrix composites offer a wide variety of mechanical properties like light weight, high stiffness and mechanical strength which can be vital for many industrial applications.

Glass fiber reinforced polymer composite has proven to have good mechanical and has found many industrial applications since a long time. The growing environmental concerns and change in regulations attracted researchers and producers to develop more environmentally friendly “green” materials. Many studies have focused on replacing synthetic fibers with natural fibers as reinforcements for composite materials due to their light weight, low price, natural abundance, and their renewability (Mohanty et al. 2004, Muralidhar, Giridev, and Raghunathan 2012, Dabade et al. 2006, Idicula, Joseph, and Thomas 2010). Using natural fibers together with traditional thermosetting resins such as

epoxy and unsaturated polyester resins will create a composite that is partly made from renewable resources.

Most commercial thermoset resins are prepared from petroleum resources. Thermoset resins prepared from renewable resources are however under development. Vegetable oil such as soybean oil and linseed oil have been used as starting material in many studies (Mosiewicki, Aranguren, and Borrajo 2005, Lu and Wool 2006, Can, Wool, and Kusefoglu 2006, Luo et al. 2013). Thermoset resins for composite applications have also been developed from lactic acid (Åkesson, Skrifvars, et al. 2010a, Bakare et al. , Chang et al. 2012a). These resins have been reinforced with various reinforcements such as flax fibers (Åkesson et al. 2009, Åkesson et al. 2011a), ramie fibers (Chen et al. 2014), regenerated cellulose (Esmaeili et al. 2014) and with montmorillonite (Åkesson, Skrifvars, Lv, et al. 2010) .

In a recent study, the group developed and synthesized another cross-linkable resin consisting of the star-shaped oligomer with three arms (Bakare et al. 2014b). This resin was synthesized in two steps. In the first step glycerol was reacted with lactic acid and in the second step, the oligomers were end-functionalized with methacrylic anhydride. By the introduction of methacrylate groups, this resin was capable of curing by free radical polymerization.

One of the main draw backs of these lactic acid based resins and their natural fiber composites is their low moisture resistance. It is well known that natural fibers are hygroscopic and biodegradable. Natural fiber reinforced composites are therefore cannot be used for outdoor applications. For this reason, it is relevant to study the reinforcement

of bio-based thermoset resins with glass fibers. This topic is presently not well studied. In this article, we have used the lactic acid-based resin mentioned above and reinforced it with glass fibers in order to investigate its compatibility with glass fibers and to investigate the resistance to hygroscopic ageing. Composites were prepared from the neat resins as well as the resin co-polymerised styrene. Co-polymerising the resin with styrene will reduce the renewable content of the resins but it could potentially improve the ageing properties. Composites were also prepared from a commercial unsaturated polyester resin for the comparison.

6.2. Experimental

6.2.1 Materials

Benzoyl peroxide (75%) -moist with water- was supplied by Merck, Germany as a free radical cross-linking initiator for curing. Styrene (99%) supplied by Sigma-Aldrich, USA was used as reactive diluent for modification of cross-linking density. As the commercial oil based unsaturated polyester used in this study was premixed with free radical accelerator, N, N-dimethylaniline (99%) Sigma-Aldrich, USA was used as an accelerator for curing to be comparable to the commercial resin.

6.2.2 Composite preparation

The resin was synthesized as described in the groups former study (Bakare et al. 2014a). Fiberglass mats were cut in 21×21 cm size and were impregnated by ordinary hand layup technique. The PLA resin was first mixed by 0.2 weight % N, N-dimethylaniline, and 2 weight % benzoyl peroxide and for styrene added composites 30

weight % styrene was added to the resin as well. The commercial polyester resin which was premixed with accelerator was mixed with 2 weight % of its supplied hardener. Composites were cured for one hour under pressure at room temperature using a Rondol press instrument and post cured under pressure in Rondol press at 150 °C for 5 minutes. Then composites were moved to an oven and kept at elevated temperature (110 °C) for an hour before cooling for further curing. Fiber loads were calculated based on the weight of composites and the initial weight of fibers and kept in 70±1 % by adjusting initial fiber/resin ratio and pressure of the Rondol press. This gave laminates with an average thickness of 1.8±0.2 mm.

6.3 Characterization

All samples were cut by automated water jet cutting to obtain tensile, flexural, Dynamical mechanical thermal analysis (DMTA) and Charpy impact test specimens. DMTA was done in dual cantilever bending mode on a Q800 instrument (TA Instruments, DE, USA). Test specimen dimensions were 35 mm length, 8 mm width, and 1.6-2 mm thickness. Temperature was set to increase from -20 to 150 ºC in a heating rate of 3 ºC/min and amplitude of 15 µm and frequency of 1 Hz were used and at least 3 specimens were tested for each type of composites.

Un-notched edgewise Charpy impact tests were performed according to ISO 179 standard using a Zwick pendulum type impact testing instrument (Zwick GmbH and Co. KG, Germany). Minimum of 10 tests were performed for each type of composite and the mean value of the absorbed energy taken.

To evaluate ageing properties of composites of different resins, flexural and tensile properties of the composites were measured and compared for two groups of identically similar composites specimens for each resin which first group was tested right after preparation and the second group were exposed to simulated temperature induced humid ageing and were tested after reconditioning for 24 hours in a desiccator. For temperature induced humid ageing, flexural and tensile specimens were placed in a climate chamber (HPP 108/749) supplied by Memmert GmbH, Germany at 50 ºC and 85% relative humidity for 800 hours.

The aged specimens were then tested by tensile and flexural testing to determine how humidity affects mechanical properties of composites of each resin. To evaluate and compare mechanical properties of composites before and after ageing, specimens were characterized by three point bending flexural test according to ISO 14129 standard with crosshead speed of 5 mm/min and holder distance of 64 mm and also by tensile test according to EN ISO 527-4:1997 with dog-bone shaped specimens both using a H10KT (Tinius Olsen, USA) instrument equipped with a 5 kN and 10 kN load cell accordingly. A minimum of 6 specimens were tested for each type of composite in each group.

6.4. Results

DMTA provides good information about viscoelastic characteristics over a wide range of temperature. The DMTA was performed on all composites. Figures 1 presents storage modulus as a measure of stiffness for all three type of composites prepared in this study (PLA resin, PLA-styrene co-polymer and commercial oil base polyester) at -20 ºC to 150 ºC temperature interval. Figure 2 presents the Tan Delta for all composites at the same temperature and DMTA results are summarized in table 1. Figure 1 shows that

storage modulus of the commercial polyester composites at -20 ºC are slightly higher than that of PLA composites, however, co-polymerizing with styrene increased the stiffness of the PLA composite considerably. This figure also shows that by increasing the temperature, the storage modulus of the commercial polyester decrease faster than that of PLA composites in a way that at temperatures above 25 ºC it goes below that of PLA-styrene composites and at temperatures above 45 ºC it goes below that of PLA composites. At temperatures between 80 and 90 ºC, PLA and PLA-styrene composites are roughly 2 and 3 times stiffer than commercial oil-based polyester composite.

Figure 2 shows Tan delta of the all three type of composites. The temperature at maximum of Tan delta is often referred as an indicator of glass transition temperature (T_g). Results indicate that peak of Tan delta which represents glass transition temperature for PLA composites is above 110 ºC which is much higher than that of the commercial polyester composite which is around 90 ºC. Also, the glass transition temperature of the PLA composite further increases to above 135 ºC by co-polymerizing with styrene that is quite high glass transition temperature for polyester composites and opens a range of new applications for this recently developed resin.

Table 6. 1. DMTA data for the studied composites

	PLA resin	PLA resin + 30% styrene	Commercial polyester
Glass transition temperature (ºC)	110.3	136.3	91.6
Storage modulus in 25 ºC (Gpa)	20.2	23.2	24.3

The storage modulus of composites decreases dramatically by entering rubbery plateau region due to the free movement of polymer chains (Bakare et al. 2014b). Results in figure 1 show that although at lower temperatures storage modulus of commercial oil based composite is higher than that of PLA based composite, at rubbery plateau region, the storage modulus of PLA based composites is much higher. This may be due to the higher crosslinking density of the PLA resin compared to that of commercial oil based resin which limits free movements of the polymer chain (more restricted network).

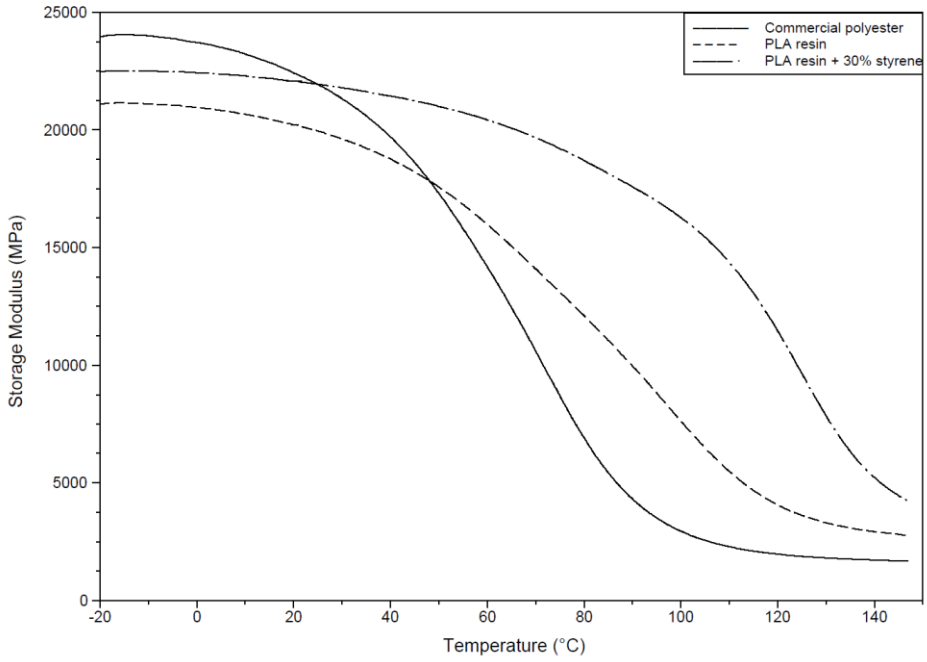

Figure 6. 1. Storage modulus vs temperature for different composites.

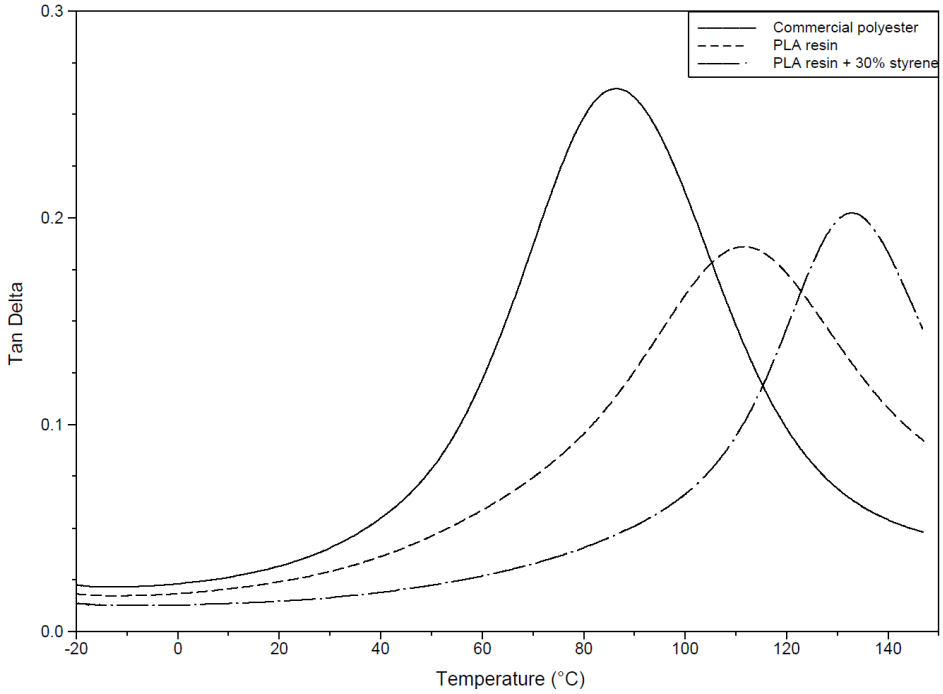

Figure 6. 2. Tan delta vs temperature for different composites in this study

Figure 3 compares flexural modulus of the composites before ageing for each type of resins. Results show that all three types of composites have roughly similar stiffness before ageing. Figure 4 also presents flexural strength of all composites which shows PLA based composite has roughly 18% higher flexural strength compared to commercial oil-based polyester composites and also co-polymerizing it with styrene further improve flexural strength of the composite by around 15%. This increase in flexural strength is a sign of good compatibility of successful co-polymerization of styrene and the PLA based resin and their good compatibility. Erden et al. reported flexural modulus of 16.6 GPa and flexural strength of 346 MPa for composited fabricated by woven glass fibre and polyester resins (Erden et al. 2010). The flexural modulus of composites made with neat PLA resin and woven glass fibre composite is above 20 GPa which indicates this resin is capable of being used as a matrix for structural composites.

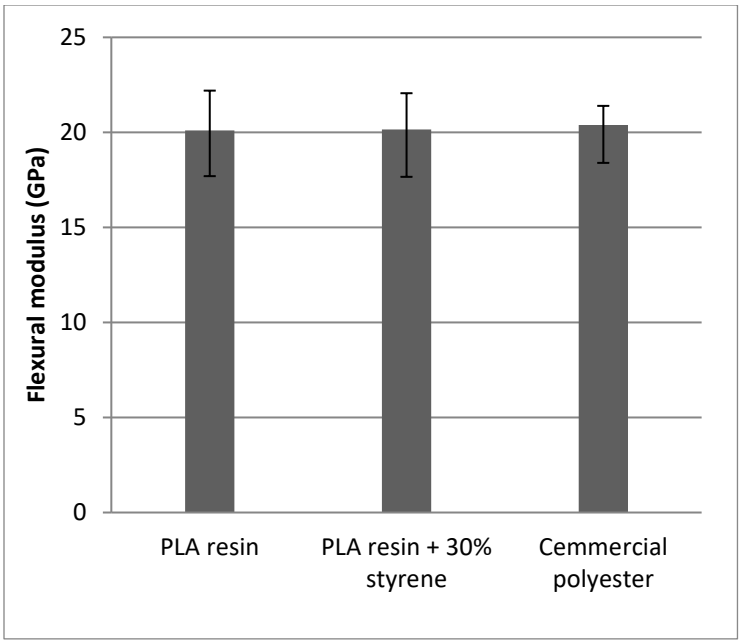

Figure 6. 3. The flexural modulus of different composites before aging

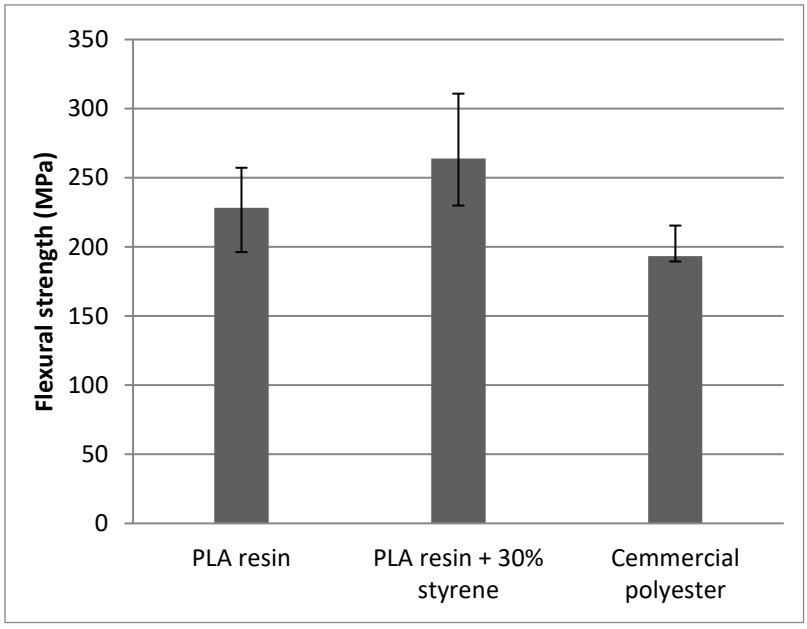

Figure 6. 4.The flexural strength of different composites before aging

Mechanical properties of all composites were also evaluated by tensile testing and results are summarized in figures 5 and 6. As figure 5 shows, the tensile modulus as a value of stiffness for all three type of composites were roughly the same before ageing

(19.8 GPa for PLA composites, 20.7 GPa for PLA-styrene composites and 20 GPa for commercial polyester resin composites). Observing similar stiffness for all three types of composites is in good agreement with flexural results. Although stiffness of composites with unidirectional or bidirectional, strong fibres greatly depends on characteristics of the fibre. Results indicate that co-polymerizing the PLA resin with styrene slightly increases the stiffness of the prepared composites and both composites made with neat and co-polymerized PLA are slightly stiffer compared to commercial polyester resin composite.

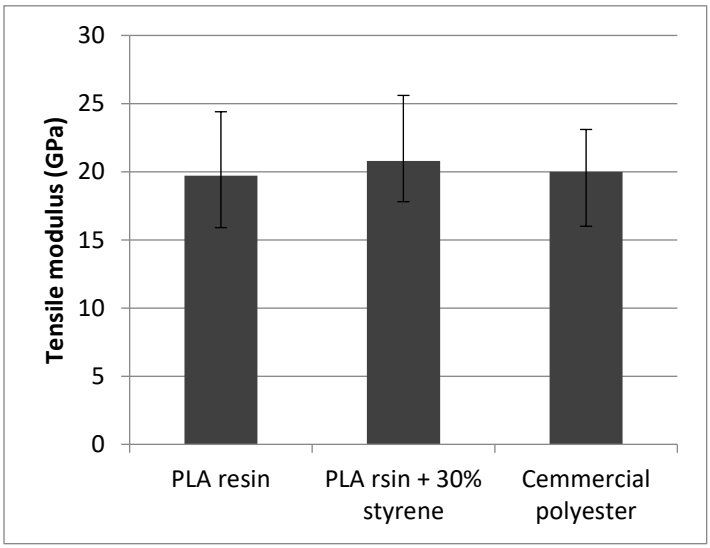

Figure 6. 5. The tensile modulus of different composites before aging

Figure 6 presents tensile max stress as an indicator of tensile strength for all composites. Results show that the tensile max stress for PLA composites were about 330 MPa which is considerably higher compared to the composites made with commercial polyester being 255 MPa. Results indicate that co-polymerization of the PLA based resin with styrene slightly reduces its composite`s tensile strength 330 MPa to about 295 MPa. Sathishkumar et al. reviewed a number of works reporting preparation of glass fibre reinforced polyester composites (Sathishkumar, Satheeshkumar, and Naveen 2014). The

tensile max stresses of composites prepared from woven glass fibre with polyester resins were reported between 200 MPa and 396 MPa in various studies. Considering that choice of glass fibres plays an important role in their tensile properties, still having relatively high tensile max stress of 330 MPa for the neat PLA resin composites indicates this resin incapable of being used as a matrix for structural composites for outdoor applications.

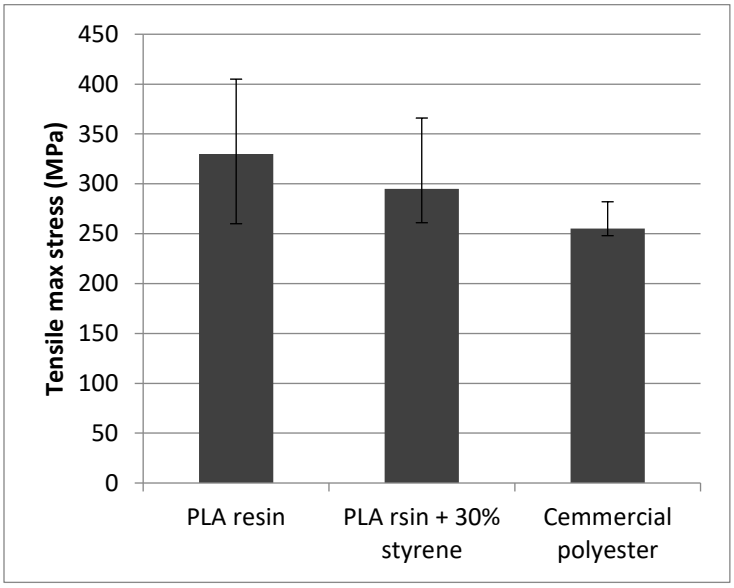

Figure 6. 6. The tensile max stress of different composites before aging

Table 2 summarizes results of Charpy impact test for all samples. Results show absorbed energies for commercial polyester resin composite was 97.1 kJ/m^2, for PLA resin composites was 119.6 kJ/m^2 and PLA+ styrene co-polymer composites was 125.1 kJ/m^2. A series of Scanning Electron Microscope (SEM) images were taken to observe the internal cracks and internal structure of the fractured surfaces and interfacial properties of the composites.

Table 6. 2. Impact analysis test data for different composites

	Absorbed energy kJ/m^2	SD

PLA resin composites	119.6	23.4
PLA/Styrene copolymer composite	125.1	18.7
Commercial polyester composites	97.1	21.7

Figure 7 a. and 7 b. and 7 c. show SEM images of the fracture area for the commercial polyester based composites, The PLA based composites and the PLA/styrene Copolymer based composites respectively. Images show that the failure process for all types of composites involved creation and growth of multiple cracks in the matrix, and fibre pull out and fibre breakage of fibres perpendicular to the impact and multiple cracks in fibre bundles parallel to the impact. During the impact of the specimen, the composite matrix of the composite materials is disintegrated in the breaking point. Figure 7 show fibres surface for all three type of composites are almost clean which indicates low fibre matrix adhesion for all types of resins.

Similar failure processes for all composites and knowing that fibre volume and fibre types were also similar for all composites, indicates that difference between absorbed energies for different composites are due to different energies absorbed during fracture of the resin matrixes thus the PLA resin absorbs considerably more energy during fracture compared to the commercial polyester and the PLA-styrene co-polymer also absorbs slightly more energy during fracture compared to neat PLA resin.

a)

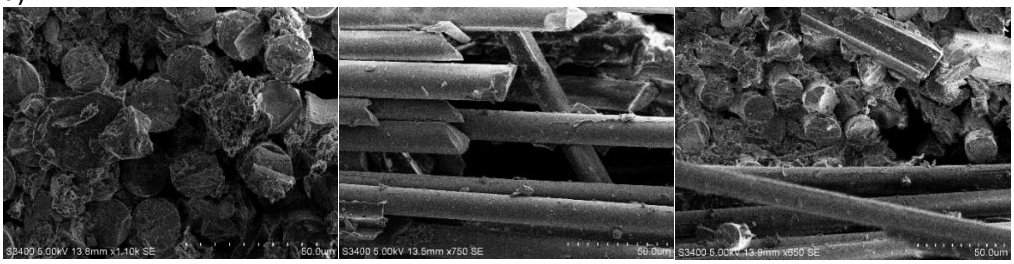

b)

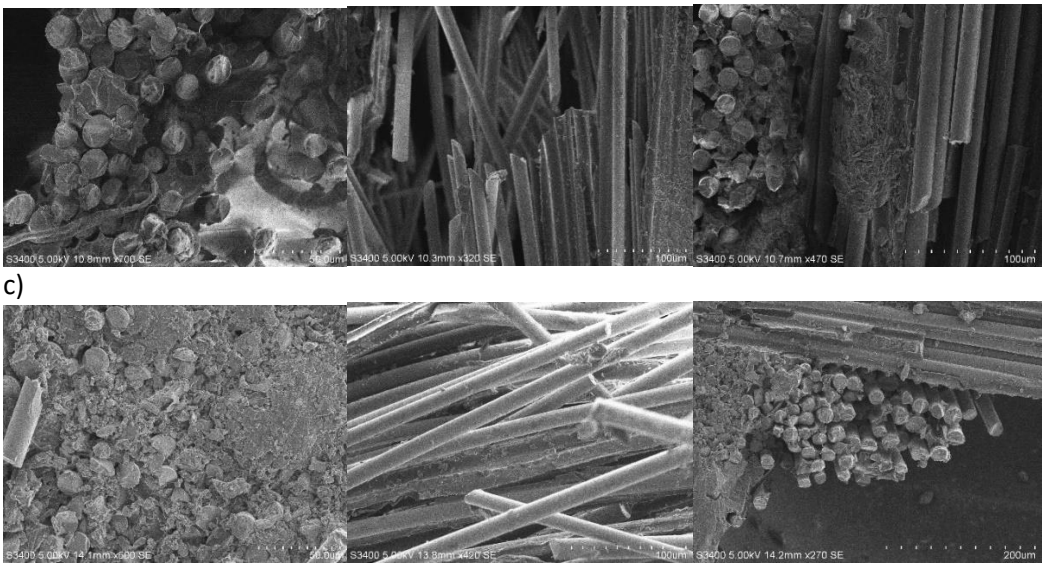

Figure 6. 7. SEM images of the fractured surfaces of the composites.

6.5. Ageing

Figure 8 shows tensile results for all composites after ageing. Results indicate the tensile modulus of PLA composites reduced dramatically after ageing from around 20 GPa to around 13 GPa while it stayed almost intact for commercial polyester resin, however, co-polymerizing with styrene considerably reduce the effect of weathering on its stiffness to less than 20%.

Figure 9 presents tensile maximum strength for all composites. Results indicate that the similar trend of reduction in tensile modulus after ageing applied for tensile strength as well. Tensile strength of the PLA resin was reduced from 330 to 180 MPa after ageing but although tensile strength of the PLA-styrene co-polymer composites being 295 MPa, was lower than that of PLA resin composites, after ageing it lost only 10% of its strength which shows adding 30% styrene the PLA resin dramatically improved its ageing behaviour.

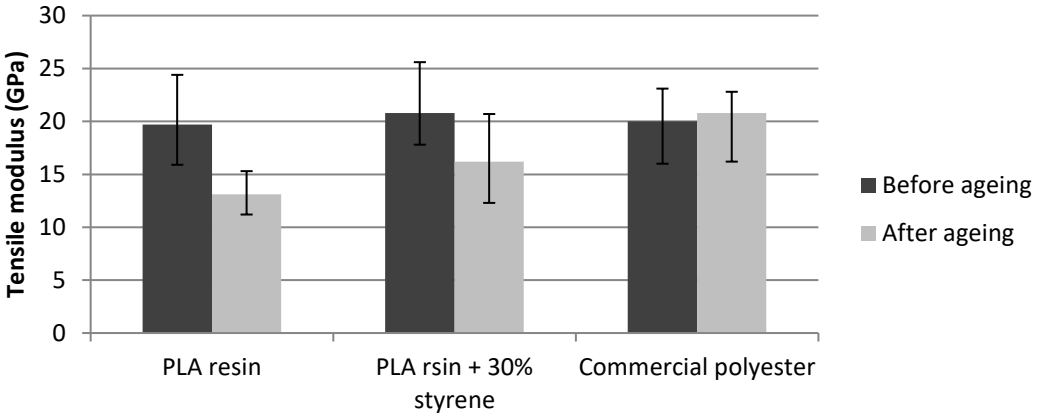

Figure 6. 8. Tensile modulus of the composites before and after aging

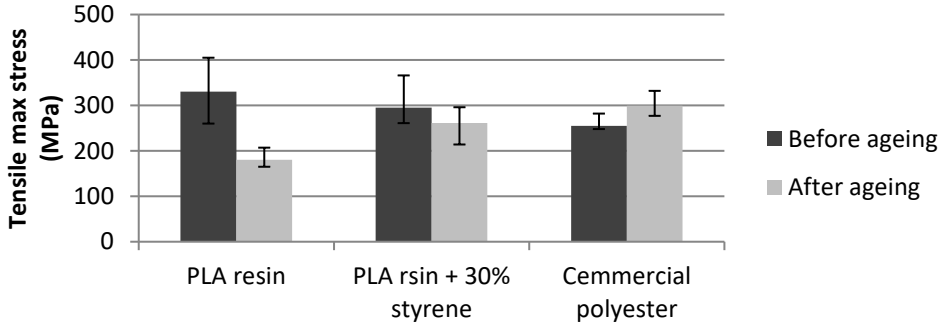

Figure 6. 9. Tensile max stress of the composites before and after aging

Figure 10 compares elongation of composites before and after ageing. Increase in elongation for all composites after ageing which is depicted in results suggests that however specimens were reconditioned for 24 hours in a desiccator, remaining water played the role of plasticizer for the composites and it can be seen that while tensile modulus of commercial polyester resin has remained intact, both max stress and elongation of the commercial polyester composite have increased. It can show improved curing at prolonginged residence at an elevated temperature during ageing. Huge fluctuation of elongation results might be due to non-uniform deterioration of the composites.

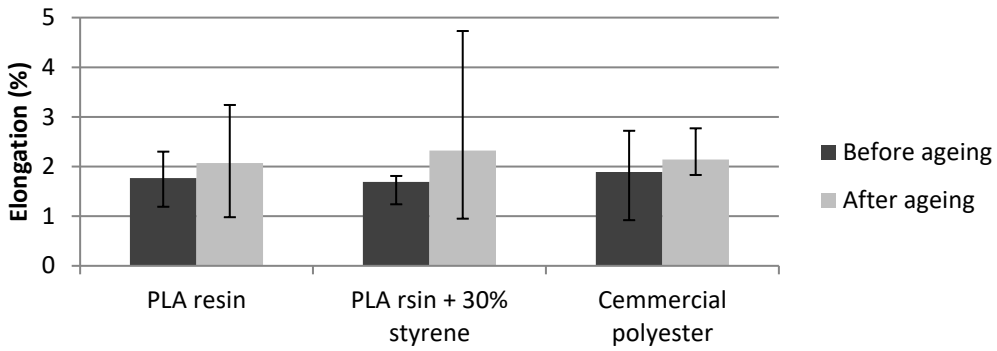

Figure 6. 10. Elongation percentage of the composites before and after aging

In the groups previous work (Esmaeili et al. 2015), ageing of bio-composites fabricated using same PLA resin and viscose fibres were reported and ageing simulation process in that study was identical to this work. In that study mechanical properties of composites made with viscose fibers were deteriorated to a considerably higher extend - more than 70% reduction in tensile modulus and tensile max stress after ageing- compared glass fibre composites in this study which indicates in that study degradation of both viscose fibers and PLA resin matrix were responsible for deterioration of mechanical properties of the composite and in order to fabricate bio-composites with higher ageing weathering properties, modification, and protection of the fibers could be considered.

These observations indicate that this resin could not be used for applications which expose them to prolonged weathering but still ageing behavior of the resin at an acceptable level for many outdoor applications especially for PLA resins which are co-polymerized by styrene.

6.6. Conclusion

In the first place, this study shows the recently developed resin is compatible with glass fibers and is a suitable bio-based alternative for oil-based commercial polyester resins for making mechanically strong and stiff glass fiber composites for many applications and specially applications in temperature above 50 ºC and also is capable of co-polymerizing with styrene which makes it suitable for high temperature environment applications in up to 120 ºC.

Results of ageing experiments and comparing them to the results of ageing experiments of viscose fiber composites in a previous study performed in the group, indicates that however weathering has a profound influence on mechanical properties of the composites with neat PLA resin matrix but deterioration in glass fiber composites are considerably less than that of glass fiber composite which shows both fiber and matrix were responsible for it in viscose fiber composites and treatment of bio-based fibers might improve the ageing behaviour of the bio-composite and as shown in the previous study, co-polymerizing the PLA resin with styrene, by adding styrene and eliminating the effect of fibers in ageing (either by using more durable fibers like glass fibers or treating bio-fibers,) bio-composites with acceptable weathering behaviour could be produced that are suitable for many outdoor applications which are not exposed to harsh weathering like interior or well-painted components in automotive industries.

Acknowledgements

The authors would like to acknowledge the funds provided by Agricultural Experiment Station, South Dakota State University, US Department of Agriculture, Washington, DC

and North Central Sun Grant through funding from USDA in support of this research work.

Chapter 7- Curing Kinetics of Methacrylated Star-Shaped Lactic Acid Based Thermosetting Resins

Arash Jahandideh[a], Kasiviswanathan Muthukumarappan[a]

[a]*Agricultural and Biosystems Engineering Department, South Dakota State University, PO Box 2120, Brookings, SD 57007, USA*

[*]Corresponding author: arash.jahandideh@sdstate.edu

Abstract

The aim of this study was to model the curing kinetics of the star-shaped lactic acid based thermosettings (*star*-La4.X). The *star*-La4.X resins were synthesized via direct condensation polymerization of the xylitol with lactic acid, followed by the end-functionalization by methacrylic anhydride. The curing behavior of the thermosetting was modeled based on the experimental data of isothermal differential scanning calorimetry, and the results were fitted to variety of phenomenological models, including *nth-rate model*, *autocatalytic model*, and *Kamal's model*. Using a nonlinear multiple regression through the Levenverg–Marquardt algorithm, the kinetic parameters of different models with different reaction orders were determined. By employing isoconversional adjustment, the apparent activation energy evolutions were obtained. The predicted models were then evaluated based on the experimental ramp differential scanning calorimetric data, to check the ability of the model for accurate predicting of the experimental data.

The results showed that the nth-rate model and its modified version are not capable of accurate predicting the experimental data. The results showed a good fit for the autocatalytic model with reaction order of 2, however no better fits were found for the autocatalytic models with reaction orders higher than 2. The Kamal's model has also been considered which showed a very good fit for the reaction order of 2. The higher reaction orders of Kamal's model have also been considered which were not capable of predicting the experimental results and extreme deviations have been resulted by using higher order reactions in Kamal's model.

KEYWORDS: thermoset; biopolymer; star-shaped poly lactic acid; curing behavior; phenomenological models

---

7.1 Introduction

Altering the architecture of a polymer from linear to star-shaped affects its physiochemical properties (Alward et al. 1986). Recently, the star-shaped thermosetting resins are gaining more attention. In brief, employing a star-shaped architecture for thermosettings results in an extended network, better thermomechanical properties, and lowers the viscosity, which in turn enhances processability of the product. The advantages of employing star-shaped architecture in thermosetting resins have been discussed elsewhere (Jahandideh, Esmaeili, and Muthukumarappan 2017, Jahandideh and Muthukumarappan 2016a, 2017). The star-shaped architecture can be achieved via poly-condensation of lactic acid with the core molecule, followed by the end-functionalization of the branches. The aim of end-functionalization is to produce resins capable of efficient crosslinking, by improving the reactivity of branches, generally by adding carbon-carbon double bonds (Åkesson et al. 2011b, Helminen, Korhonen, and Seppälä 2002, Liu,

Madbouly, and Kessler 2015, Sakai et al. 2013, Åkesson, Skrifvars, et al. 2010b, Bakare et al. 2014b, Bakare, Åkesson, et al. 2015, Chang et al. 2012b, Bakare et al. 2016). The end-functionalized thermosetting is then thermally cured, often by employing a free radical polymerization method (Jamshidian et al. 2010, Esmaeili et al. 2015, Bakare et al. 2014b, Sakai et al. 2013), which results in an irreversible transformation of oligomers into a cross-linked network (Vergnaud and Bouzon 2012).

Curing involves the irreversible transformation of low molecular weight oligomers into a solid network. Thermal curing of thermosets consists of the heating period stage and the curing reaction stage. During the heating period, the resin is heated up to a temperature at which the curing reaction starts, while in the curing reaction stage, the heat evolved from the overall curing mass at a constant temperature (Vergnaud and Bouzon 2012). Often, in the star-shaped thermosets, curing reaction starts by the assistance of a radical initiator. The tuning of curing parameters, including temperatures, pressures, time, etc. (Liang and Chandrashekhara 2006) is of importance, especially in thermosets, as it affects the properties of the final product and applying improper conditions for curing, may result in higher exotherms, faster gelation and more shrinkage due to excessive thermal zoning (Jahandideh and Muthukumarappan 2016a, Pereira and d'Almeida 2016). Understanding of the cure process is substantially important, especially for more complex systems such as industrial formulations, as a variety of additives are interfering in the curing procedure, resulting in a more complex cure kinetics. These factors indicate that an excellent control over curing process is required for production of thermosets with desired properties (Yousefi, Lafleur, and Gauvin 1997, Nawab et al. 2013).

7.2 Theoretical Background

The cure process can be evaluated based on two methods: a) monitoring the changes in concentration of the reactive groups, and b) by monitoring the changes in the physiomechanical properties of the sample (Yousefi, Lafleur, and Gauvin 1997). Cure kinetics correlate heat release rate (HRR) with the temperature (or time) and the resultant degree of cure (Liang and Chandrashekhara 2006). The analytical models of cure kinetics have wide applications in numerical simulations of composite manufacturing processes. Phenomenological –also called empirical- modeling approach is commonly employed for the analytical expression of the cure kinetics based on an Arrhenius type equation in which the approximated relationship of the curing parameters of the mathematical model are compared with the experimental data (Liang and Chandrashekhara 2006).

Several phenomenological models are presented in the literature for modeling the curing kinetics of the thermosetting resins; however, a few studies are performed for the modeling the curing kinetics of the star-shaped lactic acid based thermosettings (Liang and Chandrashekhara 2006, Chang et al. 2012b). The degree of cure, α, presents the extent of the curing reaction, and it is proportional to the amount of heat released by bond formation. The degree of cure is defined as:

$$\alpha = \frac{H}{H_u} \tag{7.1}$$

where H is accumulative reaction heat up to time t, and H_u is the total heat released during curing reaction. H_u is evaluated by

$$H_u = \int_0^{t_{fd}} \left(\frac{dQ}{dt}\right)_d dt \tag{7.2}$$

where t_{fd} is the total reaction time, and $(dQ/dt)_d$ is the instantaneous heat flow during the dynamic scanning. The curing rate, which is proportional to the rate of heat generation, is defined as:

$$\frac{d\alpha}{dt} = \frac{1}{H_u}\left(\frac{dH}{dt}\right) \qquad (7.3)$$

Table 1 provides a summary of the suggested phenomenological models in the literature.

Table 7. 1. Phenomenological models suggested for the curing kinetics of the thermosetting systems.

Model	Equation	Parameters	Dependent parameters	Ref
nth- order rate	$\frac{d\alpha}{dt} = K(1-\alpha)^n$	*K*: reaction rate constant $K = K_0 \exp\left(-\frac{\Delta E_A}{RT}\right)$	K_0: Arrhenius frequency factor ΔE_A: activation energy R: universal gas constant T: absolute temperature	(Du et al. 2004)
Autocatalytic	$\frac{d\alpha}{dt} = K\alpha^m(1-\alpha)^n$	K: reaction rate constant. $K = K_0 \exp\left(-\frac{\Delta E_A}{RT}\right)$ m, n: reaction orders defined by experimental data.	K_0: Arrhenius frequency factor ΔE_A: activation energy R: universal gas constant T: absolute temperature	(Kamal and Sourour 1973)
Kamal	$\frac{d\alpha}{dt} = (K_1 + K_2\alpha^m)(1-\alpha)^n$	Ki: reaction constants. $K_i = K_{i0} \exp\left(-\frac{\Delta E_i}{RT}\right), (i = 1,2)$ m, n: reaction orders defined by experimental data.	K_{i0}: Arrhenius frequency factors. ΔE_i: activation energy R: universal gas constant T: absolute temperature	(Kamal 1974)
Modified Kamal	$\frac{d\alpha}{dt} = (K_1 + K_2\alpha^m)(\alpha_{max} - \alpha)^n$	Ki: reaction constants. $K_i = K_{i0} \exp\left(-\frac{\Delta E_i}{RT}\right), (i = 1,2)$ m, n: reaction orders defined by experimental data. α_{max}: maximum degree of cure at a given temperature	K_{i0}: Arrhenius frequency factors. ΔE_i: activation energy R: universal gas constant T: absolute temperature	(Liang and Chandrashekhara 2006)
Cole	$\frac{d\alpha}{dt} = \frac{K\alpha^m(1-\alpha)^n}{1 + e^{C(\alpha-(\alpha_{c0}+\alpha_{CT}T))}}$	*K*: reaction rate constant. $K = K_0 \exp\left(-\frac{\Delta E_A}{RT}\right)$ *m*, *n*: reaction orders defined by experimental data. C: diffusion constant. α_{c0}: critical degree of cure at T=0 K.	K_0: Arrhenius frequency factor ΔE_A: activation energy R: universal gas constant T: absolute temperature	(Cole 1991)

	α_{CT}: increase in critical resin degree of cure with temperature.

In the authors' previous works, different star-shaped lactic acid based thermosets were synthesized and characterized (Jahandideh, Esmaeili, and Muthukumarappan 2017, Jahandideh and Muthukumarappan 2017) in which methacrylic anhydride was used for the end-functionalization of the lactic acid based resins with xylitol core molecules. The aim of this study was to model the curing kinetic of the star-shaped lactic acid based thermosettings with 4 lactic acid monomers in branches (*star*-La4.X). In this study, the *star*-La4.X thermosetting resins were synthesized via direct condensation polymerization of the xylitol with lactic acid followed by the end-functionalization of the branches by methacrylic anhydride. The curing behavior of the thermosetting was then modeled based the experimental data of isothermal differential scanning calorimetry values, and the results were fitted to the presented phenomenological models. The investigated models included nth- order rate and modified nth- order rate, autocatalytic model, and Kamal's model. For each selected model, the parameters were acquired and the reaction orders were calculated based on the isothermal curing data. The model was then evaluated based on another set of experimental ramp differential scanning calorimetric data, to check the ability of the model for predicting experimental data.

7.3 Experimental

Materials

L (+)-lactic acid (≥85%; Sigma-Aldrich), xylitol (≥99%; Sigma-Aldrich), toluene (≥99.8%; Sigma-Aldrich) and methanesulfonic acid (≥99.0%; Sigma-Aldrich) were used for poly-condensation reactions. Hydroquinone (≥99.5%; Sigma-Aldrich) and

methacrylic anhydride (≥ 94%; Sigma-Aldrich) were used as inhibitor and end-functionalization agents, respectively. Benzoyl peroxide (≥98%; Sigma-Aldrich) was used as the free radical initiator for crosslinking.

Resin synthesis

The resin was synthesized by direct condensation reaction of lactic acid monomers with xylitol core molecule, propagation of lactic acid chains, and further end-functionalizing of the hydroxyl groups of branches by methacrylic anhydride which is described in authors' previous studies in detail (Jahandideh, Esmaeili, and Muthukumarappan 2017, Jahandideh and Muthukumarappan 2016a). Toluene, containing 0.1 *wt*% of the catalyst, methanesulfonic acid, was used during condensation-polymerization step for efficient removal of water from the medium under nitrogen atmosphere. The branches were end-functionalized with methacrylic anhydride in presence of 1% hydroquinone; and the residual toluene and the released methacrylic acid were removed.

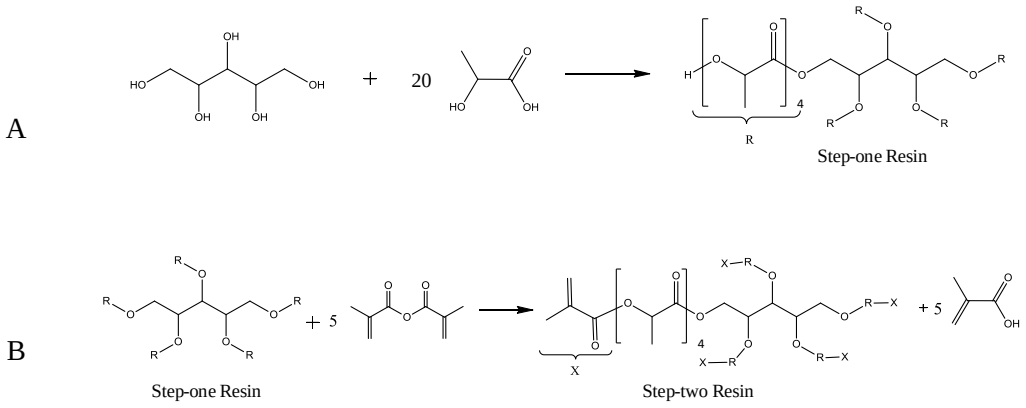

Figure 7. 1. Reaction scheme for A: synthesizing the poly-condensate (step-one) resins, and B: synthesizing the end-functionalized (step-two) resins

Curing of Resin and DSC analysis

The thermal curing was performed using an optimized free-radical polymerization method, using benzoyl peroxide 1 wt%. The end-functionalized resin was mixed with 1 wt% initiator solution in toluene, at 50 °C, and thoroughly mixed. The mixture kept under partial vacuum 10 mbar for two hours at room temperature. Approximately, 10 mg of uncured samples were sealed in hermetic aluminum hermetic pans.

Calorimetric analyses were carried out by a DSC on a TA Instrument Q 100 (V9.9 Build 303, Water LLC, DE, USA) thermal analyzer and analyzed under nitrogen atmosphere for 30 min at isotherms of 90 °C, 95 °C, 100 °C and 105 °C for isotherm DSC curing analysis, and from 0 °C to 220 °C at a heating rate of 2, 10, 15, 20, 25, 30 and 35 °C. min^{-1}. The ramp DSC curves were subsequently used for model verification purposes.

7.4 Results and Discussions

Modeling procedure

In order to model the curing kinetics of the synthesized resin, first, the isotherm DSC curing curves were fitted to a certain model, and the parameters of the best fitted model were attained for every single isotherm curve. Figure 2 presents the experimental data for isotherm curves of curing of the resin for 30 min at 90 °C, 95 °C, 100 °C and 105 °C. These isotherm curves were used for defining the parameters of the considered model. The developed model was then plotted using the former parameters and the considered heating rate versus the experimental DSC data of curing at different heating rates. Figure 3 presents the exothermic heat reaction (thermograms) of the curing reactions at different heating rates of 10 to 35 °C. min^{-1} from 0 to 220 °C.

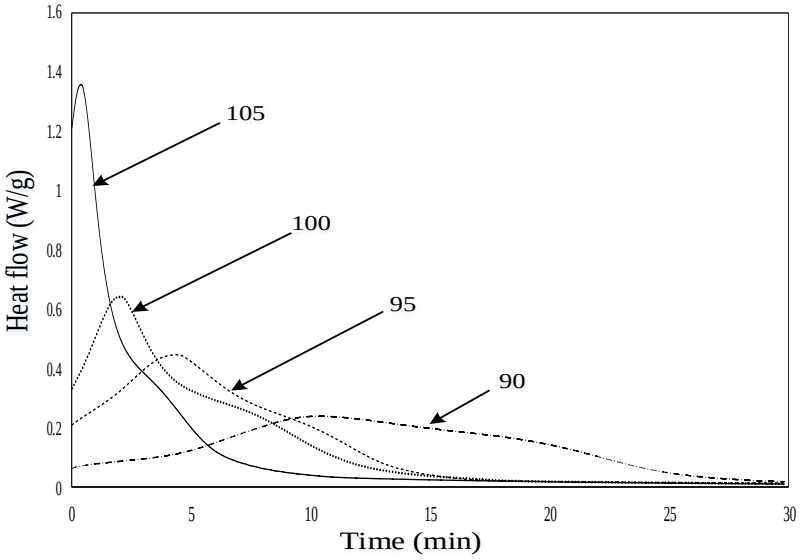

Figure 7. 2. The isotherm curves for curing of the resin for 30 min (90 °C, 95 °C, 100 °C and 105 °C)

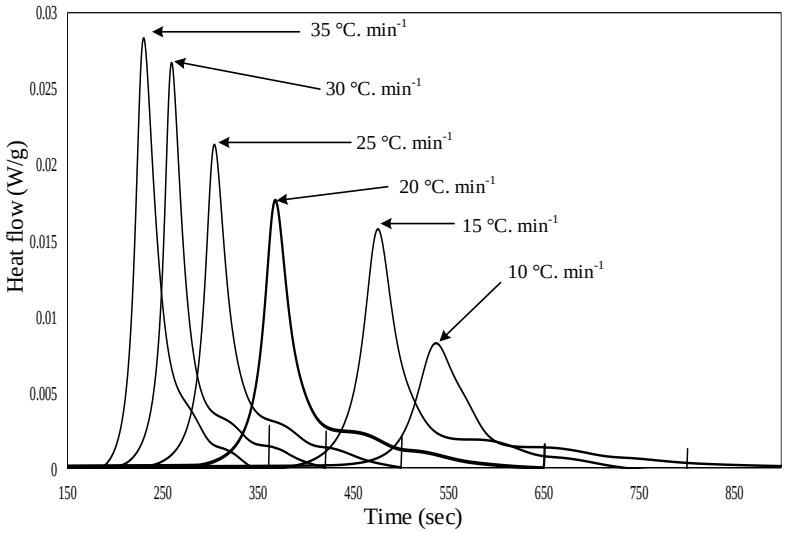

Figure 7. 3. The exothermic DSC curves of the curing reactions at different heating rates of 10 to 35 °C. min^{-1} from 0 to 220 °C.

nth- order rate model: The *nth- order* rate equation is the simplest phenomenological model proposed for predicting the rate of the curing reaction in thermosets. The *nth-order*

reaction predicts the maximum curing rate at the beginning of the curing phenomenon and does not account for the autocatalytic effect (Du et al. 2004). The model is expressed as:

$$\frac{d\alpha}{dt} = K(1-\alpha)^n \qquad (7.4)$$

Where, α is the degree of cure, n is the degree of reaction, and K is the reaction rate constant and defined as:

$$K = K_0 \exp\left(-\frac{\Delta E_A}{RT}\right) \qquad (7.5)$$

K_0: Arrhenius frequency factor

ΔE_A: Activation energy (kJ/mol)

R: universal gas constant (J / mol. K)

T: absolute temperature (K)

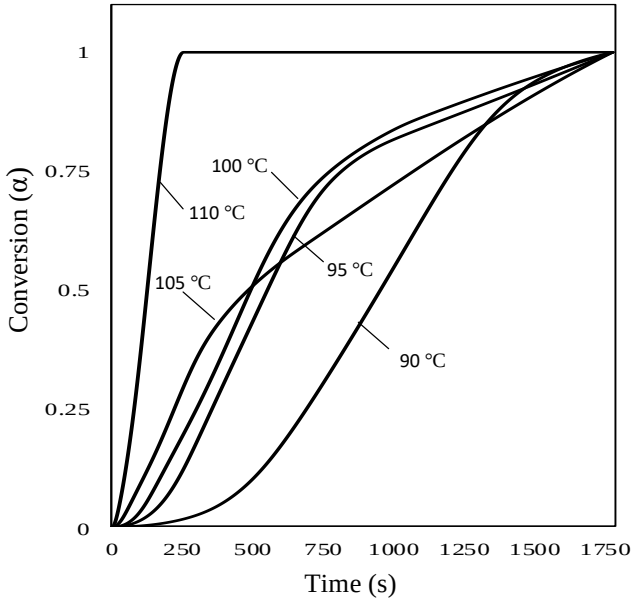

Figure 7. 4. The conversions versus curing time for samples cured at different isotherms 90-110 °C

Using a nonlinear multiple regression through the Levenberg–Marquardt algorithm (Moré 1978), the kinetic parameters of the nth-order rate model for n=2, 3 and 4 for the specified system were determined and summarized in Table 2. Employing isoconversional adjustment, it is possible to determine apparent activation energy evolution at different conversions. In addition, it is possible to check if a single activation energy evolution is capable to describe the curing process. The conversions versus time for different isotherms are depicted in Fig 4. The maximum degree of conversions after 20 minutes of curing versus temperatures were presented in the Fig 5.

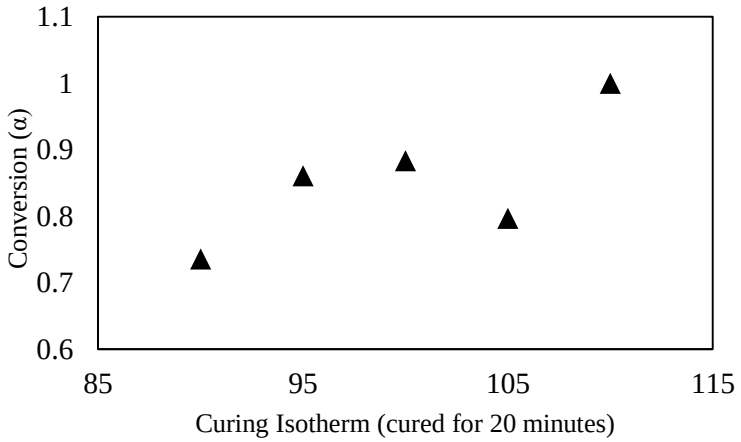

Figure 7. 5. Maximum Conversions after 20 minutes of curing for different curing isotherms

Table 7. 2. nth-rate model parameters for reaction orders of 2, 3 and 4.

Temperature (C)	90	95	100	105	110
n=2					
K	5.5761e-004	0.0011	0.0013	0.0017	0.0052

Arrhenius parameters	$K_0 = e^{22.969}$		ΔE_1 (kJ/mol) = 92.410		
nth-Rate reaction n=2	$\frac{d\alpha}{dt} = \left(e^{22.969} \times \exp(-\frac{92.410}{8.314\,.\,(273.15 + HR.t)}\right) \times (1-\alpha)^2$				
n=3					
K	4.8141e-004	9.7667e-004	0.0012	0.0017	0.0049
Arrhenius parameters	$K_0 = e^{24.708}$		ΔE_1 (kJ/mol) = 98.113		
nth-Rate reaction n=3	$\frac{d\alpha}{dt} = \left(e^{24.708} \times \exp(-\frac{98.113}{8.314\,.\,(273.15 + HR.t)}\right) \times (1-\alpha)^3$				
n=4					
K	4.2546e-004	8.8541e-004	0.0012	0.0017	0.0047
Arrhenius parameters	$K_0 = e^{36.35}$		ΔE_1 (kJ/mol) = 103.426		
nth-Rate reaction n=4	$\frac{d\alpha}{dt} = \left(e^{36.35} \times \exp(-\frac{103.426}{8.314\,.\,(273.15 + HR.t)}\right) \times (1-\alpha)^4$				

The Arrhenius equation can be written as:

$$\ln(K) = \ln(K_0) - \frac{\Delta E_A}{R}\left(\frac{1}{T}\right) \qquad (7.6)$$

By plotting ln (K) versus 1/T, the ln (K_0) and ΔE_A can be obtained – presented in Fig 6. The K_0 and ΔE_A values are presented in Table 2.

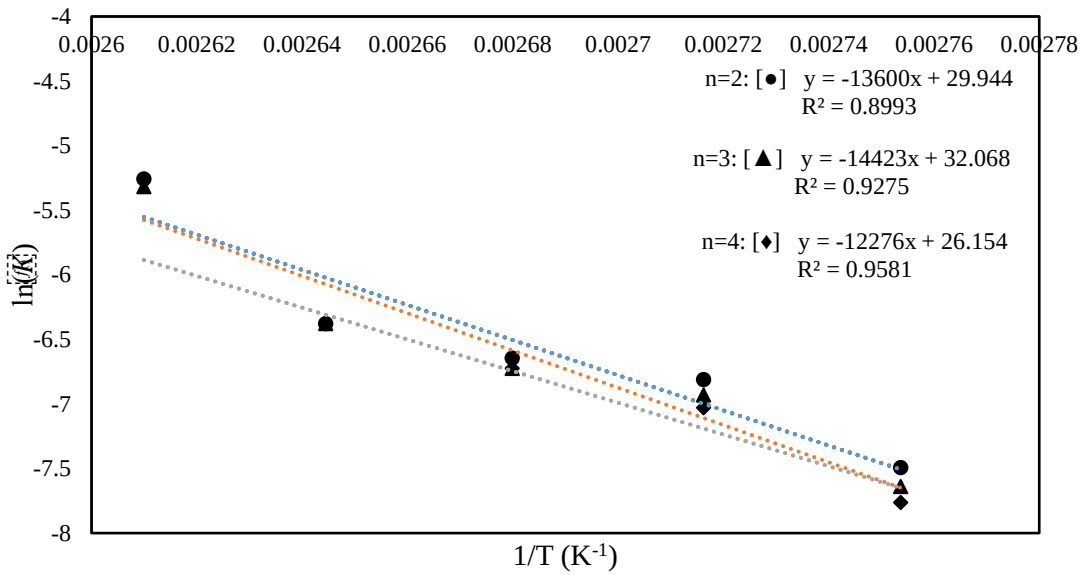

Figure 7. 6. ln(K) values vs 1/T (K^{-1}), plotted to estimate the activation energy and Arrhenius frequency factor for the nth-rate models of n=2,3 and 4.

The modeled equation for predicting the curing kinetic can be expressed as:

$$\frac{d\alpha}{dt} = \left(\mathrm{K0} \times \exp\left(-\frac{\Delta E}{R\,.(T0+HR.t)}\right)\right) \times (1-\alpha)^n \qquad (7.7)$$

Where, T0 is the initial temperature (K) and HR is the heating rate. The predicted models are presented in Table 2.

Verifications and model checking

In order to check the validity of the models, new experimental curing curves were plotted using different heating rates ranged from 2 to 30 °C.min^{-1} and compared with the predicted models - presented in Fig 7. The results showed that the nth-rate model is not capable of accurate predicting the experimental data. The experimental data versus modeled data have also been plotted and presented in Fig 8.

A

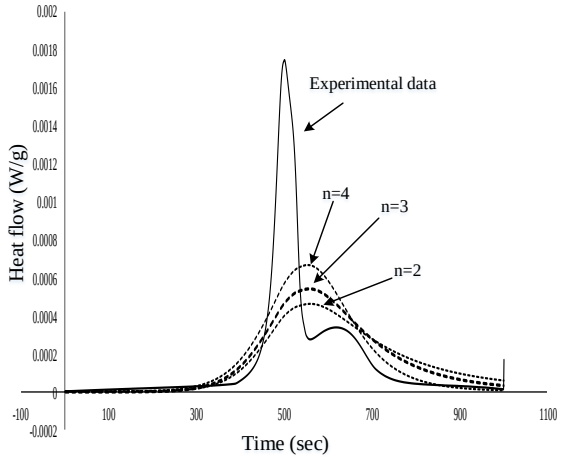
Experimental data
n=4
n=3
n=2
Heat flow (W/g)
Time (sec)

B

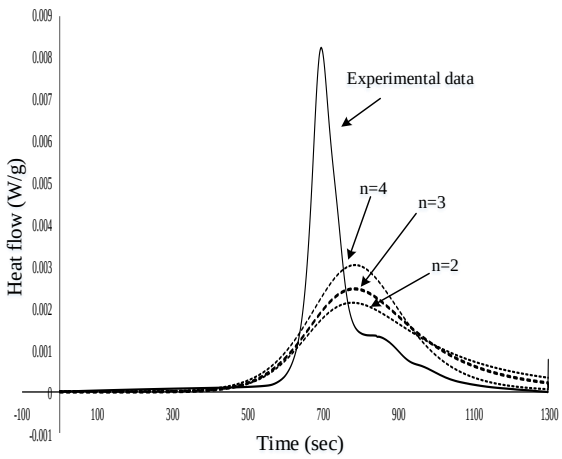
Experimental data
n=4
n=3
n=2
Heat flow (W/g)
Time (sec)

C

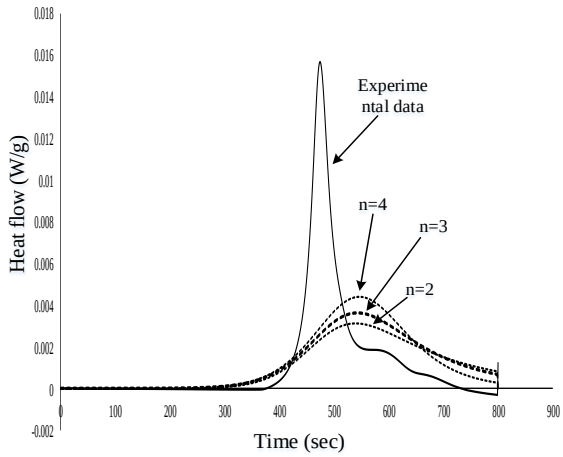
Experime
ntal data
n=4
n=3
n=2
Heat flow (W/g)
Time (sec)

D

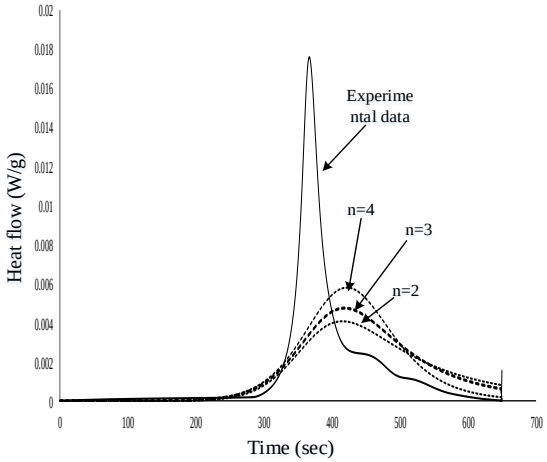
Experime
ntal data
n=4
n=3
n=2
Heat flow (W/g)
Time (sec)

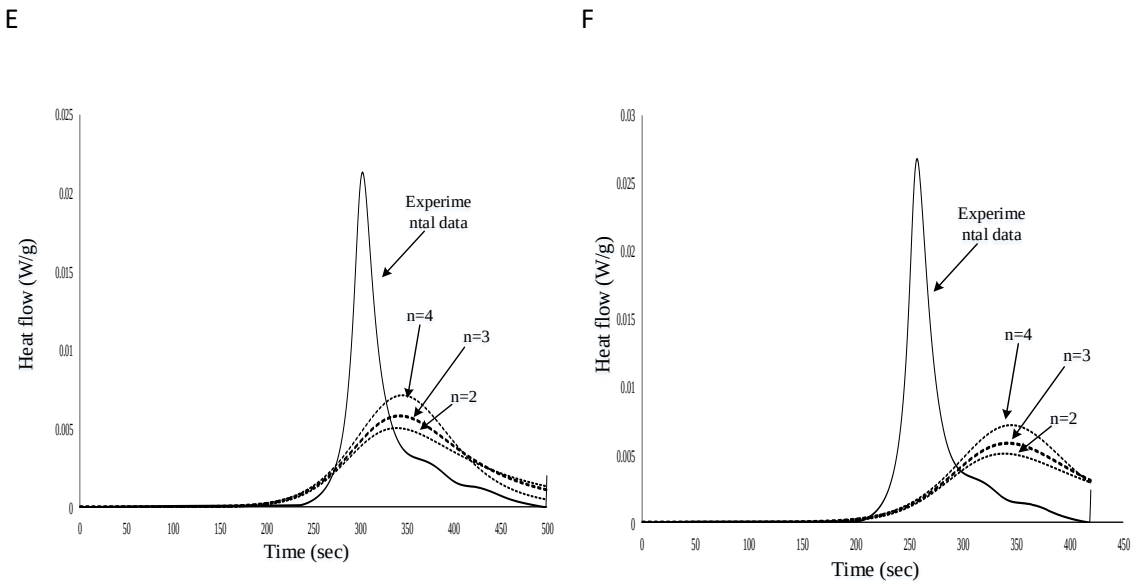

Figure 7. 7. Modeled data vs experimental data for curing with heat rate of 2 (A), 10 (B), 15 (C), 20 (D), 25 (E) and 30 (F) °C.min^{-1} for different reaction orders

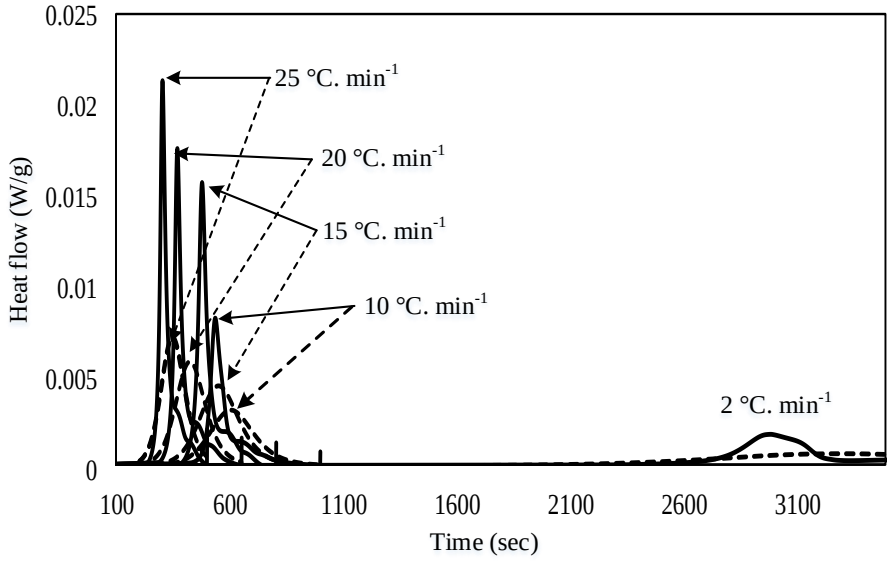

Figure 7. 8. Modeled data (dashed lines-nth-rate model, n=2) versus experimental data (solid lines) for curing of the specified system at different heating rates ranged from 0 °C to 220 °C.

In addition, the modified version of the nth-rate model was considered as:

$$\frac{d\alpha}{dt} = K\left(\frac{\alpha_{max}-\alpha}{\alpha_{max}}\right)^{x}(1-\alpha)^{n} \qquad (7.8)$$

where, α_{max} was the maximum curing degree at the corresponding temperature. However, no better fitting was obtained and the data is not presented here. The *x* value, the power of the α_{max} term, for all temperatures found to be 2.2204e-014, which is the minimum boundary of the function, indicating that the significance of the α_{max} term is negligible. This means that the model has a better fit without this term and will be reduced to the former general nth-rate model, which has been considered earlier.

Autocatalytic model: The second model which was considered was the *autocatalytic* model. The autocatalytic models represent the autocatalytic effect of the curing reactions.

This model considers a single rate constant for the reaction and the maximum reaction rate is supposed to take place in the intermediate conversion stage.

The model is expressed as:

$$\frac{d\alpha}{dt} = K\alpha^m(1-\alpha)^n \qquad (7.9)$$

Where, α is the degree of cure, *n and m* are the empirical coefficients, and the degree of reaction is expressed by n+m, and *K* is the reaction rate constant and defined by the Arrhenius equation as explained earlier in Eqn. 1. Using a nonlinear multiple regression through the Levenberg–Marquardt algorithm, the kinetic parameters of the autocatalytic model for n=2, 3 and 4 for the specified system were determined and summarized in Table 3. Employing isoconversional adjustment, it is possible to determine apparent activation energy evolution at different conversions. In addition, it is possible to check if a single activation energy evolution is capable to describe the curing process. The modeled equation for predicting the curing kinetic can be expressed as:

$$\frac{d\alpha}{dt} = \left(\mathrm{K0}\,.\exp\left(-\frac{\Delta E}{R\,.(T0+HR.t)}\right).\alpha^m\,.(1-\alpha)^n \qquad (7.10)$$

Where, *T0* is the initial temperature (K) and *HR* is the heating rate, and *n+m* is the order of reaction. The predicted models are presented in Table 3.

Table 7. 3. Autocatalytic model parameters for reaction orders of 2, 3 and 4.

Temperature (C)	90	95	100	105	110
Order of Reaction 2					
K	0.0045	0.0047	0.0047	0.0030	0.0259

m	0.9931	0.6187	0.6036	0.3013	1.0311
n	1.0069	1.3813	1.3964	1.6987	0.9689
Arrhenius parameters	$K_0 = e^{28.344}$		ΔE_1 (kJ/mol) = 102.886		
nth-Rate reaction n=2	$\frac{d\alpha}{dt} = \left(e^{28.344} \times \exp(-\frac{102886}{8.314 . (273.15 + HR.t)}\right) \times \alpha^{0.8116} \times (1-\alpha)^{1.1884}$				
Order of Reaction 3					
K	0.0097	0.0101	0.0101	0.0056	0.0547
m	1.4716	1.0048	1.0121	0.5259	1.5464
n	1.5284	1.9952	1.9879	2.4741	1.4536
Arrhenius parameters	$K_0 = e^{28.727}$		ΔE_1 (kJ/mol) = 101.722		
nth-Rate reaction n=3	$\frac{d\alpha}{dt} = \left(e^{28.727} \times \exp(-\frac{101722}{8.314 . (273.15 + HR.t)}\right) \times \alpha^{1.2587} \times (1-\alpha)^{1.7413}$				
Order of Reaction 4					
K	0.0199	0.0210	0.0209	0.0104	0.1131
m	1.9331	1.4016	1.4201	0.7633	1.9985
n	2.0669	2.5984	2.5799	3.2367	2.0015
Arrhenius parameters	$K_0 = e^{29.539}$		ΔE_1 (kJ/mol) = 101.980		

nth-Rate reaction n=4	$\frac{d\alpha}{dt} = \left(e^{29.539} \times \exp(-\frac{101980}{8.314\,.\,(273.15 + HR.t)}\right) \times \alpha^{1.6883} \times (1-\alpha)^{2.3117}$

By plotting *ln (K)* values versus *1/T*, the *ln (K_0)* and ΔE_A parameters of the model can be obtained – presented in Fig 9. The K_0 and ΔE_A values are presented in Table 3.

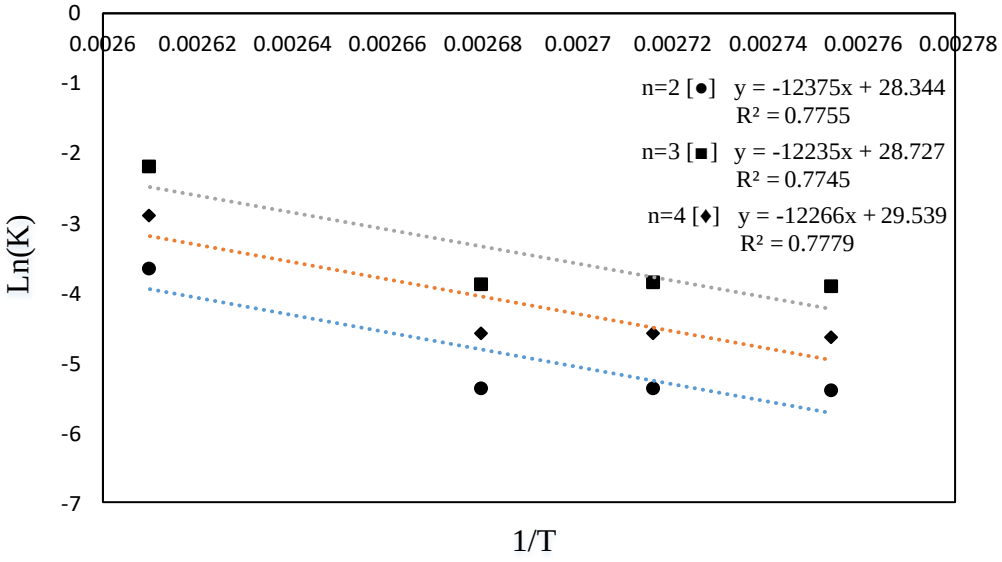

Figure 7. 9. ln(K) values vs 1/T (K^{-1}) plotted to estimate the activation energy and Arrhenius frequency factor for autocatalytic models with n+m=2,3 and 4.

Verifications and model checking of autocatalytic model

In order to check the validity of the autocatalytic model, new experimental curing curves were plotted using different heating rates ranged from 2 to 30 °C.min^{-1} versus the predicted models and presented in Fig 10. The results showed a good fit for the autocatalytic model with reaction order of 2. No better fit was found for the autocatalytic model with reaction orders higher than 2.

A

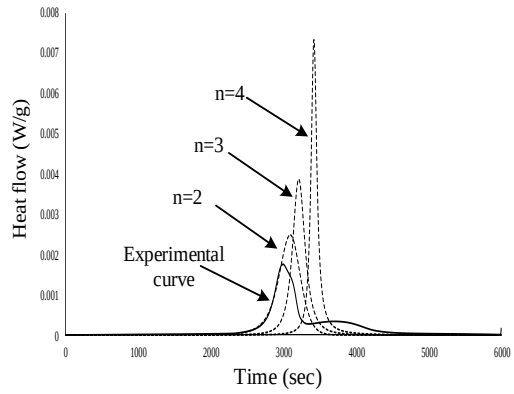
Heat flow (W/g)
0.008
0.007
0.006
0.005
0.004
0.003
0.002
0.001
0
n=4
n=3
n=2
Experimental curve
0
1000
2000
3000
4000
5000
6000
Time (sec)

B

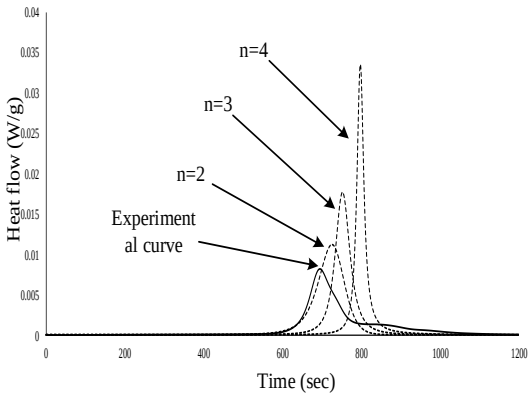
Heat flow (W/g)
0.04
0.035
0.03
0.025
0.02
0.015
0.01
0.005
0
n=4
n=3
n=2
Experiment al curve
0
200
400
600
800
1000
1200
Time (sec)

C

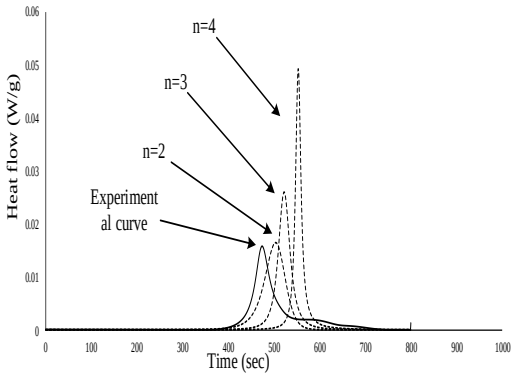
Heat flow (W/g)
0.06
0.05
0.04
0.03
0.02
0.01
0
n=4
n=3
n=2
Experiment al curve
0
100
200
300
400
500
600
700
800
900
1000
Time (sec)

D

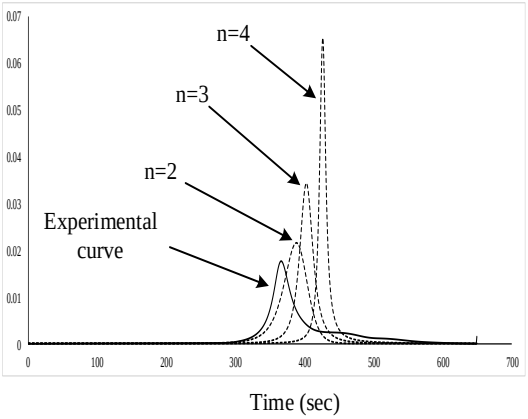
Heat flow (W/g)
0.07
0.06
0.05
0.04
0.03
0.02
0.01
0
n=4
n=3
n=2
Experimental curve
0
100
200
300
400
500
600
700
Time (sec)

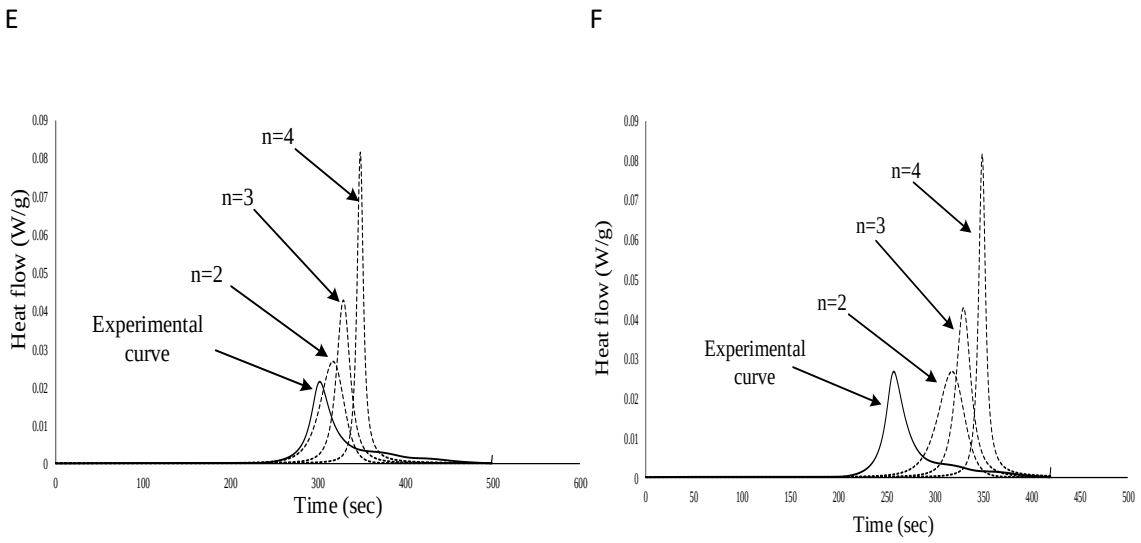

Figure 7. 10. Modeled data vs experimental data for curing with heat rate of 2 (A), 10 (B), 15 (C), 20 (D), 25 (E) and 30 (F) °C.min^{-1} for different reaction orders

The experimental results for curing at different heating rates of 2, 10, 15, 20, 25 and 30 °C.min^{-1} versus predicted data based on the autocatalytic model with n+m of 2, 3 and 4 is presented in Fig 10, and the best fitted model for all the heating rates has been presented in Fig 11. The results showed that the autocatalytic model is comparably capable of predicting the experimental data, and shows a reaction order of 2.

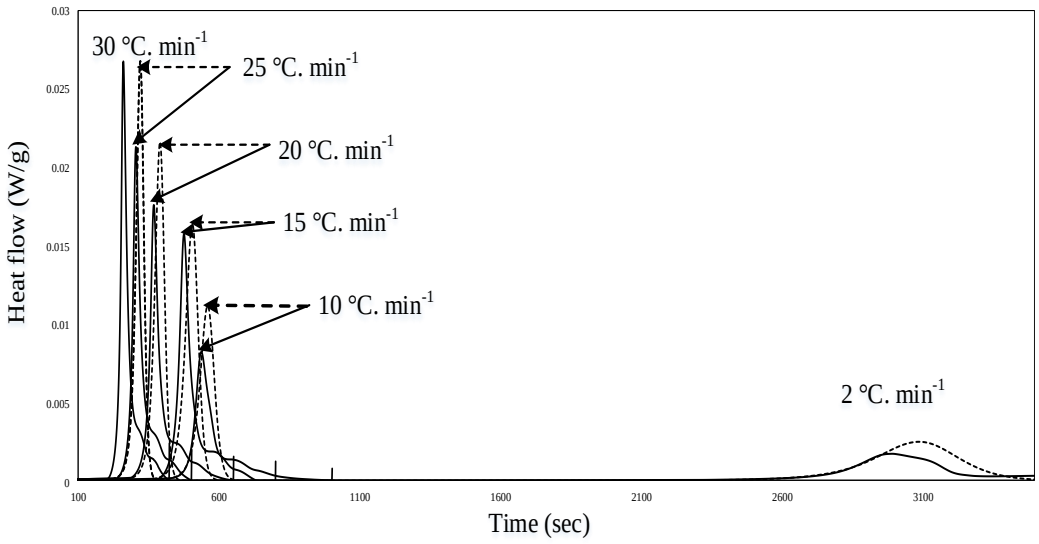

Figure 7. 11. Modeled data (dashed lines - autocatalytic model, n=2) versus experimental data (solid lines) for curing of the specified system at different heating rates ranged from 0 °C to 220 °C.

Kamal's model: A more accurate model has been proposed by Kamal and Sourour which considers two rate constants for the curing kinetics (known as *Kamal's model*) (Kamal 1974, Kamal and Sourour 1973). However, more parameters in the model have made the model to be more complicated. The limitation of Kamal's model (as well as nth-rate model and autocatalytic model) is that it is just valid when the kinetic of bond formation is considered to be the only rate controlling step in the curing reactions. The model is expressed as:

$$\frac{d\alpha}{dt} = (K_1 + K_2\alpha^m)(1-\alpha)^n \qquad (7.11)$$

Where, α is the degree of cure, *n and m* are the empirical coefficients and the degree of reaction is expressed by n+m, and K_1 and K_2 are the reaction rate constants and defined by the Arrhenius equation as explained earlier in Eqn. 1. Using a nonlinear

multiple regression through the Levenberg–Marquardt algorithm, the kinetic parameters of the Kamal's model for n=2 for the specified system were determined and summarized in Table 4. Employing isoconversional adjustment, it is possible to determine apparent activation energy evolutions at different conversions. In addition, it is possible to check if a double activation energy evolution is capable to describe the curing process. The Kamal's model equation for predicting the curing kinetic can be expressed as:

$$\frac{d\alpha}{dt} = \left(\left(\mathrm{K10} \,.\, \exp\left(-\frac{\Delta E1}{R\,.(T0+HR.t)}\right) + \left(\mathrm{K20} \,.\, \exp\left(-\frac{\Delta E2}{R\,.(T0+HR.t)}\right).\alpha^{m}\right).(1-\alpha)^{n}\right. \qquad (7.12)$$

Table 7. 4. Kamal's model parameters for reaction orders of 2.

Temperature (C)	90	95	100	105	110
Order of Reaction = 2					
K_1	2.2380e-014	2.2389e-014	7.4670e-006	2.1826e-007	0.0021
K_2	0.0041	0.0045	0.0014	0.0028	0.0191
m	0.7783	0.5694	0.0070	0.2297	1.2297
n	1.2217	1.4306	1.993	1.7703	0.7703
Arrhenius parameters	K_{10} (1/s) = $e^{11.19}$	K_{20} (1/s)= $e^{15.407}$	ΔE_1 (kJ/mol) = 142.629		ΔE_2 (kJ/mol)= 59.514
$\frac{d\alpha}{dt} = \left(e^{11.19} \times \exp\left(-\frac{142629}{8.314.(273.15+HR.t)}\right)\right) + \left(e^{15.407} \times \exp\left(-\frac{59514}{8.314.(273.15+HR.t)}\right)\right) \times \alpha^{0.763} \times (1-\alpha)^{1.237}$					

By plotting *ln* (K_i) versus *1/T*, the *ln* (K_{10}), the *ln* (K_{20}), ΔE_1, and ΔE_2 can be obtained and have been presented in Fig 12. The Ki_0 and ΔE_i values are presented in Table 4.

The higher orders of Kamal's model (m+n =3 and 4) have also been considered and the results showed that Kamal's model with higher reaction orders are not capable of predicting the experimental results and extreme deviations have been resulted by using higher order reactions in the Kamal's model.

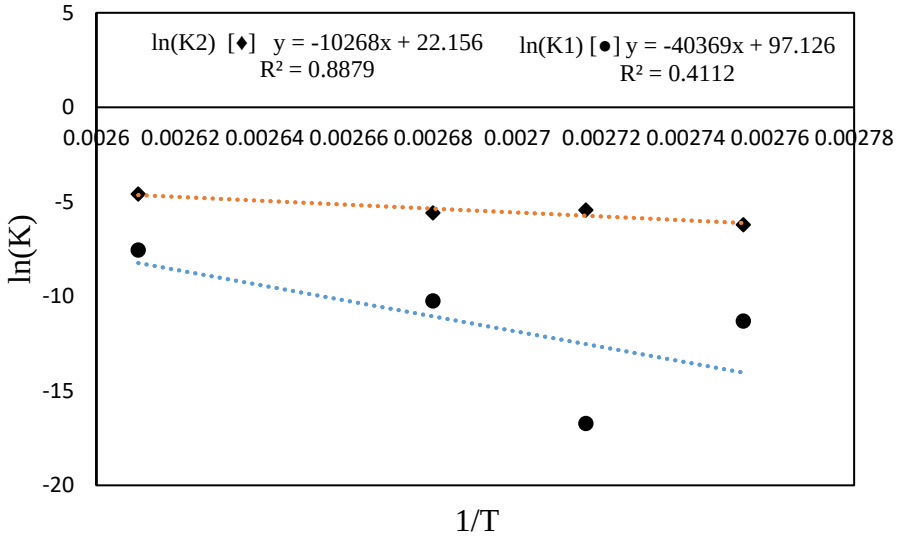

Figure 7. 12. ln(K_{i0}) values vs 1/T (K^{-1}) plotted to estimate the activation energy and Arrhenius frequency factors for Kamal's models for n+m=2.

Verifications and model checking

In order to check the validity of the Kamal's model, the experimental curing curves were plotted using different heating rates ranged from 2 to 30 °C.min^{-1} versus the Kamal's models prediction values which are presented in Fig 13 and the complete data have been presented in Fig 14. The results showed a very good fit for the Kamal's model

with reaction order of 2. It should be stated again that no better fit was found for the Kamal's model with reaction orders higher than 2.

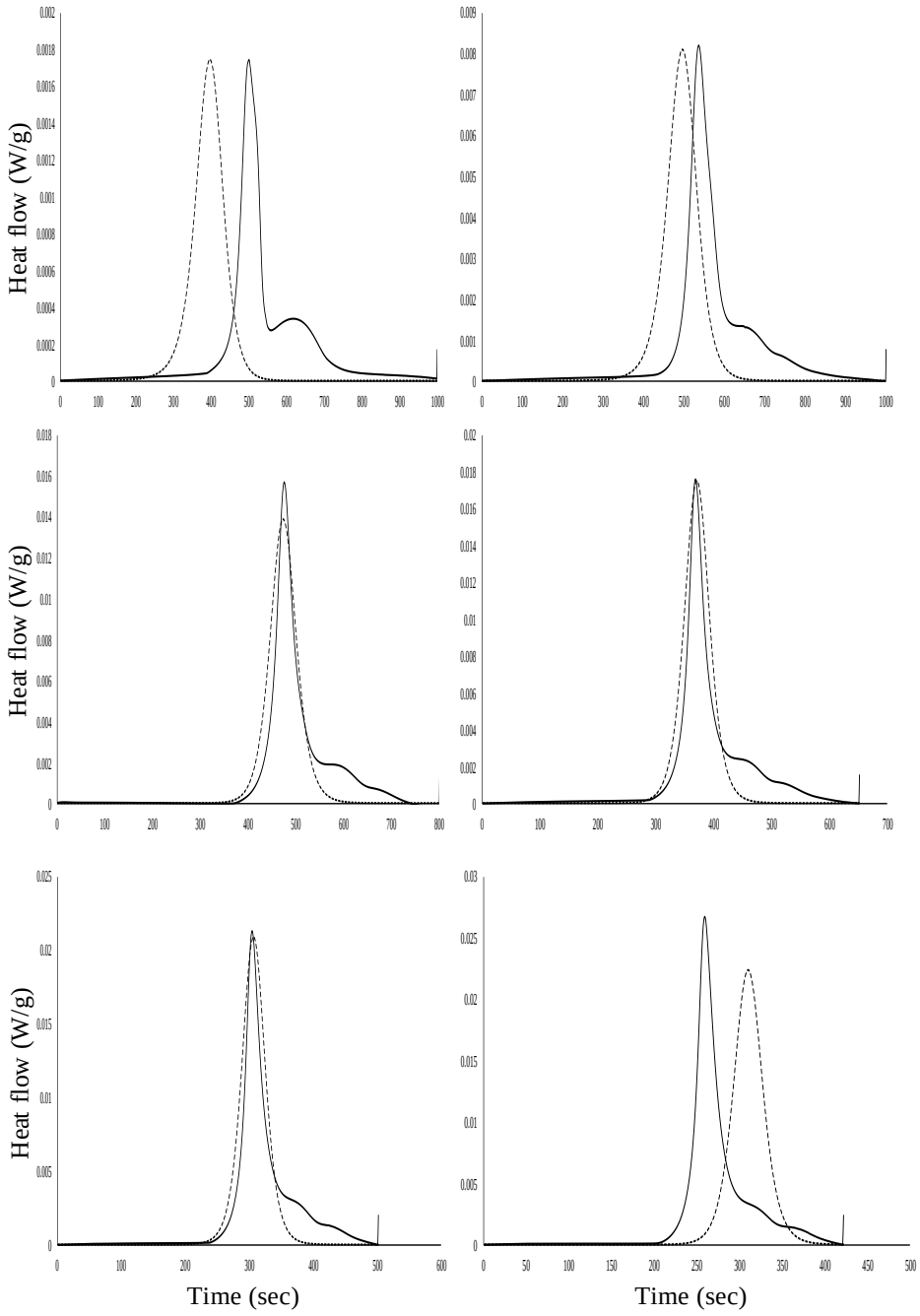

Figure 7. 13. Modeled data based on Kamal's model vs experimental data for curing with heating rates of 2 (A), 10 (B), 15 (C), 20 (D), 25 (E) and 30 (F) °C.min^{-1} for reaction order of m+n=2.

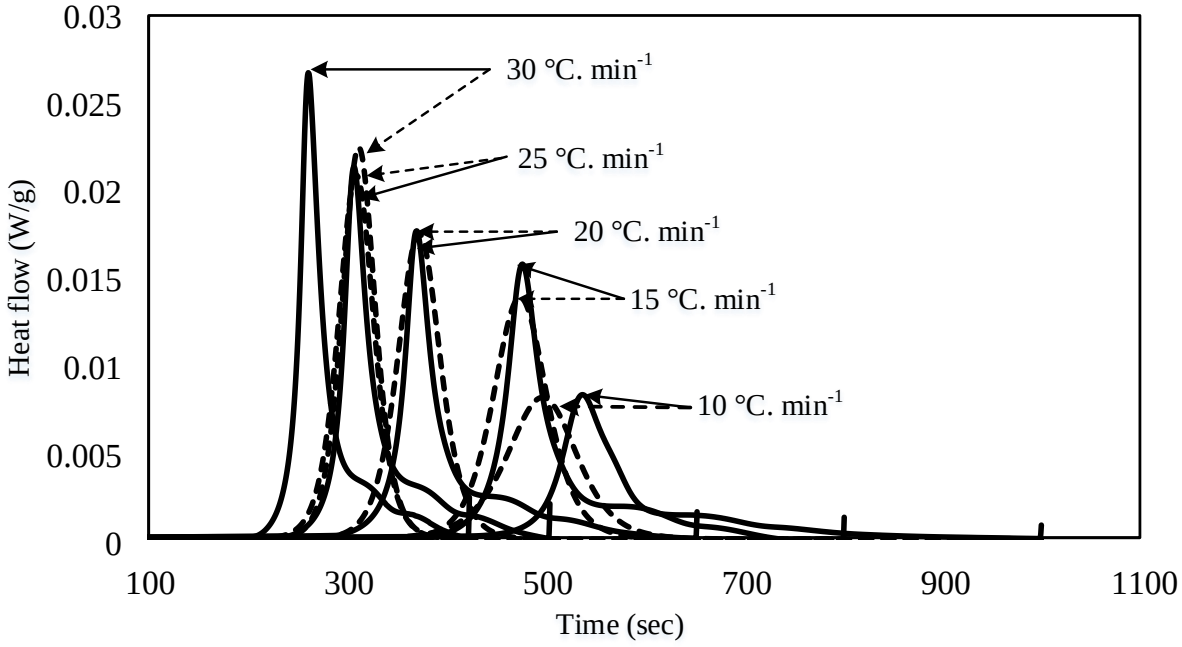

Figure 7. 14. Modeled data (dashed lines-Kamal's model, m+n=2) versus experimental data (solid lines) for curing of the specified system at different heating rates (presented in the Fig) ranged from 0 °C to 220 °C.

7.5 Conclusions

In the authors' previous works, different methacrylated star-shaped lactic acid based thermoset resins were synthesized and characterized with xylitol core molecules. The aim of this study was to model the curing kinetic of this star-shaped lactic acid based thermosettings with 4 lactic acid monomers in branches (*star*-La4.X). The *star*-La4.X thermosetting resins were synthesized via direct condensation polymerization of the xylitol with lactic acid followed by the end-functionalization of the branches by methacrylic anhydride. The curing behavior of the thermosetting was then modeled based the experimental data of isothermal differential scanning calorimetry values, and the

results were fitted to variety of available phenomenological models, including nth-rate model, autocatalytic model, and Kamal's model. For each and every considered model, the parameters were obtained based on the Arrhenius equation and the reaction orders were calculated based on the isothermal curing data. Using a nonlinear multiple regression through the Levenberg–Marquardt algorithm, the kinetic parameters of different models with different reaction orders for the specified system were determined and summarized in corresponding tables. By employing isoconversional adjustment, the apparent activation energy evolution at different conversions were obtained. The predicted model was then evaluated based on the experimental ramp differential scanning calorimetric data to check the ability of the model for predicting experimental data.

The *nth- order* rate equation is the simplest phenomenological model, proposed for predicting the rate of the curing reaction in thermosets. The *nth-order* reaction predicts the maximum curing rate at the beginning of the curing phenomenon and does not account for the autocatalytic effect. The results showed that the nth-rate model is not capable of accurate predicting the experimental data. However, higher reaction orders of 3 and 4 in the model slightly improved the prediction capability of the model. In addition, the modified version of the nth-rate model was considered with the maximum curing rate. However, no better fitting was obtained.

The *autocatalytic* model represents the autocatalytic effect of the curing reactions, and considers a single rate constant for the reaction in which the maximum reaction rate is supposed to take place in the intermediate conversion stage. The results showed a good fit for the autocatalytic model with reaction order of 2, and no better fit were found for the autocatalytic models with reaction orders higher than 2. The results showed that the

autocatalytic model is comparably capable of predicting the experimental data, and shows a reaction order of 2.

A more accurate model, known as Kamal's model, which considers two rate constants for the curing kinetics, has also been considered. However, more parameters in the model have made the model to be more complicated. The limitation of the presented models is that they are just valid when the kinetic of bond formation is considered to be the only rate controlling step in the curing reactions. However, the results showed a very good fit for the Kamal's model with reaction order of 2. The higher reaction order Kamal's model (of m+n =3 and 4) have also been considered and results showed that Kamal's model with higher order models are not capable of predicting the experimental results and extreme deviations have been resulted by using higher order reactions in the Kamal's model.

The vitrification effect (transforming to a non-crystalline amorphous solid) can also be considered in a modified version of the Kamal's model in which the fractional conversion has been considered to not exceed the degree of cure associated with vitrification. In the *Cole's model*, another controlling mechanism for the curing can also be considered in expressing the curing kinetic equation. This diffusion constant term in the equation, explicitly accounts for shifting from the kinetics to the diffusion control.

Acknowledgement

The authors would like to acknowledge the funds provided by Agricultural Experiment Station, South Dakota State University and US Department of Agriculture, Washington, DC in support of this research work.

Chapter 8 - Synthesis and Characterization of Novel Star-shaped Itaconic acid based Thermosetting Resins

Arash Jahandideh[1,*], Nima Esmaeili[2], Kasiviswanathan Muthukumarappan[1]

[1] Agricultural and Biosystems Engineering Department, South Dakota State University, PO Box

2120, Brookings, SD 57007, USA

[2] *Institute for Materials Research and Innovation, University of Bolton, Deane Road, Bolton, BL3 5AB, UK*

This chapter is under review in Journal of Polymers and the Environmental.

* Corresponding author current address: Agricultural, Biosystems & Mechanical Engineering Department, 1400 North Campus Drive Box 2120, Brookings, SD 57007, USA. Tel.: +1 (605) 6885670

Corresponding author: arash.jahandideh@sdstate.edu

Abstract

A star-shaped thermoset resin was synthesized by direct condensation reaction of itaconic acid and glycerol. In order to decrease the viscosity of the resin, the carboxyl groups of the oligomers were end-functionalized by ethanol. Chemical structures of the resins were studied by H and ^{13}C NMR and Fourier-transform infrared spectroscopy (FT-IR). The curing process was optimized by studying the residual exotherms during the curing process. Thermomechanical properties of the cured samples were studied by

Differential Scanning Calorimetry (DSC) and Dynamic Mechanical Analysis (DMA). Thermogravimetric analyses (TGA) were also carried out on both treated and pure resins to study the thermal stability of the cured samples. The viscosity of the pure and alcohol treated resins were measured at different temperatures and different stress levels. Water adsorption tests were also carried out to check the water absorption properties of treated resin's cured samples. The viscosity of the base-resin was 154.9 Pa s at room temperature which dropped to 1.8 Pa s upon increasing the temperature to 70 °C. The viscosity of the alcohol-treated resin was 0.35 Pa s at room temperature and 0.04 Pa s at 70 °C. The glass temperature (T_g) of the alcohol-treated resin was 122 °C. Fully biobased content and inexpensive raw materials, biodegradability, very good thermomechanical and comparably very promising rheological properties and processability along with good thermal stability are of advantages of the synthesized resin which makes the resin comparable with other thermosetting systems as well as the commercial unsaturated polyester resins.

Keywords: itaconic acid; synthesis; thermosets; crosslinking; star-shaped; thermal mechanical properties

---

8.1. Introduction

Altering the architecture of a polymer affects its chemical, diffusional and physical-mechanical properties (Alward et al. 1986). The star-shaped thermosetting resins are a class of branched resins with a core molecule and reactive branches which are gaining more and more attention day by day. Employing a star-shaped architecture results in an increase in the MW of the oligomers, and also reduces the viscosity and enhances

processability of the resin. The star-shaped resins offer an extended network which subsequently results in better thermomechanical properties in the final thermosetting product. In addition, the unsaturated reactive sites of the core molecule in the star-shaped structure provide the unique opportunity for the addition of a distinct functionality, e.g. flame retardancy, drug delivery, anti-microbial agents, etc.

To date, star-shaped thermosetting resins were synthesized employing different methods and different core molecules including glycolic acid (Wang et al. 2000, Lan and Jia 2006) ethylene glycol based compounds (Sawhney, Pathak, and Hubbell 1993, Kricheldorf, Hachmann-Thiessen, and Schwarz 2004, Biela et al. 2003), butanediol (Helminen, Korhonen, and Seppälä 2002), 1,6-hexanediol (Wang and Dong 2006), glycerol (Bakare et al. 2014b, Esmaeili et al. 2015, Arvanitoyannis et al. 1995), tri(hydroxymethyl)benzene (Perry and Shaver 2011), pentaerythritol (Åkesson, Skrifvars, et al. 2010b, Bakare et al. 2016, Åkesson et al. 2011b, Kim et al. 1992), xylitol (Jahandideh and Muthukumarappan 2016b, Teng et al. 2015), dipentaerythritol (Biela et al. 2003, Kim and Kim 1999), hexa(hydroxymethyl)benzene (Perry and Shaver 2011) and poly(3-ethyl-3-hydroxymethyloxetane) (Biela et al. 2003) for different applications of biocomposites (Bakare et al. 2014b, Bakare, Åkesson, et al. 2015, Bakare et al. 2016, Åkesson et al. 2011b), coating (Åkesson, Skrifvars, et al. 2010b), biomedical (Zeng et al. 2013, Kim, Kim, and Kim 2004), drug delivery (Park et al. 2003, Lin and Zhang 2010, Lin, Zhang, and Wang 2012), tissue engineering (Sakai et al. 2013), smart packaging and functionalized polymers (Finne and Albertsson 2002, Biela et al. 2005).

The star-shaped architecture can be achieved via two different methods: the *arm-first*, and the *core-first* methods. In the first-arm method, the linear arms prepared through

a controlled polymerization and then, reacted with the multifunctional terminating agents; while, in the core-first method the multifunctional core molecule reacts with the chain monomers and the propagation of the arms continue through a controlled polymerization pathway (Qiu and Bae 2006). However, the core-first method provides a better control over the polymerization process. After the poly-condensation reactions, the branches are get end-functionalized. The aim of the end-functionalization is to produce resins capable of efficient crosslinking, by improving the reactivity of branches, generally by adding carbon-carbon double bonds. Common end functionalizing agents presented in the literature are methacrylic acid (Åkesson et al. 2011b) and methacrylic anhydride (Helminen, Korhonen, and Seppälä 2002, Jahandideh and Muthukumarappan 2016b, Liu, Madbouly, and Kessler 2015, Sakai et al. 2013, Åkesson, Skrifvars, et al. 2010b, Bakare et al. 2014b, Bakare, Åkesson, et al. 2015, Chang et al. 2012b, Bakare et al. 2016, Åkesson et al. 2011b). In order to avoid gelation and unwanted cross-linking during the end-functionalization reactions, a stabilizer agent, e.g. hydroquinone, is often used. The end-functionalized thermosets are then cured, often through a thermal curing method which involves the irreversible transformation of oligomers into a cross-linked network. The thermal curing starts with the heating period and continues with the curing reactions in which the heat evolved from the reaction zone at a constant temperature (Vergnaud and Bouzon 2012). Often, a free-radical polymerization method is used to initiate the curing. Different initiators have been studied for the free radical polymerization including benzoyl peroxide (Jamshidian et al. 2010, Esmaeili et al. 2015, Bakare et al. 2014b), 2,5-bis(tert-butylperoxy)-2,5-dimethylhexane (Sakai et al. 2013), 2-butanone peroxide (Helminen, Korhonen, and Seppälä 2002), cobalt naphthenate (Finne and Albertsson

2002), *tert*-butyl peroxybenzoate (Åkesson, Skrifvars, et al. 2010b), N,N-dimethylaniline (Bakare, Åkesson, et al. 2015) and *tert*-butyl peroxybenzoate (Chang et al. 2012b, Åkesson et al. 2011b).

Developments in the emerging biobased thermosets are spectacular from a technological point of view. However, there are still several disadvantages associated with the current biobased thermosetting resins, e.g. low processability, environmental issues, expensive sources and poor thermomechanical properties. Methacrylic anhydride which is currently used for end-functionalization of resins, is a toxic and reactive liquid which does not have a known renewable source. Itaconic acid or methylenesuccinic acid is a non-toxic, readily biodegradable, fully sustainable chemical with an estimated annual global production of more than 150,000 ton which is produced commercially (since 1955 (Otsu et al. 1992)) by the fermentation of carbohydrates using *Aspergillus terreus* (Ma et al. 2013). Itaconic acid has been listed as one of the top 12 value-added chemicals by the U.S. Department of Energy (Werpy et al. 2004) and has been extensively studied to produce functional polymers (Bakare et al. 2014b, Lv et al. 2014, Avny, Saghian, and Zilkha 1972). These properties candidate the itaconic acid as an interesting sustainable industrial building block to replace the petrochemicals in chemical industries.

In the authors' previous works, different star-shaped lactic acid based thermosets resins were synthesized and characterized (Jahandideh and Muthukumarappan 2016a, Bakare et al. 2014b, Esmaeili et al. 2015, Jahandideh, Esmaeili, and Muthukumarappan 2017) in which methacrylic anhydride was used for the end-functionalization of the resin. The synthesized resins had a biobased content of up to 70-80 wt% and the viscosities ranged from 1 to 80 Pa s at room temperature which was not suitable for industrial

composite manufacturing. The aims of this study were to substitute the toxic nonrenewable methacrylic anhydride with the itaconic acid, and to overcome the viscosity barrier by end-functionalizing the resins with ethanol. In this study, the star-shaped itaconic acid based thermosetting resins were synthesized via direct condensation polymerization of the glycerol with the itaconic followed by the end-functionalization of the branches by ethanol. The chemical structures of resins were determined by H and ^{13}C NMR as well as FT-IR technique. The viscosity of the resins were measured via viscometry analysis. The curing process was optimized and the thermomechanical properties of the cured resins were investigated using dynamic mechanical analysis (DMA), differential scanning calorimetry (DSC) and the thermogravimetric analysis (TGA).

8.2. Materials and Methods

8.2.1 Materials

Itaconic acid (≥99%; Sigma-Aldrich) and glycerol (≥95.5%; Fisher) were used as the main reactants. Toluene (≥99.8%; Sigma-Aldrich) was used as the auxiliary solvent and methanesulfonic acid (≥99.0%; Sigma-Aldrich) was used the polycondensation catalysts. Ethanol (≥ 99.5%; Acros Organics) used for the end-functionalization of the oligomers in the second step of the synthesis. Dried Benzoyl peroxide (≥75%; Sigma-Aldrich) was used as the free radical initiator for crosslinking. For titration, xylenes (≥98.5%; Sigma-Aldrich), isopropyl alcohol (99.5%; Sigma-Aldrich), potassium hydroxide (≥85%; Sigma-Aldrich) and phenolphthalein (1% in ethanol, Fluka) were employed.

8.2.2 Synthesis synopsis

The star-shaped itaconic acid based resin, *star*-Ita-Gly, was synthesized by direct condensation reaction of itaconic acid and glycerol in the presence of methanesulfonic acid as the catalyst. Glycerol molecules were employed as the core molecule and the itaconic acid arms added consequently in a *core-first* synthesis fashion. The carboxyl-end of the branches of the resulted *star*-Ita-Gly oligomers were further reacted with ethanol to alter the terminal carboxyl groups to ethyl groups via another polycondensation reaction; and so, the alcohol treated resins (T*star*-Ita-Gly) were resulted. The chemical reactions and the idealized structures are presented in Fig 1.

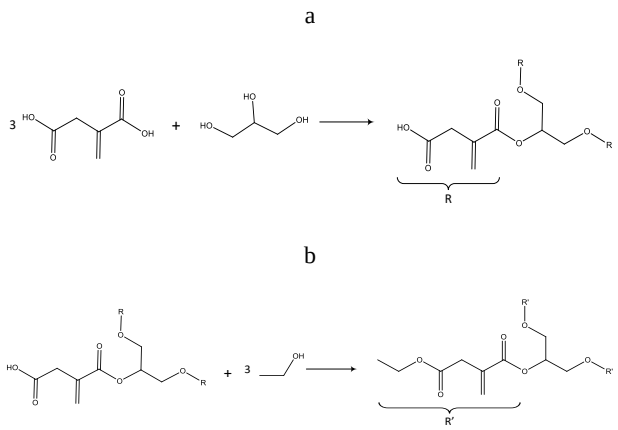

Figure 8. 1. Reaction schemes for a) the synthesis of *star*-Ita-Gly resins, and b) end-functionalization with ethanol to synthesis T*star*-Ita-Gly resins.

8.2.2.1 Synthesis of star-Ita-Gly: *polycondensation of Itaconic acid and glycerol*

The synthesis of *star*-Ita-Gly was carried out employing a direct condensation polymerization technique in the presence of toluene as an auxiliary solvent for water removal. The fine powdered itaconic acid (1.5 moles) was added to 0.5 mole of glycerol and diluted in 80 g of toluene containing 0.15% *wt* of the catalyst methanesulfonic acid in a three-neck, round-bottom flask, equipped with a magnetic stirrer in which one neck was

connected to the azeotropic distillation apparatus and the other necks were used for nitrogen flow and toluene reflux from and the azeotropic distillation apparatus and connecting a thermometer. The released water from the condensation (1.5 mole) was extracted progressively from the toluene and water-free toluene was refluxed to the reactor continuously. The temperature inside the flask was set to 140 °C and reaction was continued for 7 hours.

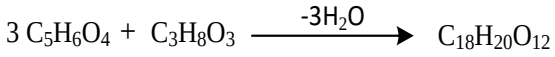

8.2.2.2 Synthesis the T*star*-Ita.Gly resin: *End functionalization of the star*-Ita.Gly *Oligomers*

The *star*-Ita.Gly resin resulted from the condensation of itaconic and glycerol would have reactive groups, but its high viscosity at room temperature made the effective casting process to be impossible. On one hand, the high viscosity of the resulted resins at the room temperature results in the improper mixing of the hardener and the resin, and on the other hand, employing higher temperatures, results in faster curing and consequently premature gelation of the samples. To overcome the viscosity problem, the branches were further functionalized with ethanol. In this step, first the resulted resin was cooled to 100 °C and under a constant stirring rate and nitrogen purge flow, 1 mole of ethanol added. The reactor was equipped with a condenser and after 30 min of reaction, the reactor was cooled to 80 °C and 1 mole of ethanol (30% excess) was added dropwise at 80 °C for two hours. In order to remove the excess ethanol, after the reaction completed, the condenser disconnected and the temperature was increased to 120 °C for two more hours. The medium was then transferred to a drop-shaped glass flask connected to a rotary

evaporator under partial vacuum conditions (~10 mbar, 1 hour at 90°C) to remove the residual ethanol and toluene. The chemical reactions and idealized structures are presented in Fig 1.

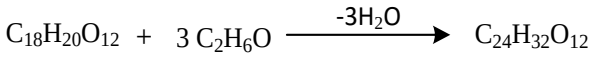

8.2.3 Curing of the resins

In this study, a free-radical polymerization method was employed for curing of the *star*-Ita.Gly and T*star*-Ita.Gly resins. The reactions were started by the assistance of a radical initiator (2 wt% of benzoyl peroxide) and continued by placing the mixture to a 70 °C preheated oven for 3 hours. The presence of the residual exotherms were investigated by DSC. The cured resins were further analyzed by TGA and FTIR. The T*star*-Ita.Gly resin samples were further analyzed by DMA.

8.2.4 Characterization

The progress of the condensation reaction of the itaconic acid and glycerol was evaluated by titrating the residual carboxyl groups of the reactants during the *star*-Ita.Gly resin synthesis based on ASTM D974-12. The conversion progress was determined by titrating aliquot samples (1 g) taken hourly during the reaction. The samples were first diluted with 20 mL of 1:1 *v/v* xylene/isopropyl alcohol solutions and then titrated with 0.5 M KOH in absolute ethanol with phenolphthalein 1% indicator.

The chemical structure of *star*-Ita.Gly and T*star*-Ita.Gly resins were evaluated with a proton and carbon Nuclear Magnetic Resonance (H NMR and ^{13}C NMR) spectrometry (Bruker BioSpin GmbH, Germany) at 400 MHz and 45 °C. Sample concentration in 5 mm tubes was ~10

wt% in $CDCl_3$ and the internal standard was tetramethylsilane, TMS. The shifts were expressed in ppm.

IR spectra of the *star*-Ita.Gly, T*star*-Ita.Gly and cured samples of the resins were recorded at room temperature on Nicolete 6700 spectrometer, supplied by Thermo Fisher Scientific, Massachusetts, USA, in the range of 4000–600 cm^{-1}. Each spectrum was recorded after the sample was scanned 60 times.

Calorimetric analyses were carried out by a DSC on a TA Instrument Q 100 (V9.9 Build 303- supplied by Water LLC, New Castle DE) thermal analyzer. Samples of approximately 10 mg were sealed in aluminum hermetic pans and tested under a nitrogen atmosphere. Uncured resin samples were analyzed from -20 °C to 220 °C at a heating rate of 10 $°C.min^{-1}$ in order to investigate the crosslinking reaction. Isothermal curing of resins was also performed at 90 °C, 100 °C, 120 °C, 130 °C, 140 °C and 150 °C for 20 minutes and residual exotherms were analyzed from 25 °C to 200 °C at a heating rate of 10 $°C.min^{-1}$.

Thermogravimetric analyses of the cured resins were carried out with a Q50 from a TA Instrument supplied by Waters LLC. Samples with an approximate mass of 30 mg were heated from 30 °C to 600 °C, at a heat rate of 10 $°C.min^{-1}$ under a helium purge gas stream of 20 $mL.min^{-1}$.

Dynamic Mechanical Analysis was performed on cured samples of T*star*-Ita.Gly resin cured at 70 °C (Q800 from TA Instruments, supplied by Waters LLC). The tests were performed on samples with dimension of approximately 60 mm ×15 mm ×3 mm from -20 °C to 180 °C in a dual cantilever bending mode with a heat rate of 10 $°C.min^{-1}$;

the frequency was 1 Hz, the amplitude was 15 µm and the tests were performed under a nitrogen atmosphere.

The viscosity of the uncured resins were determined using a viscoanalyzer rheometer (TA instrument, Sweden). All measurements were done with a truncated cone plate configuration (Ø15 mm, 5.4 °C). Viscosities of uncured resins were measured in a temperatures range of 30 °C to 120 °C in increments of 10 °C. Shear rate ranged from 1 to 200 s^{-1}.

8.2.5 Water adsorption tests

The water adsorption tests were carried out on the cured T*star*-Ita.Gly samples based on ASTM D 570–98 to determine the relative rate of absorption of water by the cured samples when immersed. The dimension of test specimens were 60 mm × 60 mm × 1 mm. The tests were perform in 3 modes: long-term immersion (23I), two-hour boiling water immersion (BI) and immersion at 50 °C (50I). In 23I, the sample was immersed in a distilled water bath at 23 ºC and the total water absorption versus time was recorded; in the BI test, the water absorption was measured after 2 hours of immersion in a boiling distilled water bath and in the 50I mode, water absorption was measured at 50 °C at different time intervals. Tests were continued until the samples got substantially saturated (achieved water absorption rates to be ≤ 1% or 5 mg between intervals).

8.3. Results and discussion

8.3.1Monitoring the progress of the polycondensation of itaconic acid and glycerol

Employing a proper retention-time is a crucial factor in polycondensation reactions. While insufficient time results in unreacted reactants, the excessive retention

time promotes the transesterification reactions (Jahandideh and Muthukumarappan 2016a, 2017). In this study, the progress of the condensation reaction of itaconic acid and glycerol was evaluated by two methods: first, by determination of the *Total Acid Number* (TAN) for residual acidic constituents (carboxyl groups) of the itaconic acid during the polycondensation and second, by monitoring the formation of (─C─O─C─ stretch) bonds between the hydroxyl groups of the core molecule and the carboxyl groups of the itaconic acid which can be identified in the FTIR spectra of the polycondensation as a signal at 1100-1200 cm^{-1} (Nouri, Dubois, and Lafleur 2015b, Lin, Zhang, and Wang 2012, Xiong et al. 2014). In the titration method, the quantity of carboxylic groups is measured with an acid-base titration method (Murillo, Vallejo, and López 2011, Xiao, Mai, et al. 2012).

The ASTM D974-12 defines the TAN as the quantity of KOH (in mg), required for the titration of 1 g of the sample dissolved in a specified solvent system. The ratio of the *reacted* to *initial* available carboxylic groups, indicates the degree of completion of the condensation reaction (Knothe 2006). The conversions during the first 660 minutes of the reaction were calculated based on the mL of consumed KOH in absolute ethanol by the 1 g samples. Figure 2 shows that the reaction is started almost after 50 minutes. The conversion reaction proceeds rapidly during the next 350 minutes. The reaction continues until 420 minutes and after that the conversion rate did not change significantly due to the progress of transesterification reactions. Based on the titration results, a 7 hours condensation-reaction period was considered to be sufficient for the polycondensation of itaconic acid and glycerol which results in a 97% conversion of the carboxylic groups. Bakare et al. employed a similar acid-base titration method for the star-shaped LA-

glycerol resins and reported a 95% conversion after 360 minutes (Bakare et al. 2014b). Using a similar polymerization method Jahandideh et al. reported a conversion of 95% for star-shaped xylitol-LA resins after 720 minutes (Jahandideh and Muthukumarappan 2016a). The differences between the conversion rates can be attributed to the differences between the numbers of hydroxyl groups of the core molecules. Increasing in the number of the hydroxyl groups of the core molecule in the star-shaped architecture is believed to affect the conversion rates of the polycondensation (Jahandideh and Muthukumarappan 2017).

Figure 3 presents the FTIR spectra of the polycondensation samples, taken after 1, 3, 5 and 7 hours of reaction. The progressive appearance of a signal at 1100-1200 cm^{-1} can be attributed to the formation of bonds between the hydroxyl groups of the core molecule and the carboxyl groups of the itaconic acid (─C─O─C─ stretching vibration) (Nouri, Dubois, and Lafleur 2015b, Lin, Zhang, and Wang 2012, Xiong et al. 2014). The signal between 1000 and 1100 cm^{-1} can also be attributed to the CO─ stretching vibration (Nouri, Dubois, and Lafleur 2015b, Lin, Zhang, and Wang 2012, Xiong et al. 2014). In addition, appearance of a weak signal at ~1800 cm^{-1} can be attributed to vinyl hydrocarbon compounds (R-CH=CH_2).

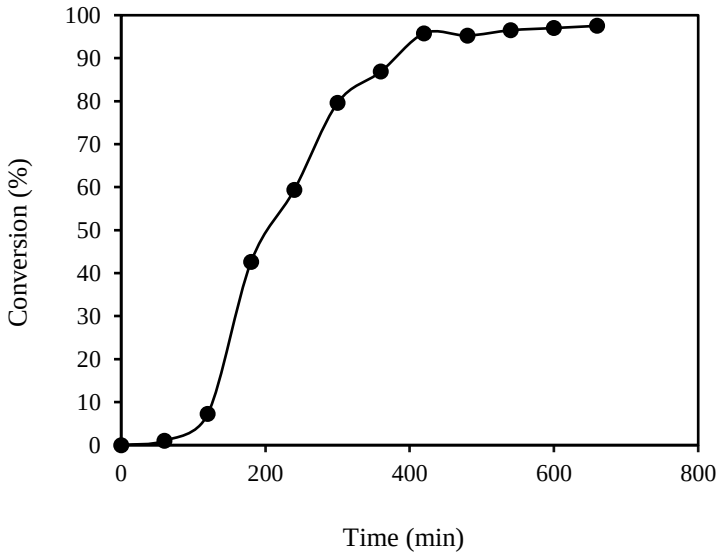

Figure 8. 2. Conversion of carboxyl groups in poly condensation reaction

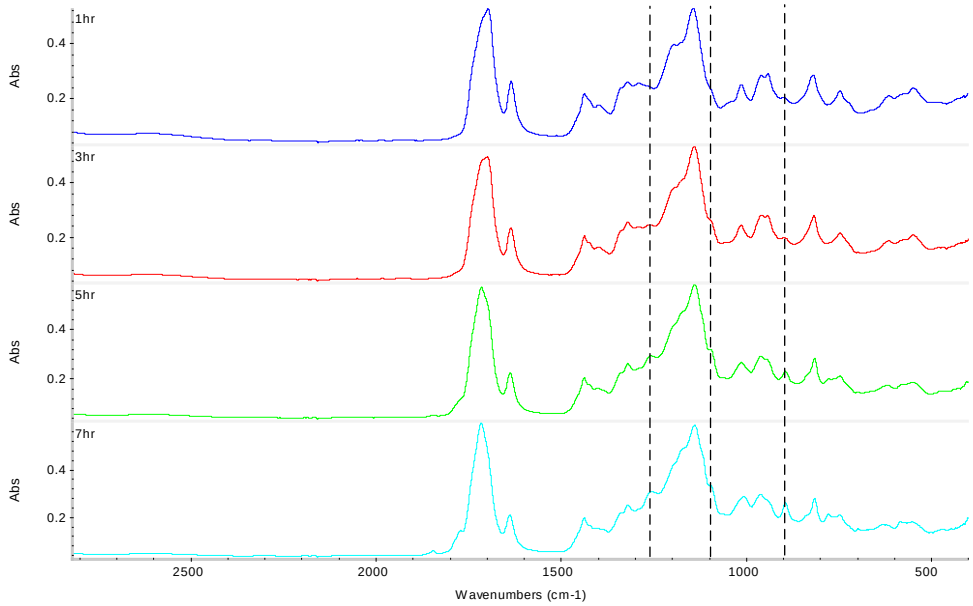

Figure 8. 3. The FTIR spectra of the poly condensation reaction, samples taken after 1, 3, 5 and 7 hours.

8.3.2 H and ^{13}C-NMR spectroscopic analysis

In order to further evaluation of the structures, the NMR techniques were employed for identifying the structure of the *star*-Ita.Gly and T*star*-Ita.Gly resins. The

NMR spectrum and the carbon environments for the ideal structures of resins are presented in Fig. 4. The peaks were assigned based on the data presented in the literature (Xiong et al. 2014, Murillo, Vallejo, and López 2011, Park et al. 2003, Choi, Bae, and Kim 1998, Abiko, Yano, and Iguchi 2012, Helminen, Korhonen, and Seppälä 2002, Åkesson, Skrifvars, et al. 2010b, Bakare et al. 2014b, Lin and Zhang 2010, Bakare, Åkesson, et al. 2015, Ma et al. 2013, Barner-Kowollik, Heuts, and Davis 2001). In the star-Ita.Gly resins, two different types of carbonyl bonds are expected, including a) The terminal carbonyls and, b) the carbonyl groups adjacent to the (–O–CH_2) group of the core molecule. In Fig. 4. A, the peaks at ~176, ~166 and ~171 ppm represent the carbonyl carbons of *a* and *e-e'* in the chemical structure of the *star*-Ita.Gly resin (presented in the same figure). The esterification between carboxyl groups and the hydroxyl groups of the core molecule usually results in a mixture of different oligomers which affect the final-use of the cured resin (Ma et al. 2013).

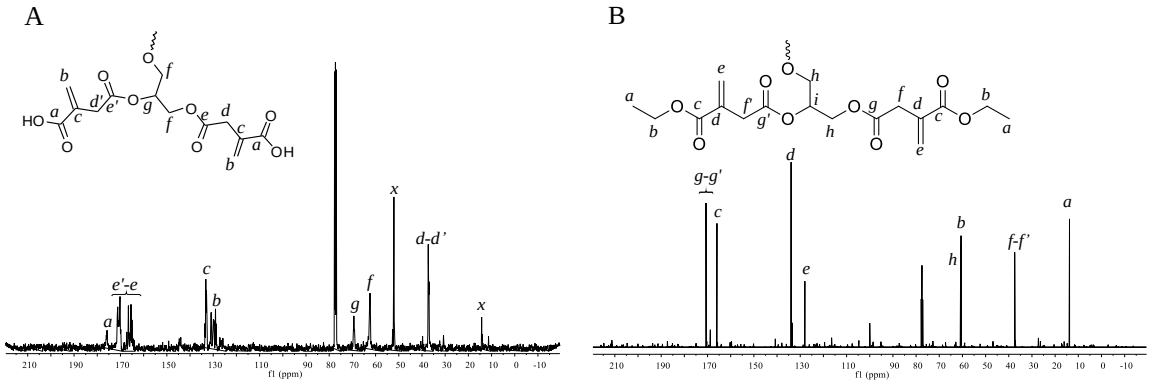

*Figure 8. 4. The 13C NMR spectra of the resins and the carbon environments for the ideal structures of resins. A: poly-condensation of itaconic acid and glycerol (star-*Ita.Gly *resin), B: end-functionalized* T*star*-Ita.Gly *resin.*

The multiple peaks at the *e* and *e'* positions indicates that the core molecule has reacted with both carbonyl ends of the itaconic acid during the polycondensation. The appearance of the other multiple peaks for the unsaturated carbons at ~128-130 ppm (which are attributed to CH_2 =C) and the peaks at ~133-134 ppm (which are attributed to the C=CH_2(C=O)(CH_2─)) also adequately indicates that the core molecule has reacted with both carbonyl ends of the itaconic acid. The peaks marked by *x* in the Fig. 4.A can be attributed to the methanol which was used for sample preparation. For the T*star*-Ita.Gly resin, a peak at ~14 ppm can be seen in the spectra shown by *a* which can be attributed to the terminal methylic group of the oligomers CH_3─(CH_2─). The absence of the peak at ~176 ppm for the terminal carboxyl in the treated resin C=O(─OH)(─C=CH_2) (which was present in the spectra of the *star*-Ita.Gly resins) is another evidence which indicates that the second polycondensation has also occurred. Other peaks at ~37 (*d-d'*), ~61(*f*) and ~69 (*g*) ppm were also identified accordingly and summarized in the table 1.

Table 8. 1. Assignment of peaks from H and ^{13}C-NMR

	Assignment	Chemical shifts (ppm)
^{13}C NMR		
	CH_3─(CH_2─)	~14
	CH_2 (─(C=O)(─C=C)	~37-38
	─CH_2─ core molecule & terminal	~61-62
	─CH─ core molecule	~69
	CH_2 =C	~128-130
	C=CH_2(C=O)(CH_2─)	~133-134
	─C=O main-chain	~166-167
	─C=O Terminal group	~170-171
	C=O(─OH)(─C=CH_2)	~176
^{1}H NMR		
	CH_3─(CH_2─)	~1.0
	CH_2 (─(C=O)(─C=C)	~2.1-2.2
	─CH_2─ in the chain	~ 3.3 & 3.6
	─CH_2─ in the core molecule	~4.2
	CH─ (Core molecule)	~ 5.2
	CH_2=C	~5.7 & 6.2
	–OH (Terminal)	~11.1

The ^{1}H NMR was also employed for characterization of the *star*-Ita.Gly and T*star*-Ita.Gly resins. The Fig. 5 and table 1 present the ^{1}H NMR results with the assigned proton environments for the ideal structures of the resins. Fig. 5.A and Fig. 5.B present the proton spectra of the *star*-Ita.Gly resin, and T*star*-Ita.Gly resin, respectively. The multiple peaks at 3.3 ppm and 3.6 ppm can be attributed to ─CH_2─ in the chain and marked with c" in the Fig 5.A. These peaks are also present in the spectra of the Tstar-Ita.Gly resin (marked as d" in the Fig. 5.B). The characteristic peak of the *star*-Ita.Gly resin spectrum would be the peak at ~11.1 ppm which can be attributed to the terminal hydroxyl group of the oligomers.

As the hydroxyl groups of the *star*-Ita.Gly resin will be esterified in the second polycondensation reaction, this peak is present in the spectrum of the T*star*-Ita.Gly resin. The other characteristic peak which indicates that the reaction of the terminal carboxyls of the oligomers of the *star*-Ita.Gly resin and the hydroxyl group of the ethanol has occurred is the presence of a peak at ~1.0 ppm in the spectrum of the T*star*-Ita.Gly resin, which can be attributed to the terminal methyl group, added to the end of the oligomers. This peak is not present in the proton spectrum of the *star*-Ita.Gly resin and marked as *a"* in the Fig. 5.B. Other peaks at ~2.2, 4.2, 5.2, 5.7 and ~6.2 ppm were also identified accordingly and summarized in the table 1. The weak peak at ~7.2 ppm (marked as *x* and *x'* in the Fig. 5) resulted from the chloroform-d solvent (also seen at ~77.1-77.8 ppm in the ^{13}C NMR spectra).

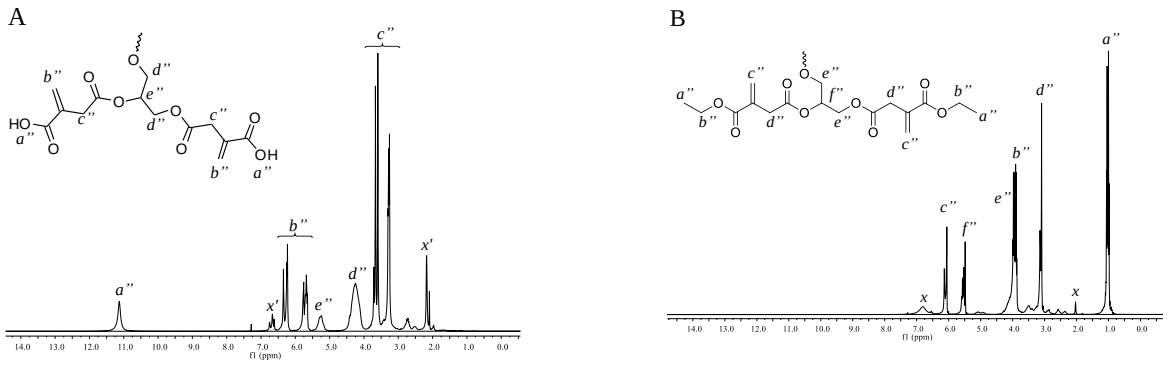

*Figure 8. 5. The H NMR spectra of the resins and the hydrogen environments for the ideal structures of a) step-one and b) step-two resins. A: poly-condensation of itaconic acid and glycerol (star-*Ita.Gly *resin), B: end-functionalized* T*star-*Ita.Gly *resin.*

8.3.3 FTIR spectroscopy analysis

Figure 6.A presents the FTIR spectra of the polycondensation and cured samples of the *star*-Ita.Gly resin and Fig. 6.B presents the FTIR spectra of the polycondensation and cured samples of the T*star*-Ita.Gly resin. The signal at 1100-1200 cm^{-1} can be attributed to the (─C─O─C─ stretching vibration) which is presented in all spectra and is an evidence of the formation of bonds between the hydroxyl groups of the core molecule and the carboxyl groups of the itaconic acid (Nouri, Dubois, and Lafleur 2015b, Lin, Zhang, and Wang 2012, Xiong et al. 2014). The peak for ─CH at ~2900 cm^{-1} (Xiao, Mai, et al. 2012) can be found in all spectra. The presence and the absence of the C=C characteristic signals at 1635 cm^{-1} (stretching C=C) (Bakare et al. 2014b) and 815 cm^{-1} (bending CH_2) (Hisham et al. 2011) confirm that the unsaturated carbons are available in polycondensation resins and the curing is occurred in the solid samples. The signal between 1000 and 1100 cm^{-1} can also be attributed to the CO─ stretching vibration (Nouri, Dubois, and Lafleur 2015b, Lin, Zhang, and Wang 2012, Xiong et al. 2014).

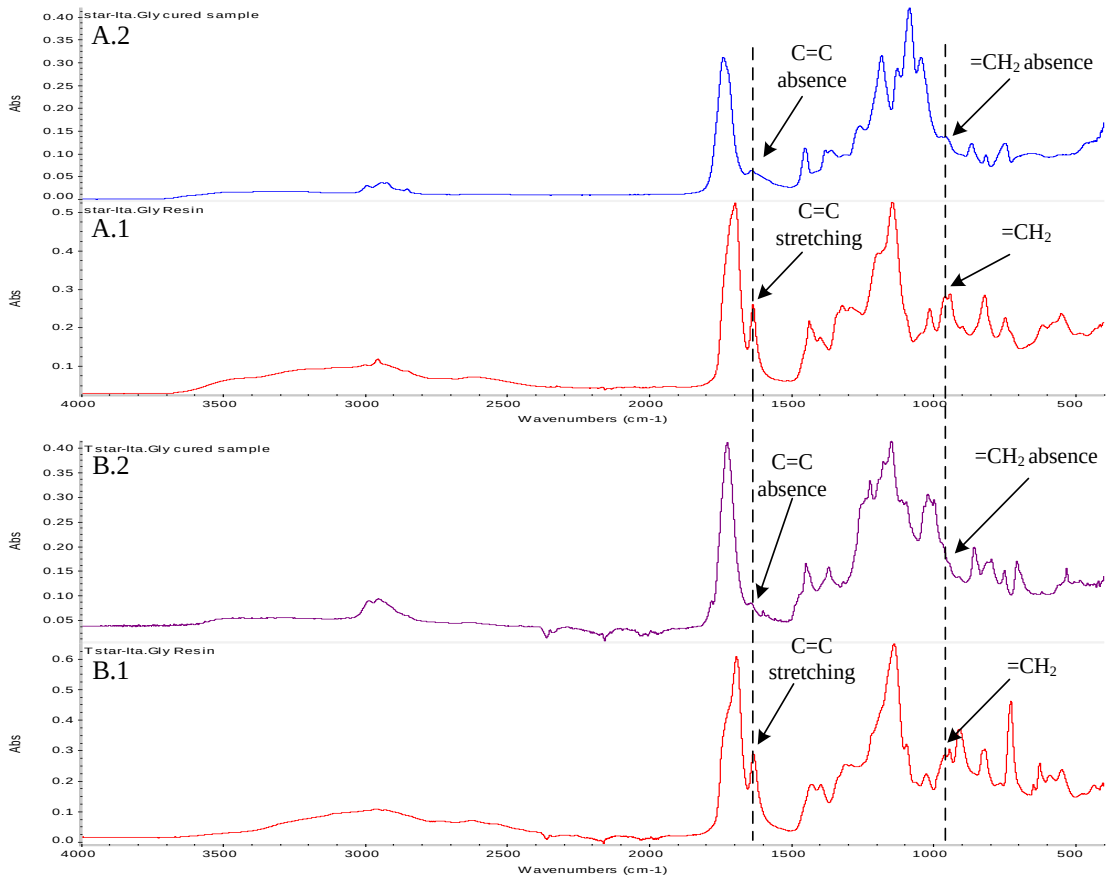

Figure 8. 6. The FTIR spectra of the star-Ita.Gly resin *(A.1)* and the *star*-Ita.Gly cured sample *(A.2), and the* T*star*-Ita.Gly *resin (B.1) and the* T*star*-Ita.Gly *cured samples (B.2).*

8.3.4 Differential Scanning Calorimetry

DSC is a thermoanalytical technique currently employed to study the curing of thermoset resins by detecting the crosslinking, and the residual reaction heats and of the cured samples (Liang and Chandrashekhara 2006, Mohan, Ramesh Kumar, and Velmurugan 2005, Bakare, Ramamoorthy, et al. 2015). The peak exotherms in Fig 7.A present the residual exotherms of the cured *star*-Ita.Gly resin from 50 °C to 200 °C for samples cured at 70 °C for two hours and post cured at different temperatures of 80 °C, 90 °C, 100 °C, 110 °C, 120 °C and 130°C for 30 minutes. The presence of residual heats in the curves, marked as *a*, *b* and *c* in Fig 7.A, shows that samples cured at temperatures

below 110 °C did not cured completely. There is almost no reaction heat exists in the exotherms of samples cured at temperatures above 130 °C which indicates that the curing is complete, and so, in this study, the post curing conditions for curing was selected as 20 minutes at 120 °C.

Figure 7.B presents the exothermic heat reactions of the curing reaction of *star*-Ita.Gly (marked as *a*), and T*star*-Ita.Gly (marked as *b*) resins. Figure 7.B shows that the *star*-Ita.Gly resin is cured between 70 °C and 150 °C, (revealing a sharp exothermic peak), while the T*star*-Ita.Gly resin is cured between 60 °C and 140 °C.

For the *star*-Ita.Gly resin, the reaction heat was measured as 94.4 $J.g^{-1}$, and the peak temperature and the onset temperature were 132.8 °C and 104.3 °C, respectively. For the T*star*-Ita.Gly resin, the reaction heat was measured as 117.7 $J.g^{-1}$, and the peak temperature and the onset temperature were 129.3 °C and 93.2 °C, respectively. For comparison, in the star-shaped glycerol-lactic acid based resins, the curing temperatures reported between 80 °C to 130 °C and the heat reaction was 227.4 $J.g^{-1}$ (Bakare et al. 2014b), and for star-shaped xylitol-lactic acid based resins, the curing temperatures reported between 100 °C to 140 °C and the heat reaction was 275.5 $J.g^{-1}$ (Jahandideh and Muthukumarappan 2016a).

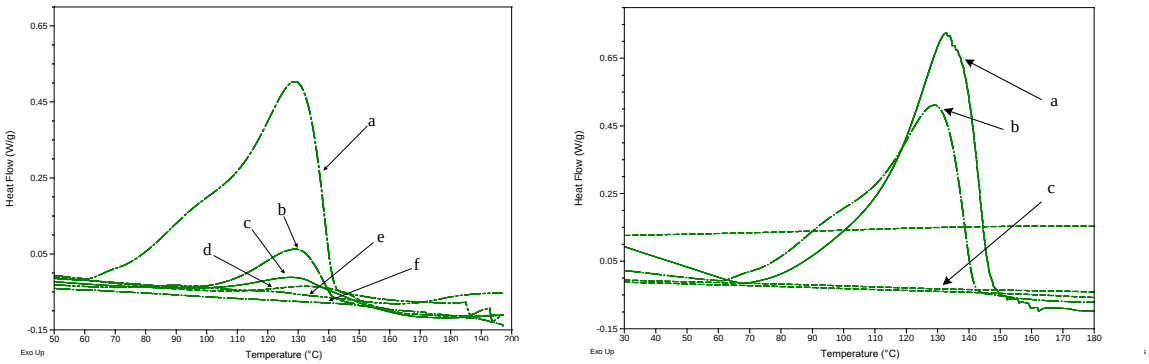

*Figure 8. 7. A) The DSC curves for residual exotherms for samples cured for 20 minutes at 80 °C (a), 90 °C (b), 100 °C (c), 110 °C (d), 120 °C (e) and 130 °C (f). B) The DSC curves for the unreacted star-*Ita.Gly *resin (a) and the unreacted (b) and the cured resin (c) at a heat rate of 10 °C.min^{-1} in the heat range of 30 to 180 °C.min^{-1}*

8.3.5 Thermogravimetric analysis

Thermogravimetric analysis (TGA) was performed in order to investigate the thermal stability of both cured resins by recording mass loss by heating samples from room temperature to 600 °C at 10 °C.min^{-1} heating rate under a nitrogen atmosphere. Typical weight loss and derivative thermograms for crosslinked *star*-Ita.Gly and T*star*-Ita.Gly are shown in Fig 8. The *star*-Ita.Gly starts to decompose at 286 °C in a single broad degradation stage with maximum rate at 380 °C, leaving ~10% solid residue at 450 °C. It can be seen that while *star*-Ita.Gly shows a single decomposition stage, the T*star*-Ita.Gly has two major thermal decomposition stages starting at 180 °C with maximum rates at 200 °C and 380 °C followed by a slow weight loss at 420-600 °C temperature

range. Although onset of thermal decomposition of the T*star*-Ita.Gly occur at about 120 °C lower temperatures compared to the *star*-Ita.Gly, which implies it has considerably lower thermal stability compared to the *star*-Ita.Gly, it leaves around 25% solid residue at 450 °C which is much higher than that of *star*-Ita.Gly. This relatively high char formation makes T*star*-Ita.Gly a promising resin for development of flame retardant systems using minimal additives.

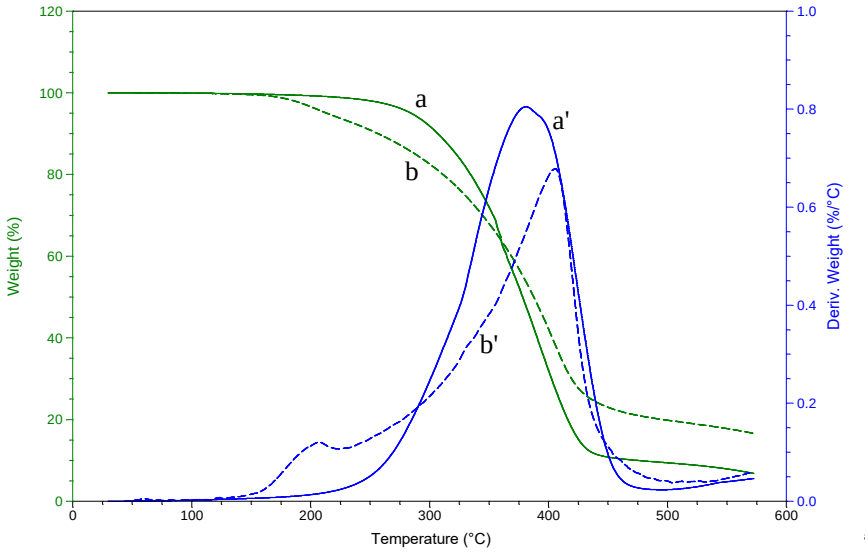

Figure 8. 8. TGA curves for the cured samples of the star-Ita.Gly *(a-a'), and* T*star*-Ita.Gly (b-b'), *solid-line presents Weight (%) and dashed-typed pattern shows Derivative Weight (%.°C^{-1})*

8.3.6 Dynamic Mechanical Thermal Analysis

DMA is often employed for analyzing the thermal-mechanical properties of the crosslinked resin in which a sinusoidal stress is applied and the displacement is measured and the storage modulus, loss of modulus and T_g are measured (Menard 2008). Figure 9

presents the storage modulus G' in the temperature range of -20 °C to 170 °C for the crosslinked T*star*-Ita.Gly samples. The G' value is related to the molecular packing density in the glassy state (Vergnaud and Bouzon 2012, Chang et al. 2012b); therefore, the higher G', the better mechanical properties. The free movement of the polymer chains in the rubbery plateau region (Bakare, Ramamoorthy, et al. 2015) decreases the G' value in this temperature interval (between 48 °C and 120 °C).

In the authors' previous study, a stepwise curing method employed for curing of the methacrylated star-shaped lactic acid thermosets with xylitol core molecules which induces gradual solidification and more relaxed state with less built in stresses (Jahandideh and Muthukumarappan 2016a, Vergnaud and Bouzon 2012) and resulted in superior G' compared to the other curing methods. In this study, a similar curing technique was applied. Figure 9 also presents the loss modulus G", which is an indicator of the dissipated energy in the temperature range of -20 °C to 170 °C for the crosslinked T*star*-Ita.Gly samples. Often, smaller G" indicates superior mechanical properties and the strong tendency for reversibility (Bakare, Ramamoorthy, et al. 2015). The DMA results are summarized in Table 2.

The T_g of the crosslinked thermosets often presented based on the peak of tan δ in DMA curves. Figure 10 shows the tan δ curve in the temperature range of -20 °C to 170 °C for the crosslinked T*star*-Ita.Gly samples. The tan δ peak was observed at 122 °C. Generally, the higher tan δ peak values are desired and indicate better mechanical properties.

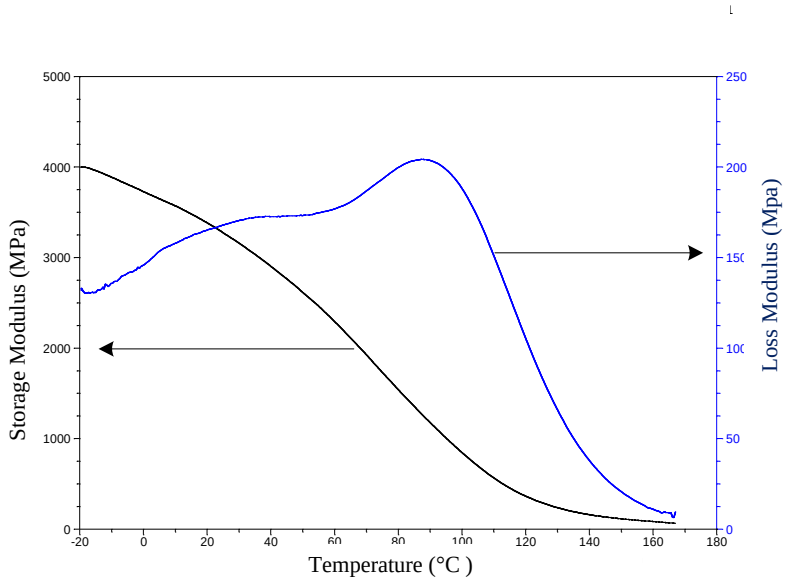

Figure 8. 9. Storage modulus and Loss modulus curves for the crosslinked T*star*-Ita.Gly *samples in the temperature range of -20 °C to 170 °C*

For comparison, the T_g (based on the peak of tan δ) for the linear PLA is ~50 °C (Oksman, Skrifvars, and Selin 2003), and for other similar star-shaped lactic acid based resins with glycerol, PENTA, and xylitol core molecules were reported as 83 °C, 97 °C and 98 °C, respectively (Bakare et al. 2014b, Jahandideh and Muthukumarappan 2016a, Åkesson, Skrifvars, et al. 2010b). The T*star*-Ita.Gly thermosets suggest a substantial higher T_g compared to the other thermoset systems which is also believed to get improved more after applying the reinforcement fibers due to the adhesion of the fibers to the matrix (Adekunle, Åkesson, and Skrifvars 2010, Bakare, Ramamoorthy, et al. 2015)

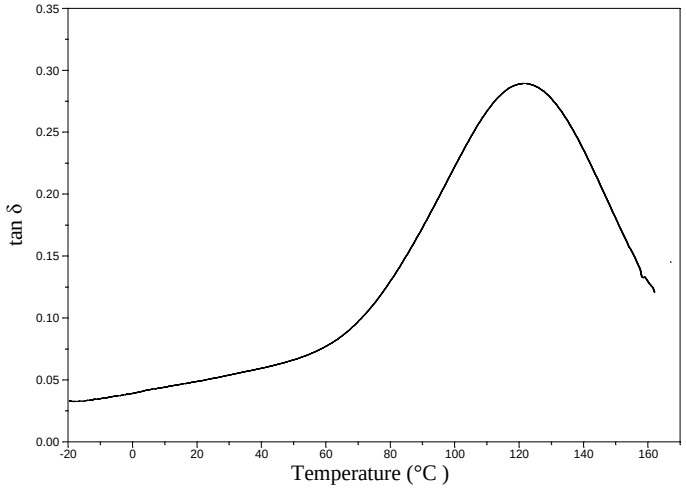

Figure 8. 10. Tan δ curve for the crosslinked T*star*-Ita.Gly *samples in the temperature range of -20 °C to 160 °C*

8.3.7 Viscosity measurements

Inadequate and poor impregnation of a resin to fibers results in a slow composite production process and has impact on the mechanical strength of the composites [12, 13]. Comparably lower viscosities of thermosets, results in better processability and impregnation, which candidates thermosets desirable for composite applications. For a satisfactory composite manufacturing, the viscosity of the resin is required to be below 0.5 Pa s (Li, Wong, and Leach 2010). Changing the structure of oligomers from linear into a star-shaped architecture results in smaller hydrodynamic volume, which in turn reduces the viscosity (Corneillie and Smet 2015, Chang et al. 2012b, Finne and Albertsson 2002).

In this study, the viscosity of *star*-Ita.Gly and T*star*-Ita.Gly resins were measured based on stress viscometry technique at different temperature intervals (30 °C to 100 °C) and the results are presented in Fig. 11. The *star*-Ita.Gly resin has a viscosity of 154.9 Pa s which dropped to 1.8 Pa s upon increasing the temperature to 70 °C. This high viscosity makes the resin unsuitable for composite manufacturing, even at elevated temperatures (up to curing temperature of the thermoset). After treating the resin with ethanol and shifting the carboxyl-ends to a methylene group, the viscosity was dropped substantially. The T*star*-Ita.Gly resin showed a viscosity of 0.35 Pa s at room temperature which dropped to 0.04 Pa s at 70 °C (see Fig. 11). This low viscosity, even at room temperature, is substantially desirable for the fiber reinforcement composites manufacturing. The reported viscosities for other star-shaped thermosetting systems are relatively higher than the viscosity of this new synthesized resin.

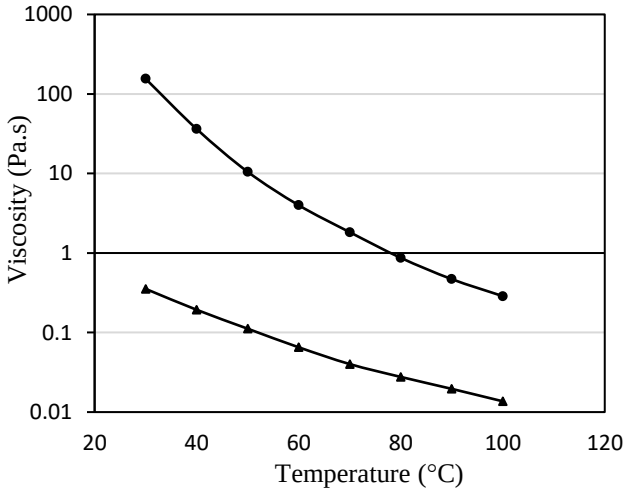

Figure 8. 11. Viscosities of the star-Ita.Gly *resin (•) and the* T*star*-Ita.Gly *resin (▲) as a function of the temperature.*

For comparison, at room temperature, the four armed, star-shaped resins of pentaerythritol and LA has a viscosity of 7000 Pa s (Åkesson, Skrifvars, et al. 2010b), the three armed, star-shaped resins of glycerol and LA has a viscosity of 1.09 Pa s (Bakare et al. 2014b), and the five-armed star-shaped resins of xylitol and LA has a viscosity of 2.97 Pa s (Jahandideh and Muthukumarappan 2016b). The viscosity of the T*star*-Ita.Gly resin is comparable with the viscosity of the commercial unsaturated polyester with a viscosity of 0.3 at room temperature (Bakare et al. 2016).

8.3.8 Water adsorption tests

The water absorption rates of polymers is of interest, especially when the material is supposed to exposure to relatively humid conditions. The moisture content affects polymers' properties such as electrical insulation resistance, dielectric losses, mechanical strength, appearance, and dimensions. It is believed that the diffusion of water into polymeric matrix is dependent to several factors, including a) the square root of immersion time, b) the type of immersion, c) dimensions and shape of the specimen, and d) the inherent properties of the polymer (Jahandideh and Muthukumarappan 2016a, Qiu and Bae 2006, ASTM D570-98(2010)e1 2010). In this study, samples with water adsorption rates of less than 1 % or 5 mg between intervals, were considered to be substantially saturated.

Figure 12.A presents the percent of absorbed water versus immersing time for the 50I test. For the 23I test, the absorbed water was reported as a function of the square root of immersion time- Fig. 12.B. The initial slope of the water-absorption versus time curve is proportional to the diffusion constant of water in the matrix (Qiu and Bae 2006) and calculated as 0.304 and 0.397 for 50I and 23I methods, respectively. The water saturation

for the I23 method was 336 h and for 50I was 48 h. the percentage water adsorbed after saturation I50 and I23 immersions were 8.51±0.33 and 10.49±0.25%, respectively. The percentage of the saturated water adsorption by BI was recorded as 6.57±0.36 %. The authors previously reported the diffusion constants of 0.252 after 504 h of immersion with 14.02 ±0.35% water adsorption for 23I and the diffusion constants of 0.699 after 110 h of immersion with 8.08 ± 0.61% water adsorption, employing 50I for the S-LA resins with xylitol core molecules (Jahandideh and Muthukumarappan 2016a).

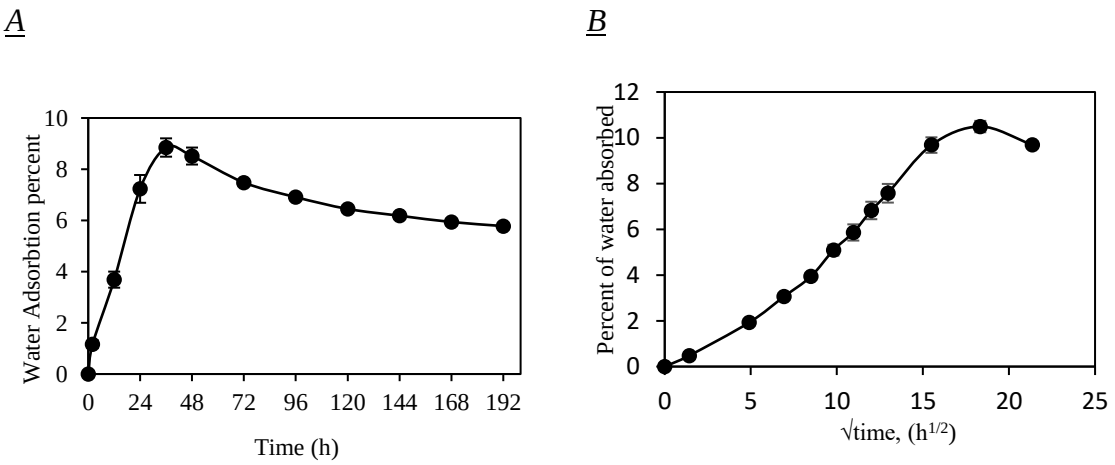

Figure 8. 12. A) Percent of absorbed water versus immersing time at 50°C, B) long-term immersion procedure water adsorption; reported as a function of the square root of immersion time for T*star*-Ita.Gly *samples*

Table 8. 2, Thermal-Mechanical Characterization Results of the Resins

DSC		*star*-Ita.Gly resin	T*star*-Ita.Gly resin
	Heat of exotherm for uncured resin ($J.g^{-1}$)	94.4	117.7
	Curing temperature interval	70 °C - 150 °C	60 °C - 140 °C
	Heat of exotherm for cured resin ($J.g^{-1}$) at 120 °C	0	0
	Peak temperature	132.8 °C	129.3 °C
	Onset temperature	104.3 °C	93.2 °C
DMA			
		T*star*-Ita.Gly resin	
	tan δ peak (T_g °C)	122 °C	
	Storage modulus (MPa) at 25°C	3109 ± 133	
	Loss modulus (MPa) at 25°C	162 ± 9	
TGA		*star*-Ita.Gly resin	T*star*-Ita.Gly resin
	Degradation temperature range	286 – 460 °C	180 – 460 °C
	Maximum degradation (°C)	380 °C	380 °C
	Solid residue at 450 °C	~10%	~25%

8.4 Conclusion

In this study, a star-shaped biobased thermoset resin was synthesized by poly-condensation of itaconic acid and glycerol. In order to reduce the viscosity of the synthesized resin, the branches were end-functionalization with ethanol. Chemical structure of the base resin and the alcohol treated resins were confirmed employing H and

^{13}C NMR and FTIR techniques. The resins were thermally cured via free-radical polymerization using benzoyl peroxide. The residual exotherms of samples cured at 70 °C for 1 hour and different post curing temperatures for 20 min were investigated to optimize the post curing process. Thermogravimetric analyses of the cured resins were also carried out to study the thermal properties of the cured resins. The viscosity of the base resin, and the alcohol treated resin were measured at temperatures in the range of 30 °C to 100 °C. The results showed that the base resin has a relatively high viscosity which makes the resin unsuitable for any industrial biocomposite manufacturing. However, the substitution of the carboxyl end groups of the branches with a methyl group substantially reduced the viscosity of the star-shaped resins resulted in a viscosity of 0.35 Pa s at room temperature and 0.04 Pa s at 70 °C which makes the resin very promising for industrial manufacturing production.

The water adsorption properties of the cured samples of the treated star-shaped resin were also investigated via standard water adsorption tests. DMA analysis of the crosslinked thermoset resin showed a T_g, substantially higher than that of other star-shaped systems as well as the thermoplast PLA, at 122 °C. Fully biobased and inexpensive raw materials, biodegradability, good thermomechanical and comparably very promising rheological properties along with good thermal stability are of advantages of this novel star-shaped itaconic based resin which make the resin comparable with, and superior in some aspects, than other star-shaped thermosetting systems as well as the commercial unsaturated polyester resins.

Acknowledgement

The authors would like to acknowledge the funds provided by Agricultural Experiment Station, South Dakota State University and US Department of Agriculture, Washington, DC in support of this research work.

Chapter 9 - Facile Synthesis and Characterization of Activated Star-shaped Itaconic acid based Thermosetting Resins

Arash Jahandideh[1,*], Nima Esmaeili[2], Kasiviswanathan Muthukumarappan[1]

[1] Agricultural and Biosystems Engineering Department, South Dakota State University, PO Box

2120, Brookings, SD 57007, USA

[2] *Institute for Materials Research and Innovation, University of Bolton, Deane Road, Bolton, BL3 5AB, UK*

* Corresponding author current address: Agricultural, Biosystems & Mechanical Engineering Department, 1400 North Campus Drive Box 2120, Brookings, SD 57007, USA. Tel.: +1 (605) 6885670

Corresponding author: arash.jahandideh@sdstate.edu

Abstract

Activated star-shaped itaconic acid based thermosetting resins were synthesized by direct condensation reaction of itaconic acid and glycerol, followed by activation of the oligomers, by methanol and allyl alcohol treatments. Chemical structures of the resins were studied and confirmed by ^{1}H-^{13}C NMR and Fourier-transform infrared spectroscopy (FT-IR). The curing and thermomechanical properties were studied by Differential Scanning Calorimetry (DSC) technique and Dynamic Mechanical Analysis (DMA).

Thermogravimetric analyses (TGA) and viscometry analysis were also carried out on resins to study the rheological properties and thermal stability of the cured samples. The methanol-treated resin showed a viscosity of 4.2 Pa.s at room temperature which dropped to 0.25 Pa.s upon increasing the temperature to 70 °C; while, the allyl alcohol-treated resin showed a lower viscosity of 1.8 Pa.s at room temperature, and 0.14 Pa.s at 70 °C. The glass temperature (T_g) of the methanol-treated resin was 150 °C, substantially higher than that of the allyl alcohol-treated resin (observed at 93 °C) and to date reported star-shaped bio-thermosets. DMA results also showed very good mechanical properties for the methanol-treated resin in terms of storage modulus, compared to the allyl alcohol treated resin (61% higher G' was obtained for the methanol-treated resin). Biodegradability and inexpensive raw materials, good rheological properties along with promising thermomechanical properties are of advantages of this novel resin, which make the resin comparable with, and superior in some aspects, than other thermosetting systems as well as the commercial unsaturated polyester resins.

Keywords: Itaconic Acid; Synthesis; Thermosets; Crosslinking; Star-Shaped; Thermal Mechanical Properties

---

9.1. Introduction

From a technological point of view, recently, substantial developments have been emerged in the field of biobased thermosetting. It is believed that the employment of a star-shaped architecture for thermosetting resins results in an engineerable, processable and more reactive resin, with comparably lower viscosity. The extended network, provided by the star-shaped structure, also results in better thermomechanical properties of the final product. Different authors employed different core molecules, including

glycerol (Bakare et al. 2014b, Esmaeili et al. 2015, Arvanitoyannis et al. 1995), tri(hydroxymethyl)benzene (Perry and Shaver 2011), erythritol and pentaerythritol (Åkesson, Skrifvars, et al. 2010b, Bakare et al. 2016, Åkesson et al. 2011b, Kim et al. 1992), xylitol (Jahandideh and Muthukumarappan 2016b, Teng et al. 2015), dipentaerythritol (Biela et al. 2003, Kim and Kim 1999), for synthesizing of the star-shaped thermosetting resins. Two different methods have been suggested for achieving a star-shaped structure: the *arm-first* method, in which the arms are prepared first, and then reacted with a multifunctional core molecule, and the *core-first* method, in which the core molecule reacts with the chain monomers first, and then the length of the arms increased via a controlled polymerization pathway (Qiu and Bae 2006).

Often, the core-first method is preferred, as it provides a better control over the polymerization. The oligomers' branches are then end-functionalized by adding unsaturated bonds to the branches. The most common reactive agent which has been used for efficient end-functionalization is methacrylic anhydride (Helminen, Korhonen, and Seppälä 2002, Jahandideh and Muthukumarappan 2016b, Liu, Madbouly, and Kessler 2015, Sakai et al. 2013, Åkesson, Skrifvars, et al. 2010b, Bakare et al. 2014b, Bakare, Åkesson, et al. 2015, Chang et al. 2012b, Bakare et al. 2016, Åkesson et al. 2011b). The thermosetting resins are then cured, via thermal curing methods and by assistance of a free-radical polymerization method, which leads into an irreversible cross-linked network (Vergnaud and Bouzon 2012). Benzoyl peroxide (Jamshidian et al. 2010, Esmaeili et al. 2015, Bakare et al. 2014b), 2,5-bis(tert-butylperoxy)-2,5-dimethylhexane (Sakai et al. 2013), 2-butanone peroxide (Helminen, Korhonen, and Seppälä 2002), cobalt naphthenate (Finne and Albertsson 2002), *tert*-butyl peroxybenzoate (Åkesson, Skrifvars,

et al. 2010b), N,N-dimethylaniline (Bakare, Åkesson, et al. 2015) and *tert*-butyl peroxybenzoate (Chang et al. 2012b, Åkesson et al. 2011b) are of initiators, which have been used for free-radical polymerization. Although currently synthesized star-shaped thermosetting systems are interesting from different aspects, yet, there are still several drawbacks exist which have to be highlighted. These limitations include low processability of the resin, environmental issues, expensive sources and poor thermomechanical properties.

In the authors' previous work, the substitution of toxic-nonrenewable methacrylic anhydride with itaconic acid was investigated and star-shaped itaconic acid based thermosets were produced. The base-resin was synthesized by direct condensation reaction of itaconic acid and glycerol. The resin was fully biobased and showed good thermomechanical properties; however, the resin was not suitable for industrial manufacturing purposes, due to its high viscosity, even at the elevated temperatures. In an attempt to reduce the viscosity of the resin into satisfactory levels, the resin was treated with ethanol, which led to transformation of carboxyl end-groups branches into methyl ones. The treatment was successful and substantially reduced the viscosity of the resin, from 194 Pa s (for the base resin) to 0.35 Pa s (for the treated resin), at room temperature. The aim of this study is to alter the terminal methyl-group of the oligomer, with a more reactive agent, to increase the cross-linking density and consequently, the thermomechanical properties of the cured resins. In this study, the star-shaped itaconic acid based thermosetting resins were synthesized via direct condensation polymerization of the glycerol with the itaconic acid followed by the esterification of the branches by methanol and allyl alcohol. Instead of ethanol which has been used in the former resin,

methanol was suggested, as the expected hindrance of the terminal methyl-group is supposed to be lower than that of the ethyl group.

Therefore, the access to the unsaturated bond of itaconic acid might be increased, which in turn results in more efficient crosslinking and, consequently better thermomechanical properties of the cured samples. The allyl alcohol, which has an unsaturated C-C bond, was also considered to study the effect of the unsaturated carbon-carbon bond density on the rheological and thermomechanical properties of the finished product. Introducing the allyl group at the end of the itaconic acid branches will double the unsaturated bond density, which results in plausible higher crosslinking density and consequently better thermomechanical properties of the cured resins. The star-methyl (and allyl) itaconic acid based resins were synthesized using the glycerol core molecule and the chemical structures of resins were determined by H and ^{13}C NMR as well as by FT-IR technique. The viscosity of the resins were measured via viscometry analysis. The thermomechanical properties of the cured resins were also investigated using dynamic mechanical analysis (DMA), differential scanning calorimetry (DSC) and the thermogravimetric analysis (TGA).

9.2. Materials and Methods

9.2.1 Materials

Itaconic acid (≥99%; Sigma-Aldrich) and glycerol (≥95.5%; Fisher) were used for synthesis of the base resin. Toluene (≥99.8%; Sigma-Aldrich) and and methanesulfonic acid (≥99.0%; Sigma-Aldrich) were used as the auxiliary solvent and catalysts, respectively. Methanol (≥ 99.9%; Sigma-Aldrich) and allyl alcohol (≥ 99 %; Sigma-

Aldrich) were used for the activation of the oligomers. Dried Benzoyl peroxide (≥75%; Sigma-Aldrich) was used as the free radical initiator for curing.

9.2.2 Synthesis synopsis

The synthesis of the star-shaped itaconic acid based thermoset has been described in the authors' previous work. In summary, itaconic acid was reacted with glycerol, in the presence of 0.15% w/w methanesulfonic acid, and toluene as an auxiliary solvent for water removal. An azeotropic distillation apparatus was used for toluene reflux and the reactions were occurred under nitrogen atmosphere at 140 °C for 7 hours. The results of the previous study have shown that the star-shaped resin, resulted from the condensation of itaconic and glycerol, is capable of crosslinking, but its high viscosity hindered the improper mixing of the hardener and the resin, and consequently, makes the resin not suitable for casting purposes. Previously, ethanol has been used for treating the resin which resulted in a substantial reduction in the viscosity of the resin. In this study, the oligomers' branches were reacted with methanol and allyl alcohol.

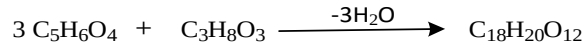

9.2.2.1 Synthesis of methanol-treated star-shaped itaconic acid based thermosets

The base-resin, resulted from the condensation of itaconic and glycerol, was cooled to 90 °C, and under a constant stirring rate and nitrogen purge flow, 1 mole of methanol per mole of itaconic acid was added to the reactor. Under condensation condition and after 30 min of reaction, the reactants were cooled to 70 °C and 0.3 mole of methanol per mole of itaconic acid (30% excess) was added dropwise. After two hours of reaction, the excess methanol was removed by disconnecting the condenser and

increasing the temperature to 110 °C for two more hours. The medium was then transferred to a drop-shaped glass flask connected to a rotary evaporator and under partial vacuum conditions (~10 mbar, 1 hour at 90°C) the residual methanol and toluene were removed. The chemical reactions and idealized structures are presented in Fig 1.

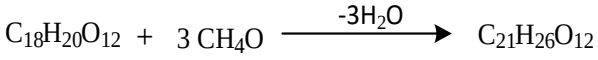

9.2.2.2 Synthesis of allyl-treated star-shaped itaconic acid based thermosets

In a similar way, the cooled base-resin (at 120 °C) was initially reacted with 1 mole of allyl alcohol per mole of itaconic acid used, and after 30 min of reaction, extra 30% mol/mol of allyl alcohol was added dropwise at 100 °C for two hours. The excess allyl alcohol was removed in a similar way explained in the former section but at 130 °C. The medium was then transferred to a drop-shaped glass flask connected to a rotary evaporator, and under partial vacuum conditions (~10 mbar, 1 hour at 94°C) the residual allyl alcohol and toluene were removed. The chemical reactions and idealized structures are presented in Fig 1.

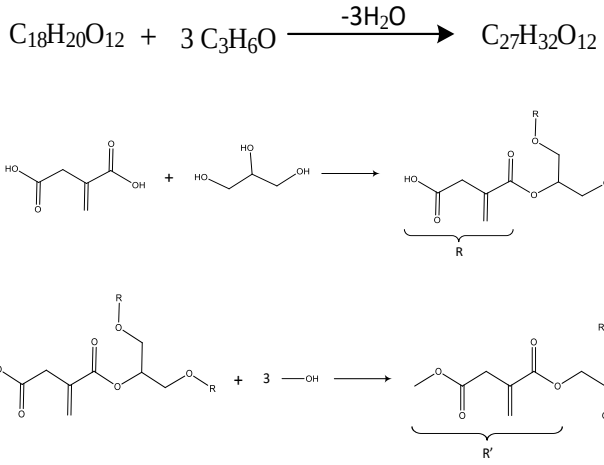

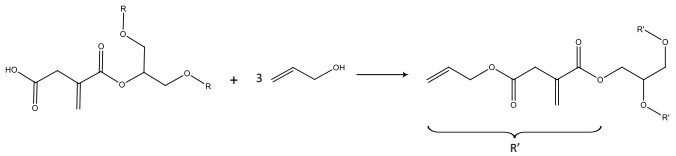

Figure 9. 1. Reaction schemes for the synthesis of (a) star-shaped itaconic acid based resin (base-resin), (b) methanol-treated and (c) allyl alcohol treated star-shaped Itaconic acid based resins.

In this study, a free-radical polymerization method was employed for thermal curing of the synthesized resins based on the method used in the previous study (2 wt% of benzoyl peroxide used at 70 °C, for 3 hours and post curing for 20 mins at 140 °C).

9.2.3 Characterization

The chemical structure of methanol and allyl treated star-shaped resins were evaluated via Nuclear Magnetic Resonance (H NMR and ^{13}C NMR) spectrometry technique (Bruker BioSpin GmbH, Germany) at 400 MHz. Sample concentration in 5 mm tubes was ~10 wt% in $CDCl_3$. The shifts were expressed in ppm. FTIR spectra of the methanol and allyl treated resins and their corresponding cured samples were recorded at room temperature on Nicolete 6700 spectrometer, supplied by Thermo Fisher Scientific, Massachusetts, USA, in the range of 4000–400 cm^{-1}. Each spectrum was recorded after the sample was scanned 36 times. Calorimetric analyses were carried out, to investigate the crosslinking reaction, by a DSC on a TA Instrument Q 100 (V9.9 Build 303- supplied by Water LLC, New Castle DE) thermal analyzer. Samples of approximately 10 mg were sealed in aluminum hermetic pans and tested under a nitrogen atmosphere. The mixtures of the resin and the initiator were analyzed at temperatures in range of -20 °C to 220 °C at a heating rate of 10 °C.min^{-1}. Thermogravimetric analyses of the cured resins were carried

out with a Q50 from a TA Instrument supplied by Waters LLC. Samples with an approximate mass of 30 mg were heated from 30 °C to 600 °C, at a heating rate of 10 °C.min^{-1} under a nitrogen purge gas stream of 20 mL.min^{-1}. Dynamic Mechanical Analysis was performed using a Q800 from TA Instruments, supplied by Waters LLC from -20 °C to 180 °C in a dual cantilever bending mode with a heat rate of 10 °C.min^{-1}; the frequency was 1 Hz, the amplitude was 15 µm and the tests were performed under a nitrogen atmosphere. The viscosity of the uncured treated resins were determined using a viscoanalyzer rheometer (TA instrument, Sweden). All measurements were done with a truncated cone plate configuration (Ø15 mm, 5.4 °C) in a temperatures range of 30 °C to 120 °C, at a shear rate ranged between 1 to 200 s^{-1}.

9.3. Results and discussion

9.3.1 ^{1}H and ^{13}C-NMR spectroscopic analysis

The NMR technique was employed to evaluate the chemical structure of the methanol-treated and allyl alcohol-treated resins. Figure 2 presents the ^{13}C-NMR spectrum of both resins and according ideal structures. The peaks were assigned according to the previous data as well as the data presented in literature (Xiong et al. 2014, Murillo, Vallejo, and López 2011, Park et al. 2003, Choi, Bae, and Kim 1998, Abiko, Yano, and Iguchi 2012, Helminen, Korhonen, and Seppälä 2002, Åkesson, Skrifvars, et al. 2010b, Bakare et al. 2014b, Lin and Zhang 2010, Bakare, Åkesson, et al. 2015, Ma et al. 2013, Barner-Kowollik, Heuts, and Davis 2001). The peaks at ~170-173 ppm were attributed to the different carbonyls of the treated resins (marked as *d* and *f* in Fig 2.A for methanol-treated resin, and, as *h"* and *d"* for allyl alcohol-treated resin in Fig. 2.B). The presence of multiple peaks at *h"-d"* carbonyl position (see Fig. 2.B),

indicates that glycerol has probably reacted with both carbonyl ends of the itaconic acid. This can be further confirmed by the presence of other multiple peaks between ~129-133 ppm for both methanol-treated (see Fig. 2.A- *e* position) and allyl alcohol-treated samples (see Fig 2.B. *g''* position).

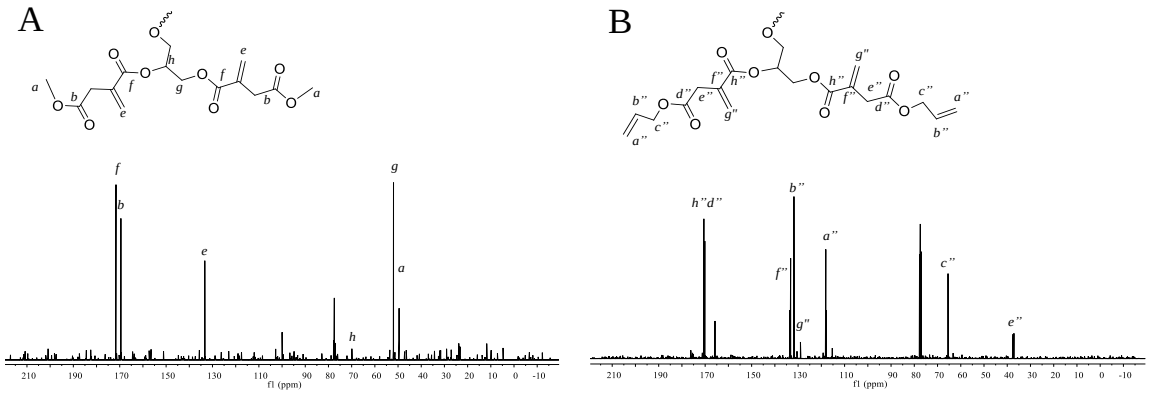

Figure 9. 2. The 13C NMR spectra of the alcohol treated resins and the carbon environments for the ideal structures. A: Methanol-treated itaconic acid based resin, B: Allyl alcohol-treated itaconic acid based resin.

These multiple peaks can be attributed to the unsaturated carbon bonds of CH_2 =C and C=CH_2(C=O)(CH_2─). For the methanol-treated resin, a peak at ~50 ppm can be seen in the spectra (marked by *a* in Fig.2.A), which can be attributed to the terminal methyl group of the oligomers ─O─CH_3. This peak is substituted with a peak at ~ 118 ppm in the spectra of the allyl alcohol-treated resin, which is attributed to the unsaturated terminal group of arms (marked as a'' in the Fig. 2.B.). Other peaks at ~65 ppm (*c''*), ~69 ppm (*h*) and ~130-135 ppm (*b''* and *f''*) were also identified accordingly, and summarized in the Table 1.

Table 9. 1. Assignment of peaks from ^{1}H and ^{13}C-NMR

Assignment	Chemical shifts (ppm)
^{13}C NMR	
CH_2─(C=O)─(C=C)	~37
CH_3─O─	~50
─CH_2─ core molecule & terminal	~53
CH(=CH_2)(─CH_2─)	~66
─CH─ core molecule	~69
CH_2= Terminal group	~118
CH_2 =C(─CH_2) (─CH=O)	~129-133
C=O(─O─)(─C=CH_2)	~171-173
^{1}H NMR	
CH_2 (─(C=O)(─C=C)	~3.1-3.3
CH_3─O─	~3.5-3.6
─CH_2─ in the core molecule	~4.1-4.3
CH_2(C=)(–O–)	~4.5
CH─ (Core molecule)	~ 5.2
CH_2=C (Terminal)	~5.1-5.3
CH_2 =C(─CH_2) (─CH=O)	~5.7
CH_2=C in the chain	~ 5.6 & 6.2

The ^{1}H NMR was also employed for characterization of the methanol-treated and allyl alcohol-treated resins. Figure 3 and Table 1 present the ^{1}H NMR results with the assigned proton environments for the ideal structures of the resins. Figure 3 presents the ^{1}H-NMR spectrum of alcohol treated resins and the according ideal structures. The multiple peaks at ~3.1-3.3 ppm can be attributed to CH_2 (─(C=O)(─C=C) and marked as *b* and *d"* in Fig 3.A and 3.B, respectively. The peak at ~3.5-3.6 ppm can be attributed to the terminal methyl group of the methanol-treated resin (marked as *a* in Fig 3.A). However, the peak at ~4.1-4.3 can be attributed to the ─CH_2─ groups in the core molecule (marked as *d* and *f"* in Fig 3.A and Fig 3.B, respectively). The other characteristic peak, which indicates that the unsaturated bonds are present in the allyl alcohol-treated resin, is seen at ~5.2 ppm in the spectrum of the allyl alcohol-treated resin and marked as *a"* in Fig 3.B. This peak is not present in the spectrum of the methanol-treated resin. Other peaks at ~4.5, ~ 5.2, ~5.7, ~ 5.6 and 6.2 ppm were also identified accordingly, and summarized in the Table 1. The peak at ~8-9 ppm (marked as *x* and *x'* in Fig. 3) resulted from the chloroform-d solvent (also seen at ~75-80 ppm in the ^{13}C NMR spectra).

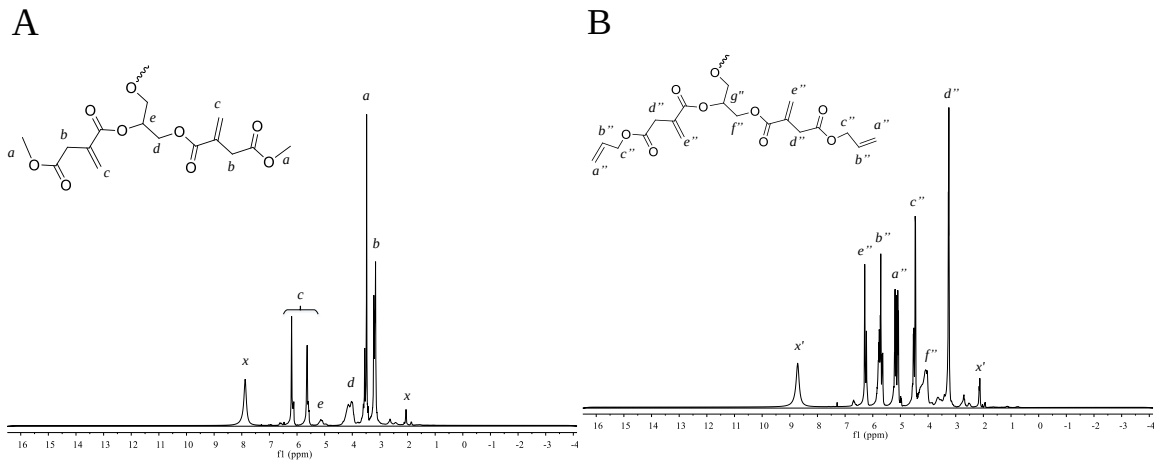

Figure 9. 3. The H NMR spectra of the alcohol treated resins and the hydrogen environments for the ideal structures. A: Methanol-treated itaconic acid based resin, B: Allyl alcohol-treated itaconic acid based resin.

9.3.2 FTIR spectroscopy analysis

Figure 4.A presents the FTIR spectra of the methanol-treated resin (Fig. 4.A.1), and the methanol-treated cured sample (Fig. 4.A.2). Figure 4.B presents the FTIR spectra of the allyl alcohol-treated resin (Fig. 4.B.1), and the allyl alcohol-treated cured sample (Fig. 4.B.2). The presence of a signal at 1100-1150 cm^{-1}, in the spectra of both methanol-treated and allyl alcohol-treated samples, can be attributed to the (─C─O─C─ stretching vibration) is an evidence of the reaction between the hydroxyl groups of the glycerol and the carboxyl groups of the itaconic acid (Nouri, Dubois, and Lafleur 2015b, Lin, Zhang, and Wang 2012, Xiong et al. 2014). The signal at ~1635 cm^{-1} can be attributed to the stretching C=C (Bakare et al. 2014b), and the signal at ~815 cm^{-1} can be attributed to the bending CH_2 (Hisham et al. 2011) in the methanol-treated and allyl alcohol-treated resins. The absence of these signals in the spectra of the cured samples is an evidence that the

curing is occurred (Nouri, Dubois, and Lafleur 2015b, Lin, Zhang, and Wang 2012, Xiong et al. 2014).

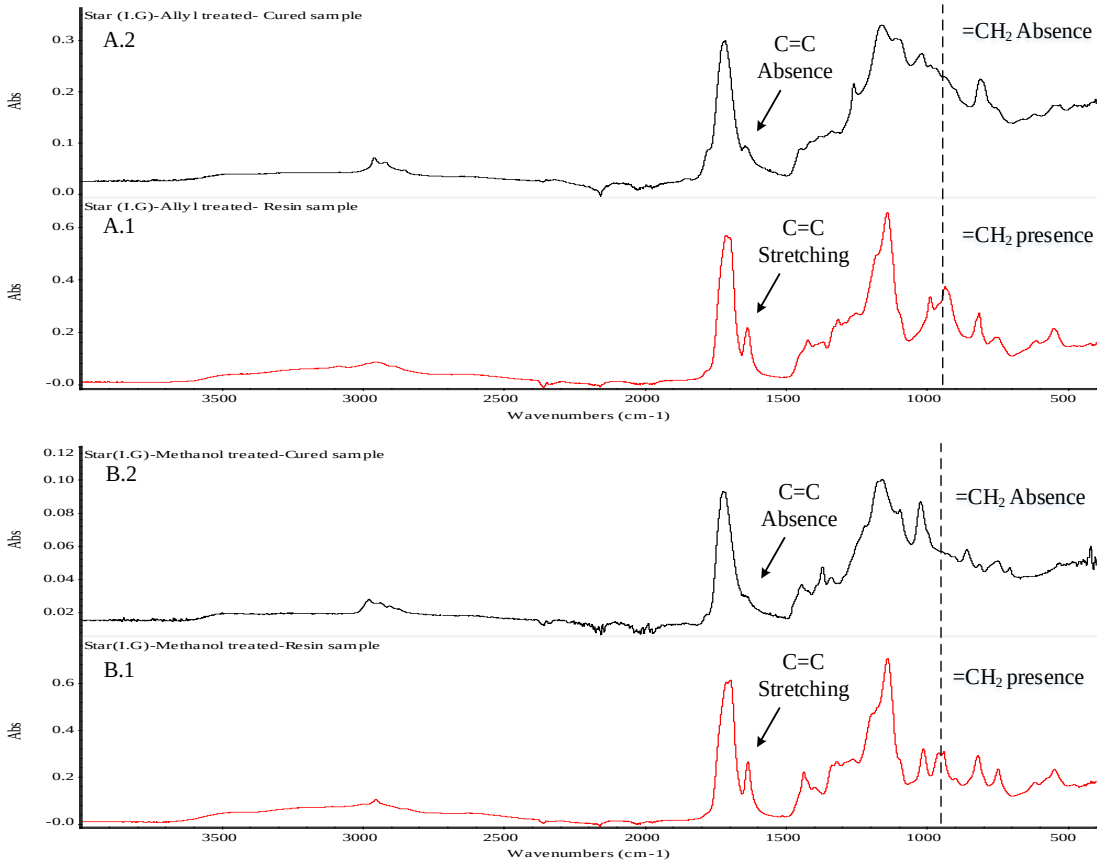

Figure 9. 4. The FTIR spectra of (A.1) the Methanol-treated resin, (A.2) the Methanol-treated cured sample, (B.1) the Allyl alcohol-treated resin, and (B.2) the Allyl alcohol-treated cured sample.

9.3.3 Differential Scanning Calorimetry

DSC technique was employed to study the curing behavior, by detecting the reaction heat of the crosslinking of methanol-treated and allyl alcohol-treated resins. Figure 5 presents the exothermic heat reactions of the curing reaction of methanol-treated (solid line) and the allyl alcohol-treated (dashed line) resins. It can be seen that the

methanol-treated resin was cured between 65 °C and 150 °C, the reaction heat was measured as 141.9 J/g, the peak temperature was 106.8 °C and the onset temperature was 71.1 °C. On the other hand, the allyl alcohol-treated resin was cured between 73 °C and 160 °C, the reaction heat was measured as 197.1 J/g, the peak temperature was 136.2 °C and the onset temperature was 104.8 °C. The higher reaction heat of the curing of the allyl alcohol-treated resin, compared to that of methanol-treated resin, might be explained based on the higher density of double bonds in the allyl alcohol-treated resin. This can also be observed as a shift in the exothermic peak of this resin. Previously, reaction heats of 94.4 $J.g^{-1}$, and 117.7 $J.g^{-1}$, and the peak temperatures of 132.8 °C and 129.3 °C, were reported for the *star*-Ita.Gly resin (The base-resin), and the ethanol-treated resin, respectively. Comparably, higher reaction heats have been reported for the other star-shaped lactic acid-based resins; for example, the heat of reaction of 227.4 $J.g^{-1}$ has been reported for the star-shaped resins with glycerol core molecules(Bakare et al. 2014b), and the heat of reaction of 275.5 $J.g^{-1}$ has been reported for the star-shaped lactic acid based resins with xylitol core molecules (Jahandideh and Muthukumarappan 2016a).

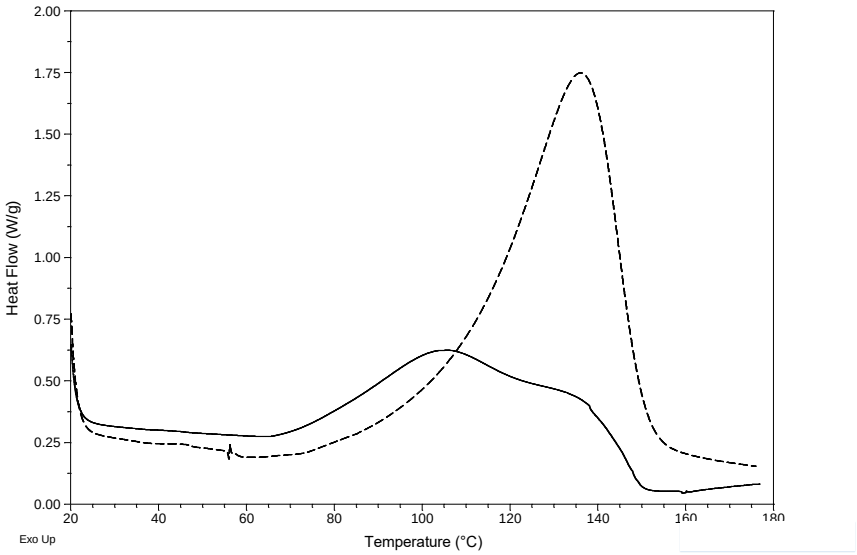

Figure 9. 5. The DSC curves for curing of the methanol-treated resin (solid line) and the allyl alcohol-treated resin (dashed line) at a heat rate of 10 °C.min^{-1} in the heat range of 30 to 180 °C.min^{-1}

9.3.4 Thermogravimetric analysis

The thermal stability of the cured methanol-treated and allyl alcohol-treated resins was investigated using TGA. The percentage of mass loss versus temperature and derivative thermograms were plotted from room temperature to 650 °C and presented in Fig 6. The cured methanol-treated sample started to decompose at 248 °C and showed its maximum rate at 412 °C and ~23% solid residue at 450 °C. However, the cured sample of allyl alcohol-treated started to decompose at 243 °C, and showed two thermal degradation stages below 450 °C, with maximum degradation rates at 337 °C and 430 °C. The allyl alcohol-treated resin also leaves ~37% solid residue at 450 °C. The methanol-treated sample and allyl alcohol-treated sample also showed a slow weight loss at 509-

671 °C and 501-661 °C temperature range, respectively. The recorded onset temperature of the methanol-treated sample (317 °C) was higher than that of the allyl alcohol-treated samples 276 °C, indicating better thermal stability for the methanol-treated resin. In the authors' previous work, it was shown that the thermal degradation of the base-resin and the ethanol-treated resin started at 286 °C and 180 °C, respectively. However, the maximum degradation rates of both resins were reported at 380 °C.

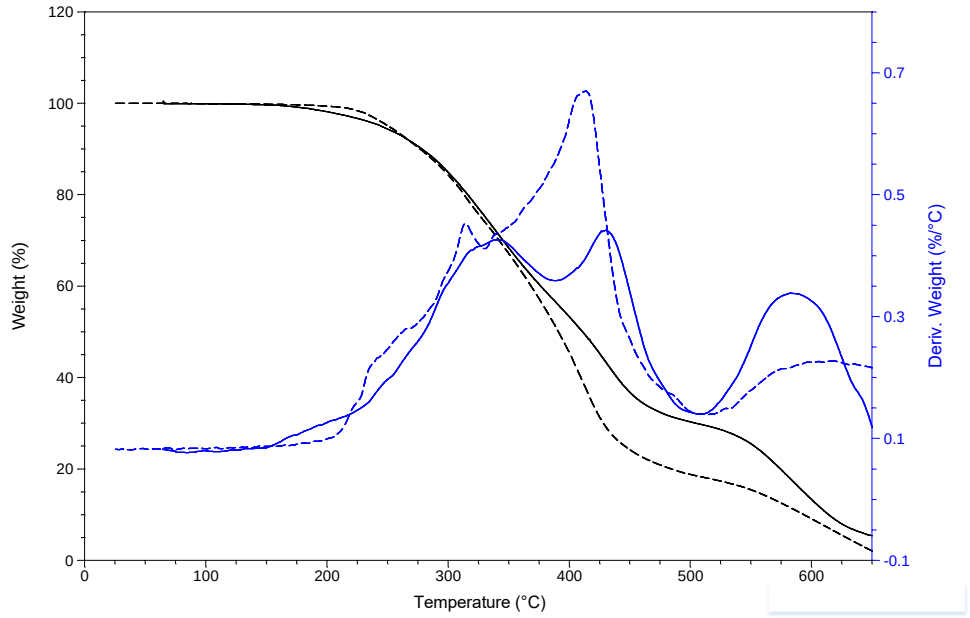

Figure 9. 6. TGA curves for the cured samples of the methanol-treated (solid line), and allyl alcohol-treated samples (dashed line).

9.3.5 Dynamic Mechanical Analysis

DMA was employed for analyzing the thermomechanical properties of the methanol-treated and allyl alcohol-treated samples, and the storage modulus, loss of modulus and T_g were measured. Figure 7 presents the storage modulus *G'* of both resins,

in the temperature range of -20 °C to 170 °C, and the measured storage modulus of both resins with standard deviations at 25°C are given in table 2. It is believed that a stepwise curing method induces gradual solidification, and consequently results in more relaxed state with less built in stresses (Jahandideh and Muthukumarappan 2016a, Vergnaud and Bouzon 2012). The G' is a measure of the molecular packing density in the glassy state of the polymer (Vergnaud and Bouzon 2012, Chang et al. 2012b), and is proportional to the mechanical properties of the tested sample. Figure 7 shows that the methanol-treated sample has a higher storage modulus (~5170 ± 142 MPa at 25 °C) than allyl alcohol-treated resins (3192 ± 80 MPa at 25 °C), and consequently, better mechanical properties are expected for this resin (in range of -20 °C up to 130 °C). In the authors' previous work, the storage modulus of 3109 ± 133 MPa was reported at 25°C for ethanol-treated samples. The G' value of methanol-treated sample was substantially higher than that of other star-shaped itaconic acid based resins.

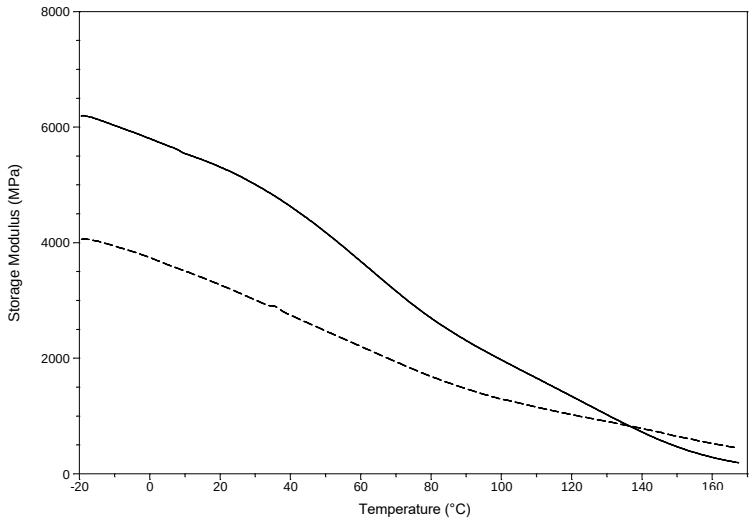

Figure 9. 7. Storage modulus curves of the crosslinked methanol-treated and allyl alcohol-treated *samples in the temperature range of -20 °C to 170 °C*

Figure 8 presents the loss modulus G" curves of the crosslinked methanol-treated and allyl alcohol-treated samples, in the temperature range of -20 °C to 170 °C. G' is an indicator of the dissipated energy, and represents the viscous part of the sample. Therefore, better mechanical properties and strong tendency for reversibility are expected for samples with smaller G' value (Bakare, Ramamoorthy, et al. 2015). In this study, the G' values were found to be relatively small and broad which is similar to the reported G' values in the crosslinked S-LA thermosets (Jahandideh and Muthukumarappan 2016a). The loss modulus results at 25 °C were presented in Table 2.

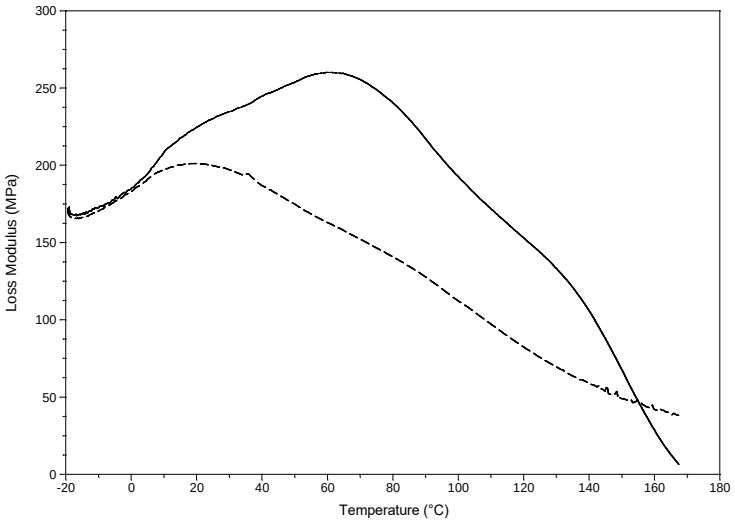

Figure 9. 8. Loss modulus curves of the crosslinked methanol-treated and allyl alcohol-treated samples in the temperature range of -20 °C to 170 °C

Figure 9 presents tan δ curve for the crosslinked methanol-treated (solid line) and allyl alcohol-treated (dashed line) samples in the temperature range of -20 °C to 170 °C. The glass temperature (T_g) of thermosets can be presented based on the peak of tan δ curves. The tan δ peak or the T_g of the allyl alcohol-treated sample was recorded at 93.5 °C, which is comparable to the other reported T_g values of the lactic acid-based thermosets. However, substantially higher T_g value was observed for the methanol-treated resin at 150 °C. Previously, a T_g of 122 °C was recorded for ethanol-treated itaconic acid based resins. Higher T_g values indicate better thermomechanical properties, and are desired for biocomposite manufacturing. To the best of authors' knowledge, the reported T_g (based on the peak of tan δ) for the methanol-treated sample was substantially higher than that of other biobased star-shaped thermosets, which has been reported in range of 50 to 98 °C. (Oksman, Skrifvars, and Selin 2003, Bakare et al. 2014b,

Jahandideh and Muthukumarappan 2016a, Åkesson, Skrifvars, et al. 2010b). The T_g values are also believed to get more improved by applying the reinforcement fibers, which happens due to the adhesion of the fibers to the matrix (Adekunle, Åkesson, and Skrifvars 2010, Bakare, Ramamoorthy, et al. 2015)

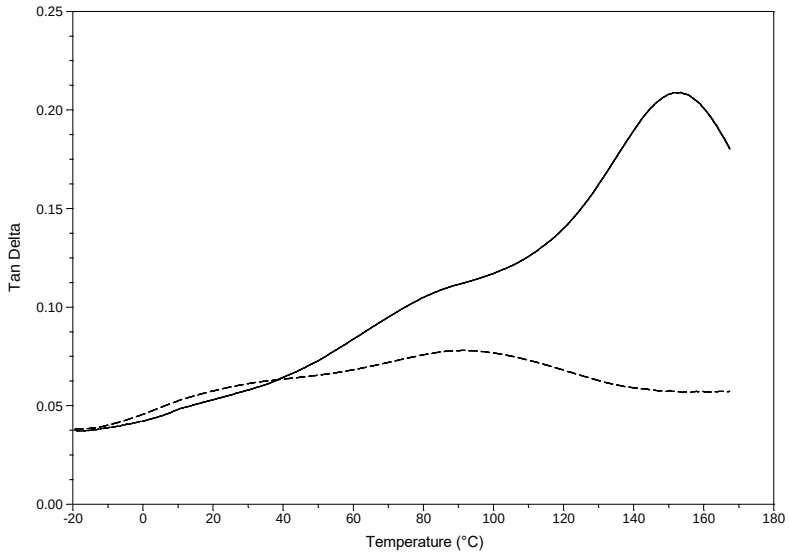

Figure 9. 9. Tan δ curve for the crosslinked methanol-treated (solid line) and allyl alcohol-treated (dashed line) samples in the temperature range of -20 °C to 170 °C

Table 9. 2. Thermal-Mechanical Characterization Results of the Resins

DSC	methanol-treated resin	allyl alcohol-treated resin
Heat of exotherm for uncured resin ($J.g^{-1}$)	140.1	198.9
Curing temperature interval	65 °C - 151 °C	72 °C - 158 °C
Heat of exotherm for cured resin ($J.g^{-1}$) at 140 °C	0	0
Peak temperature	106.8 °C	136.2 °C
Onset temperature	71.4 °C	104.7 °C
DMA	**methanol-treated resin**	**allyl alcohol-treated resin**
tan δ peak (T_g °C)	153.5	91
Storage modulus (MPa) at 25°C	5170 ± 142	3192 ± 80
Loss modulus (MPa) at 25°C	257 ± 11	210 ± 9
TGA	**methanol-treated resin**	**allyl alcohol-treated resin**
Degradation temperature range °C	248 – 460	243 – 450
Maximum degradation (°C)	412	337 & 430
Solid residue at 450 °C	~23%	~37%

9.3.6 Viscosity measurements

Lower viscosities are of interest for composite production processes. Compared to thermoplasts, thermosets provide lower viscosities which make them suitable for composite applications. In addition, there is evidence that changing the structure of oligomers, from linear into a star-shaped one, results in a reduction in the viscosity by reducing the hydrodynamic volume of the oligomers (Corneillie and Smet 2015, Chang et al. 2012b, Finne and Albertsson 2002). It is believed that for a satisfactory composite manufacturing, resins with viscosities below 0.5 Pa s (at the processing temperature) are

required (Li, Wong, and Leach 2010). Figure 10 presents the viscosities of the methanol-treated resin and the allyl alcohol-treated resin as a function of the temperature at temperature intervals of 30 to 100 °C. The methanol-treated resin has a viscosity of 4.2 Pa.s at room temperature which dropped to 0.25 Pa.s upon increasing the temperature to 70 °C. However, the allyl alcohol-treated resin showed a lower viscosity of 1.8 Pa.s at room temperature, and 0.14 Pa.s at 70 °C. Overall, the viscosities of both resins at elevated temperatures, or even at room temperature, are rather lower than the viscosities reported for other star-shaped biobased thermosets, and satisfactory for manufacturing purposes (Åkesson, Skrifvars, et al. 2010b, Jahandideh and Muthukumarappan 2016b). However, in the previous study, the authors reported a viscosity of 0.35 Pa.s at room temperature and 0.04 Pa s at 70 °C, for a star-shaped ethanol-treated itaconic acid-based resin.

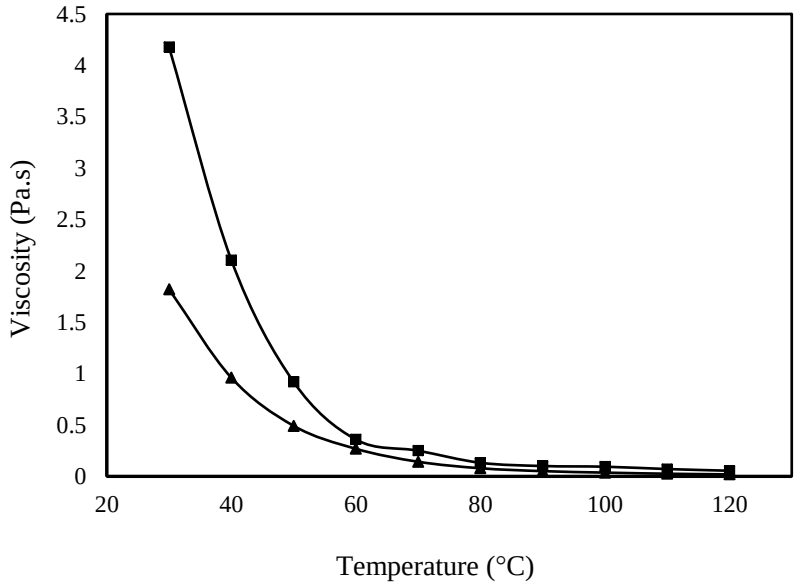

Figure 9. 10. Viscosities of the methanol-treated resin (■) and the allyl alcohol-treated resin (▲) as a function of the temperature.

9.4. Conclusion

In the authors' previous work, synthesis of a fully biobased star-shaped itaconic acid-based thermosets via direct condensation reaction of itaconic acid and glycerol was investigated. The base-resin had good thermomechanical properties, but also showed high viscosity. The viscosity of the resin was substantially reduced by treating the base-resin with ethanol, and dropped from 194 Pa.s (for the base-resin) into 0.35 Pa.s (for the treated resin), at room temperature. Although the alcohol treatment was successful for reducing the viscosity, it adversely affected the thermomechanical properties. The aim of this study is to maintain the viscosity in satisfactory levels, while increasing the cross-linking density and improving the thermomechanical properties of the cured resins. In this study, instead of ethanol-treatment, methanol-treatment was employed, to reduce the hindrance associated to the terminal ethyl-group. The allyl alcohol was also employed to study the effect of the crosslinking density on the thermomechanical properties of the finished resin. Employing allyl alcohol treatment resulted in higher crosslinking density and consequently better thermomechanical properties of the cured resins. Therefore, the star-shaped itaconic acid base thermosetting resins were synthesized via direct condensation polymerization of the glycerol with the itaconic acid as explained in the authors' previous work. The branches of the base-resin were then activated with methanol and allyl alcohol. The results of this study showed that employing methanol-treatment resulted in the better thermomechanical properties, probably by increasing the access to the unsaturated bonds of itaconic acids.

Chemical structures of the methanol and allyl alcohol treated resins were confirmed employing H and ^{13}C NMR and FTIR techniques. The resins' curing behavior

were investigated by DSC analysis, showed a complete curing after curing at 70 °C for 2 h and post curing at 120 °C for 20 min. The reaction heat of allyl alcohol treated-resin was higher than that of methanol treated resin, due to the higher density of unsaturated bonds. Thermogravimetric analyses of the cured resins showed that both resins were comparably stable up to 240 °C. The viscometry analysis showed that the allyl-treated resins has comparably lower viscosities than methanol-treated resins. Overall, the viscosities of both resins at elevated temperatures, are rather lower than the viscosities reported for other star-shaped biobased thermosets, and satisfactory for manufacturing purposes. DMA analysis of the crosslinked methanol-treated resin showed a T_g of 150 °C, substantially higher than that of the other resin (at 93 °C), as well as to-date other synthesized star-shaped systems. The storage modulus of the methanol-treated resin was also substantially higher than that of the allyl alcohol-treated resin (compare the storage modulus of methanol-treated cured samples (5170 ± 142 MPa) to the storage modulus of allyl alcohol-treated cured samples at 25 °C (3192 ± 80 MPa). The results of this study showed that by reactivating the branches of the star-shaped itaconic acid based resins with methanol, the viscosity of the resin will be slightly increased, but the thermomechanical properties will be substantially improved. However, increasing the crosslinking density, by treating the resins with allyl alcohol necessarily does not improve the mechanical properties. Biodegradable and inexpensive raw materials, good rheological properties and promising thermomechanical properties are of advantages of this novel star-shaped itaconic acid based resin, which make the resin comparable with, and superior in some aspects, than other thermosetting systems.

Acknowledgement

The authors would like to acknowledge the funds provided by Agricultural Experiment Station, South Dakota State University and US Department of Agriculture, Washington, DC in support of this research work.

Chapter 10 - Summary and Conclusions

Increasing attentions toward sustainable development, economic and environmental issues have led to many attempts toward replacing the petroleum based materials with renewables. Versatile and economical renewable sources of lactic acid and Itaconic acid make these corn based materials suitable sources for production of bioplastics. It is believed that the employment of a star-shaped architecture for thermosetting resins results in an engineerable, processable and more reactive resin, with comparably lower viscosity. The extended network, provided by the star-shaped structure, also results in better thermomechanical properties of the final product. Different studies have been performed on synthesis of star-shaped thermosetting resins. It is presumed that more hydroxyls of the core molecule provide a better extended network of the final thermosets. In addition, unsaturated hydroxyl groups of the core molecule may ultimately increase the hydrophilicity of the produced resin which makes the resin more compatible with hydrophilic inexpensive natural fibers. The major goal of this dissertation was to synthesize bioresins and biocomposites made from natural fibers and novel star-shaped bioresins. The privilege of this state-of-the-art thermoset systems over other systems is that this resin can be engineered for a certain functionality by changing the chemical structure or altering the crosslinking density.

This dissertation was consisted of two different parts. In the first part (part A), the synthesis and characterization of various star-shaped lactic acid based resins with different core molecules were investigated. The employed core molecules included: glycerin, pentaerythritol, ethylene glycol and xylitol. In the second part (part B), the star-

shaped biobased thermoset resins were synthesized employing itaconic acid molecules and glycerin core molecule.

The first objective of part A of this dissertation was to synthesize, characterize and optimize the curing process of the novel star-shaped lactic acid based resins employing xylitol core molecule. This biobased thermoset resin was successfully synthesized by direct condensation reaction of lactic acid with xylitol followed by the end-functionalization of the hydroxyl groups of branches by methacrylic anhydride, and results were presented in chapter III of this dissertation. Inexpensive raw materials, high biobased content, biodegradability, good thermomechanical and rheological properties, good processability and good thermal stability were of advantages of the synthesized resin which made the resin comparable with commercial unsaturated polyester resins.

The second and third objectives of part A were to evaluate the effect of lactic acid chain lengths on thermomechanical properties of star-LA-xylitol resins and production of jute reinforced biocomposites. An evaluation of the effect of chain length showed that the resin with five LAs exhibited the most favorable thermomechanical properties. Also, the resin's glass transition temperature (103 °C) was substantially higher than that of the thermoplast PLA (~55 °C). The resin had low viscosity at its processing temperature (80 °C). The compatibility of the resin with natural fibers was also investigated for biocomposite manufacturing. Composites were produced from the n5-resin (resin with 5 lactic acid monomers in chains) (80 *wt*% fiber content) using jute fiber. The thermomechanical and morphological properties of the biocomposites were compared with jute-PLA composites and a hybrid composite made of the impregnated jute fibers with n5 resin and PLA. SEM and DMA showed that the n5-jute composites had better

mechanical properties than the other composites produced. The results have been presented in chapter IV of this dissertation.

In chapter V, the synthesis and characterization of methacrylated star-shaped poly(lactidc acid), employing core molecules with different hydroxyl groups was presented. In this chapter, a set of novel bio-based star-shaped thermoset resins were synthesized via ring-opening polymerization of lactide and employing different multi-hydroxyl core molecules, including ethylene glycol, glycerol and erythritol. The branches were end-functionalized with methacrylic anhydride. The effect of the core molecule on the melt viscosity, the curing behavior of the thermosets and also, the thermomechanical properties of the cured resins were investigated. The erythritol-based resin showed superior thermomechanical properties compared to the other resins, and also lower melt viscosity compared to the glycerol-based resin. In addition, the experimental results indicated that erythritol-based resin with 82% bio-based content has superior thermomechanical properties, compared to the commercial polyester resin.

In chapter VI, glass fiber reinforced composites were prepared from lactic acid based thermosetting resin, and their hygroscopic ageing properties were investigated. In this study, three different type of thermoset glass fibre composites were produced and characterized using star-shaped lactic acid based resin with glycerol core molecule (1), its blend with styrene (2), and a commercial oil-based polyester resin (3). Results showed that bio-based composites had roughly similar mechanical properties at room temperature, but thermomechanical properties at higher temperatures were considerably superior compared to that of commercial polyester composites. Ageing test results showed that bio-based resin composites deteriorate by ageing, while commercial

polyester composites remained intact; however, co-polymerizing with styrene improved the ageing behaviour of the bio-based resin and made it suitable for many applications.

In chapter VII the curing kinetics of the star-shaped lactic acid based resin with xylitol core molecule was investigated and modelled. For cure kinetics, the DSC was used to measure the heat flow of dynamic and isothermal curing processes. Non-isothermal curing experiments were performed to study the curing kinetics of the reactions. The curing process was then modeled by the change of various kinetic parameters, reaction orders and evolutions of activated energy under the test reaction conditions. Different models of curing have been investigated including nth-rate model, autocatalytic model, modified autocatalytic model, Kamal's model, and modified models based on Kamal's model. Different order of reactions were also considered for modelling purpose. The results showed that the star-shaped resins' curing can be expressed by autocatalytic model with order 2. Also, a better fit was obtained using Kamal's model with order 2. However, other models were failed accurate predicting of the curing behaviour of the resin.

In chapter IIX, (part B.1) another star-shaped thermoset resin was synthesized by direct condensation reaction of itaconic acid and glycerol. The resin had high viscosity which made it unsuitable for manufacturing purposes. In order to decrease the viscosity of the resin, the carboxyl groups of the oligomers were end-functionalized by ethanol. The viscosity of the base-resin was substantially higher than that of alcohol-treated resin which was only 0.35 Pa s at room temperature and 0.04 Pa s at 70 °C. The glass temperature (T_g) of the alcohol-treated resin was 122 °C. Fully biobased content and inexpensive raw materials, biodegradability, very good thermomechanical and very

promising rheological properties along with good thermal stability were of advantages of the synthesized resin.

In chapter IX (part B.2), activated star-shaped itaconic acid based thermosetting resins were synthesized by direct condensation reaction of itaconic acid and glycerol, followed by activation of the oligomers, by methanol and allyl alcohol treatments. Instead of ethanol, in this study, methanol and allyl alcohol were suggested to improve the thermomechanical properties of the resin by increasing the cross-linking density of the samples. The viscosity of both resins were slightly higher than the ethanol treated itaconic acid based resin, but still lower than other reported biobased thermosets. However, the glass temperature (T_g) of the methanol-treated resin was 150 °C, substantially higher than that of the allyl alcohol-treated resin (observed at 93 °C) and to date reported star-shaped bio-thermosets. DMA results also showed very good mechanical properties for the methanol-treated resin in terms of storage modulus, compared to that of allyl alcohol treated resin (61% higher G' was obtained for the methanol-treated resin). The results have shown that these resin are capable of competing with or even surpassing fossil fuel based resins in terms of cost and eco-friendliness aspect.

Chapter 11-Recommendations for Further Study

- Studying the Curing kinetics of the synthesized polyol resins-Ethylene Glycol (EG), Glycerol (GL), Pentaerythritol (PE) and Xylitol (Xyl) based resins. The details of synthesis have been explained in chapter 5.
- Studying the curing kinetic and rheological modeling of Itaconic acid based resins. The details of synthesis of Itaconic acid-based resins have been introduced in chapters 8 and 9.
- Composite preparation from the Itaconic acid based resins-Ethanol-Allyl and Methanol treated resins and natural fibers i.e. flax, jute, hemp and cotton.
- Employment of the itaconic acid based resin for 3D printing purposes-for preparation of novel engineered composites.
- Employing Lactic acid chains in the structure of the star-shaped itaconic acid based resin-Synthesis studies and assessment of its thermomechanical properties.
- Functionalization of Itaconic acid based resins for fire retardancy purposes, by employing phosphorous groups.
- Functionalization of Itaconic acid based resins for embedding antibacterial agents in the structure for drug delivery purposes.
- Technoeconomic feasibility studies of itaconic acid based resins and also composite production.
- Conducting LCA studies for the itaconic acid based resin composites

Chapter 12 – Literature Cited

Abiko, Atsushi, Shin-ya Yano, and Makoto Iguchi. 2012. "Star-shaped poly (lactic acid) with carboxylic acid terminal groups via poly-condensation." *Polymer* no. 53 (18):3842-3848.

Adekunle, Kayode, Dan Åkesson, and Mikael Skrifvars. 2010. "Synthesis of reactive soybean oils for use as a biobased thermoset resins in structural natural fiber composites." *Journal of applied polymer science* no. 115 (6):3137-3145.

Ajioka, Masanobu, Katashi Enomoto, Kazuhiko Suzuki, and Akihiro Yamaguchi. 1995. "The basic properties of poly (lactic acid) produced by the direct condensation polymerization of lactic acid." *Journal of Environmental polymer degradation* no. 3 (4):225-234.

Åkesson, Dan, Mikael Skrifvars, Bengt Hagström, Pernilla Walkenström, and Jukka Seppälä. 2009. "Processing of Structural Composites from Biobased Thermoset Resins and Natural Fibres by Compression Moulding." *Journal of Biobased Materials and Bioenergy* no. 3 (3):215-225.

Åkesson, Dan, Mikael Skrifvars, Shichang Lv, Wenfang Shi, Kayode Adekunle, Jukka Seppälä, and Minna Turunen. 2010. "Preparation of nanocomposites from biobased thermoset resins by UV-curing." *Progress in Organic Coatings* no. 67 (3):281-286.

Åkesson, Dan, Mikael Skrifvars, Jukka Seppälä, and Minna Turunen. 2011a. "Thermoset lactic acid-based resin as a matrix for flax fibers." *Journal of Applied Polymer Science* no. 119 (5):3004-3009.

Åkesson, Dan, Mikael Skrifvars, Jukka Seppälä, and Minna Turunen. 2011b. "Thermoset lactic acid-based resin as a matrix for flax fibers." *Journal of Applied Polymer Science* no. 119 (5):3004-3009.

Åkesson, Dan, Mikael Skrifvars, Jukka Seppälä, Minna Turunen, Anna Martinelli, and Aleksandar Matic. 2010a. "Synthesis and characterization of a lactic acid-based thermoset resin suitable for structural composites and coatings." *Journal of Applied Polymer Science* no. 115 (1):480-486.

Åkesson, Dan, Mikael Skrifvars, Jukka Seppälä, Minna Turunen, Anna Martinelli, and Aleksandar Matic. 2010b. "Synthesis and characterization of a lactic acid-based thermoset resin suitable for structural composites and coatings." *Journal of applied polymer science* no. 115 (1):480-486.

Alward, David B, David J Kinning, Edward L Thomas, and Lewis J Fetters. 1986. "Effect of arm number and arm molecular weight on the solid-state morphology of poly (styrene-isoprene) star block copolymers." *Macromolecules* no. 19 (1):215-224.

Arvanitoyannis, Ioannis, Atsuyoshi Nakayama, Norioki Kawasaki, and Noboru Yamamoto. 1995. "Novel star-shaped polylactide with glycerol using stannous octoate or tetraphenyl tin as catalyst: 1. Synthesis, characterization and study of their biodegradability." *Polymer* no. 36 (15):2947-2956.

Astete, Carlos E, and Cristina M Sabliov. 2006. "Synthesis and characterization of PLGA nanoparticles." *Journal of Biomaterials Science, Polymer Edition* no. 17 (3):247-289.

ASTM D570-98(2010)e1. 2010. "Standard Test Method for Water Absorption of Plastics, ." *ASTM International, West Conshohocken, PA, 2010, www.astm.org*.

Auvergne, Rémi, Sylvain Caillol, Ghislain David, Bernard Boutevin, and Jean-Pierre Pascault. 2013. "Biobased thermosetting epoxy: present and future." *Chemical reviews* no. 114 (2):1082-1115.

Avny, Yair, Nasser Saghian, and Albert Zilkha. 1972. "Thermally Stable Polymers Derived from Itaconic Acid." *Israel Journal of Chemistry* no. 10 (5):949-957.

Baghaei, Behnaz, Mikael Skrifvars, and Lena Berglin. 2013. "Manufacture and characterisation of thermoplastic composites made from PLA/hemp co-wrapped hybrid yarn prepregs." *Composites Part A: Applied Science and Manufacturing* no. 50:93-101.

Baghaei, Behnaz, Mikael Skrifvars, and Lena Berglin. 2015. "Characterization of thermoplastic natural fibre composites made from woven hybrid yarn prepregs with different weave pattern." *Composites Part A: Applied Science and Manufacturing* no. 76:154-161.

Baghaei, Behnaz, Mikael Skrifvars, Marja Rissanen, and Sunil Kumar Ramamoorthy. 2014. "Mechanical and thermal characterization of compression moulded polylactic acid natural fiber composites reinforced with hemp and lyocell fibers." *Journal of Applied Polymer Science* no. 131 (15):1-10.

Baghaei, Behnaz, Mikael Skrifvars, Masoud Salehi, Tariq Bashir, Marja Rissanen, and Pertti Nousiainen. 2014. "Novel aligned hemp fibre reinforcement for structural biocomposites: porosity, water absorption, mechanical performances and viscoelastic behaviour." *Composites Part A: Applied Science and Manufacturing* no. 61:1-12.

Baiardo, Massimo, Giovanna Frisoni, Mariastella Scandola, Michel Rimelen, David Lips, Kurt Ruffieux, and Erich Wintermantel. 2003. "Thermal and mechanical properties of plasticized poly (L-lactic acid)." *Journal of Applied Polymer Science* no. 90 (7):1731-1738.

Bakare, Fatimat O, Sunil Kumar Ramamoorthy, Dan Åkesson, and Mikael Skrifvars. 2015. "Thermomechanical properties of bio-based composites made from a lactic acid thermoset resin and flax and flax/basalt fibre reinforcements." *Composites Part A: Applied Science and Manufacturing*.

Bakare, Fatimat O, Sunil Kumar Ramamoorthy, Dan Åkesson, and Mikael Skrifvars. 2016. "Thermomechanical properties of bio-based composites made from a lactic acid thermoset resin and flax and flax/basalt fibre reinforcements." *Composites Part A: Applied Science and Manufacturing* no. 83:176-184.

Bakare, Fatimat Oluwatoyin, Dan Åkesson, Mikael Skrifvars, Tariq Bashir, Petri Ingman, and Rajiv Srivastava. "Synthesis and characterization of unsaturated lactic acid based thermoset bio-resins." *European Polymer Journal* (0).

Bakare, Fatimat Oluwatoyin, Dan Åkesson, Mikael Skrifvars, Tariq Bashir, Petri Ingman, and Rajiv Srivastava. 2015. "Synthesis and characterization of unsaturated lactic acid based thermoset bio-resins." *European Polymer Journal* no. 67:570-582.

Bakare, Fatimat Oluwatoyin, Mikael Skrifvars, Dan Åkesson, Yanfei Wang, Shahrzad Javanshir Afshar, and Nima Esmaeili. 2014a. "Synthesis and characterization of bio-based thermosetting resins from lactic acid and glycerol." *Journal of Applied Polymer Science*:n/a-n/a.

Bakare, Fatimat Oluwatoyin, Mikael Skrifvars, Dan Åkesson, Yanfei Wang, Shahrzad Javanshir Afshar, and Nima Esmaeili. 2014b. "Synthesis and characterization of bio-based thermosetting resins from lactic acid and glycerol." *Journal of Applied Polymer Science* no. 131 (13):1-9.

Barner-Kowollik, Christopher, Johan Heuts, and Thomas P Davis. 2001. "Free-radical copolymerization of styrene and itaconic acid studied by 1H NMR kinetic experiments." *Journal of Polymer Science Part A: Polymer Chemistry* no. 39 (5):656-664.

Biela, Tadeusz, Andrzej Duda, Harald Pasch, and Karsten Rode. 2005. "Star-shaped poly (L-lactide) s with variable numbers of hydroxyl groups at polyester arms chain-ends and directly attached to the star-shaped core—Controlled synthesis and characterization." *Journal of Polymer Science Part A: Polymer Chemistry* no. 43 (23):6116-6133.

Biela, Tadeusz, Andrzej Duda, Stanislaw Penczek, Karsten Rode, and Harald Pasch. 2002. "Well-defined star polylactides and their behavior in two-dimensional chromatography." *Journal of Polymer Science Part A: Polymer Chemistry* no. 40 (16):2884-2887.

Biela, Tadeusz, Andrzej Duda, Karsten Rode, and Harald Pasch. 2003. "Characterization of star-shaped poly (L-lactide) s by liquid chromatography at critical conditions." *Polymer* no. 44 (6):1851-1860.

Biwa, Shiro, and Bertil Storåkers. 1995. "An analysis of fully plastic Brinell indentation." *Journal of the Mechanics and Physics of Solids* no. 43 (8):1303-1333.

Bourbigot, Serge, and Gaëlle Fontaine. 2010. "Flame retardancy of polylactide: an overview." *Polymer Chemistry* no. 1 (9):1413-1422.

Bozaci, Ebru, Kutlay Sever, Mehmet Sarikanat, Yoldas Seki, Asli Demir, Esen Ozdogan, and Ismail Tavman. 2013. "Effects of the atmospheric plasma treatments on surface and mechanical properties of flax fiber and adhesion between fiber–matrix for composite materials." *Composites Part B: Engineering* no. 45 (1):565-572.

Bruining, Monique J, Harriet GT Blaauwgeers, Roel Kuijer, Elisabeth Pels, Rudy MMA Nuijts, and Leo H Koole. 2000. "Biodegradable three-dimensional networks of poly (dimethylamino ethyl methacrylate). Synthesis, characterization and in vitro studies of structural degradation and cytotoxicity." *Biomaterials* no. 21 (6):595-604.

Bummer, Paul M. 2004. "Physical chemical considerations of lipid-based oral drug delivery—solid lipid nanoparticles." *Critical Reviews™ in Therapeutic Drug Carrier Systems* no. 21 (1).

Byun, Youngjae, Young Teck Kim, and Scott Whiteside. 2010. "Characterization of an antioxidant polylactic acid (PLA) film prepared with α-tocopherol, BHT and polyethylene glycol using film cast extruder." *Journal of Food Engineering* no. 100 (2):239-244.

Cai, Qing, Youliang Zhao, Jianzhong Bei, Fu Xi, and Shenguo Wang. 2003. "Synthesis and properties of star-shaped polylactide attached to poly (amidoamine) dendrimer." *Biomacromolecules* no. 4 (3):828-834.

Callister, William D, and David G Rethwisch. 2007. *Materials science and engineering: an introduction*. Vol. 7: Wiley New York.

Campbell Jr, Flake C. 2003. *Manufacturing processes for advanced composites*: Elsevier.

Can, E., R. P. Wool, and S. Kusefoglu. 2006. "Soybean and castor oil based monomers: synthesis and copolymerization with styrene." *Journal of Applied Polymer Science* no. 102 (3):2433-2447.

Carfagna, C, E Amendola, and M Giamberini. 2013. Liquid crystalline epoxy resins. Paper read at Liquid Crystalline Polymers: Proceedings of the International Workshop on Liquid Crystalline Polymers, WLCP 93, Capri, Italy, June 1-4 1993.

Chang, ShaoKun, Chao Zeng, Jianbo Li, and Jie Ren. 2012a. "Synthesis of polylactide-based thermoset resin and its curing kinetics." *Polymer International*:n/a-n/a.

Chang, ShaoKun, Chao Zeng, Jianbo Li, and Jie Ren. 2012b. "Synthesis of polylactide-based thermoset resin and its curing kinetics." *Polymer International* no. 61 (10):1492-1502.

Chatterjee, Amit. 2009. "Thermal degradation analysis of thermoset resins." *Journal of applied polymer science* no. 114 (3):1417-1425.

Chen, Xie, Naiwen Zhang, Shuying Gu, Jianbo Li, and Jie Ren. 2014. "Preparation and properties of ramie fabric-reinforced thermoset poly lactic acid composites." *Journal of Reinforced Plastics and Composites*. doi: 10.1177/0731684413520264.

Cheng, Jianjun, Benjamin A Teply, Ines Sherifi, Josephine Sung, Gaurav Luther, Frank X Gu, Etgar Levy-Nissenbaum, Aleksandar F Radovic-Moreno, Robert Langer, and Omid C Farokhzad. 2007. "Formulation of functionalized PLGA–PEG nanoparticles for in vivo targeted drug delivery." *Biomaterials* no. 28 (5):869-876.

Choi, Young Kweon, You Han Bae, and Sung Wan Kim. 1998. "Star-shaped poly (ether-ester) block copolymers: synthesis, characterization, and their physical properties." *Macromolecules* no. 31 (25):8766-8774.

Cole, KC. 1991. "A new approach to modeling the cure kinetics of epoxy/amine thermosetting resins. 1. Mathematical development." *Macromolecules* no. 24 (11):3093-3097.

Cooper-White, Justin J, and Michael E Mackay. 1999. "Rheological properties of poly (lactides). Effect of molecular weight and temperature on the viscoelasticity of poly (l-lactic acid)." *Journal of Polymer Science Part B: Polymer Physics* no. 37 (15):1803-1814.

Corneillie, Stijn, and Mario Smet. 2015. "PLA architectures: the role of branching." *Polymer Chemistry* no. 6 (6):850-867.

Cui, Yanjun, Xiaozhen Tang, Xiaobin Huang, and Yan Chen. 2003. "Synthesis of the star-shaped copolymer of ε-caprolactone and l-lactide from a cyclotriphosphazene core." *Biomacromolecules* no. 4 (6):1491-1494.

Dabade, B. M., G. Ramachandra Reddy, S. Rajesham, and C. Udaya Kiran. 2006. "Effect of Fiber Length and Fiber Weight Ratio on Tensile Properties of Sun hemp and Palmyra Fiber Reinforced Polyester Composites." *Journal of Reinforced Plastics and Composites* no. 25 (16):1733-1738. doi: 10.1177/0731684406068418.

Dainelli, Dario, Nathalie Gontard, Dimitrios Spyropoulos, Esther Zondervan-van den Beuken, and Paul Tobback. 2008. "Active and intelligent food packaging: legal aspects and safety concerns." *Trends in Food Science & Technology* no. 19:S103-S112.

Datta, Rathin, and Michael Henry. 2006. "Lactic acid: recent advances in products, processes and technologies—a review." *Journal of Chemical Technology and Biotechnology* no. 81 (7):1119-1129.

Dobrzynski, Piotr, Janusz Kasperczyk, Henryk Janeczek, and Maciej Bero. 2002. "Synthesis of biodegradable glycolide/L-lactide copolymers using iron compounds as initiators." *Polymer* no. 43 (9):2595-2601.

Dong, Chang-Ming, Kun-Yuan Qiu, Zhong-Wei Gu, and Xin-De Feng. 2001. "Synthesis of star-shaped poly (ε-caprolactone)-b-poly (dl-lactic acid-alt-glycolic acid) with multifunctional initiator and stannous octoate catalyst." *Macromolecules* no. 34 (14):4691-4696.

Drumright, Ray E, Patrick R Gruber, and David E Henton. 2000. "Polylactic acid technology." *Advanced materials* no. 12 (23):1841-1846.

Du, Shanyi, Zhan-Sheng Guo, Boming Zhang, and Zhanjun Wu. 2004. "Cure kinetics of epoxy resin used for advanced composites." *Polymer international* no. 53 (9):1343-1347.

Erden, S, K Sever, Y Seki, and M Sarikanat. 2010. "Enhancement of the mechanical properties of glass/polyester composites via matrix modification glass/polyester composite siloxane matrix modification." *Fibers and Polymers* no. 11 (5):732-737.

Esmaeili, Nima, Fatimat Oluwatoyin Bakare, Mikael Skrifvars, Shahrzad Javanshir Afshar, and Dan Åkesson. 2015. "Mechanical properties for bio-based thermoset composites made from lactic acid, glycerol and viscose fibers." *Cellulose* no. 22 (1):603-613.

Esmaeili, Nima, FatimatOluwatoyin Bakare, Mikael Skrifvars, Shahrzad Javanshir Afshar, and Dan Åkesson. 2014. "Mechanical properties for bio-based thermoset composites made from lactic acid, glycerol and viscose fibers." *Cellulose*:1-11.

Esmaeili, Nima, and Shahrzad Javanshir. 2013. *Eco Friendly Composites Prepared from Lactic Acid Based Resin and Natural Fiber*. 30 ECTS credits Master of Science. Major in Resource recovery – Sustainable engineering, No. 6/2013, Högskolan i Borås/Ingenjörshögskolan (IH), University of Borås, University of Borås/School of Engineering, Sweden.

Finne, Anna, and Ann-Christine Albertsson. 2002. "Controlled synthesis of star-shaped L-lactide polymers using new spirocyclic tin initiators." *Biomacromolecules* no. 3 (4):684-690.

Fu, Hui-Li, Tao Zou, Si-Xue Cheng, Xian-Zheng Zhang, and Ren-Xi Zhuo. 2007. "Cholic acid functionalized star poly (DL-lactide) for promoting cell adhesion and proliferation." *Journal of tissue engineering and regenerative medicine* no. 1 (5):368-376.

Fukui, Hiroji, Mitsuo Sawamoto, and Toshinobu Higashimura. 1994. "Multifunctional coupling agents for living cationic polymerization. 3. Synthesis of tri-and tetra-armed poly (vinyl ethers) with tri-and tetrafunctional silyl enol ethers." *Macromolecules* no. 27 (6):1297-1302.

Gabbott, Paul. 2008. *Principles and applications of thermal analysis*. Vol. 1: John Wiley & Sons.

Garlotta, Donald. 2001a. "A literature review of poly (lactic acid)." *Journal of Polymers and the Environment* no. 9 (2):63-84.

Garlotta, Donald. 2001b. "A Literature Review of Poly(Lactic Acid)." *Journal of Polymers and the Environment* no. 9 (2):63-84. doi: 10.1023/a:1020200822435.

Ghahremankhani, Ali Afshar, Farid Dorkoosh, and Rassoul Dinarvand. 2008. "PLGA-PEG-PLGA tri-block copolymers as in situ gel-forming peptide delivery system: effect of formulation properties on peptide release." *Pharmaceutical development and technology* no. 13 (1):49-55.

Gledhill, RA, AJ Kinloch, S Yamini, and RJ Young. 1978. "Relationship between mechanical properties of and crack progogation in epoxy resin adhesives." *Polymer* no. 19 (5):574-582.

Go, Dong Hyun, Yoon Ki Joung, Sun Young Park, Yong Doo Park, and Ki Dong Park. 2008. "Heparin-conjugated star-shaped PLA for improved biocompatibility." *Journal of Biomedical Materials Research Part A* no. 86 (3):842-848.

Gu, ShuYing, Ming Yang, Tao Yu, TianBin Ren, and Jie Ren. 2008. "Synthesis and characterization of biodegradable lactic acid-based polymers by chain extension." *Polymer International* no. 57 (8):982-986.

Han, Gyeong-Soon, Youn-Soo Shim, Yu-Ri Choi, and Sun-Ok Jang. 2015. "Viscosity, Micro-Leakage, Water Solubility and Absorption in a Resin-based Temporary Filling Material." *Indian Journal of Science and Technology* no. 8 (25).

Hardis, Ricky, Julie LP Jessop, Frank E Peters, and Michael R Kessler. 2013. "Cure kinetics characterization and monitoring of an epoxy resin using DSC, Raman spectroscopy, and DEA." *Composites Part A: Applied Science and Manufacturing* no. 49:100-108.

Hartmann, M. H. 1998. "High Molecular Weight Polylactic Acid Polymers." In *Biopolymers from Renewable Resources*, edited by David L. Kaplan, 367-411. Berlin, Heidelberg: Springer Berlin Heidelberg.

Heinrich, Christian, Michael Aldridge, Alan S Wineman, John Kieffer, Anthony M Waas, and Khaled W Shahwan. 2013. "The role of curing stresses in subsequent response, damage and failure of textile polymer composites." *Journal of the Mechanics and Physics of Solids* no. 61 (5):1241-1264.

Helminen, Antti O, Harri Korhonen, and Jukka V Seppälä. 2002. "Structure modification and crosslinking of methacrylated polylactide oligomers." *Journal of applied polymer science* no. 86 (14):3616-3624.

Herrmann, Konrad. 2011. *Hardness testing: principles and applications*: ASM International.

Hisham, Siti Farhana, Ishak Ahmad, Rusli Daik, and Anita Ramli. 2011. "Blends of LNR with unsaturated polyester resin from recycled PET: comparison of mechanical properties and morphological analysis with the optimum blend by commercial resin." *Sains Malaysiana* no. 40 (7):729-735.

Hodgkinson, John M. 2000. *Mechanical testing of advanced fibre composites*: Elsevier.

Houchin, ML, and EM Topp. 2009. "Physical properties of PLGA films during polymer degradation." *Journal of applied polymer science* no. 114 (5):2848-2854.

Huda, Masud S., Lawrence T. Drzal, Manjusri Misra, Amar K. Mohanty, Kelly Williams, and Deborah F. Mielewski. 2005. "A Study on Biocomposites from Recycled Newspaper Fiber and Poly(lactic acid)." *Industrial & Engineering Chemistry Research* no. 44 (15):5593-5601. doi: 10.1021/ie0488849.

Hult, Anders, Mats Johansson, and Eva Malmström. 1999. "Hyperbranched polymers." In *Branched Polymers II*, 1-34. Springer.

Ibay, Augusto C, and Linwood P Tenney. 1993. Polymers from hydroxy acids and polycarboxylic acids. Google Patents.

Idicula, Maries, Kuruvilla Joseph, and Sabu Thomas. 2010. "Mechanical Performance of Short Banana/Sisal Hybrid Fiber Reinforced Polyester Composites." *Journal of Reinforced Plastics and Composites* no. 29 (1):12-29. doi: 10.1177/0731684408095033.

Iwatake, Atsuhiro, Masaya Nogi, and Hiroyuki Yano. 2008. "Cellulose nanofiber-reinforced polylactic acid." *Composites Science and Technology* no. 68 (9):2103-2106.

Jahandideh, Arash, Nima Esmaeili, and Kasiviswanathan Muthukumarappan. 2017. "Effect of lactic acid chain lengths on thermomechanical properties of star-LA-xylitol resins and jute reinforced biocomposites." *Polymer International*:1-10.

Jahandideh, Arash, and Kasiviswanathan Muthukumarappan. 2016a. "Synthesis, characterization and curing optimization of a biobased thermosetting resin from xylitol and lactic acid." *European Polymer Journal* no. 83:344-358. doi: http://dx.doi.org/10.1016/j.eurpolymj.2016.08.033.

Jahandideh, Arash, and Kasiviswanathan Muthukumarappan. 2016b. "Synthesis, Characterization and Curing Optimization of a Biobased Thermosetting Resin from Xylitol and Lactic Acid." *European Polymer Journal*.

Jahandideh, Arash, and Kasiviswanathan Muthukumarappan. 2017. "Star-shaped lactic acid based systems and their thermosetting resins; synthesis, characterization, potential opportunities and drawbacks." *European Polymer Journal* no. 87:360-379. doi: http://dx.doi.org/10.1016/j.eurpolymj.2016.12.035.

Jamshidian, Majid, Elmira Arab Tehrany, and Stéphane Desobry. 2012. "Release of synthetic phenolic antioxidants from extruded poly lactic acid (PLA) film." *Food Control* no. 28 (2):445-455.

Jamshidian, Majid, Elmira Arab Tehrany, Muhammad Imran, Muriel Jacquot, and Stéphane Desobry. 2010. "Poly-Lactic Acid: production, applications, nanocomposites, and release studies." *Comprehensive Reviews in Food Science and Food Safety* no. 9 (5):552-571.

Jeong, B, YK Choi, You Han Bae, G Zentner, and Sung Wan Kim. 1999. "New biodegradable polymers for injectable drug delivery systems." *Journal of Controlled Release* no. 62 (1):109-114.

Jeong, Byeongmoon, You Han Bae, and Sung Wan Kim. 2000. "In situ gelation of PEG-PLGA-PEG triblock copolymer aqueous solutions and degradation thereof." *Journal of biomedical materials research* no. 50 (2):171-177.

Jeong, Ji Hoon, Dong Woo Lim, Dong Keun Han, and Tae Gwan Park. 2000. "Synthesis, characterization and protein adsorption behaviors of PLGA/PEG di-block co-polymer blend films." *Colloids and Surfaces B: Biointerfaces* no. 18 (3–4):371-379. doi: http://dx.doi.org/10.1016/S0927-7765(99)00162-9.

Jimenez, Alfonso, Mercedes Peltzer, and Roxana Ruseckaite. 2014. *Poly (lactic acid) science and technology: processing, properties, additives and applications*: Royal Society of Chemistry.

Jonoobi, Mehdi, Jalaluddin Harun, Aji P Mathew, and Kristiina Oksman. 2010. "Mechanical properties of cellulose nanofiber (CNF) reinforced polylactic acid

(PLA) prepared by twin screw extrusion." *Composites Science and Technology* no. 70 (12):1742-1747.

Kabir, MM, H Wang, KT Lau, and F Cardona. 2012. "Chemical treatments on plant-based natural fibre reinforced polymer composites: An overview." *Composites Part B: Engineering* no. 43 (7):2883-2892.

Kalpakjian, Serope, Steven R Schmid, and KS Vijay Sekar. 2014. *Manufacturing engineering and technology*: Prentice Hall.

Kamal, MR, and S Sourour. 1973. "Kinetics and thermal characterization of thermoset cure." *Polymer Engineering & Science* no. 13 (1):59-64.

Kamal, Musa R. 1974. "Thermoset characterization for moldability analysis." *Polymer Engineering & Science* no. 14 (3):231-239.

Kanaoka, Shokyoku, Mitsuo Sawamoto, and Toshinobu Higashimura. 1991. "Star-shaped polymers by living cationic polymerization. 1. Synthesis of star-shaped polymers of alkyl and vinyl ethers." *Macromolecules* no. 24 (9):2309-2313.

Kim, Eun Sub, Byoung Chul Kim, and Soo Hyun Kim. 2004. "Structural effect of linear and star-shaped poly (L-lactic acid) on physical properties." *Journal of Polymer Science Part B: Polymer Physics* no. 42 (6):939-946.

Kim, Soo Hyun, Yang-Kyoo Han, Kwang-Duk Ahn, Young Ha Kim, and Taihyun Chang. 1993. "Preparation of star-shaped polylactide with pentaerythritol and stannous octoate." *Die Makromolekulare Chemie* no. 194 (12):3229-3236.

Kim, Soo Hyun, Yang-Kyoo Han, Young Ha Kim, and Sung Ill Hong. 1992. "Multifunctional initiation of lactide polymerization by stannous octoate/pentaerythritol." *Die Makromolekulare Chemie* no. 193 (7):1623-1631.

Kim, Soo Hyun, and Young Ha Kim. 1999. Direct condensation polymerization of lactic acid. Paper read at Macromolecular Symposia.

Knothe, Gerhard. 2006. "Analyzing biodiesel: standards and other methods." *Journal of the American Oil Chemists' Society* no. 83 (10):823-833.

Komkov, MA, VA Tarasov, and VM Kuznetsov. 2015. "The influence of epoxide resin viscosity on impregnation of fiber reinforcement." *Polymer Science Series D* no. 8 (4):292-295.

Kricheldorf, Hans R, and Ruth Dunsing. 1986. "Polylactones, 8. Mechanism of the cationic polymerization of L, L-dilactide." *Die Makromolekulare Chemie* no. 187 (7):1611-1625.

Kricheldorf, Hans R, Heiko Hachmann-Thiessen, and Gert Schwarz. 2004. "Telechelic and star-shaped poly (L-lactide) s by means of bismuth (III) acetate as initiator." *Biomacromolecules* no. 5 (2):492-496.

Kumari, Avnesh, Sudesh Kumar Yadav, and Subhash C Yadav. 2010. "Biodegradable polymeric nanoparticles based drug delivery systems." *Colloids and Surfaces B: Biointerfaces* no. 75 (1):1-18.

Kurcok, P, A Matuslonicz, and Z Jedlinski. 1995. "Anionic-polymerization as a tool in the synthesis of biodegradable polymers." *JOURNAL OF POLYMER MATERIALS* no. 12 (2):161-174.

Lan, Ping, and Lv Jia. 2006. "Thermal Properties of Copoly (L-lactic acid/glycolic acid) by Direct Melt Polycondensation." *Journal of Macromolecular Science, Part A: Pure and Applied Chemistry* no. 43 (11):1887-1894.

Langer, Robert. 1994. "Biodegradable polymer scaffolds for tissue engineering." *Nat. Biotechnol*.

Lasprilla, Astrid JR, Guillermo AR Martinez, Betânia H Lunelli, André L Jardini, and Rubens Maciel Filho. 2012. "Poly-lactic acid synthesis for application in biomedical devices—A review." *Biotechnology advances* no. 30 (1):321-328.

Le Corre, Kristell S, Christoph Ort, Diana Kateley, Belinda Allen, Beate I Escher, and Jurg Keller. 2012. "Consumption-based approach for assessing the contribution of hospitals towards the load of pharmaceutical residues in municipal wastewater." *Environment international* no. 45:99-111.

Li, Wei Helen, Alex Wong, and David Leach. 2010. Advances in benzoxazine resins for aerospace applications. Paper read at Proc 2010 SAMPE International Symposium, Seattle WA, SAMPE Covina CA.

Liang, Guanghui, and K Chandrashekhara. 2006. "Cure kinetics and rheology characterization of soy-based epoxy resin system." *Journal of applied polymer science* no. 102 (4):3168-3180.

Lim, L. T., R. Auras, and M. Rubino. 2008. "Processing technologies for poly(lactic acid)." *Progress in Polymer Science* no. 33 (8):820-852. doi: http://dx.doi.org/10.1016/j.progpolymsci.2008.05.004.

Lin, Yaling, and Anqiang Zhang. 2010. "Synthesis and characterization of star-shaped poly (d, l-lactide)-block-poly (ethylene glycol) copolymers." *Polymer bulletin* no. 65 (9):883-892.

Lin, Yaling, Anqiang Zhang, and Lianshi Wang. 2012. "Synthesis and characterization of star-shaped poly (ethylene glycol)-block-poly (L-lactic acid) copolymers by melt polycondensation." *Journal of Applied Polymer Science* no. 124 (6):4496-4501.

Liu, Kunwei, Samy A Madbouly, and Michael R Kessler. 2015. "Biorenewable thermosetting copolymer based on soybean oil and eugenol." *European Polymer Journal* no. 69:16-28.

Liu, L, YD Huang, ZQ Zhang, ZX Jiang, and LN Wu. 2008. "Ultrasonic treatment of aramid fiber surface and its effect on the interface of aramid/epoxy composites." *Applied Surface Science* no. 254 (9):2594-2599.

Lu, J., and R. P. Wool. 2006. "Novel thermosetting resins for smc applications from linseed oil. synthesis, characterization, and properties." *Journal of Applied Polymer Science* no. 99 (5):2481-8.

Lucke, Andrea, Jörg Teßmar, Edith Schnell, Georg Schmeer, and Achim Göpferich. 2000. "Biodegradable poly (D, L-lactic acid)-poly (ethylene glycol)-monomethyl ether diblock copolymers: structures and surface properties relevant to their use as biomaterials." *Biomaterials* no. 21 (23):2361-2370.

Lunt, James. 1998. "Large-scale production, properties and commercial applications of polylactic acid polymers." *Polymer Degradation and Stability* no. 59 (1):145-152. doi: http://dx.doi.org/10.1016/S0141-3910(97)00148-1.

Luo, Qiang, Min Lui, Yijin Xu, Mihail Ionescu, and Zoran S. Petrovic. 2013. "Thermosetting allyl resins derived from soybean fatty acids." *Journal of Applied Polymer Science* no. 127 (1):432-438.

Lutz, Pierre, and Paul Rempp. 1988. "New developments in star polymer synthesis. Star-shaped polystyrenes and star-block copolymers." *Die Makromolekulare Chemie* no. 189 (5):1051-1060.

Lv, An, Zi-Long Li, Fu-Sheng Du, and Zi-Chen Li. 2014. "Synthesis, functionalization, and controlled degradation of high molecular weight polyester from itaconic acid via ADMET polymerization." *Macromolecules* no. 47 (22):7707-7716.

Ma, Songqi, Xiaoqing Liu, Yanhua Jiang, Zhaobin Tang, Chuanzhi Zhang, and Jin Zhu. 2013. "Bio-based epoxy resin from itaconic acid and its thermosets cured with anhydride and comonomers." *Green Chemistry* no. 15 (1):245-254.

Madhavan Nampoothiri, K., Nimisha Rajendran Nair, and Rojan Pappy John. 2010. "An overview of the recent developments in polylactide (PLA) research." *Bioresource Technology* no. 101 (22):8493-8501. doi: http://dx.doi.org/10.1016/j.biortech.2010.05.092.

Mahalle, Lal, Ayse Alemdar, Mihaela Mihai, and Nathalie Legros. 2014. "A cradle-to-gate life cycle assessment of wood fibre-reinforced polylactic acid (PLA) and polylactic acid/thermoplastic starch (PLA/TPS) biocomposites." *The International Journal of Life Cycle Assessment* no. 19 (6):1305-1315. doi: 10.1007/s11367-014-0731-4.

Makadia, Hirenkumar K, and Steven J Siegel. 2011. "Poly lactic-co-glycolic acid (PLGA) as biodegradable controlled drug delivery carrier." *Polymers* no. 3 (3):1377-1397.

Marsalko, TM, I Majoros, and JP Kennedy. 1993. "Multi-arm star polyisobutylenes." *Polymer Bulletin* no. 31 (6):665-672.

Martín, J. L., A. Cadenato, and J. M. Salla. 1997. "Comparative studies on the non-isothermal DSC curing kinetics of an unsaturated polyester resin using free radicals

and empirical models." *Thermochimica Acta* no. 306 (1):115-126. doi: http://dx.doi.org/10.1016/S0040-6031(97)00311-0.

Martinez, Fabio Andres Castillo, Eduardo Marcos Balciunas, José Manuel Salgado, José Manuel Domínguez González, Attilio Converti, and Ricardo Pinheiro de Souza Oliveira. 2013. "Lactic acid properties, applications and production: a review." *Trends in food science & technology* no. 30 (1):70-83.

Mashouf Roudsari, Ghodsieh, Amar K Mohanty, and Manjusri Misra. 2014. "Study of the curing kinetics of epoxy resins with biobased hardener and epoxidized soybean oil." *ACS Sustainable Chemistry & Engineering* no. 2 (9):2111-2116.

McCabe-Sellers, Beverly J, and Samuel E Beattie. 2004. "Food safety: emerging trends in foodborne illness surveillance and prevention." *Journal of the American Dietetic Association* no. 104 (11):1708-1717.

Menard, Kevin P. 2008. *Dynamic mechanical analysis: a practical introduction*: CRC press.

Mezzenga, Raffaele, Louis Boogh, and Jan-Anders E Månson. 2001. "A review of dendritic hyperbranched polymer as modifiers in epoxy composites." *Composites Science and Technology* no. 61 (5):787-795.

Mohan, TP, M Ramesh Kumar, and R Velmurugan. 2005. "Rheology and curing characteristics of epoxy–clay nanocomposites." *Polymer International* no. 54 (12):1653-1659.

Mohanty, S., S. K. Nayak, S. K. Verma, and S. S. Tripathy. 2004. "Effect of MAPP as a Coupling Agent on the Performance of Jute–PP Composites." *Journal of*

Reinforced Plastics and Composites no. 23 (6):625-637. doi: 10.1177/0731684404032868.

Moon, Sung-Il, Ikuo Taniguchi, Masatoshi Miyamoto, Yoshiharu Kimura, and Chan-Woo Lee. 2001. "Synthesis and properties of high-molecular-weight poly (L-lactic acid) by melt/solid polycondensation under different reaction conditions." *High Performance Polymers* no. 13 (2):S189-S196.

Moré, Jorge J. 1978. "The Levenberg-Marquardt algorithm: implementation and theory." In *Numerical analysis*, 105-116. Springer.

Morgan, Alexander B, and Jeffrey W Gilman. 2013. "An overview of flame retardancy of polymeric materials: application, technology, and future directions." *Fire and Materials* no. 37 (4):259-279.

Mosiewicki, M., M. I. Aranguren, and J. Borrajo. 2005. "Mechanical properties of linseed oil monoglyceride maleate/styrene copolymers." *Journal of Applied Polymer Science* no. 97 (3):825-36.

Mujika, F. 2006. "On the difference between flexural moduli obtained by three-point and four-point bending tests." *Polymer testing* no. 25 (2):214-220.

Muralidhar, B. A., V. R. Giridev, and K. Raghunathan. 2012. "Flexural and impact properties of flax woven, knitted and sequentially stacked knitted/woven preform reinforced epoxy composites." *Journal of Reinforced Plastics and Composites* no. 31 (6):379-388. doi: 10.1177/0731684412437987.

Murillo, Edwin A, Pedro P Vallejo, and Betty L López. 2011. "Effect of tall oil fatty acids content on the properties of novel hyperbranched alkyd resins." *Journal of Applied Polymer Science* no. 120 (6):3151-3158.

Nawab, Yasir, Pascal Casari, Nicolas Boyard, and Frédéric Jacquemin. 2013. "Characterization of the cure shrinkage, reaction kinetics, bulk modulus and thermal conductivity of thermoset resin from a single experiment." *Journal of Materials Science* no. 48 (6):2394-2403.

Nouri, Sahar, Charles Dubois, and Pierre G Lafleur. 2015a. "Effect of chemical and physical branching on rheological behavior of polylactide." *Journal of Rheology (1978-present)* no. 59 (4):1045-1063.

Nouri, Sahar, Charles Dubois, and Pierre G Lafleur. 2015b. "Synthesis and characterization of polylactides with different branched architectures." *Journal of Polymer Science Part B: Polymer Physics* no. 53 (7):522-531.

Oksman, Kristiina, Mikael Skrifvars, and J-F Selin. 2003. "Natural fibres as reinforcement in polylactic acid (PLA) composites." *Composites science and technology* no. 63 (9):1317-1324.

Olabisi, Olagoke, and Kolapo Adewale. 2016. *Handbook of thermoplastics*. Vol. 41: CRC press.

Othman, Norhayani, Alberto Acosta-Ramírez, Parisa Mehrkhodavandi, John R Dorgan, and Savvas G Hatzikiriakos. 2011. "Solution and melt viscoelastic properties of controlled microstructure poly (lactide)." *Journal of Rheology (1978-present)* no. 55 (5):987-1005.

Otsu, Takayuki, Hiroyuki Watanabe, Jian-Zhong Yang, Masahiro Yoshioka, and Akikazu Matsumoto. 1992. Synthesis and characterization of polymers from itaconic acid derivatives. Paper read at Makromolekulare Chemie. Macromolecular Symposia.

Park, Sang Yeob, Bo Ryeong Han, Kwang Myoung Na, Dong Keun Han, and Sung Chul Kim. 2003. "Micellization and gelation of aqueous solutions of star-shaped PLLA-PEO block copolymers." *Macromolecules* no. 36 (11):4115-4124.

Pascault, Jean-Pierre, Henry Sautereau, Jacques Verdu, and Roberto JJ Williams. 2002. *Thermosetting polymers*. Vol. 64: CRC Press.

Pereira, Ayrton Alef Castanheira, and José Roberto Moraes d'Almeida. 2016. "Effect of the hardener to epoxy monomer ratio on the water absorption behavior of the DGEBA/TETA epoxy system." *Polímeros* no. 26 (1):30-37.

Perry, Mitchell R, and Michael P Shaver. 2011. "Flexible and rigid core molecules in the synthesis of poly (lactic acid) star polymers." *Canadian Journal of Chemistry* no. 89 (4):499-505.

Phillips, DC, JM Scott, and M Jones. 1978. "Crack propagation in an amine-cured epoxide resin." *Journal of Materials Science* no. 13 (2):311-322.

Plate, NA, and VP Shibayev. 1971. "Structure and physical properties of "comb-like" polymers." *Polymer Science USSR* no. 13 (2):466-483.

Qin, Lijun, Jianhui Qiu, Mingzhu Liu, Shenglong Ding, Liang Shao, Shaoyu Lü, Guohong Zhang, Yang Zhao, and Xie Fu. 2011. "Mechanical and thermal properties of poly (lactic acid) composites with rice straw fiber modified by poly (butyl acrylate)." *Chemical Engineering Journal* no. 166 (2):772-778.

Qiu, Li Yan, and You Han Bae. 2006. "Polymer architecture and drug delivery." *Pharmaceutical research* no. 23 (1):1-30.

Ramamoorthy, Sunil Kumar, Fatimat Bakare, Rene Herrmann, and Mikael Skrifvars. 2015. "Performance of biocomposites from surface modified regenerated cellulose fibers

and lactic acid thermoset bioresin." *Cellulose* no. 22 (4):2507-2528. doi: 10.1007/s10570-015-0643-x.

Ramamoorthy, Sunil Kumar, Mikael Skrifvars, and Marja Rissanen. 2015. "Effect of alkali and silane surface treatments on regenerated cellulose fibre type (Lyocell) intended for composites." *Cellulose* no. 22 (1):637-654.

Raquez, J-M, M Deléglise, M-F Lacrampe, and P Krawczak. 2010a. "Thermosetting (bio) materials derived from renewable resources: a critical review." *Progress in Polymer Science* no. 35 (4):487-509.

Raquez, J. M., M. Deléglise, M. F. Lacrampe, and P. Krawczak. 2010b. "Thermosetting (bio)materials derived from renewable resources: A critical review." *Progress in Polymer Science* no. 35 (4):487-509. doi: http://dx.doi.org/10.1016/j.progpolymsci.2010.01.001.

Ratna, Debdatta. 2009. *Handbook of thermoset resins*: ISmithers Shawbury, UK.

Ray, Suprakas Sinha, and Mosto Bousmina. 2005. "Biodegradable polymers and their layered silicate nanocomposites: in greening the 21st century materials world." *Progress in materials science* no. 50 (8):962-1079.

Rowell, Roger M. 2007. "Challenges in Biomass–Thermoplastic Composites." *Journal of Polymers and the Environment* no. 15 (4):229-235. doi: 10.1007/s10924-007-0069-0.

Sachlos, E, and JT Czernuszka. 2003. "Making tissue engineering scaffolds work. Review: the application of solid freeform fabrication technology to the production of tissue engineering scaffolds." *Eur Cell Mater* no. 5 (29):39-40.

Sakai, Reika, Baiju John, Masami Okamoto, Jukka V Seppälä, Jayasheelan Vaithilingam, Husnah Hussein, and Ruth Goodridge. 2013. "Fabrication of Polylactide-Based Biodegradable Thermoset Scaffolds for Tissue Engineering Applications." *Macromolecular Materials and Engineering* no. 298 (1):45-52.

Saltzman, W Mark, and William L Olbricht. 2002. "Building drug delivery into tissue engineering design." *Nature Reviews Drug Discovery* no. 1 (3):177-186.

Saltzman, W. Mark, and Themis R. Kyriakides. 2014. "Chapter 20 - Cell Interactions with Polymers A2 - Lanza, Robert." In *Principles of Tissue Engineering (Fourth Edition)*, edited by Robert Langer and Joseph Vacanti, 385-406. Boston: Academic Press.

Sathishkumar, TP, S Satheeshkumar, and J Naveen. 2014. "Glass fiber-reinforced polymer composites–a review." *Journal of Reinforced Plastics and Composites* no. 33 (13):1258-1275.

Sawhney, Amarpreet S, Chandrashekhar P Pathak, and Jeffrey A Hubbell. 1993. "Bioerodible hydrogels based on photopolymerized poly (ethylene glycol)-co-poly (. alpha.-hydroxy acid) diacrylate macromers." *Macromolecules* no. 26 (4):581-587.

Shao, Jingai, and F Agblevor. 2015. "New Rapid Method for the Determination of Total Acid Number (Tan) of Bio-Oils." *American Journal of Biomass and Bioenergy* no. 4 (1):1-9.

Sheridan, MH, LD Shea, MC Peters, and DJ Mooney. 2000. "Bioabsorbable polymer scaffolds for tissue engineering capable of sustained growth factor delivery." *Journal of Controlled Release* no. 64 (1):91-102.

Shin, Heungsoo, Seongbong Jo, and Antonios G Mikos. 2003. "Biomimetic materials for tissue engineering." *Biomaterials* no. 24 (24):4353-4364.

Soto-Cantú, CD, AZ Graciano-Verdugo, E Peralta, AR Islas-Rubio, A González-Córdova, A González-León, and H Soto-Valdez. 2008. "Release of butylated hydroxytoluene from an active film packaging to asadero cheese and its effect on oxidation and odor stability." *Journal of dairy science* no. 91 (1):11-19.

Storey, Robson F, Stephen C Warren, Charles J Allison, Jeffrey S Wiggins, and AD Puckett. 1993. "Synthesis of bioabsorbable networks from methacrylate-endcapped polyesters." *Polymer* no. 34 (20):4365-4372.

Suryanegara, Lisman, Antonio Norio Nakagaito, and Hiroyuki Yano. 2009. "The effect of crystallization of PLA on the thermal and mechanical properties of microfibrillated cellulose-reinforced PLA composites." *Composites Science and Technology* no. 69 (7–8):1187-1192. doi: http://dx.doi.org/10.1016/j.compscitech.2009.02.022.

Sutivisedsak, Nongnuch, HN Cheng, MK Dowd, GW Selling, and Atanu Biswas. 2012. "Evaluation of cotton byproducts as fillers for poly (lactic acid) and low density polyethylene." *Industrial Crops and Products* no. 36 (1):127-134.

Tabata, Yasuhiko. 2000. "The importance of drug delivery systems in tissue engineering." *Pharmaceutical science & technology today* no. 3 (3):80-89.

Takamura, Masumi, Tomoyuki Nakamura, Tatsuhiro Takahashi, and Kiyohito Koyama. 2008. "Effect of type of peroxide on cross-linking of poly (l-lactide)." *Polymer Degradation and Stability* no. 93 (10):1909-1916.

Teng, Lijing, Xiaohong Xu, Wangyan Nie, Yifeng Zhou, Linyong Song, and Pengpeng Chen. 2015. "Synthesis and degradability of a star-shaped polylactide based on l-lactide and xylitol." *Journal of Polymer Research* no. 22 (5):1-7.

Tiwari, Gaurav, Ruchi Tiwari, Birendra Sriwastawa, L Bhati, S Pandey, P Pandey, and Saurabh K Bannerjee. 2012. "Drug delivery systems: An updated review." *International journal of pharmaceutical investigation* no. 2 (1):2.

Tsuji, Hideto, Yu Sugiura, Yuzuru Sakamoto, Leevameng Bouapao, and Shinichi Itsuno. 2008. "Crystallization behavior of linear 1-arm and 2-arm poly (l-lactide) s: Effects of coinitiators." *Polymer* no. 49 (5):1385-1397.

Tunca, Umit. 2013. "Triple click reaction strategy for macromolecular diversity." *Macromolecular rapid communications* no. 34 (1):38-46.

Vergnaud, Jean-Maurice, and Jean Bouzon. 2012. *Cure of thermosetting resins: modelling and experiments*: Springer Science & Business Media.

Wambua, Paul, Jan Ivens, and Ignaas Verpoest. 2003. "Natural fibres: can they replace glass in fibre reinforced plastics?" *composites science and technology* no. 63 (9):1259-1264.

Wang, Lu, and Chang-Ming Dong. 2006. "Synthesis, crystallization kinetics, and spherulitic growth of linear and star-shaped poly (L-lactide) s with different numbers of arms." *Journal of Polymer Science Part A: Polymer Chemistry* no. 44 (7):2226-2236.

Wang, Nuo, Xue Shen Wu, Chao Li, and Mei Fang Feng. 2000. "Synthesis, characterization, biodegradation, and drug delivery application of biodegradable

lactic/glycolic acid polymers: I. Synthesis and characterization." *Journal of Biomaterials Science, Polymer Edition* no. 11 (3):301-318.

Wang, Yiqing, David E Noga, Kunsang Yoon, Abigail M Wojtowicz, Angela SP Lin, Andrés J García, David M Collard, and Marcus Weck. 2008. "Highly Porous Crosslinkable PLA-PNB Block Copolymer Scaffolds." *Advanced Functional Materials* no. 18 (22):3638-3644.

Wang, Yongbin, Liang Yang, Yanhua Niu, Zhigang Wang, Jun Zhang, Fengyuan Yu, and Hongbin Zhang. 2011. "Rheological and topological characterizations of electron beam irradiation prepared long-chain branched polylactic acid." *Journal of Applied Polymer Science* no. 122 (3):1857-1865.

Werpy, Todd, Gene Petersen, A Aden, J Bozell, J Holladay, J White, Amy Manheim, D Eliot, L Lasure, and S Jones. 2004. Top value added chemicals from biomass. Volume 1-Results of screening for potential candidates from sugars and synthesis gas. DTIC Document.

Wessling, C, T Nielsen, and J R Giacin. 2001. "Antioxidant ability of BHT-and α-tocopherol-impregnated LDPE film in packaging of oatmeal." *Journal of the Science of Food and Agriculture* no. 81 (2):194-201.

Wessling, Carolina, Tim Nielsen, Anders Leufven, and Margaretha Jaegerstad. 1999. "Retention of α-tocopherol in low-density polyethylene (LDPE) and polypropylene (PP) in contact with foodstuffs and food-simulating liquids." *Journal of the Science of Food and Agriculture* no. 79 (12):1635-1641.

Whang, Kyumin, Thomas K Goldstick, and Kevin E Healy. 2000. "A biodegradable polymer scaffold for delivery of osteotropic factors." *Biomaterials* no. 21 (24):2545-2551.

Wise, Donald Lee. 1995. *Encyclopedic Handbook of Biomaterials and Bioengineering: v. 1-2. Applications*: CRC Press.

Wolf, Florian K, and Holger Frey. 2009. "Inimer-promoted synthesis of branched and hyperbranched polylactide copolymers." *Macromolecules* no. 42 (24):9443-9456.

Wool, Richard, and Xiuzhi Susan Sun. 2011. *Bio-based polymers and composites*: Academic Press.

Wu, Wei, Weigang Wang, and Jianshu Li. 2015. "Star polymers: Advances in biomedical applications." *Progress in Polymer Science* no. 46:55-85.

Wu, Xue Shen, and Nuo Wang. 2001. "Synthesis, characterization, biodegradation, and drug delivery application of biodegradable lactic/glycolic acid polymers. Part II: Biodegradation." *Journal of Biomaterials Science, Polymer Edition* no. 12 (1):21-34. doi: 10.1163/156856201744425.

Xiao, Lin, Yiyong Mai, Feng He, Longjiang Yu, Limin Zhang, Huiru Tang, and Guang Yang. 2012. "Bio-based green composites with high performance from poly (lactic acid) and surface-modified microcrystalline cellulose." *Journal of Materials Chemistry* no. 22 (31):15732-15739.

Xiao, Lin, Bo Wang, Guang Yang, and Mario Gauthier. 2012. *Poly (lactic acid)-based biomaterials: synthesis, modification and applications*: INTECH Open Access Publisher.

Xiong, Jin-Feng, Qun-Fang Wang, Pai Peng, Jie Shi, Zhao-Yang Wang, and Chong-ling Yang. 2014. "Design, synthesis, and characterization of a potential flame retardant poly (lactic acid-co-pyrimidine-2, 4, 5, 6-tetramine) via direct melt polycondensation." *Journal of Applied Polymer Science* no. 131 (10).

Xiong, Zhu, Chao Li, Songqi Ma, Jianxian Feng, Yong Yang, Ruoyu Zhang, and Jin Zhu. 2013. "The properties of poly (lactic acid)/starch blends with a functionalized plant oil: Tung oil anhydride." *Carbohydrate polymers* no. 95 (1):77-84.

Xu, Gang, Wenfang Shi, and Shijun Shen. 2004. "Curing kinetics of epoxy resins with hyperbranched polyesters as toughening agents." *Journal of Polymer Science Part B: Polymer Physics* no. 42 (14):2649-2656.

Yam, Kit L, Paul T Takhistov, and Joseph Miltz. 2005. "Intelligent packaging: concepts and applications." *Journal of Food Science* no. 70 (1):R1-R10.

Yousefi, A, PG Lafleur, and R Gauvin. 1997. "Kinetic studies of thermoset cure reactions: a review." *Polymer Composites* no. 18 (2):157-168.

Zeng, Xiaowei, Wei Tao, Lin Mei, Laiqiang Huang, Chunyan Tan, and Si-Shen Feng. 2013. "Cholic acid-functionalized nanoparticles of star-shaped PLGA-vitamin E TPGS copolymer for docetaxel delivery to cervical cancer." *Biomaterials* no. 34 (25):6058-6067.

Zhao, You-Liang, Qing Cai, Jing Jiang, Xin-Tao Shuai, Jian-Zhong Bei, Chuan-Fu Chen, and Fu Xi. 2002. "Synthesis and thermal properties of novel star-shaped poly(l-lactide)s with starburst PAMAM–OH dendrimer macroinitiator." *Polymer* no. 43 (22):5819-5825. doi: http://dx.doi.org/10.1016/S0032-3861(02)00529-3.

Appendix 1

Figure A1- 24. top: Casted samples of methanol-treated itaconic acid based resins after the DMA analysis. bottom: Casted samples of allyl alcohol-treated itaconic acid based resins after the DMA analysis.

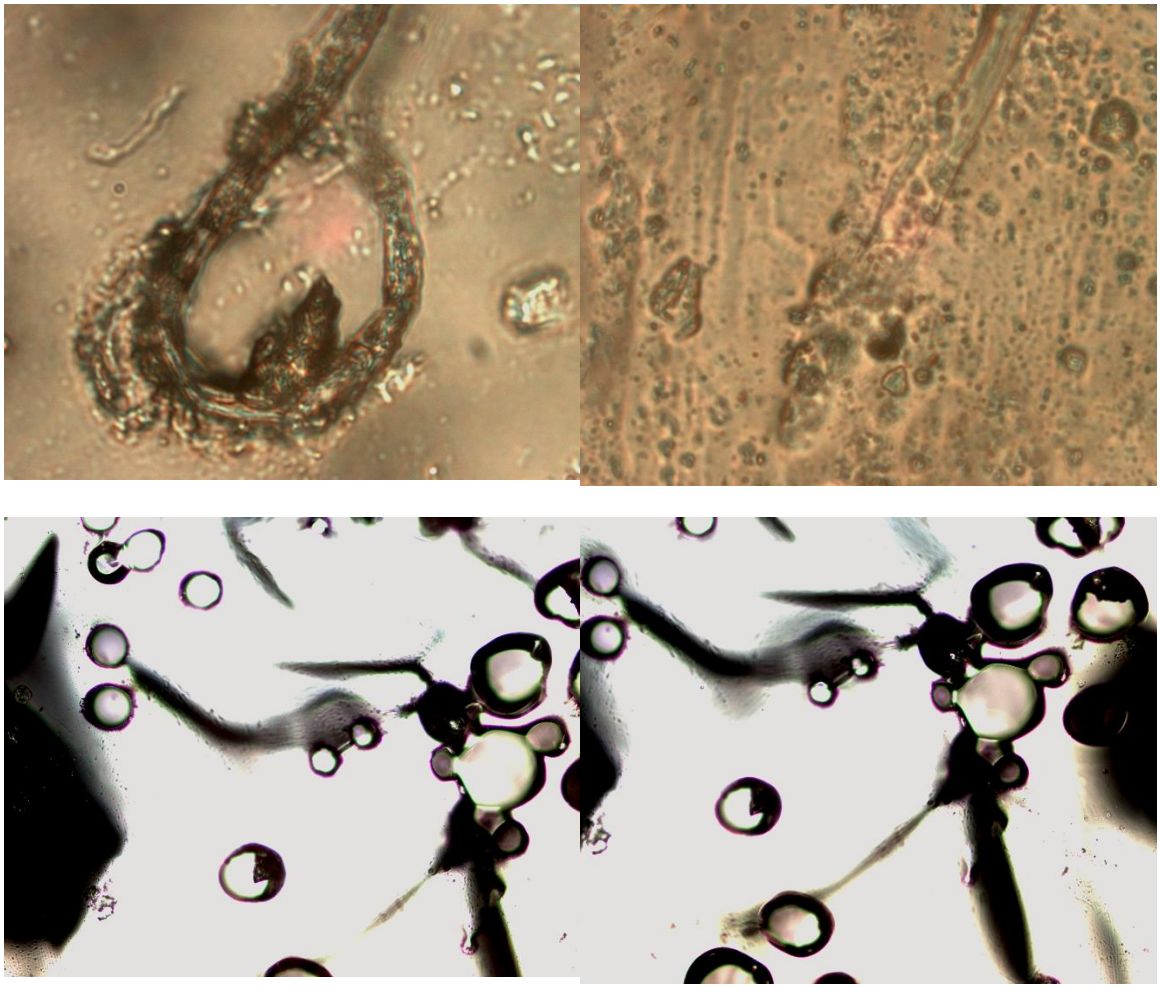

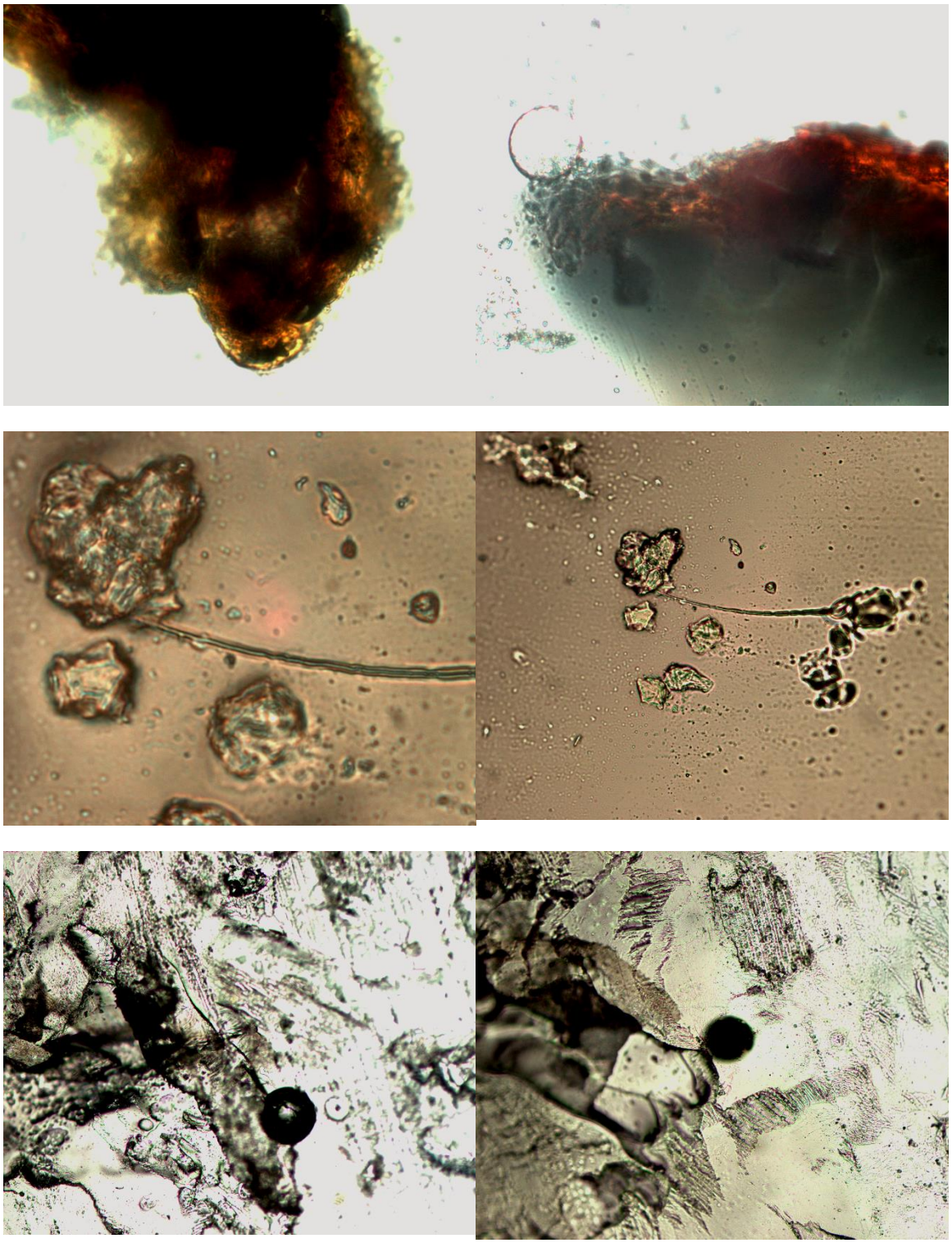

Figure A1- 1 Effect of curing methods on distribution and propagation of bubbles and cracks-100X

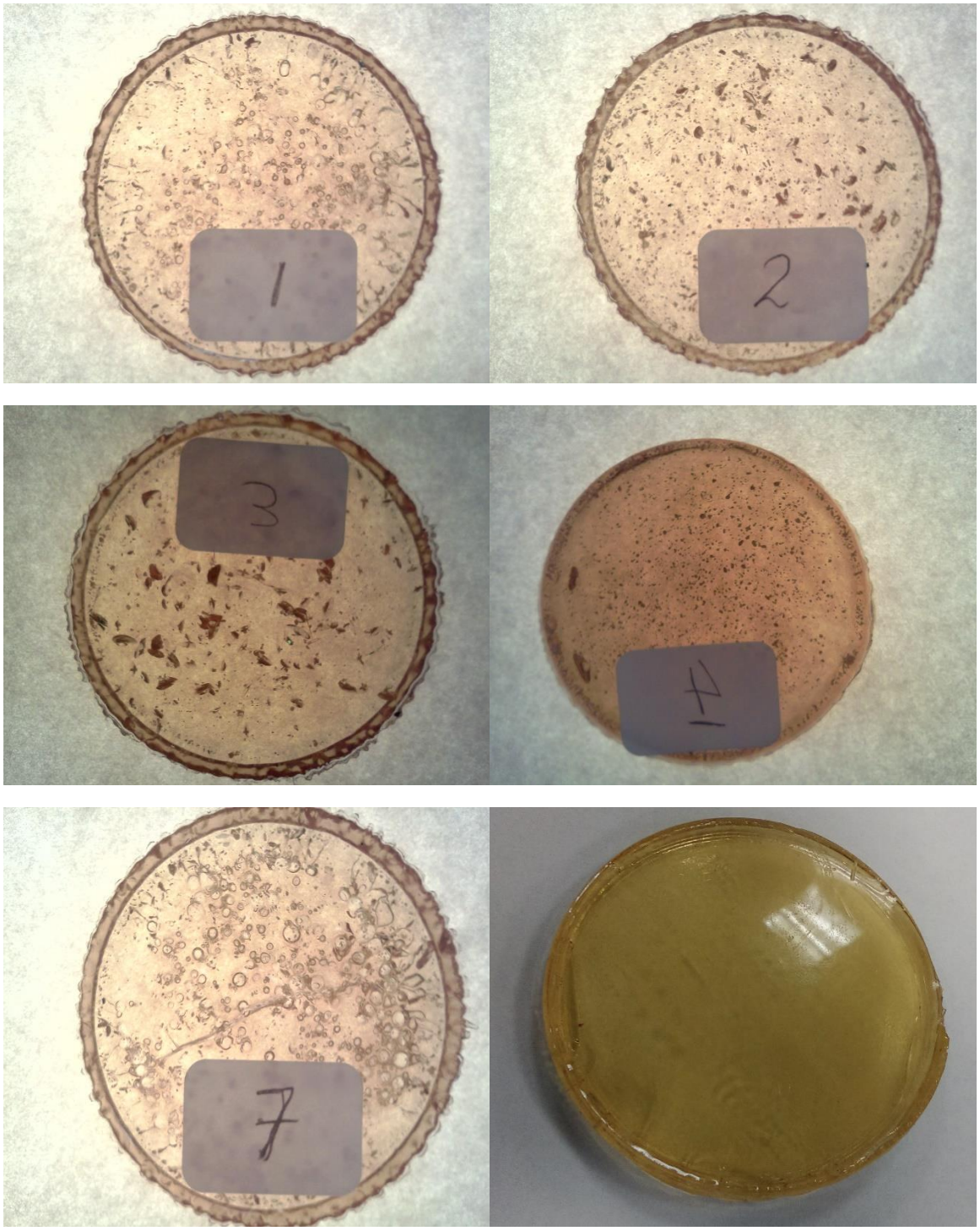

Figure A1- 2 Optimization of heating regimes on distribution and propagation of bubbles and cracks-Explanations given in Chapter one

Figure A1- 3 Left: Reactor set up for polycondensation reactions-Right: Azeotropic separation of water and toluene in the azeotropic distilation column.

Figure A1- 4 Polycondensation's reactor with the condensated resin

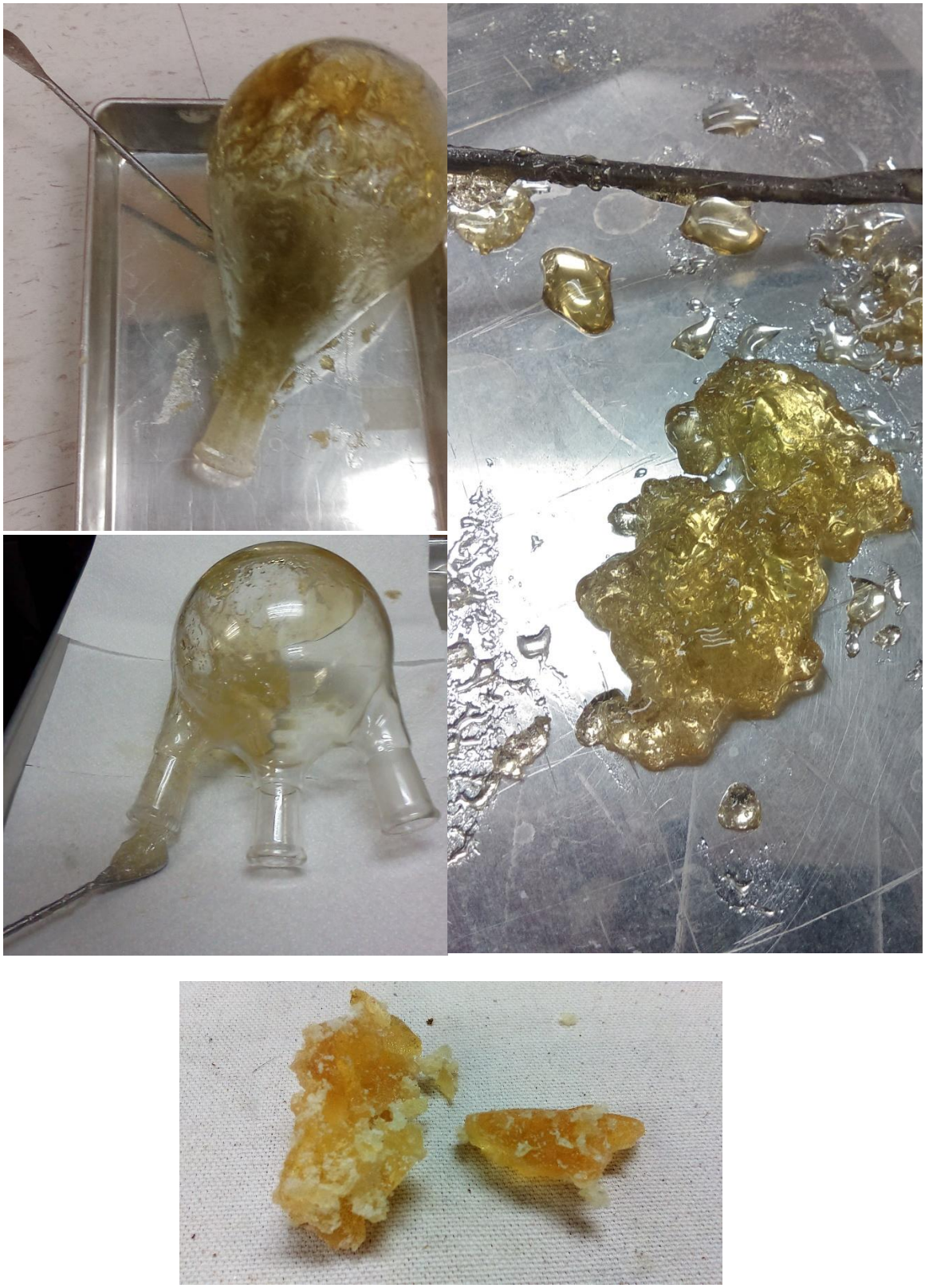

Figure A1- 5 Gel problem happening during different stages of the experiments

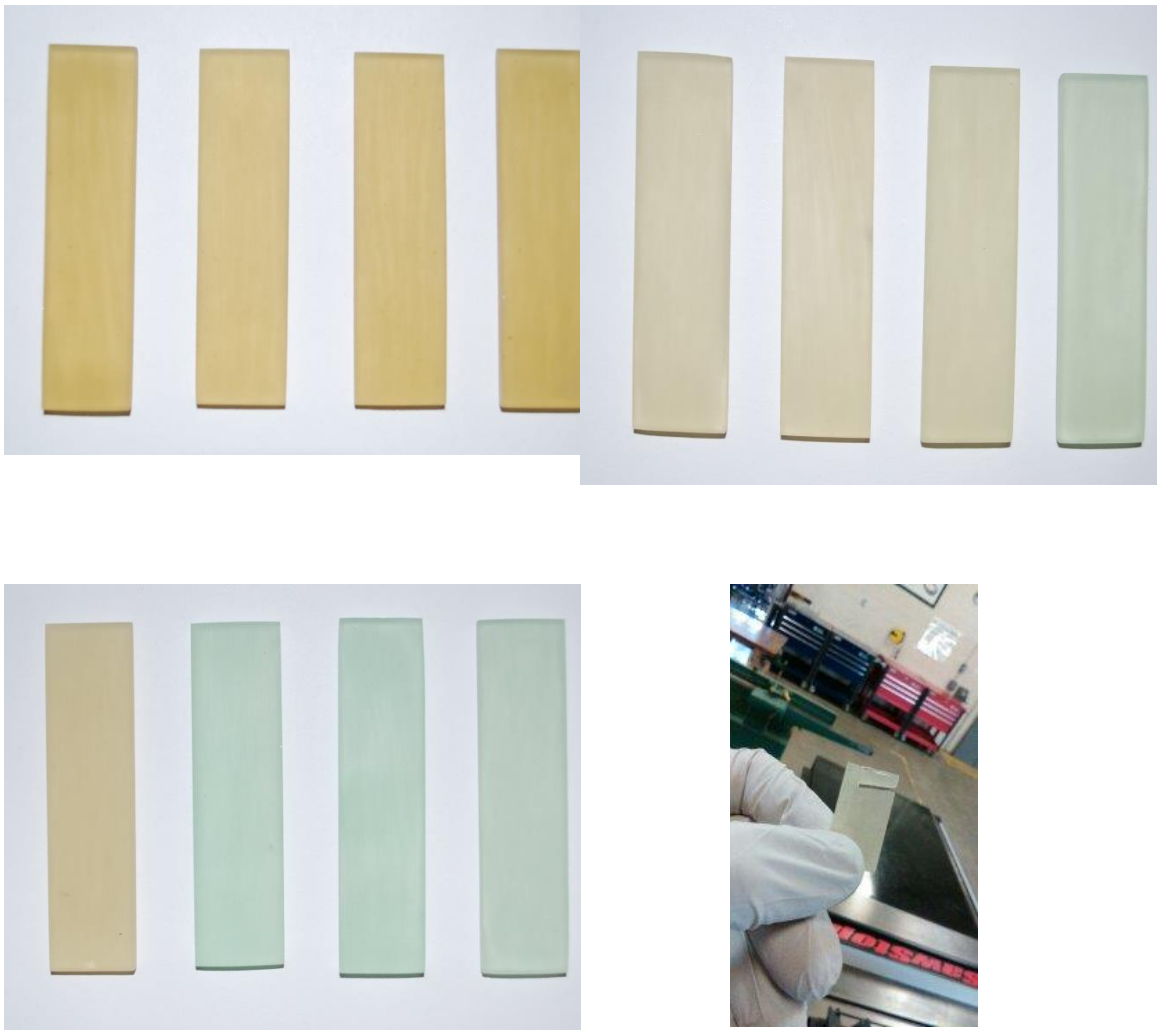

Figure A1- 6. Casted samples of n3, n5 and n7 resin samples, prepared for DMA analysis. Cutted samples of n5 resin.

Figure A1- 7. top: sputter gold machine, bottom: SEM machine used in microscopy of the composites.

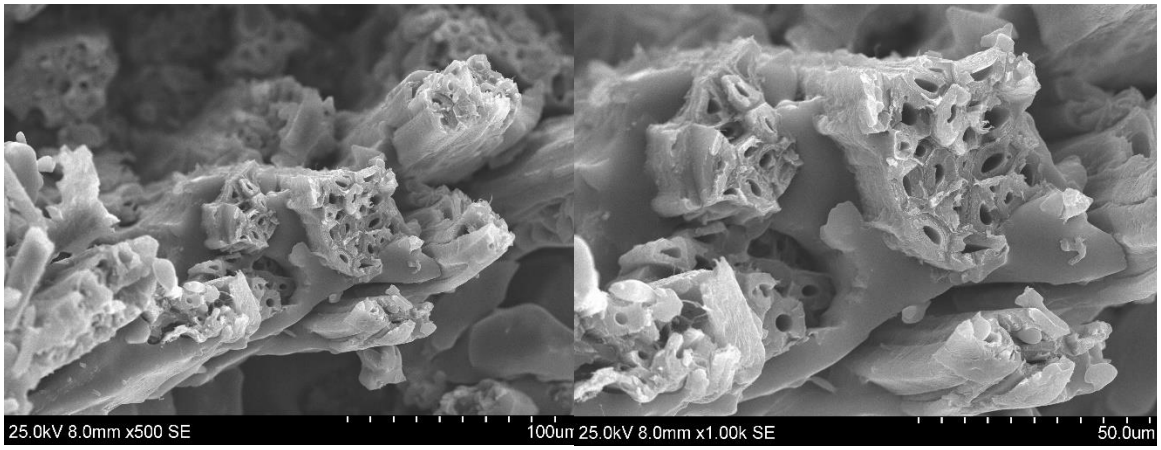
25.0kV 8.0mm x500 SE
100um
25.0kV 8.0mm x1.00k SE
50.0um

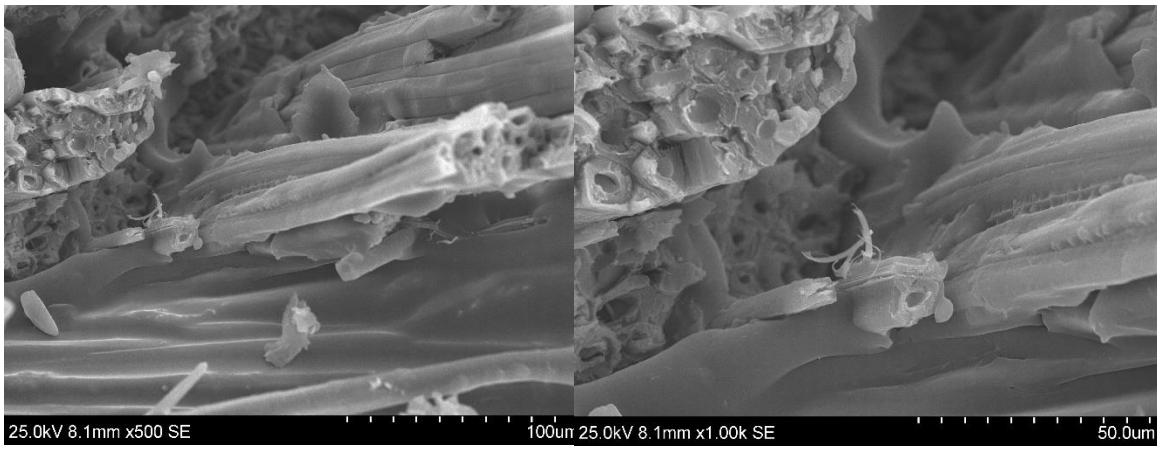
25.0kV 8.1mm x500 SE
100um
25.0kV 8.1mm x1.00k SE
50.0um

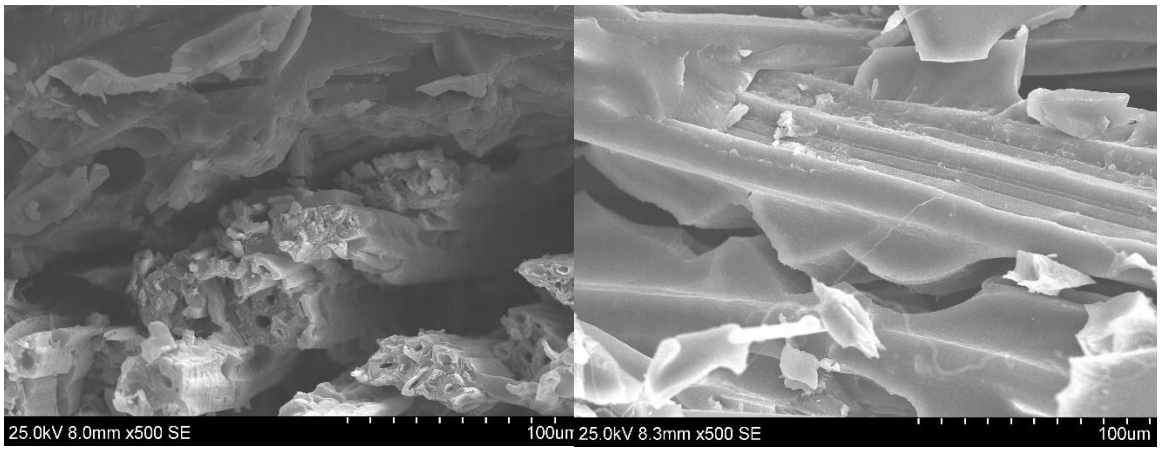
25.0kV 8.0mm x500 SE
100um
25.0kV 8.3mm x500 SE
100um

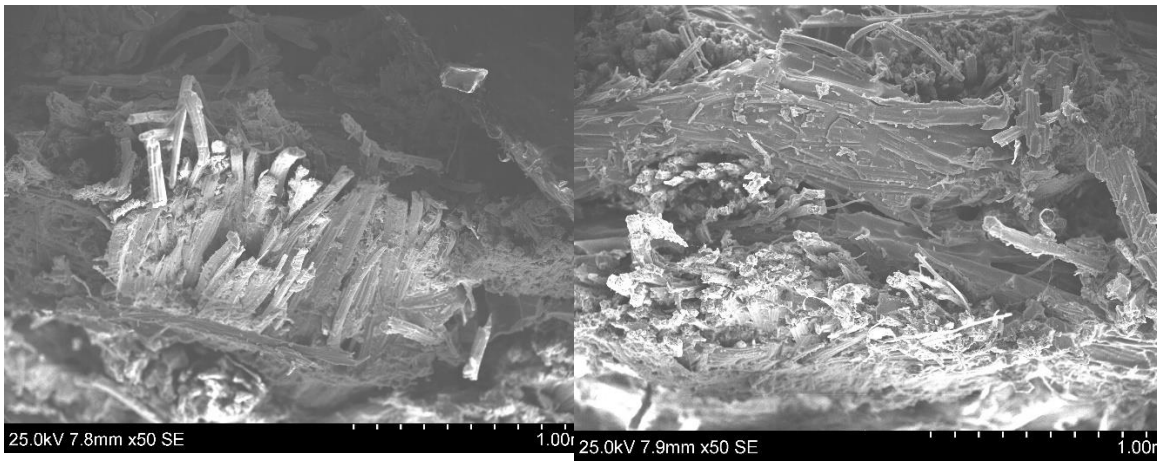

Figure A1- 8. SEM micrographs of the cross-sections of PLA-jute composite. More explanation in chapter 3.

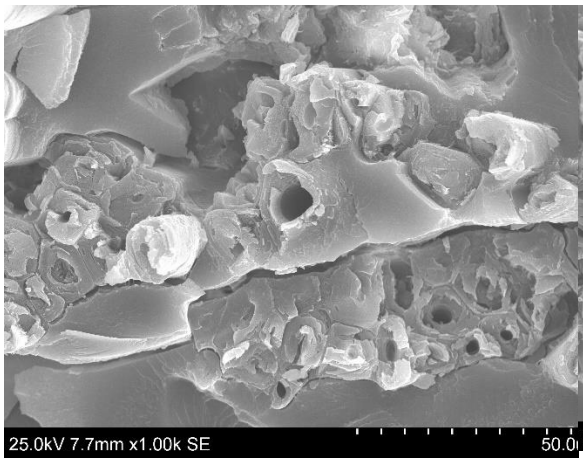
25.0kV 7.7mm x1.00k SE
50.0

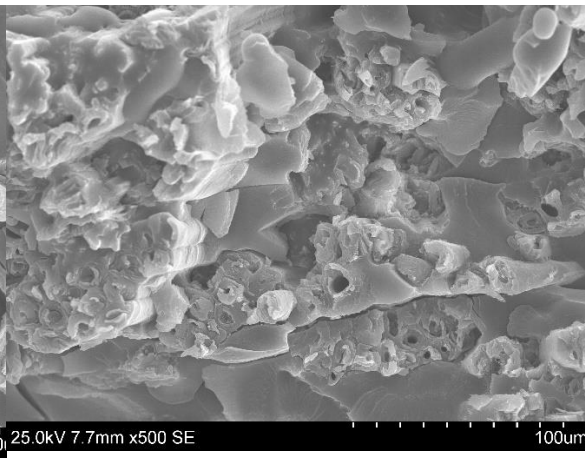
25.0kV 7.7mm x500 SE
100um

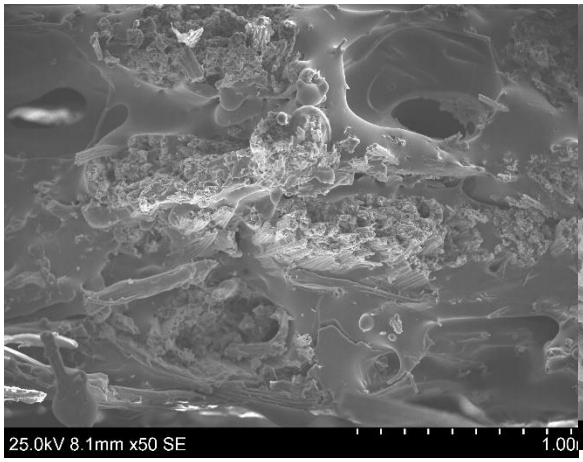
25.0kV 8.1mm x50 SE
1.00

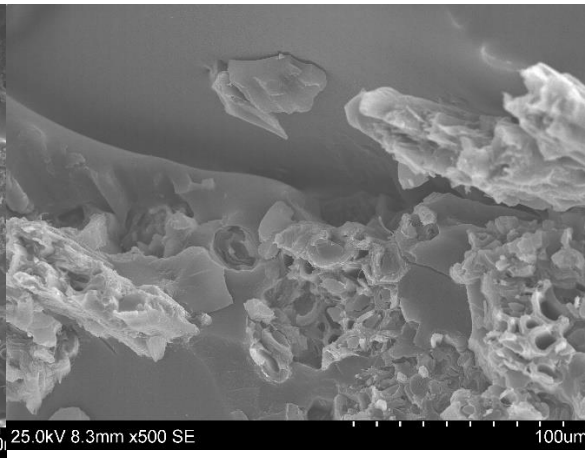
25.0kV 8.3mm x500 SE
100um

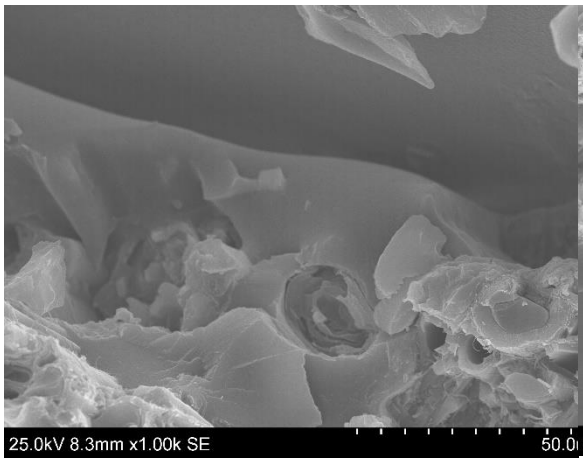
25.0kV 8.3mm x1.00k SE
50.0

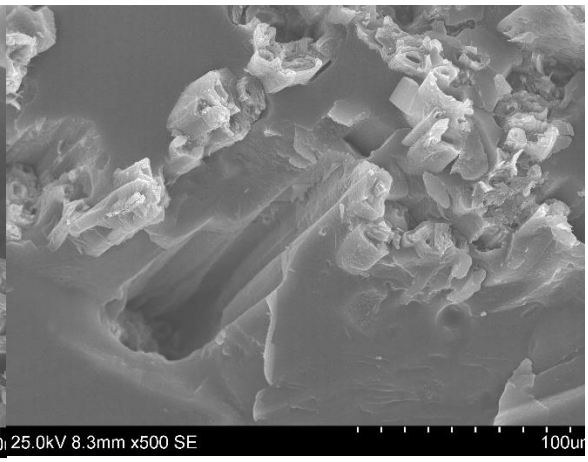
25.0kV 8.3mm x500 SE
100um

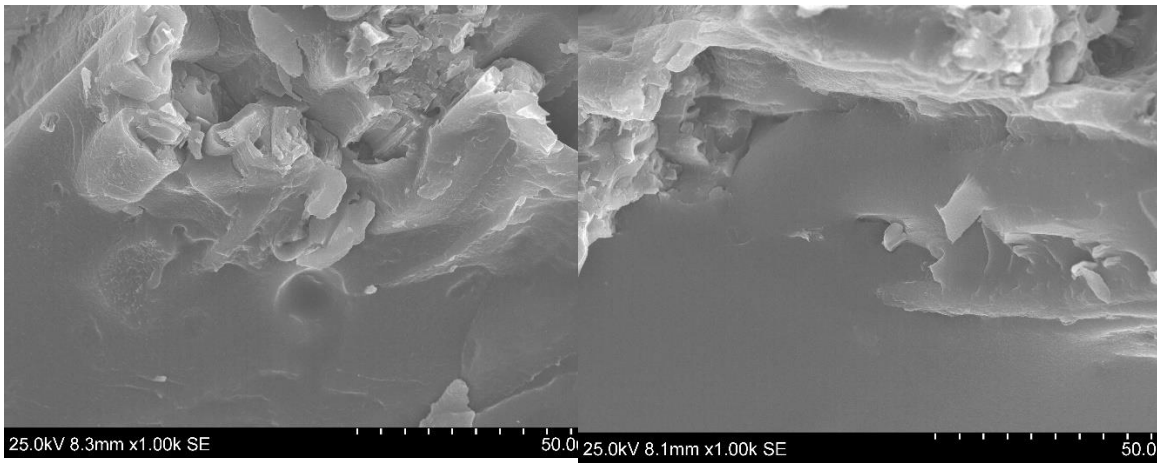

Figure A1- 9. SEM micrographs of the (n5-PLA)-jute composites. More explanation in chapter 3.

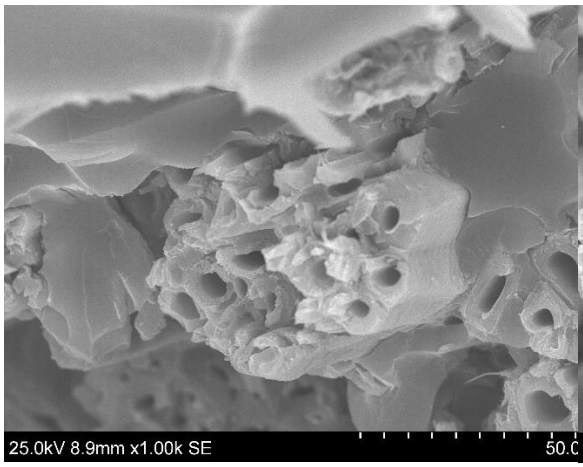
25.0kV 8.9mm x1.00k SE
50.0

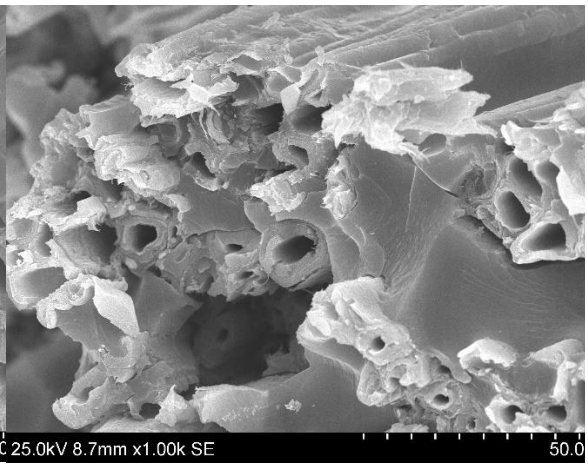
25.0kV 8.7mm x1.00k SE
50.0

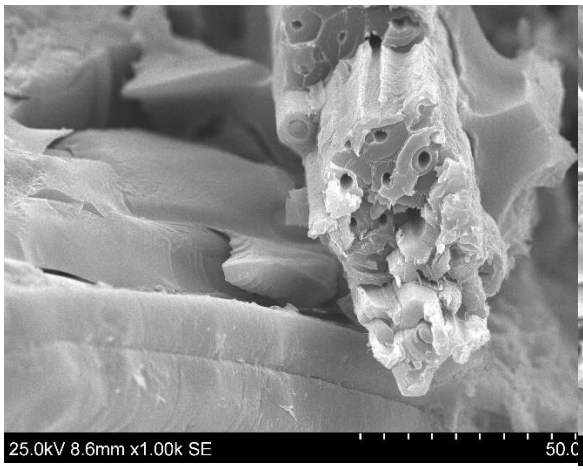
25.0kV 8.6mm x1.00k SE
50.0


25.0kV 8.6mm x500 SE
100

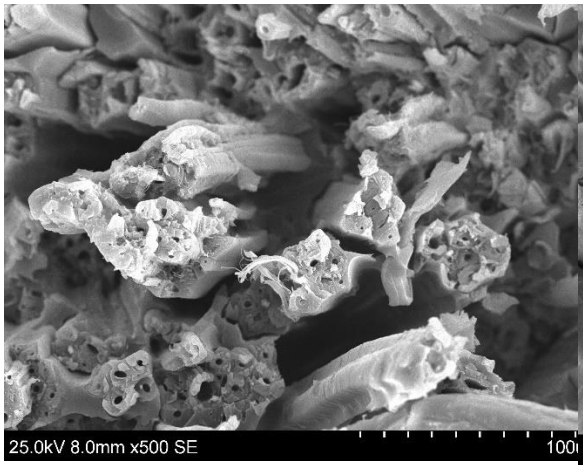
25.0kV 8.0mm x500 SE
100

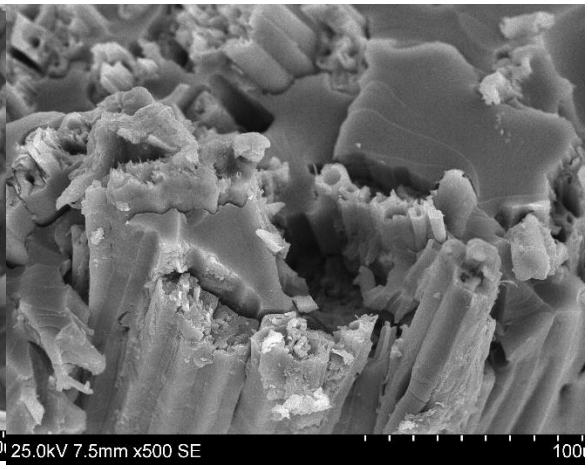
25.0kV 7.5mm x500 SE
100

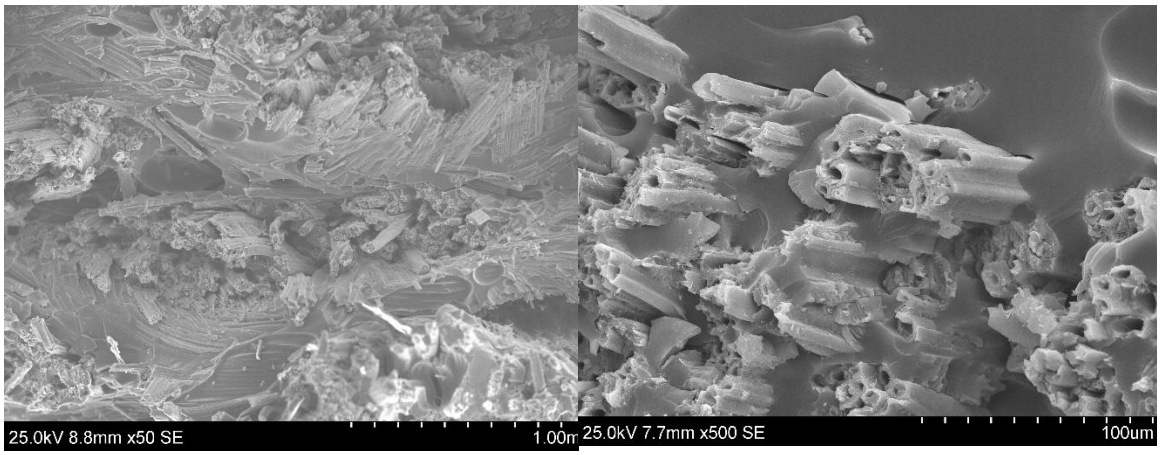

Figure A1- 10. SEM micrographs of the cross-sections of n5-jute composite. More explanation in chapter 3.

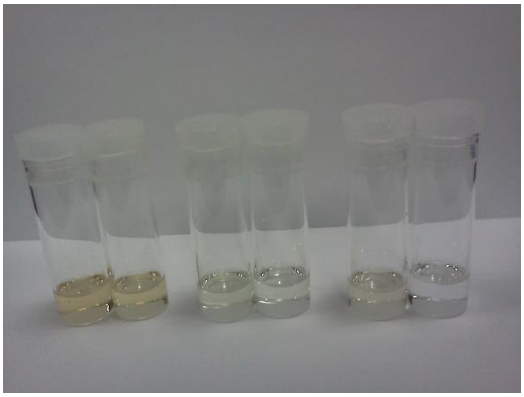

Figure A1- 11. Sample preparation for NMR studies. n3, n5 and n7 samples in $CDCl_3$ from left to right

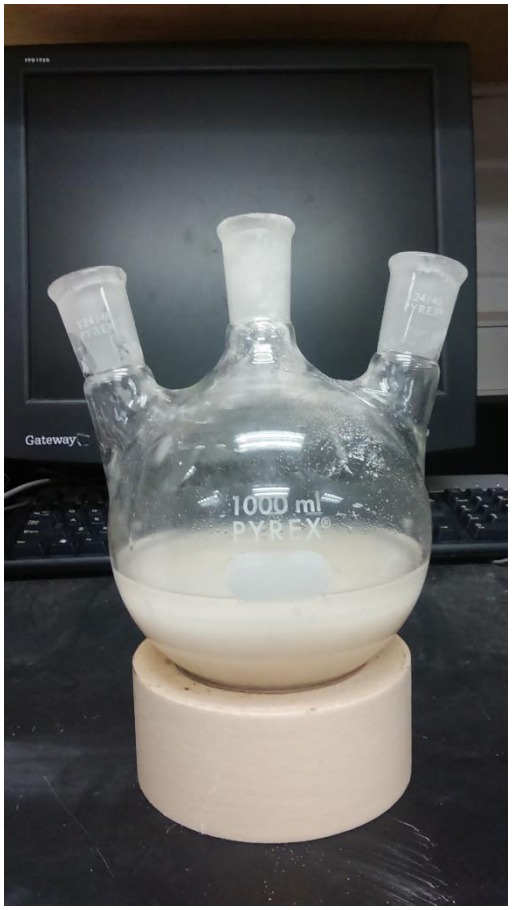

Figure A1- 12. Reactor and reactants of the itaconic acid based resin experiment. Itaconic acid+Glycerol+Toluene and Catalyst

Figure A1- 13. Polycondensation's reactor with the condensated resin, for Itaconic acid based resin

Figure A1- 14. Polycondensated Star-Ita.Gly resin with high viscosity, unsutable for processing. More explanation in chapter 8.

Figure A1- 15. Cured sample of Star-Ita.Gly resin. More explanation in chapter 8.

Figure A1- 16. Preparation of itaconic acid crystals inside the reactor, during the production of Star-Ita.Gly resin

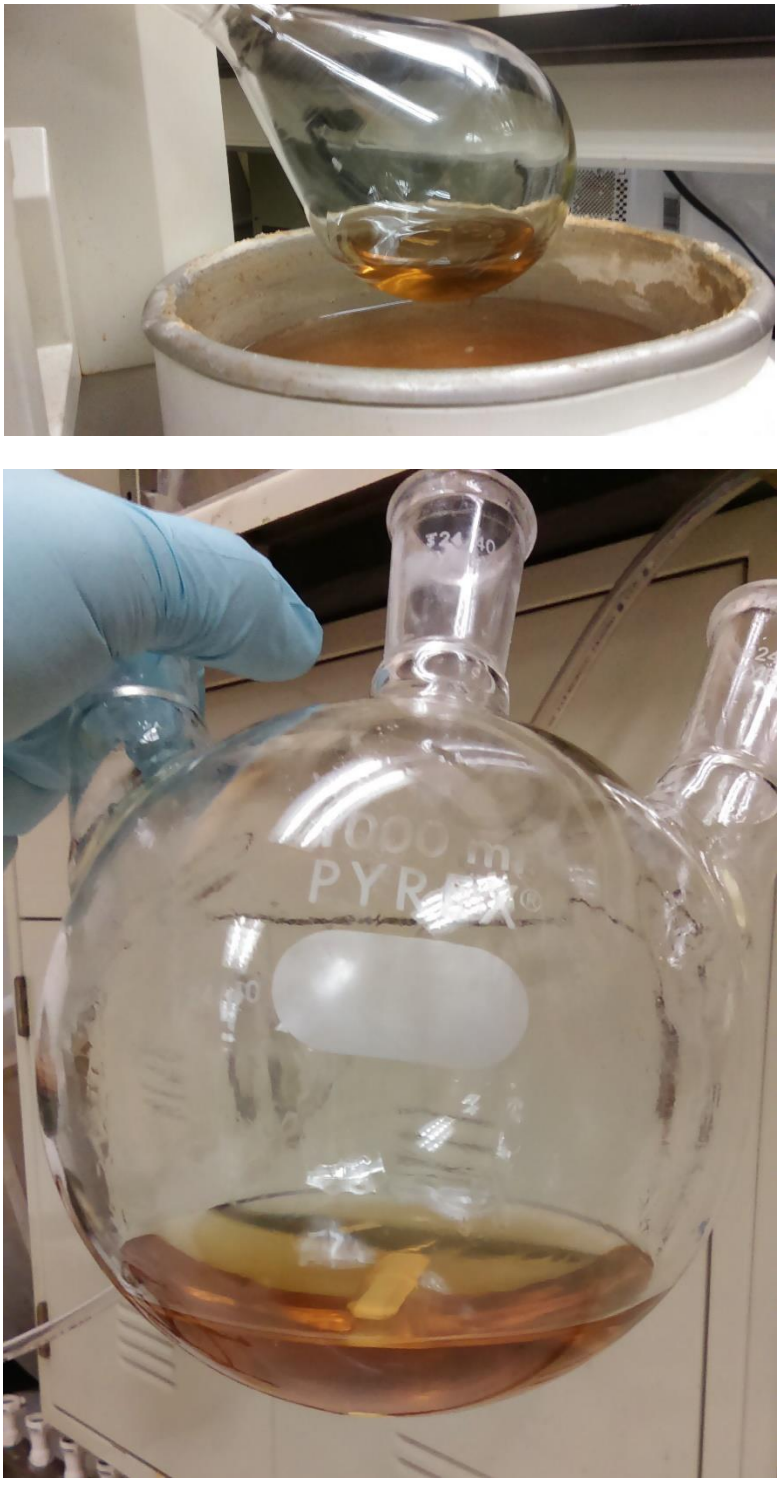

Figure A1- 17. Polycondensation's resin (bottom) and the condensated resin after vaccuum removal of extra solvent (top) for Itaconic acid based resin

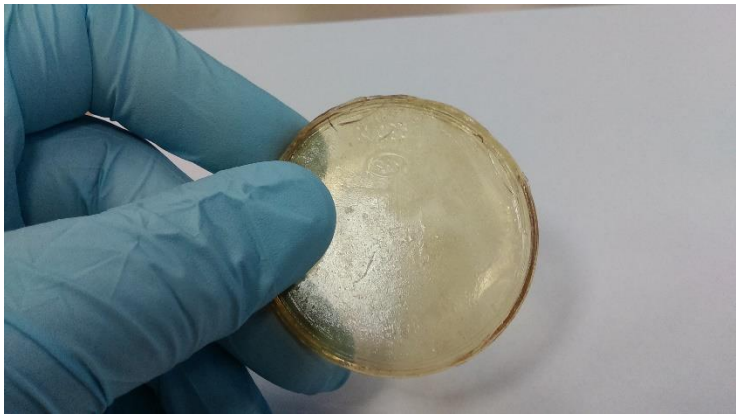

Figure A1- 18. Successfully casted and cured optimized TStar-Ita.Gly resin. More explanation in chapter 8.

Figure A1- 19. Polycondensate Star-Ita.Gly resin. Samples taken during the time-course of polycondensation reaction.

Figure A1- 20. From left to right: Star-Ita.Gly resin-Base resin, Ethanol-treated Star-Ita.Gly resin, Methanol-treated Star-Ita.Gly resin, and Allyl alcohol treated Star-Ita.Gly resin.

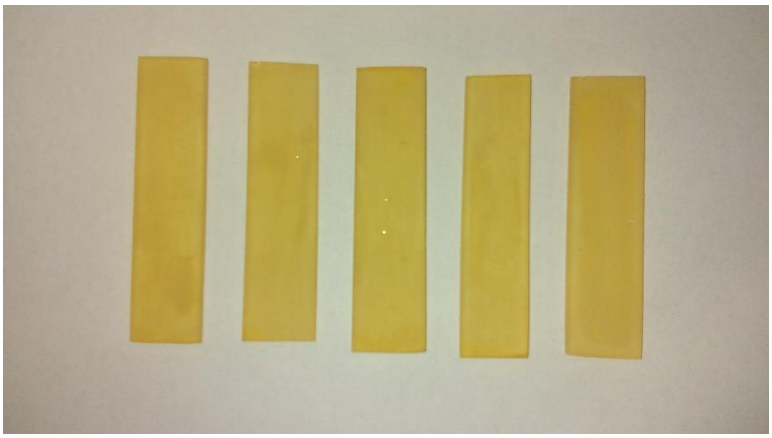

Figure A1- 21. Casted samples of star-shaped ethanol-treated itaconic acid based resin samples, prepared for DMA analysis- The samples of Methanol-treated and allyl alcohol-treated samples were similar and are not presented here.

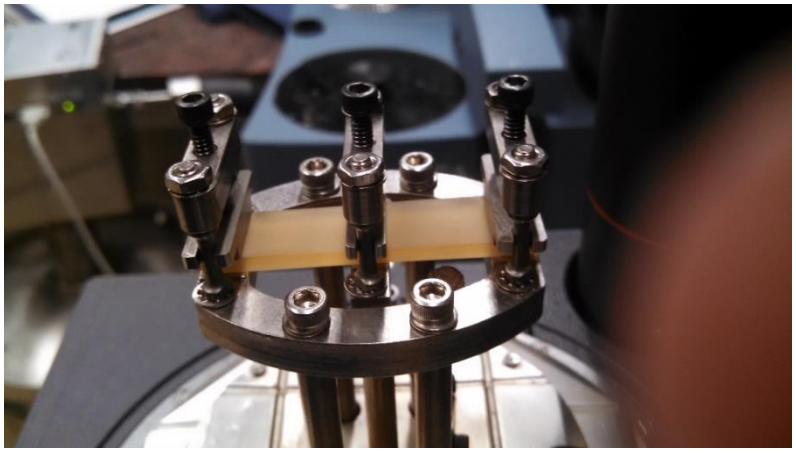

Figure A1- 22. DMA analysis set up for allyl alcohol treated samples. More explanation in chapter 9.

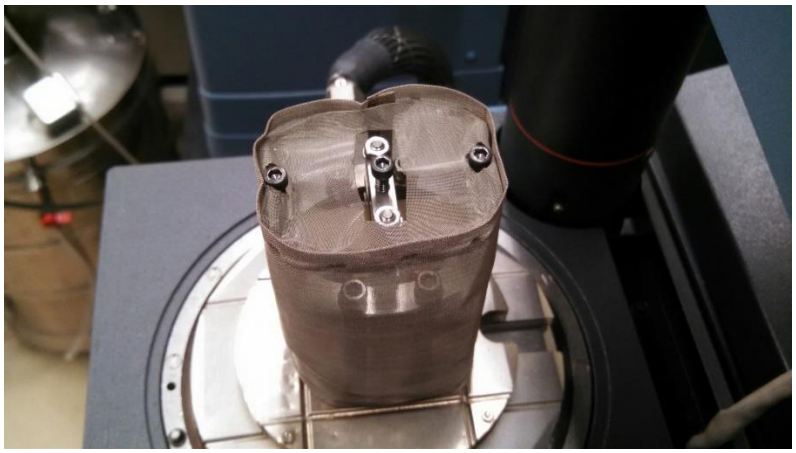

Figure A1- 23. Temperature mesh set up configuration used in DMA analysis of the activated itaconic acid based resins.

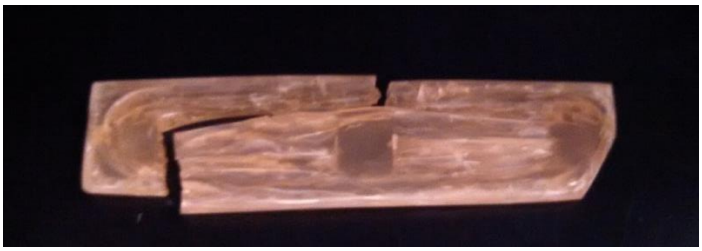

Figure A1- 24. top: Casted samples of methanol-treated itaconic acid based resins after the DMA analysis. bottom: Casted samples of allyl alcohol-treated itaconic acid based resins after the DMA analysis.

Appendix 2

1. Synthesis of PLLAs with ethylene glycol core molecule.
2. Synthesis of PLLAs with glycolic acid core molecule.
3. Synthesis of PLLAs with 1,4-butanediol core molecule.
4. Synthesis of PLLAs with diethylene glycol core molecule.
5. Synthesis of PLLAs with 1,6-hexanediol core molecule.
6. Synthesis of S-LA with glycerol core molecule.
7. Synthesis of S-LA with 1,1,1-tri(hydroxymethyl)propane core molecule.
8. Synthesis of S-LA with 1,3,5-benzenetrimethanol core molecule.
9. Synthesis of S-LA with pentaerythritol (PENTA) core molecule.
10. Synthesis of S-LA with di(trimethylolpropane) core molecule.
11. Synthesis of S-LA with xylitol core molecules with five hydroxyl groups using LA
12. Synthesis of S-LA with xylitol core molecules with five hydroxyl groups using lactide
13. Synthesis of S-LA with dipentaerythritol core molecule.
14. Synthesis of S-LA with hexa(hydroxymethyl)benzene
15. Synthesis of S-LA with poly(3-ethyl-3-hydroxymethyloxetane) core molecule.
16. End functionalization agents:1: methacrylic anhydride (MAAH),2: methacrylic acid (MAA), 3: itaconic acid (IT) and 4: 2-Butene-1,4-diol
17. 1: PLA esterification promotion functionalization, 2: End functionalized LA oligomers capable of free radical crosslinking.
18. Reaction scheme for the step-one resins of xylitol and lactic acid n=3, 5 and 7.

1 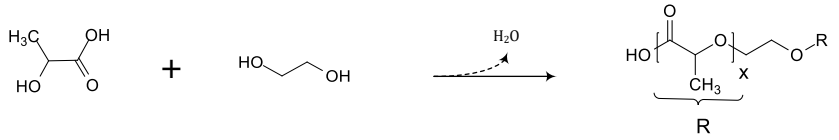

2 

3 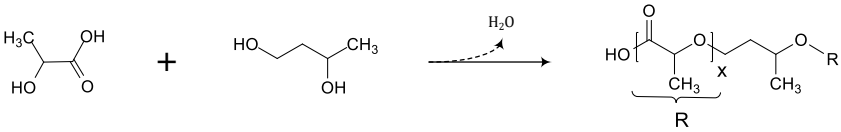

4 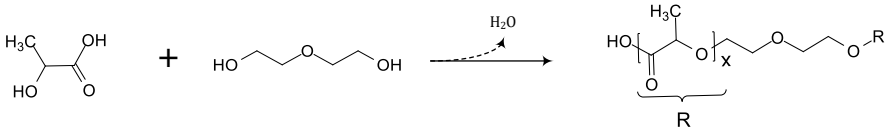

5 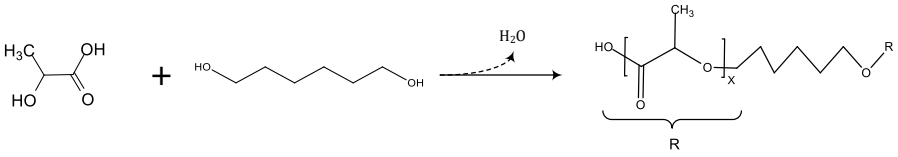

6 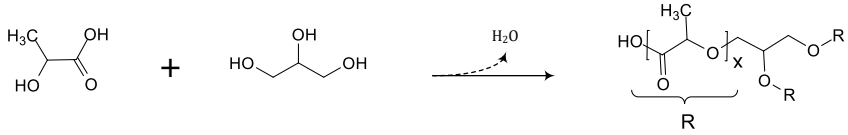

7 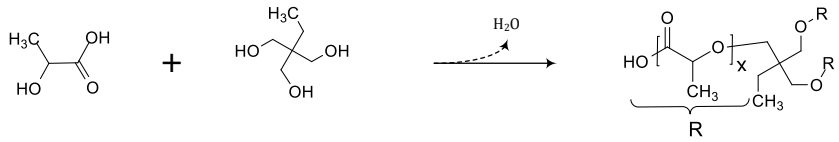

8 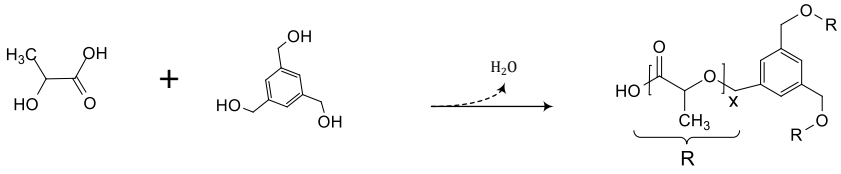

9 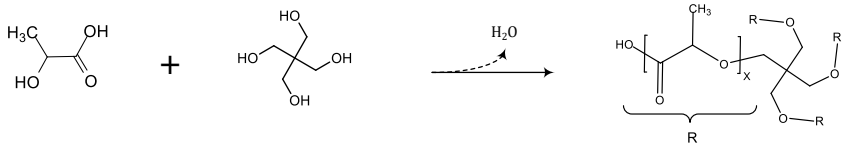

10 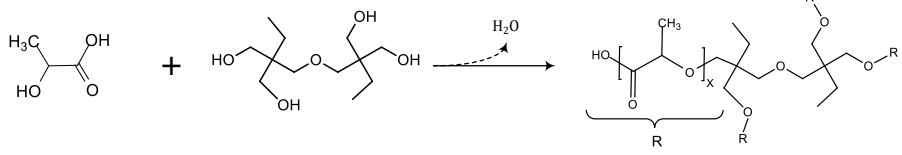

11 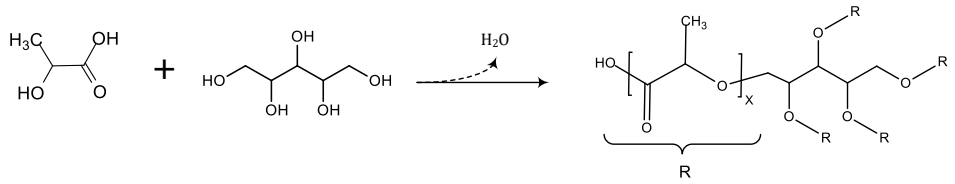

12 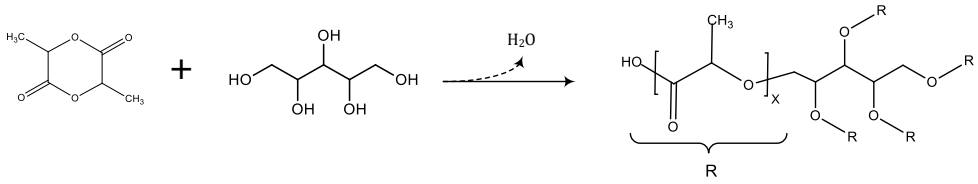

13 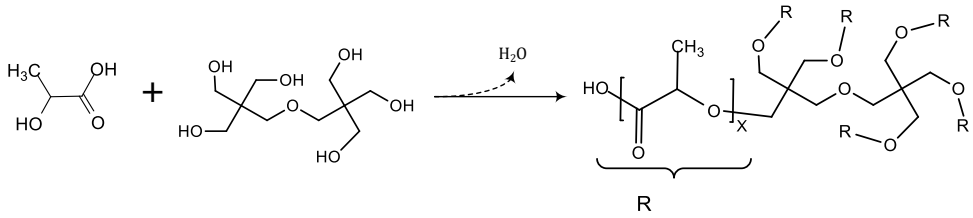

14 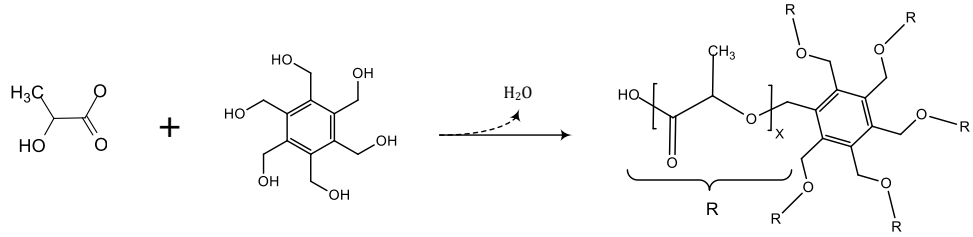

15 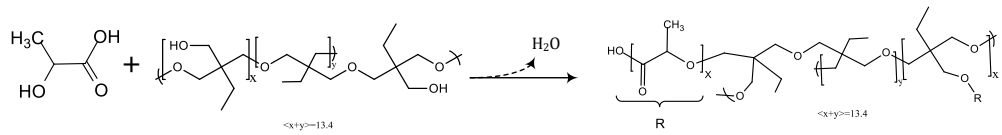

16 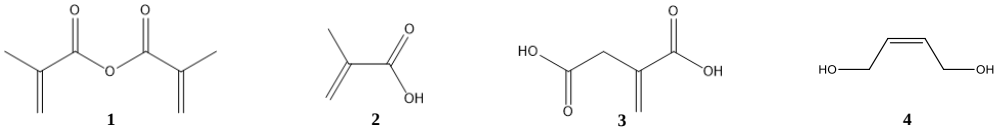

17 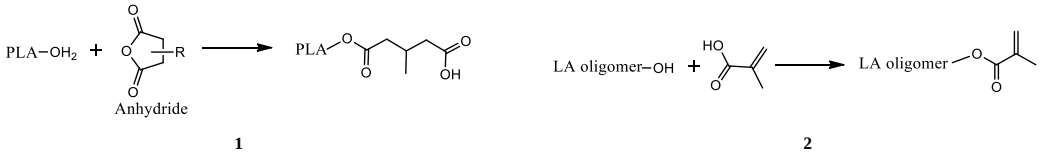

18

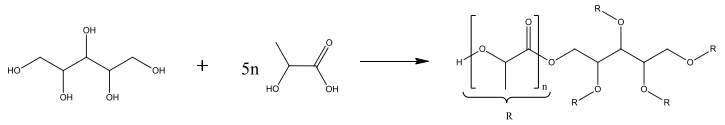

Xylitol Lactic acid Step-one Resin

19

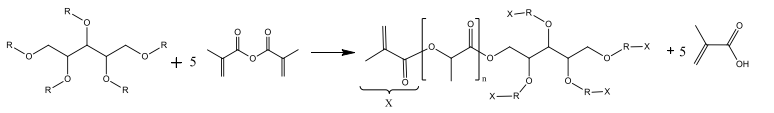

Step-one Resin Methacrylic anhydride Step-two Resin Methacrylic acid

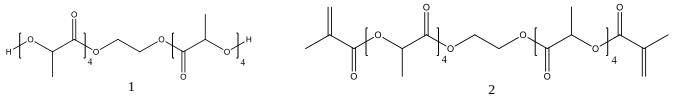

1 2

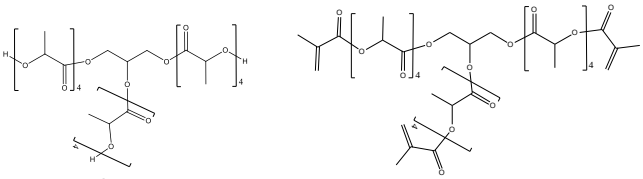

3 4

20

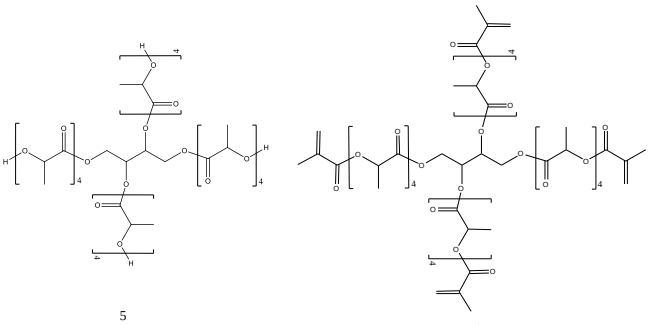

5 6

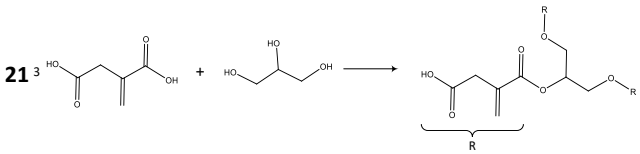

21

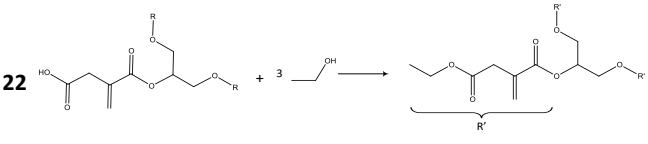

22

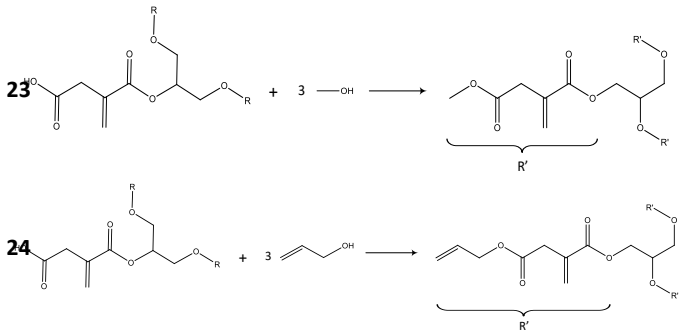
23
3
OH
R'
24
3
OH
R'